The ecological effects of slope and aspect in chalk grassland

Bennie, Jonathan James

The Ecological Effects of Slope and Aspect in Chalk Grassland

Jonathan James Bennie B.A. M.Sc.

School of Biological and Biomedical Sciences
University of Durham

2003

This thesis is submitted in candidature
for the degree of
Doctor of Philosophy

Frontispiece: South-facing sward on Hambledon Hill.

Table of Contents

List of figures

List of tables

List of plates

Declaration

The material contained within this thesis has not previously been submitted for a degree at the University of Durham or any other university. The research reported within this thesis has been conducted by the author unless reported otherwise.

Abstract

The microclimate of plants growing close to the ground is strongly influenced by the orientation of a soil/vegetation surface with respect to the sun's rays (slope and aspect). In chalk grassland in the UK, slopes of contrasting aspect frequently have distinctive patterns of vegetation.

A series of climatic and microclimatic measurements were made at field sites in different regions on the English chalk (North Dorset and the Yorkshire Wolds) during the period June 2000 to September 2002. Using digital terrain models (DTMs), process-based models of microclimatic variables at different points in the landscape were developed. The mechanisms through which topography may influence vegetation and species distribution were investigated with field experiments and measurements. Both existing vegetation data from Perring (1956) and new data collected from the field sites were analysed using detrended correspondence analysis (DCA) and generalised additive models (GAMs), to elucidate the relationships between vegetation and soil, topography and climate.

A consistent gradient in chalk grassland vegetation was found across spatial scales, associated with the frequency of species with a "stress tolerant" strategy. This gradient in vegetation is apparently driven by species' responses to several separate, but often correlated, variables including soil moisture, maximum summer temperatures and soil fertility.

Over the past 50 years, stress tolerant species have declined in frequency at the North Dorset field site, Ellenberg fertility indices have increased and light indices have decreased. The observed changes are consistent with fertilisation from atmospheric N deposition and/or relaxation of rabbit grazing after the myxomatosis outbreak in the 1950s. Plots on sloping ground, and in particular, south-west facing slopes, were least affected by these changes, suggesting that high temperatures, phosphorus and water limitation have acted as a buffer against vegetation change, and that complex topography creates refuges for stress tolerant species in the landscape.

Acknowledgements

This study was funded by NERC grant number GT04/1999/TS/0056, a CASE studentship with CEH Monk's Wood.

A great many people have helped me in the preparation of this thesis. I am indebted to Brian Huntley and Bob Baxter at Durham and Mark Hill at Monks Wood for their supervision; all three have been very generous with their time and invaluable sources of information and opinion. Peter North kindly gave up his time to run solar radiation models for me even after leaving Monk's Wood for Swansea. Frank Perring very generously allowed me to use his unique set of chalk grassland data; fifty years on, his detailed, legible notes put my rain-smudged notebooks to shame. Mike Austin gave useful advice in using Generalised Additive Models to analyse this data, and Jeremy Thomas kindly lent me tinytalk data loggers for the first field season.

Thanks are due to past and present members of the ecology group for help, advice and all those mugs of coffee. Judy Allen, Steve Willis, Trish Rannor, Hannah Drewitt, Yvonne Collingham, Matt Davey Steve Oswald and Richard Fuller have all helped solve a thousand minor (and some major) problems. Andy Dean was my guide in the dark art of extracting terrain models from aerial photographs. Andy Joyce was a valuable source of information on meteorology and the logistics of weather stations; Eric Henderson was an invaluable help in the logistics of getting them back from Dorset. Thanks are also due to Matt Davey and Hannah Drewitt for their help in the lab with the auto-analyser. I am grateful to all those at Warter Priory Farms, Chisel Farm and to Ian Nichol at English Nature, for allowing me to erect various bits of equipment on their land, and in their help in making it all sheep and cattle-proof.

I owe a great deal to friends who have been supportive throughout, not least during the dark days of the Foot and Mouth outbreak. Special thanks to Susie Roy, and to Nick Baker and Jens Lamping. Finally, my greatest debt of thanks is to my family, who have never failed to be supportive, encouraging, and very patient. This thesis is dedicated to them.

Notes on nomenclature used in this thesis

Vascular plants follow Stace (1991).

Bryophytes follow Smith (1980).

Glossary of acronyms

ANOVA	Analysis of variance
AWS	Automatic weather station
DAWS	AWS plot at Hambledon Hill, Dorset
DCA	Detrended correspondence analysis
DR	Modelled number of drought days (<30% volumetric soil moisture)
DTM	Digital terrain model
GAM	Generalised additive model
GCP	Ground control position
JMAX	Modelled mean daily maximum temperature in July
LIDAR	Light detection and radar
LOI	Loss on ignition
NNR	National Nature Reserve
PAR	Photosynthetically active radiation
RWC	Relative water content
SSSI	Site of special scientific interest
TSUM	Modelled soil temperature sum above 5 °C threshold, March-May
WUE	Water use efficiency
YAWS	AWS plot at Millington Pastures, Yorkshire Wolds
YNF	North-facing plot in Sylvan Dale, Yorkshire Wolds
YSF	South-facing plot in Sylvan Dale, Yorkshire Wolds

Chapter 1: Introduction and Aims

1.1 Introduction to slope and aspect

1.1.1 Slope, aspect and microclimate

Climate has long been accepted as a major factor in determining the structure and function of vegetation communities and the distribution of species. However, the climatic data collected by national meteorological networks are designed to provide a representative "average" climate for a region at a standardised height above a horizontal surface (Linacre, 1992). These data do not capture the full spatial and temporal variability of the microclimates of plants and animals living close to the ground in complex landscapes (Geiger *et al.*, 1995; Oke, 1987).

A major source of variability in microclimate is the orientation of the ground/vegetation surface with respect to the sun's rays. At mid to high latitudes the solar radiation flux at a surface facing towards the equator is significantly higher than that at a surface facing towards the pole. The slope and aspect of the ground can therefore have a considerable effect on the microclimate of plants and animals. The annual mean temperature difference between slopes facing north and south in a UK calcareous grassland has been recorded as 2.5 to 3° C (Rorison *et al.*, 1986) – roughly equivalent to a shift of 5° in latitude or 300 m in altitude in the British Isles (Barry, 1992).

1.1.2 Slope and aspect in ecological studies

Körner (1999) has argued that, while climatic gradients associated with latitude and altitude have been widely studied by ecologists, there is considerable potential to make further use of topographic microclimate gradients in ecological studies. While the slope and aspect of sites are routinely recorded when collecting ecological data, this information is often neglected in analysis due to the indirect nature of these variables. Converting data in the form of slope (usually measured in degrees from horizontal) and aspect (measured in degrees clockwise from magnetic north) into a biologically meaningful environmental gradient is

problematic for several reasons. In order to estimate the relative direct radiation load on a surface, slope and aspect must be transformed using tables such as those in Buffo (1972) or trigonometric equations such as those in Oke (1987). These provide an index of potential (clear sky) radiation for a particular time of day; to integrate potential direct radiation fluxes over longer periods requires integrating equations, typically with a time-step of one hour (Weiss *et al.*, 1988) or an empirical equation such as that proposed by McCune and Keon (2002). Diffuse solar radiation, cloud cover and long wave radiation exchange act to lessen the differences in net radiation flux between different aspects. Potential direct radiation is symmetrical around a north-south axis; however observed patterns in vegetation often show a deflection towards a southwest-northeast axis (Dargie, 1987; Lakhani and Davis, 1982), usually attributed to higher maximum temperatures on slopes receiving afternoon sun (Geiger *et al.*, 1995; McCune and Keon, 2002). In order to quantify the ecological effects of slope and aspect, and their interactions with spatial and temporal climatic variation in cloudiness, temperature, humidity and rainfall, there is a need for process-based models of biologically relevant variables.

1.1.3 Slope and aspect in chalk grassland

Calcareous grasslands, particularly those on the southern English Chalk, have long attracted the attention of British ecologists due in part to their species-rich assemblages of plants and small-scale diversity. Early ecological studies of British chalk grasslands noted that there are often consistent differences in the vegetation on different aspects (Tansley and Adamson, 1925, 1926). A systematic attempt to study the effects of slope and aspect in chalk grassland in the context of large-scale climatic gradients was made in a series of papers by Perring (1956; 1958; 1959; 1960). Since these studies, advances in technology have greatly increased the potential to quantify the effects of slope and aspect on microclimate, both through direct measurement and computer modelling. Meanwhile, increasing concern about the effects of future anthropogenic climate change on ecosystems has led to a resurgence in interest in the relationships between climate and vegetation. In this context a better understanding of the ways in which topographic microclimate influences vegetation and species distribution has several

applications. Microclimatic gradients might be used as "space-for-time" proxies to predict vegetation change under possible future climates (Körner, 1999); areas of complex topography may provide "refugia" where species might persist in areas of suitable microclimate where regional climatic conditions become unsuitable; and changes in the topographic distribution of a species at its range margins might be an early indicator of change in its geographical range – for example the butterfly species *Hesperia comma* is expanding onto north-facing slopes in the South Downs (Thomas et al., 2001).

1.2 Scope and aims of thesis

The overall aim of this study was to investigate the mechanisms through which slope and aspect influence vegetation composition in British chalk grasslands. Firstly, literature on the effects of climate on plants, and of topography on microclimate, was reviewed, and vegetation data collected by Perring (1956) was analysed using modern statistical methods to elucidate the associations between regional climate, topography and vegetation.

In order to examine the ways in which topography influences microclimate, models of selected microclimatic variables were developed, using digital terrain models (DTMs) of two chalk grassland field sites with contrasting climates in the UK. Hourly climatic measurements at the sites were adjusted for radiation input to model the effects of landscape position and slope orientation on soil moisture and temperature close to the ground at different points in the landscape, and under different climates. These models were tested against microclimatic measurements made over a period of two years at both sites.

To examine possible mechanisms by which microclimate influences ecological processes, a series of experiments and measurements were carried out to investigate the influence of microclimate on soil processes, and on seed germination and gas exchange in selected chalk grassland species.

The vegetation composition of plots at both field sites was surveyed, and the extent to which the modelled microclimatic variables could explain the observed vegetation composition and the distribution of individual species was examined.

Finally, vegetation plots surveyed by Perring (1956) in Dorset in 1953, were compared with plots in the same positions surveyed in this study in 2000. The differences in vegetation between the two surveys are discussed with reference to landscape position and vegetation change.

A brief outline of the thesis is given below:

In chapter 2, the relevant literature is discussed, and the study of topographic and climatic gradients in chalk grassland by F. H. Perring is introduced; Perring's original data are analysed using detrended correspondence analysis (DCA) and generalised additive models (GAMs).

In chapter 3, the two study sites are described and climatic and microclimatic measurements at these sites taken from June 2000 to September 2002 at each site are summarised.

In chapter 4, an approach to modelling topographic microclimate is defined; process-based models of topographic microclimate (soil moisture, soil temperature and sward temperature) are described, and tested against measurements taken at both study sites.

In chapter 5, field experiments and observations are described, including *in-situ* soil incubations and organic matter decomposition, seasonal variation in plant-available N and P concentration within the soil and gas-exchange measurements of five selected species on contrasting slopes, and a novel method of manipulating soil microclimate using mirrors and shades in a germination experiment.

In chapter 6,gradients in vegetation composition at both field sites are examined. DCA is used to examine differences in vegetation within and between field sites,

and GAMs are used to investigate the relationships between microclimatic variables as modelled in chapter 3, and the frequency of species found within plots. Changes in vegetation between 1953 and 2000 are analysed in the context of slope and aspect.

In chapter 7 the results of the study are discussed with reference to previous work, their wider relevance and suggestions for future research.

Chapter 2: Background to Study

2.1 Introduction

In this chapter, literature concerning the effect of climatic variables on the distribution of organisms is considered, including correlations between climate and vegetation distribution across spatial scales. The physiological mechanisms by which microclimate influences plant survival, growth and regeneration and the biological relevance of topographic and climatic variables are discussed. The effect of topography on microclimate in grasslands and similar ecosystems, and the relationship between macro- and microclimates, and macro- and micro-scale species distributions is considered. The classic studies of topographic and climatic gradients in chalk grassland by Perring (1956; 1958; 1959; 1960) are introduced. Finally, two modern methods of exploratory analysis, Detrended Correspondence Analysis (DCA) and Generalised Additive Models (GAM) are applied to Perring's original data in order to elucidate the factors influencing the distribution of vegetation and species in chalk grassland.

2.2 Literature review

2.2.1 The effects of climate on the distribution of plants

Climatic phenomena can be studied across a range of spatial and temporal scales; different atmospheric processes dominate at different scales (Oke, 1987; Geiger *et al.*, 1995;). Similarly the distribution of vegetation has been studied across a range of scales.

2.2.1.1 The global scale

At a continental or global scale, it has been demonstrated that the principal features of higher plant distribution are determined primarily by macroclimate, as governed by large-scale atmospheric circulation systems and modified by altitude. The response of vegetation to climate may be considered through the individual responses of different species, in the response of vegetation units such as

communities, biomes (Smith *et al.*, 1992) or functional types (Box, 1996) or in terms of characteristics such as leaf area index (Woodward, 1987; Smith *et al.*, 1992). The limits of climatic tolerance of a species are often reflected in the geographical limits to the distribution of the species, which may follow the isometric lines of climatic variables (Pigott, 1970). Multi-dimensional climate response surfaces have been proposed for a range of species at large scales, describing the observed spatial distribution in terms of bioclimatic variables such as mean temperature of the coldest month, degree days above a 5° C threshold and ratio of actual to potential evapotranspiration (AET/PET) (Huntley *et al.*, 1989; Huntley *et al.*, 1995). Stephenson (1990) has correlated the distribution of North American plant formations with spatial variation in the water balance on a continental scale and Smith *et al.* (1992) have modelled the response of vegetation to global change using Holdridge's life-zones classification based on potential evapotranspiration and rainfall. Criddle *et al.* (1996) have argued that the response of plant respiration to climate is the primary determinant of distribution on a global scale. Over time, paleoecological evidence shows that patterns of vegetation change follow climate change, but also that plant communities and biomes are not fixed entities, and that the individual responses of species have combined to form associations in the past that do not currently exist in nature (Huntley, 1991). Indirect effects of climate, such as competition, which define the species' realised, rather than fundamental niche (Sætersdal *et al.*, 1998) may be important. If a species comes into contact with a mix of species with which it does not currently come into contact, then its realised niche, and hence its climate response, may be modified.

Multivariate statistics have been frequently used to investigate the relationship between of vegetation and climate. For example relationships in Atlantic European calcareous grasslands have been investigated using DCA (Duckworth *et al.*, 2000a; Duckworth *et al.*, 2000b; Duckworth *et al.*, 2000c), and have shown correlations between climatic factors (temperature and rainfall) and vegetation axes; however at this scale other environmental factors, such as land-use and geology, are also significant.

2.2.1.2 The landscape scale

At regional (~10^4 m) to local (~10 m) scales, the macroclimate may be modified considerably by topography. Whereas continental-scale studies have successfully used spatial interpolation techniques such as kriging to provide climate data between weather stations, at local and regional scales digital terrain models (DTMs) are often used to predict climatic variables such as soil moisture or temperature (Franklin, 1995, 1998; Rich and Fu, 2000) or more often to derive terrain-related variables such as slope, aspect and altitude as proxies for climatic variables (Gottfried *et al.*, 1998; Zimmermann and Kienast, 1999; Franklin *et al.*, 2000). Studies at a regional to local scale may have to incorporate variations in geology, soils and land-use that are important determinants of plant distribution at these scales. Franklin (1995) reviews attempts at predictive vegetation mapping at the landscape scale, with climatic, topographic and other variables typically incorporated as data layers in geographical information systems (GIS) (1995). Guisan, Weiss and Weiss (1999) have compared a constrained ordination technique (CCA) with Generalized Linear Models (GLMs) in predicting plant species distribution using topographic variables. Burnside *et al.* (2002) have used a weighted scoring approach to identify a GIS-based habitat suitability index for calcareous grassland restoration on the South Downs. However, the derived model, based on the present distribution of calcareous grassland, predicts higher suitability on north-facing slopes due to the current abundance of chalk grassland on the steep north-facing slopes on the South Downs escarpment, despite the more species-rich nature of swards on south-facing slopes. This example demonstrates the advantages of models based on ecological processes rather than correlations between terrain-derived variables and vegetation.

Spatial models of species distribution require an ecological model concerning the ecological theory to be used or tested as well as a data model concerning sampling and collection of data and a statistical model describing the statistical theory and methods used (Austin, 2002). The ecological theory behind most models of the distribution of species with respect to climate has its roots in niche theory and

gradient analysis (Franklin, 1995). Austin and Smith (1989) identified three types of variables, or gradients, affecting vegetation distribution. Indirect gradients, such as slope and aspect, influence the distribution of species through their effect on other variables, or are used as proxies for other, less easily measured variables. Interpretation of indirect variables may be complex and specific to a particular location. Direct gradients are those that influence plant distribution directly through known physiological mechanisms. Resource gradients are those that involve a resource that is directly consumed by the plant. Direct and resource gradients define the ecological niche of a species or the limits of a vegetation type. Alternatively, variables may be defined as more or less proximal or distal, depending on their proximity to known physiological mechanisms influencing plant establishment, survival and reproduction. By this definition, mean canopy temperature may be a more proximal variable than terrain-derived attributes such as slope or aspect or macroclimatic variables such as air temperature at screen height, while the meristem temperature of an individual plant may be more proximal still.

The distinctions between direct, indirect and resource gradients, and between proximal and distal variables, are not always straightforward. Pigott (1975) has shown that the Eastern limits of many European higher plant species follow the isotherms of mean temperature during the coldest month of the year, while the northern limits of many species run south-west to north-east, following isotherms of mean summer temperature. For species with a lowland distribution, the upper limits decrease with latitude. However, he argues that this does not imply a simple causal connection, since many climatic variables are correlated with one another, and plants are likely to respond physiologically to all variables, and to interactions between them.

A study of *Sedum rosea* and *Sedum telephium* grown together and separately at different altitudes showed that the upper altitudinal limit of *S. telephium* at 400 m could be explained as a physiological response of the species to climate (the growth rate of the species declines linearly with altitude). However, the lower limit of *S.rosea* at the same altitude cannot be explained as easily since it grows at the

same rate at lower altitudes when grown separately. The lower limit of *S. rosea* is probably due to a lack of competitive ability compared to lowland species (Woodward and Pigott, 1975).

Competition from other species is often invoked as an explanation for the limits to distribution of species when a physiological constraint cannot be identified. However, a similar study of growth rates of *Geum rivale* and *Geum urbanum*, the latter of which is restricted to lower altitudes and more southerly latitudes, showed no consistent differences in the growth rates of the two species at different altitudes (Graves and Taylor, 1986).

It is clear that a single climatic factor cannot explain the distributions of all species. It may however be possible to define general groups of species on the basis of factors that control their distribution. The British flora has been divided into geographical elements on the basis of their European (Matthews, 1955) and Northern Hemisphere (Preston and Hill, 1997) distribution; it might be considered that common processes limit groups of species with a common pattern of distribution. Field observations of life cycles show that low winter survival prevents the establishment of both the oceanic species *Digitalis purpurea* and the continental species *Eupatorium cannabinum* at high altitudes in Wales, while the continental species *Potentilla reptans* is limited by a combination of low seed germination, winter survival and seed production. However, similar observations of the life cycles of *Oxyria digyna* and *Saxifraga stellaris* do not explain their absence from the Welsh lowlands. Again, it has been suggested that this is due to their low competitive ability due to slow leaf area expansion (Woodward and Jones, 1984; Beerling, 1993).

Dahl (1997) suggests that species with an Atlantic distribution in Northern Europe are limited by winter frost and that Arctic and Alpine species are limited by competition from faster-growing species, drought and high summer temperatures. High temperatures may act to limit the distribution of some Arctic-Alpine species directly through overheating, as their growth form is adapted to retain heat (Gauslaa, 1984). In a few species the mechanism that controls distribution has

been convincingly identified. For example, *Tilia cordata* does not set seed at its northern limit in Britain unless the summer is exceptionally warm (Pigott and Huntley, 1978, 1980, 1981), while at the temperate-Mediterranean ecotone in Southern France it is restricted to North-facing slopes and valleys by low soil moisture (Pigott and Pigott, 1993). *Cirsium acaule* has been shown to be restricted by the failure of the development of the embryo in low summer temperatures and is limited to south-west facing slopes at the northern limit of its range in Britain in calcareous grasslands (Pigott, 1975).

2.2.2 Physiological mechanisms

The climatic control of plant distribution must operate through the physiological response of plants to their microclimate or to factors indirectly dependent on climate. The distribution of plants can be considered to be a response to environmental stress, where stress is defined as any factor that decreases plant growth and reproduction below the genotype's potential (Osmond *et al.*, 1987). However, understanding the physiological basis of plant distribution is complex because as Grace (1987) points out, there are hundreds of physiological and biochemical reactions which could be considered, all of which are likely to be sensitive to climatic variables but only a few of which may be critical in determining the long-term survival of a particular species at a particular site. Rare climatic events may be as important in controlling plant distributions as "average" climate. Furthermore, the limits to distribution may not be the absolute physiological limits that the species can tolerate, but may be affected by biotic processes such as competition or herbivory.

2.2.2.1 Temperature

Temperature may limit the distribution of plants in several ways. Extreme low temperatures can lead to irreversible injury to plant tissues or fatality through chilling or freezing injury; in addition, most biochemical reactions are temperature-sensitive and persistent low, but non-fatal, temperatures can slow the rate of

development. Woodward (1987) states that low temperatures limit plant distributions primarily through an effect on one particular limiting phase on the life cycle (for example failure of pollen germination below 16 - 18° C in *Tilia cordata* (Pigott and Huntley, 1981)). Since both the highest and lowest temperatures a plant is likely to experience occur near the soil surface, the mortality of juveniles usually determines the ecological impact of temperature extremes (Osmond *et al.*, 1987). As a general rule, absolute minimum temperatures in winter may limit plant distributions by killing foliage or the entire organism, while low average temperatures in summer may prevent a species from successfully completing its life cycle (Grace, 1987).

Woodward and Jones (1984) have modelled the effect of temperature on populations of both annual and perennial species by estimating the probability of survival of individuals at different stages of the life cycle at different temperatures. Temperature is considered to affect seed production, germination, establishment, growth and (in perennials) winter survival, post-winter establishment and survival to flowering. In models run on a range of species using data from field experiments at different altitudes, the effects of changes in the viability of different phases of the life cycle were often not obvious until after several annual cycles had been simulated (Woodward and Jones, 1984). As might be expected, annual species were found to be particularly sensitive to low growing season temperatures which did not allow them to complete their life-cycle, while perennial species are sensitive to winter temperatures as well as the length of the growing season (Woodward, 1988). The distribution of annual species is likely to be more closely correlated with recent extreme climatic events, while perennial species, which do not necessarily need favourable conditions for reproduction in every year, respond to longer-term climatic trends (Woodward, 1997). Plants restricted to warm-temperate climates or from lowland Britain were shown to suffer reduced yields or death when exposed to a regime of chill stress for a short period of the growing season under controlled conditions (Thorpe *et al.*, 1993).

The cell membranes are thought to be the primary sites of injury for both chilling injury (at temperatures above 0°C), and freezing injury (Jones, 1992; Woodward,

1987). Chilling injury is common in tropical or subtropical plants below around 10°C, and is thought to result from a phase change in the cell membranes from a fluid to a gel structure. Freezing injury occurs when ice starts to form within extracellular water; as ice has a lower vapour pressure than water at the same temperature, this leads to rapid dehydration of cells as water is drawn out to the site of freezing. The cell contracts, and its solute concentration increases (Jones, 1992); once ice has formed, cell death is thought to be inevitable. The exact temperature at which freezing injury occurs, however, varies as many temperate and boreal species are frost-resistant, and can maintain supercooled water in a liquid state at sub-zero temperatures.

Different parts of a plant may have different sensitivities to cold (Dahl, 1997), and the difference in temperature between the parts of a plant in the field, for example leaves and meristem, can be considerable (Grace, 1987). Furthermore, many species show an ability to acclimate to low temperatures through biochemical changes, and show seasonal differences in their resistance to cold (Alberdi and Corcuera, 1991). The age of a plant may also affect its vulnerability to low temperatures. In experiments in a controlled environment, *Verbena officinalis* showed full survival over winter if temperatures remained above -4°C, but full mortality of young plants if temperatures fell below –10 °C and full mortality of older plants if they fell below –17 °C (Woodward, 1997). Hunt and Neal (1993) consider that the response to low night temperatures is linked to nuclear DNA content; shorter cell-cycles in low DNA species may be expected to suffer proportionally more under low temperatures and so species growing in cold conditions are selected for high nuclear DNA content.

Heat injury may occur in plants in hot climates, or even at air temperatures as low as 20 °C for Arctic-Alpine species that are adapted to minimise heat loss. As with chilling injury, the exact temperature at which damage occurs varies between plants, although plants from cold climates do not necessarily have lower lethal temperatures than those from warmer climates. If plants are exposed to sub-lethal high temperatures, their lethal temperatures may be increased in a process known as "heat hardening". In many species, including *Picea abies,* the lethal

temperature varies on an annual cycle, probably determined by photoperiod (Gauslaa, 1984).

When temperatures are non-lethal, the effects of temperature on growth and development in the growing season are complex. The rates of both photosynthesis and respiration in leaves are temperature dependent. Photosynthesis does not occur below a certain temperature (although in some plants it may continue to freezing conditions). Above this cold limit, net CO_2 assimilation increases up to a temperature optimum, then decreases (Larcher, 1995). Körner and Diemer (1987) found that, for 12 pairs of plant species separated altitudinally in the Austrian Alps, the temperature optimum was similar, but that alpine species had higher assimilation rates at low temperatures and a lower cold limit. However, the rate of leaf extension of a plant has been found to be more sensitive to the temperature of the meristem than to leaf temperature (Grace, 1987). Dahl (1997) considers that this is because the production of adenosine triphosphate (ATP) through respiration, rather than photosynthesis, is usually the limiting factor in growth. In Mediterranean systems, during both low winter temperatures and summer drought, non-structural carbohydrates (NSC) reserves in several different species were never found to be exhausted, suggesting that structural growth (a carbon sink) was constrained under these conditions more than photosynthesis (a carbon source) (Körner, 2003). Körner presents data from several other climatic zones to show that tree growth in a range of climatic zones is rarely, if ever, limited by carbon. Criddle *et al.* (1996) consider that plant respiration responses to climate are the main determinant of geographic distribution on a global scale. The processes of cell division and extension within the meristem are also sensitive to low temperature, with the process of cell extension predominating in the short-term response, and cell division becoming important over a longer timescale (Pollock and Eagles, 1988).

The distinction between the effects on growth of meristem and leaf temperatures is significant because while leaf temperatures are primarily influenced by air temperature, fluctuations in radiation and wind speed may be more important in determining meristem temperature (Grace, 1988). The temperature of the

meristems of dwarf vegetation growing in the Cairngorms was found to be up to 7 °C higher than air temperature, and the difference between air and meristem temperatures was shown to be correlated with both windspeed and vegetation height (Grace *et al.*, 1989). The temperature of leaves of alpine plants has been found to be up to 22 °C above air temperature in full insolation, and 3.5 °C below air temperature in the shade, being primarily influenced by incoming radiation under clear skies and air temperature under overcast skies (Salisbury and Spomer, 1964).

C_3 plants growing under temperate conditions have been generally found to show a linear relationship of leaf extension rate with temperature that is not directly dependent on the rate of photosynthesis (Grace, 1987). At a certain temperature, the growth rate is effectively zero – this temperature varies between plants. Woodward *et al.* (1986) showed that, for five upland and five lowland species, leaf extension rates measured in the field were significantly correlated with temperature. While the lowland species had higher coefficients of temperature, and higher growth rates at high temperatures, all species had threshold temperatures below which no measurable leaf extension occurred. In laboratory experiments comparing the growth rates of the grasses *Holcus lanatus* and *Deschampsia flexuosa* under a simulated seasonal regime of autumn-winter-spring temperatures it was found that while *H. lanatus* had a significantly higher growth rate in the autumn and spring regime (day/night temperatures of 20°C/15°C), *D. flexuosa* had a higher growth rate in the winter regime (10°C/5°C) (Rorison, 1981). Since different species have different minimum threshold temperatures and different optimum temperatures for growth, changes in the seasonal temperature regime may reverse the competitive advantage of species.

For some species, including *Tilia cordata* (Pigott and Huntley, 1981) and *Cirsium acaule* (Pigott, 1970), the production of viable seed at low temperatures has been shown to be a limiting factor in their distribution. In the case of *T. cordata* it has been found that pollen requires temperatures above 16-18 °C for a significant proportion to germinate. In *C. acaule*, flower heads begin to develop in June as a

response to vernalization and exposure to a daily light period of over 15 hours. The rate of development of the flower heads increases with temperature, and around five weeks pass between the opening of the outer flowers to the detachment of the fruit from the capitulum. The stigma of each ring of flowers remains receptive for between 24 to 48 hours, and the weather during this period may affect the chance of pollination by insects. More significantly, however, the rate of development of the embryo after pollination was found to be dependent on the temperature of the flower heads; if the late summer is cold, then the embryos fail to develop fully. It has been shown that *Verbena officinalis* only flowers above a threshold temperature of 16 °C, and seed germination only occurs when mean temperatures are above 14 °C and daytime temperatures are above 19 °C (Woodward, 1997). These examples suggest that the temperature of the flowering parts of a plant at key times of the year may be an important factor in its ability to produce viable seed. Furthermore, once dormancy is lost, the rate of germination of seeds increases linearly with temperature to an optimum, then decreases linearly (Roberts, 1988). In both field observations at Lathkill Dale, Derbyshire, and germination tests in the laboratory, germination of both *Scabiosa columbaria* and *Centaurea nigra* seeds depended on a mean air temperature above 9 °C and 10 °C, even if minimum temperatures were much lower (Rorison, 1981; Rorison and Sutton, 1975). Conversely, germination of *Arrhenatherum elatius* occurred all year round in field experiments and at temperatures as low as 0 °C. However, climatic control of seed germination does not explain the distribution of these species at Lathkill Dale. Mean air temperatures are above 10 °C on both north- and south-facing slopes from May to September, yet *S. columbaria* and *A. elatius* are limited to the south-facing slopes, while *C. nigra* is limited to north-facing slopes (Rorison, 1981).

Thermal time (i.e. degree days above a threshold temperature) and mean temperatures have been shown to be a useful predictor of germination success in some grassland species (Arnold and Monteith, 1974; Trudgill *et al.*, 2000). However, temperature fluctuations are a requirement for germination in some species (Thompson and Grime, 1983). Complex responses to diurnal fluctuations in temperature have been proposed drawing on data from temperature gradient

plates (Murdoch *et al.*, 1989) and field studies (Hardegree and Vactor, 1999a, b). Williams (1983) found that the effects of temperature, light and pre-chilling interacted to produce germination response in grassland plants. In a study of four chalk grassland species van Tooren *et al.* (1988) found that fluctuating temperatures and exposure to different red/far-red light ratios had an effect on species germination rates, but this did not easily explain their distribution in terms of microhabitat.

Chalk grassland floras have been found to have wide variations in seed dormancy (Pons, 1991). Seed germination strategies may vary in order to avoid light competition (Olff *et al.*, 1994) or summer drought (Thompson, 1970) at the seedling stage. The regeneration niche (Grubb, 1977) may be an important factor in determining the distribution of plant species at a range of scales; Thompson *et al.* (1996) suggest that spatial and temporal variation in regeneration opportunities is an important structuring force in limestone grasslands. Temperature dependence of critical life cycle processes may be an important factor in determining the distribution of species, but identifying the critical life-cycle process is not straightforward.

2.2.2.3 Radiation

Incoming solar radiation is clearly the most significant input of energy to the earth's surface (Geiger *et al.*, 1995). The quantity of solar radiation that is received by a surface is therefore likely to affect plant distribution indirectly through its effect on the temperature of air, soil and the parts of plants themselves, through the eco-physiological mechanisms described above. However, the timing and quantity of certain wavelengths of radiation also affects plants directly. Short-wave radiation is a source of information for the photoperiodic responses of plants. Photoperiodism is a reaction to day-length that induces flowering; for example, "short-day" plants require a certain minimum number of days with a number of hours of darkness, while "long-day" plants require a minimum number of days with a number of hours of daylight. These responses can vary between ecotypes of a single species (Jones, 1992). Short-wave radiation between c. 400 and 700 nm wavelength is

also the energy source for photosynthesis (photosynthetically active radiation, PAR). Light deficiency in shaded sites may be a limitation on photosynthesis. Photosynthetic rates increase with increasing irradiance, up to a saturation level; this varies between species, and between both phenotypes and genotypes of the same species, as well as between leaves of the same plant grown in sun and shade conditions. A shade-grown leaf may be saturated at 5% full sunlight, while "sun leaves" may respond up to full sunlight (Jones, 1992). Radiation is clearly not independent of temperature, and the effects of each on photosynthesis are interconnected. The temperature optimum for photosynthesis for several alpine plants has been shown to correspond to the median air temperature for hours with saturating light conditions, rather than to mean air temperatures (Körner and Diemer, 1987).

Light intensity of different wavelengths has been shown experimentally to have an effect on the germination of seeds of a range of grassland and woodland species. Grime and Jarvis (1975) found that far-red radiation inhibited all of the species examined in their study, while in most species red, green or blue light promoted germination with red light being most efficient and blue light least efficient. Some species characteristic of bare ground (such as *Juncus effusus* and *J. articulatus*) required high intensity red light to germinate, while woodland and grassland species usually germinated at lower intensities; in all habitats, some species germinated most efficiently in shade and others in full light.

2.2.2.3 The Water Balance of soil and plants

Perring (1959) showed that the topographic gradients in vegetation on chalk grasslands in Cambridgeshire, North Dorset and the East Riding of Yorkshire were associated with soil moisture and other related edaphic factors. Slope and aspect may affect the water balance of a surface through their effects on precipitation, evapotranspiration and drainage. Furthermore, slope and aspect may influence factors such as soil depth and organic content, which control the water capacity of the soil. However, water and energy do not act independently on plants, as they cannot utilise water without sufficient energy in the form of radiation and heat, and

energy in the absence of water will only cause heat stress to the plant. When a plant is under water stress, its stomata begin to close, and reduce its capacity for gas exchange; if stomata are totally closed, gas exchange may completely cease (Larcher, 1995). For a plant, an environment where soil moisture is low because of a high evapotranspiration rate may be very different to an environment where soil moisture is low due to lack of precipitation and rapid drainage. Osmond *et al.* (1987) have suggested that water stress has its main influence during seedling establishment, since seedlings have shallower roots than adult plants. Summerfield (1975) showed that successful germination in *Narthecium ossifragum* was restricted to a narrow band of moisture, light and temperature conditions under experimental conditions. In a field experiment with wet and dry microsites, Oomes and Elberse (1976) showed that small scale variations in surface moisture can strongly influence seed germination rates in a calcareous grassland.

Stephenson (1990,1998) has argued that actual evapotranspiration (AET) and deficit (D) are biologically meaningful variables combining both the water and energy balances, applicable across a range of spatial scales. AET is defined as the evaporative water loss from a hypothetical "standard crop" given the prevailing water availability; D is the difference between AET and potential evapotranspiration (PET), the evaporative water loss under excess available water. To accurately calculate water balances, reliable information on the energy balance, humidity and wind speed are necessary. Alternative variables that might approximate a biologically meaningful measure of the interaction between the energy and water balances include the integrated solar radiation over the period when soil moisture is adequate for a standard crop to maintain open stomata, or integrated solar radiation over the period when soil moisture is too low to maintain open stomata (Stephenson, 1998).

Measurements of the relative water content (RWC) of leaves of plant species in a limestone dale at Buxton, Derbyshire during the extreme drought of summer 1995 found that low RWC, which was taken to indicate drought stress, was only present in plants in shallow soils on the slopes and rock outcrops (Buckland *et al.*, 1997). Even at these sites a few species with taproots were able to maintain relatively

high RWC values. For a number of species with distributions that were concentrated on the deeper soils, it was found that a declining frequency of occurrence was correlated with falling RWC values. It was concluded that this relationship existed because outlying populations on shallower soils were suffering from extreme moisture stress, and that the drought was acting as a "resetting" mechanism, restricting the expansion of drought-sensitive species onto shallower soils. The effects of the 1976 drought on species abundance in a Sussex chalk grassland were recorded by Hopkins (1978). The area of bare ground increased dramatically and several species decreased considerably in abundance. Water stress may therefore have a major impact on plant distribution in these environments through occasional drought events killing sensitive species even if sufficient water is available in most years. For those species without taproots, even those associated with shallow soils showed a negative relationship between abundance and leaf RWC, implying that shallow soils are not optimal for these species, but that they provide a refuge from competition. Seeds of the tap-rooted species *Scabiosa columbaria* sown on plots on horizontal, north- and south-facing slopes at Lathkill Dale, Derbyshire established and showed good early survival rates on all three sites. However, after three years, only those on the south-facing slope remained; the other plots had been invaded by more vigorous vegetation. The shallow-soiled south-facing slopes were more likely to be water stressed, and so may provide a refuge against competitors (Rorison and Sutton, 1975).

In Erschbamer *et al*'s. (1983) study of the distribution of dry grassland species in the central Alps, it was found that the correlation of grass species with soil depth depended on the ability of their roots to penetrate water in deep rock crevices. The distribution of dwarf shrubs was not explained by soil moisture, however, despite some species apparently having strong stomatal control and others having little or no control.

2.2.2.4 Wind

The word "exposure" has been widely used by ecologists to describe the stresses that plants experience in windy conditions, and relates to a number of different

mechanisms. Wind increases the coupling of the vegetation to the atmosphere, and limits the extent to which leaf and stem temperatures can exceed that of the atmosphere. Generally, tall vegetation and small leaved plants are more closely coupled to the atmosphere (Grace, 1981). Wind decreases the boundary layer resistance of the air around leaves, and so usually increases evaporation rates, although if air temperatures are cooler than leaf temperatures, its cooling effect may decrease evaporation.

Plants exposed to high winds may suffer from impaired water status due to high evaporation rates, but Grace (1981) considers that the direct effect of wind on both transpiration rates and CO_2 exchange is usually small and may be positive or negative. Exposed plants may suffer greater extremes of temperature than those in sheltered situations, and decreased leaf temperature due to wind may be an important factor in determining the distribution of alpine plants (Jones, 1992). Mechanical damage due to wind pressure may cause stunting and deformation, or even uprooting or buckling of plant stems; shaking or structural damage to plants may impair their ability to control their transpiration rates (Grace, 1981).

2.2.2.5 Indirect effects of microclimate – biotic interactions

The potential effects of competition in restricting the range of species which are individually physiologically capable of surviving beyond their geographical limits has been described above, particularly with reference to slow-growing upland and Arctic-alpine plants (Woodward and Pigott, 1975; Woodward and Jones, 1984; Dahl, 1997; Sætersdal *et al.*, 1998;). The lowland annual ruderal *Lactuca serriola* has been shown to regenerate from self-sown seed and survive for several generations when introduced beyond its natural geographical distribution. It has been suggested that the distribution must be related to the secondary effects of climate on populations and metapopulations (Prince and Carter, 1985). Other biotic factors may also be responsible for the distribution of plants in the landscape. For example, in an experiment designed to explain the distribution of *Medicago lupulina* along a topographic gradient, it was found that rates of invertebrate

herbivory on seedlings were significantly higher in damper microsites (Hogenbirk and Reader, 1989).

2.2.2.6 Indirect effects of microclimate – soil processes

The physical and chemical development of soils on calcareous substrates in Britain has been shown to be correlated with topography and climate, particularly rainfall and angle of slope (Balme, 1953; Perring, 1960; Grime, 1963; Trudgill, 1976). Rendzinas form on chalk and limestone where a shallow organic A horizon lies directly above the bedrock C horizon. Water percolating through the soil profile picks up organic acids from the A horizon, and removes calcium and carbonates from the soil. As soil development progresses, calcareous brown earths with a defined B horizon may develop and soil pH decreases (Trudgill, 1976). Increasing soil depth, decreasing pH and leaching may eventually lead to the formation of chalk heath vegetation, with a characteristic mixture of calcicoles and calcifuges, developing. In extremely wet areas, such as the Burren in Ireland, peat deposits or limestone rankers may form directly over limestone bedrock (Trudgill, 1976).

Topography has an effect on soil independent of microclimate as steeper slopes encourage mass movement of soil downslope and retard soil development, while valley bottoms accumulate deep deposits – soils on slopes are therefore typically less developed unstable rendzinas with higher pH and calcium carbonate content than soils on hilltops or in valleys (Balme, 1953). Perring (1960) showed that the pH and $CaCO_3$ content of chalk soils increased significantly at slope angles of over 15 to 20°, more or less independently of aspect, and decreased with increasing rainfall. This angle of slope coincides with that at which grazing-step terraces form in temperate grasslands (Howard and Higgins, 1987), suggesting that mass movement of soils becomes significant at these slope angles. Thomas (1963) reports that a footpath (and presumably surface soil) moved down slope at a rate of 1 m in six years on a Sussex chalk grassland, although the angle of slope is not specified. On chalk and limestone under damp climates, for example on the Yorkshire Wolds and Derbyshire Dales, calcareous brown earths form on shallow

slopes but on steeper slopes soil formation is restricted to shallow rendzinas by mass movement down the slope (Balme, 1953; Furness *et al.*, 1981; Ellis and Newsome, 1991). However, this climatic pattern may be exaggerated by the effect of drift materials incorporated in plateau soils; Grime (1963) considered that in the absence of drift material, rendzinas develop into limestone rankers.

Biological processes within the soil, particularly organic matter decomposition and soil nitrogen mineralisation, are likely to be influenced by microclimate. Decomposition rates of leaf litter are influenced by temperature and moisture (Witkamp, 1966). Nitrogen mineralisation has been shown to be sensitive to temperature regime in many systems; in calcareous grasslands, however, it has been suggested that low water availability or low availability of organic substrate during summer may be a limiting factor in nitrogen cycling (Jamieson *et al.*, 1998; Jamieson *et al.*, 1999; Uncovich *et al.*, 1998). Time course studies of N mineralisation in calcareous soils have shown peaks in mineralisation during spring (Davy, 1974; Jamieson *et al.*, 1999).

Calcareous soils are typically very low in available phosphates, as phosphorus is bound up in non-exchangeable forms at high pH. Low phosphorus solubility has been implicated as a factor restricting "calcifuge" species from calcareous grassland (Tyler, 1994), although inability to solubilise iron appears to be the limiting factor in some species (Tyler, 1996). Different calcareous grasslands have been shown to be either phosphorus or nitrogen limited (Uncovich *et al.*, 1998; Köhler *et al.*, 2001); however Janssens (1998) suggests that phosphorus availability may limit microbial nitrogen mineralisation in calcareous soils, and therefore that a single limiting factor theory is inappropriate. Furthermore, variations in soil moisture have been shown to influence the concentration of mineral nutrients in calcareous soil solutions (Misra and Tyler, 1999), and *Arrhenatherum elatius* has been shown to be increasingly vulnerable to drought when deficient in N and P when grown in calcareous soils (Grime and Curtis, 1976). The feedbacks between soil moisture, soil pH, nitrogen and phosphorus availability in calcareous soils are therefore potentially complex. Fine-scale patchiness of nutrients in chalk grassland has been correlated with the distribution

of species using pattern analysis (Hall, 1971); soil heterogeneity at a fine scale may be an important factor in determining vegetation composition at larger scales.

Summary of plant responses to microclimate

Low temperatures can damage plants, and while the lowest temperatures are likely to occur in winter, less severe frosts in spring or autumn when plants are not acclimated and new growth is exposed may be equally important. Heat sum above a threshold during the growing season is likely to be an important control on annual growth, but the temperature of the reproductive parts of a plant at critical times of the year may also be important in many species. Solar radiation may directly affect the timing of the life cycle of the plant through photoperiodic responses, and integrated levels of irradiance in the photosynthetic wavelengths are also likely to be an important control on growth. This energy can only be utilised if sufficient water is available to maintain open stomata, so the rate of evapotranspiration and water deficit may be useful indicators of plant response. Exposure to wind can lower the temperature of parts of a plant and increase evaporation, causing water stress. All of these microclimatic variables are likely to vary with slope and aspect. Furthermore, these responses to microclimate may not act directly by pushing the species to its physiological limits of survival, but may act indirectly by stressing the plants and therefore changing the relative competitive advantage between species, or putting species at risk from herbivory or pathogens. Microclimate is also likely to influence soil processes that are critical to plant survival; topography also has an effect on soil development that is more-or-less independent of microclimate.

The examples given above show that plants respond physiologically to a number of different but not independent climatic variables. Studies of vegetation-climate relationships often use indirect gradients and distal variables to predict distributions. They may not have an explicit ecological model of the ways in which climate affects plant survival and reproduction. This can make interpretation of the physiological processes involved difficult. Applying the results of such studies to different geographical areas or to future climates can therefore be problematic.

2.2.3 Microclimate and topography in grasslands

2.2.3.1 Radiation

On a sunny summer day at mid-latitudes, a 20° slope facing south receives around twice the radiation of a flat surface (Geiger *et al.*, 1995). On a south-facing slope in Lathkill Dale, Derbyshire, direct radiation is effectively doubled in winter, when the solar elevation is least; while on north-facing slopes it is eliminated entirely (Rorison *et al.*, 1986b). However, Olyphant (1986) found that in mountainous terrain the effects of diffuse radiation dampened the differences in direct radiation between sites of different slope and aspect. Oliver (1991) found that north-facing slopes received consistently low net radiation in winter, with little variation between days, due to the lack of direct radiation, while south-facing slopes had lower mean values than summer, but considerable variation between sunny and cloudy days. In summer, although mean north-facing values were lower than south-facing slopes, there was considerable variation on both slopes. In Lathkill Dale, the lowest relative values for diffuse radiation came at the equinoxes, with peaks in both winter and summer, probably due to cloudiness in winter and atmospheric conditions in summer (Rorison *et al.*, 1986b). Differences in net radiation between south and north-facing slopes have been found to be greater in winter in the Arctic (Young *et al.*, 1997) and at 43° latitude in New Zealand uplands (Radcliffe and Lefever, 1981), but greater in summer in Britain (Oliver, 1991), probably due to the effect of cloud cover.

2.2.3.2 Temperature and the energy balance

Slope and aspect would be expected to affect the temperatures of soil and plant parts primarily through their effects on radiation. The energy balance of the soil surface is driven by incident short and long wave radiation from the sun, atmosphere and surroundings. Radiation losses are due to reflected short wave radiation, and long-wave heat loss. Energy is also exchanged through conductive

heat exchange between the surface and deeper layers of soil, convective heat loss between the surface and the air and latent heat loss from evaporation (Monteith, 1981). Rorison and Sutton (1975) found that, at Lathkill Dale in Derbyshire, 1 cm soil temperatures tended to follow the diurnal solar radiation pattern with greater daily fluctuations on south-facing than north-facing slopes. Maximum daily temperature was strongly correlated with net radiation, but minimum and mean daily temperatures were only weakly correlated.

Over a period of several years of measurement at Lathkill Dale, Rorison, Sutton and Hunt (1986b) found considerable variation (around 8 °C) between annual mean temperatures of both soil (at 20 mm depth) and air (at 20 mm above ground) temperatures. Soil temperatures were generally lower than air temperatures, and north-facing slopes were generally colder than south-facing slopes. The difference in mean temperatures between slopes was 2.4 °C for soil temperatures and 2.9 °C for air temperatures. However, this mean figure hides much larger diurnal variations – while the differences between slopes were mainly less than 2 °C at night, they reached 11 °C in air and 7 °C in soil during the day. Påhlsson (1974) found a similar pattern of soil and air temperature on slopes of a sandy hill in southern Sweden.

During the winter, Oliver (1991) found soil temperatures on south-facing slopes on the Chilterns to be radiation-driven, following the diurnal cycles, while north-facing slopes varied with longer term temperature changes, with a net heat flux out of the soil through the winter months. In the summer, both slopes were radiation-driven with a net heat flux into the soil, although the heat flux into the north slope was only one third of that into the south-facing slope. He also found that, while on south facing slopes, annual cumulative temperatures at 5 mm depth were higher than north-facing slopes, at 300 mm depth this was reversed and cumulative temperatures on north-facing slopes were higher. Radcliffe and Lefever (1981) found that both mean annual soil temperatures and air temperatures were higher on (southern hemisphere) north-facing slopes than south-facing slopes. On the north aspect, soil temperatures under short grass were found to vary much more

than those under tussock, while on the ridge topsoil temperatures were consistently lower than those under tussocks. This may be because long grass provides air pockets that insulate the soil surface from extremes due to radiative warming and heat loss.

2.2.3.3 Soil moisture and the water balance

The main supply of water to plants is through soil moisture absorbed by the root system. Soil moisture is dependent on precipitation, throughflow, soil characteristics and evapotranspiration rate. All of these variables may be affected to some extent by the slope and/or aspect of a surface. Rorison and Sutton (1975) found that soils on the north slope of Lathkill Dale were deeper and had more organic matter (and therefore greater water-holding capacity) than soils on south-facing slopes. They observed that in summer, the shallow soils of the south-facing slope dried out much more quickly, and so surface soil temperatures fluctuated widely and plants were put under water stress.

The input of energy from solar radiation, temperature, and the humidity of the atmosphere determine the potential evapotranspiration rate (PET) of a surface. The actual evapotranspiration rate (AET) is less than the PET if there is not excess water available. In alpine tundra in Colorado, it was found that AET was controlled by energy availability immediately after precipitation events, and subsequently by soil moisture availability (Isard and Belding, 1989).

Radcliffe and Lefever (1981) calculated PET in New Zealand pastures using net solar radiation and Stevenson screen air temperatures, assuming soil heat flux to be negligible. Calculated values for PET on the north (equivalent to south in the Northern Hemisphere) aspect of a ridge were double those for the south aspect. The north-facing slopes were consistently drier than the south-facing slopes through the growing season, with intermediate moisture content on the top of the ridge.

2.2.4 Topography, soils and vegetation in calcareous grasslands

Several studies have examined the effects of slope and aspect on the ecology and biogeography of calcareous grasslands or other short vegetation. Some studies have concentrated on the distribution of a single species in the landscape, taking data from a representative sample of slopes and aspects; others have taken a more holistic approach and compared vegetation, soils and/or microclimate on contrasting slopes. Perring (1958; 1959; 1960) compared topographic gradients in both vegetation and soils across chalk grassland sites with a range of macroclimates in England, France and Germany.

In a classic study, Pigott (1970) demonstrated that *Cirsium acaule* is limited to south- and south-west facing slopes towards the north of its range, and identified the failure of the development of the embryo under low summer temperatures as a proximal cause. In calcareous grasslands, similar distributions have been noted for *Hippocrepis comosa* (Fearn, 1973), *Helianthemum* species (Lakhani and Davis, 1982; Proctor, 1958) and *Thymus* species (Pigott, 1955), among others. Watson (1960) identified several bryophyte species with predominantly north- or south-facing distributions in chalk grassland. In some, but not all, of these examples the distributions are centred on southwestern, rather than southern aspects. Lakhani and Davis (1982) quantified this effect for *Helianthemum nummularium.* Using multiple regression techniques they found an optimal aspect of between 188° and 205°. This phenomenon has been explained as due to the highest temperatures occurring in the afternoon (Geiger *et al.*, 1995). Using ordination techniques, Dargie (1987) found that semi-arid vegetation in SE Spain follows an optimal axis of 199° at four sites and 187° at another. However, this tendency is not apparent in all studies (for example Hutchings (1983) found the south-facing aspect in a chalk grassland to be similar in vegetation and diversity to the east-facing aspect, and west to be more similar to north), and the angle of rotation may be species and/or site-specific if it depends on interactions between macroclimate, topography and the physiology of the species involved.

Studies of microclimate in grassland or other low vegetation on contrasting slopes have found dramatic differences in both temperatures at or below the surface and in evapotranspiration and soil moisture. These differences can often be associated with differences in the soil and vegetation of the slopes. Growth experiments on *Arrhenatherum elatius* and *Centaurea nigra* in pots on Lathkill Dale slopes showed that, while growth rates in watered pots increased with temperature sum, soil moisture stresses were of overriding importance in production and nutrient uptake (Rorison *et al.*, 1986a). Påhlsson (1974) examined microclimate, vegetation and soils on contrasting north- and south-facing slopes on a sandy hill in Sweden, and considered soil moisture, and its effects on soil structure and chemistry, to be a determining factor. Radcliffe and Lefever (1981) found considerable variation in radiation, temperature and soil moisture between north- and south-facing slopes in a New Zealand pasture. Hutchings (1983) found differences in diversity and its components between slopes in chalk grassland. Most of these studies stress the importance of soil moisture and linked soil properties as a driving force behind soil and vegetation patterns.

2.2.5 Integrating macro- and micro-scale distributions

Boyko (1947) observed that the distribution of many plants with respect to slope and aspect in Palestine mirrored their geographical distribution at larger scales. Saharan species, for example, were absent from cooler, damper north-facing slopes, where Mediterranean and Eurasian species were more common. He suggested that the climatic factors that controlled plant "macro-distribution" were the same as those that controlled "micro-distribution" (the "geo-ecological law of distribution"). Körner (1999) observed that, while large-scale altitudinal and latitudinal gradients in climate have been well studied and used as proxies for future climate change, topographic gradients in microclimate had often been neglected.

Quantifying the relationship between micro- and macro-scale distributions requires a theoretical model of the interaction between macro- and micro-climate, and also

a model of the way in which microclimate affects plant distribution. Perring (1958) proposed an approach to studying the relationship between vegetation, macroclimate and topography based on the approach of Jenny (1941) to soil development, in which the vegetation-soil complex is a function of climate, the parent material of the soil, topography, biotic factors and time, represented by:

$$v = f(cl, p, r, o, t) \qquad \textbf{Equation 2.1}$$

where v = some property of the vegetation, cl is climate, p is parent material, r is topography, o is the biotic factor and t is time.
By comparing sites where one of these variables differs, but the others are similar, the effect of individual variables can be studied.

This approach formed the basis for an extensive study of chalk grassland sites in which areas with different macroclimates (Northern France (Rouen), North Dorset, Yorkshire Wolds, East Anglia, Kent), with similar chalk geology, were surveyed systematically with a representative sample of sites with different slopes, aspects, grazing and disturbance regimes.

2.2.6 Soil and vegetation "toposequences"

According to Perring, the most important independent variable influencing both vegetation and soil characteristics is humidity. Soil and vegetation sequences were considered to follow a gradient of increasing humidity in the order Rouen > Cambridge > Dorset > Yorkshire. Wetter soil conditions were shown to be associated with lower total carbonates, higher organic matter and lower pH values in the surface soil. These associations were represented on an idealised hill diagram, a polar ordination with an angular axis representing aspect and a radial axis representing slope, which can be considered as an overhead view of an idealised hemispherical hill. Plotting individual diagrams for different subsets of the data allows a visualisation of the effects of climate and topography. Fig 2.1 shows the distributions of five species representative of groups of species with similar topographic distributions; the interaction of topography and climate can be clearly

seen here as species with widespread distributions in the regions with drier macroclimates are restricted to south-facing aspects in wetter regions.

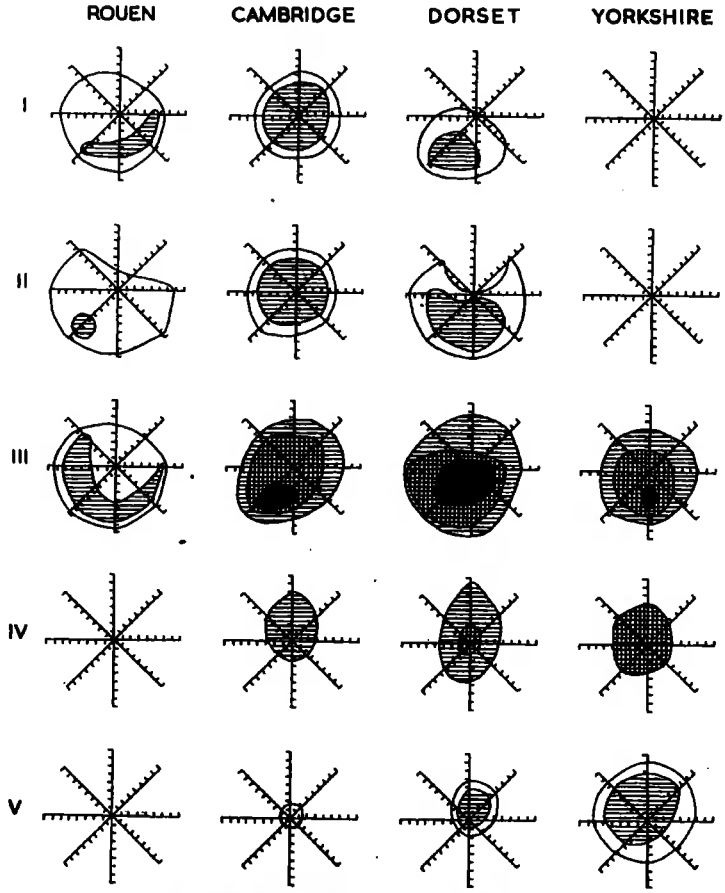

Fig. 13. Distribution of species in Groups I–V – Series I.
I = Hippocrepis comosa
II = Asperula cynanchica
III = Poterium sanguisorba
IV = Plantago lanceolata
V = Holcus lanatus

Key

Groups I–II	White	– All sites at which species recorded
	Single hatching	– All sites with cover over 5%
Groups III–V	White	– All sites at which species recorded
	Single hatching	– All sites with cover over 10%
	Cross hatching	– All sites with cover over 20%
	Black	– All sites with cover over 25%

Figure 2.1: Distributions of selected species with reference to region, slope and aspect, from Perring (1959). Note: *Poterium sanguisorba = Sanguisorba minor.*

Perring's analysis of this dataset was largely based on interpretation of this form of diagram, constructed from data in a punched-card filing system. Modern statistical techniques and the use of computers has greatly increased the potential of large datasets such as this. Austin (*pers. comm.*) has used a subset of this data set (the

North Dorset sites) to carry out a multivariate classification and general additive model (GAM) of selected species.

F. H. Perring has kindly made the original data available for this study, and M. P. Austin has given advice on expanding his GAM approach to the larger data set.

2.3 Further analysis of Perring's data

2.3.1 The data set

The data used in this analysis consist of Perring's original data from 263 sites of chalk grassland from four broad areas; North Dorset (including nearby sites in Hampshire and Wiltshire), the East Riding of Yorkshire, Cambridgeshire (including sites in Bedfordshire and Hertfordshire), and Kent. Full sampling methodology is given in Perring (1959). Sampling took place during the flowering seasons of 1952 to 1954. Each site comprised of an area of approximately 50 m^2 with uniform slope and aspect, each with twenty 10 cm $\times$ 10 cm quadrats thrown randomly within it; cover of all vascular plants and bryophytes was recorded in each quadrat. In this analysis, frequency scores for each species are calculated from the proportion of quadrats at a site in which the species occurs. Data were originally recorded on punched-hole cards, and were entered into electronic form for analysis. Environmental data were recorded for most sites; variables used in these analyses are slope, aspect (recorded to nearest 8-point compass bearing), mean vegetation height, soil depth, pH, organic matter content and total carbonates. An index of estimated grazing intensity was also recorded on the cards. Three derived topographic variables were also used in these analyses, based on the radiation index described by Oke (1987):

$$Ri = cos\beta cosZ + sin\beta sinZcos(\Omega - \Omega_s) \qquad \textbf{Equation 2.2}$$

Where β is the angle of slope, Z is the solar zenith (angle of the sun from vertical), Ω is the solar azimuth (angle of the sun from due north), Ω_s is the aspect of the slope, and Ri is a radiation index estimating the proportion of potential direct irradiance intercepted by the slope for a given solar zenith and azimuth. Three

values of Ri were calculated with different values of Z and Ω corresponding to different times of day and year. $Ri(1)$ represents solar radiation at noon at the summer solstice, $Ri(2)$ at noon at the winter solstice, and $Ri(3)$ at 1500h in mid-August. The latter was chosen to estimate maximum summer temperatures, and to allow for the south-west centred distributions observed for many species.

Three regional climatic variables were also included, in order to rank the areas. These were derived from the nearest available data from Met Office stations in the region of the sites, and means were taken from the ten years prior to the first survey, i.e. the period 1942 to 1952. These variables were mean annual rainfall, mean summer (June-August) rainfall, and mean maximum July temperature.

2.3.2 Methods of analysis

2.3.2.1 Detrended correspondence analysis

Multivariate ordination techniques facilitate the visualisation of the main axes of variation in large datasets of vegetation data. Detrended Correspondence Analysis (DCA) (Hill and Gauch, 1980) was used in preference to a linear model such as Principal Components Analysis (PCA) to avoid problems associated with species turnover along the gradient; and in preference to Correspondence analysis to avoid the "arch effect" (Kent and Coker, 1994). An indirect ordination of the data, with environmental data subsequently correlated with the axes was used rather than a direct ordination such as Canonical Correspondence Analysis (CCA) in which the ordination is constrained by the choice of environmental variables at this stage. The ordination was therefore not constrained by the choice of environmental variables or the nature of the relationship between environmental variables and ordination axes (e.g. linear, logarithmic etc.). Ordination was carried out using the DECORANA FORTRAN program (Hill, 1979) using default options for DCA.

2.3.2.2 Ellenberg and CSR scores

Ellenberg indicator scores and CSR scores were calculated for each plot using MAVIS plot analyser software (Stuart, 2000). Plot scores represent weighted mean species scores, from the Ellenberg indicator dataset extended to Great

Britain (Hill *et al.*, 1999) and CSR scores for British species from Grime (1974; Grime, 1988). The Ellenberg indices are L (light), M (moisture), R (reaction) and N (nitrogen); the latter is probably best interpreted as a "productivity" indicator rather than a measure of nitrogen availability to plants (Hill and Carey, 1997; Schaffers and Sýkora, 2000). Grime's CSR scores represent the proportion to which a species is attributable to each of three strategies S (stress tolerators), R (ruderals) or C (competitors). A high S score for a plot would indicate resource shortages that limit photosynthetic production such as drought, shade, or nutrient limitation; a high R score would indicate disturbance associated with destruction of biomass; and a high C score indicates the absence of these constraints on the accumulation of plant biomass. Plot scores were plotted on a triangular ordination. For descriptive purposes, sample plots were matched to NVC community (Rodwell, 1992) using MAVIS Plot analyser (Stuart, 2000).

2.3.2.3 Generalised Additive Models

Generalised Additive Models (GAMs), a non-parametric extension of General Linear Models (GLMs) (Hastie and Tibshirani, 1990) have been used as an exploratory tool in the analysis of species with climate (Yee and Mitchell, 1991). With a logistic link function they can be used to form a model of species presence/absence or frequency as the sum of smooth functions of one or more variables. These functions are estimated from the data using techniques for smoothing scatterplots. As they are data-driven, the smoothed values do not come from an *a priori* model and allow the structure of the data to be examined. Since the structure of the model is additive, if interaction terms are not used, the contribution of individual variables to the fitted model can be examined separately. This technique is roughly analogous to Perring's approach of examining the effect of one variable independently of others.

Austin (*pers. comm.*) has used GAMs to model the effect of topographic and soil variables on presence/absence of several species using Perring's North Dorset data, and has presented the results for *Hippocrepis comosa*, showing the effects of topographic variables and exchangeable calcium. In the present study, I carried

out GAMs for the first two DCA axes, and for the five representative species in figure 2.1, using the larger dataset of British data, to explore the effects of soils, topography and regional climate on distributions. The analysis was carried out using the GAM procedure in S-PLUS v6.0 (Insightful Corp., Seattle) with frequency data (expressed as a fraction between 0 and 1) using a logistic regression with a logit link function. A forward stepwise procedure was used to create the models. At each step, explanatory variables were added firstly with a linear response function, then with a cubic smoothing spline. The change in residual deviance and degrees of freedom were examined using χ^2-tests, and terms were included if they significantly reduced the residual deviance of the model at $p < 0.05$. To simplify the final model, smooth functions were replaced by linear functions if this was possible without a significant increase in deviance.

2.3.3 Results

2.3.3.2 DCA ordination

The first four axes of the DCA ordination have eigenvalues of 0.368, 0.260, 0.170 and 0.125 respectively. The first two axes only are considered here. Fig 2.2 shows the distribution of sites with respect to the first two axes. Although plots from the same region show some signs of clustering together, there is considerable overlap along both axes. The centroids (mean sample scores) of the five species illustrated in figure 2.1 are plotted on the same diagram; they are clustered around the centre of the plot but arranged along axis 1 in order of their affinity to south-facing slopes.

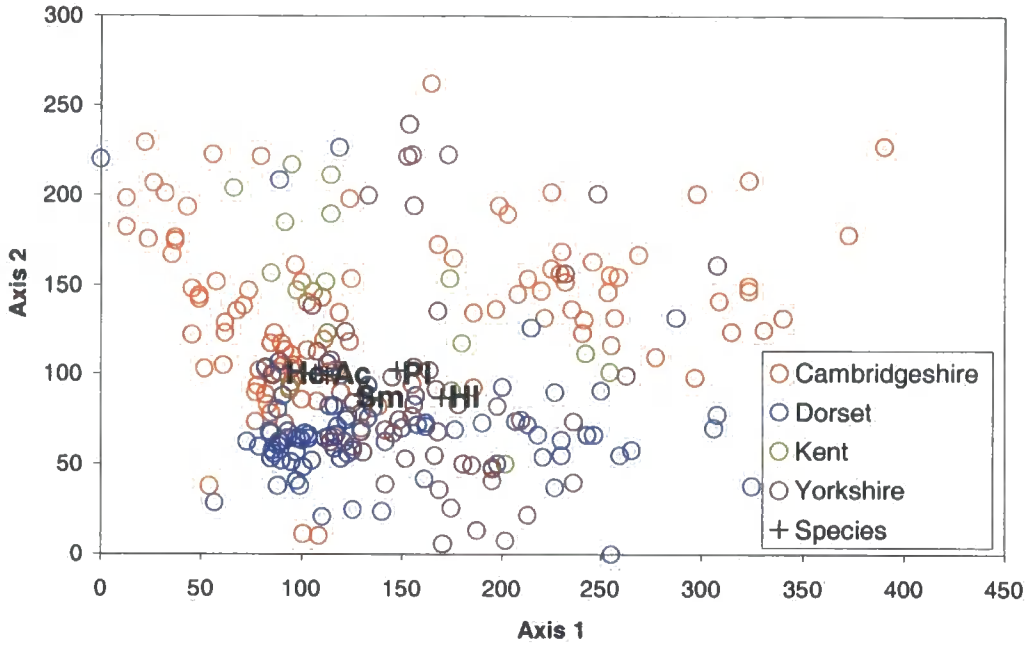

Figure 2.2: Ordination of first two DCA axes showing plots coded by region. Centroids of selected species: Hc *Hippocrepis comosa*, Ac *Asperula cynanchica*, Sm *Sanguisorba minor*, Pl *Plantago lanceolata*, Hl *Holcus lanatus*.

The magnitude of CSR and Ellenberg indices for each plot are shown on the same diagram in figures 2.3 and 2.4. The cluster of plots in the bottom left of the diagram have high S indices; high C indices are concentrated towards the top of the diagram and high R indices are concentrated towards the left. High Ellenberg light indices are towards the bottom right, and moisture and fertility increases along axis 1 while pH decreases.

Triangular ordination of the CSR indices for each plot (figure 2.5) show a striking pattern with virtually all plots arranged along a gradient from the middle of the plot (representing CSR strategies) to the bottom left (representing S strategies).

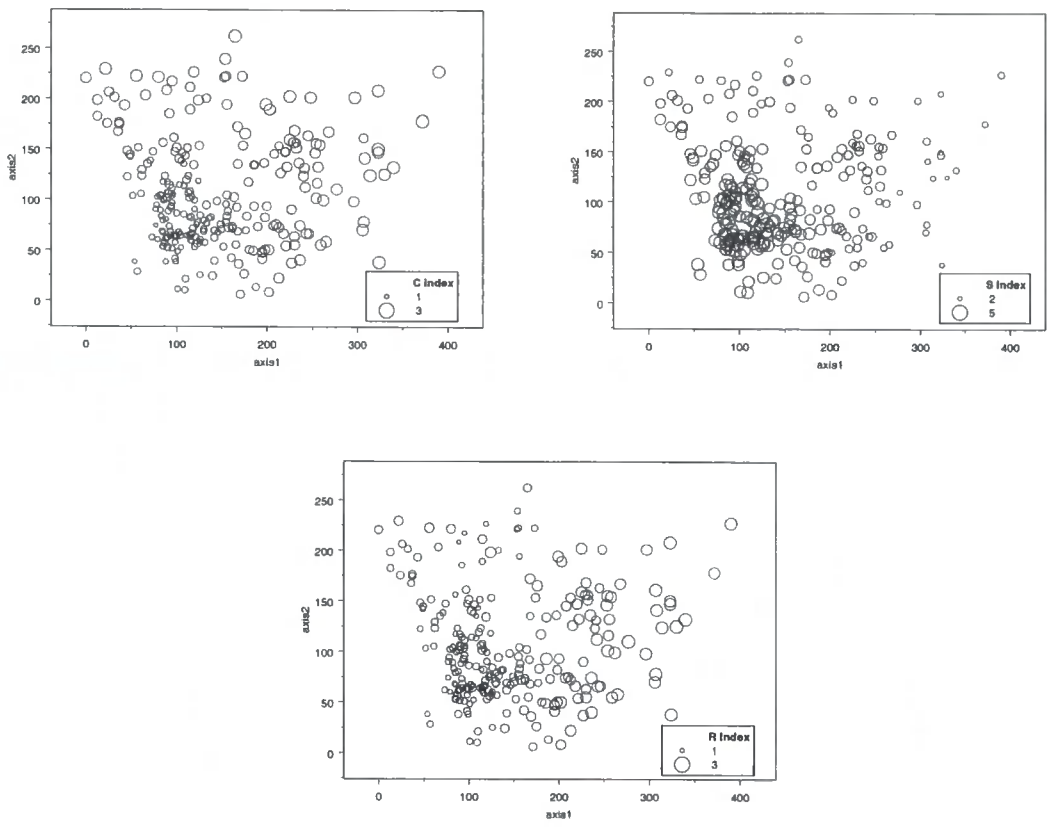

Figure 2.3: Ordination of first two DCA axes; symbol size scaled to Grimes CSR indices for each plot: (a) C (competitors) (b) S (stress tolerators) (c) r (ruderals)

Table 2.1 shows Spearman's Rank correlation coefficients between the first two axes, plot indices and environmental variables (adjusted for multiple comparisons using the Bonferroni correction). Axis 1 is strongly correlated M, R and N Ellenberg values and all three CSR indices. Low values along this axis are associated with conditions of low moisture, high pH and low fertility, and stress tolerator strategies. It may be interpreted as a gradient from relatively stressed conditions with a sunny, dry microclimate and shallow unleached soils and low nutrient status, to shaded, moist conditions with deeper, leached soils and higher nutrient availability. Axis 1 is also significantly correlated with all three radiation indices, consistent with the interpretation that it is a microclimatic gradient. The correlations with P, K and total carbonates are also consistent with the interpretation that this axis represents a gradient from rendzina soils with high chalk content to more fertile calcareous brown earths.

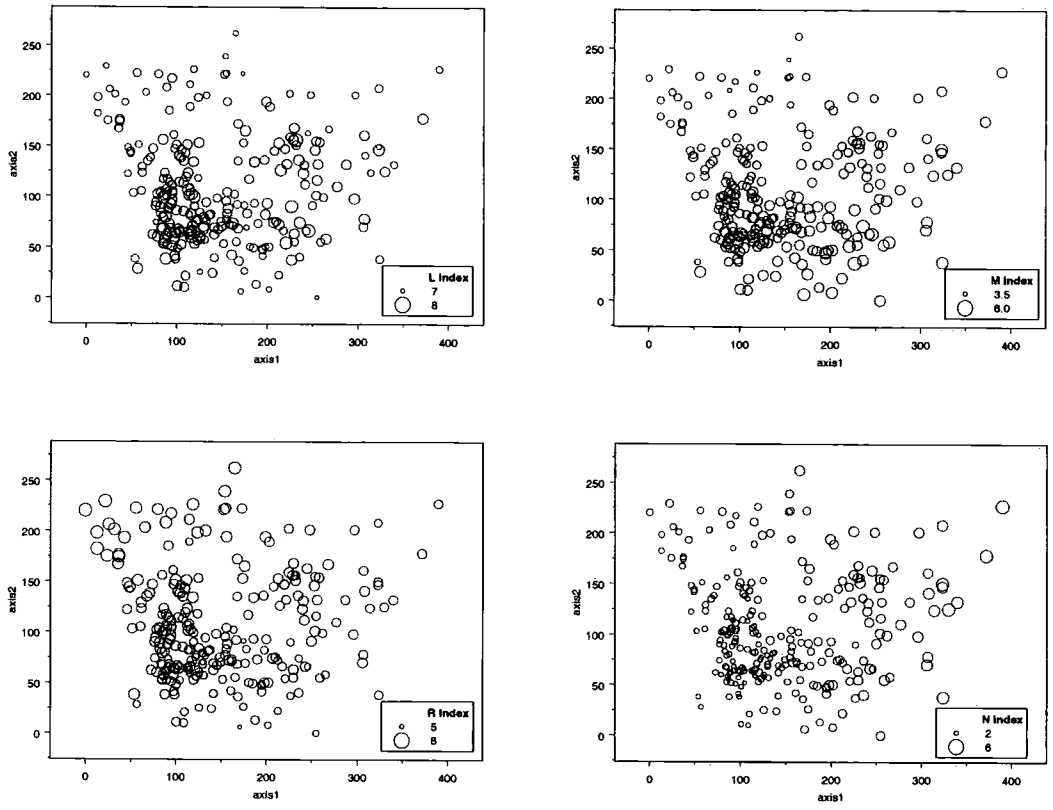

Figure 2.4: Ordination of first two DCA axes; symbol size scaled to Ellenberg indices for each plot: (a) L (light) (b) M (moisture) (c) R (reaction) (d) N (fertility)

Axis 2 is correlated with all four Ellenberg values, C and S indices, as well as with vegetation height, grazing index and presence/absence of rabbits, macroclimatic variables and organic matter, soil pH and total carbonates. It is suggested that this axis primarily represents a gradient in grazing pressure, from relatively diverse, short swards with low nutrient status to less diverse ungrazed swards dominated by rank grasses. However the further correlations of this axis may be an artefact due to the fact that many of the Cambridgeshire and Kent grasslands, which have higher pH values, low rainfall and higher July temperatures than the other plots, were not grazed at the time of this survey.

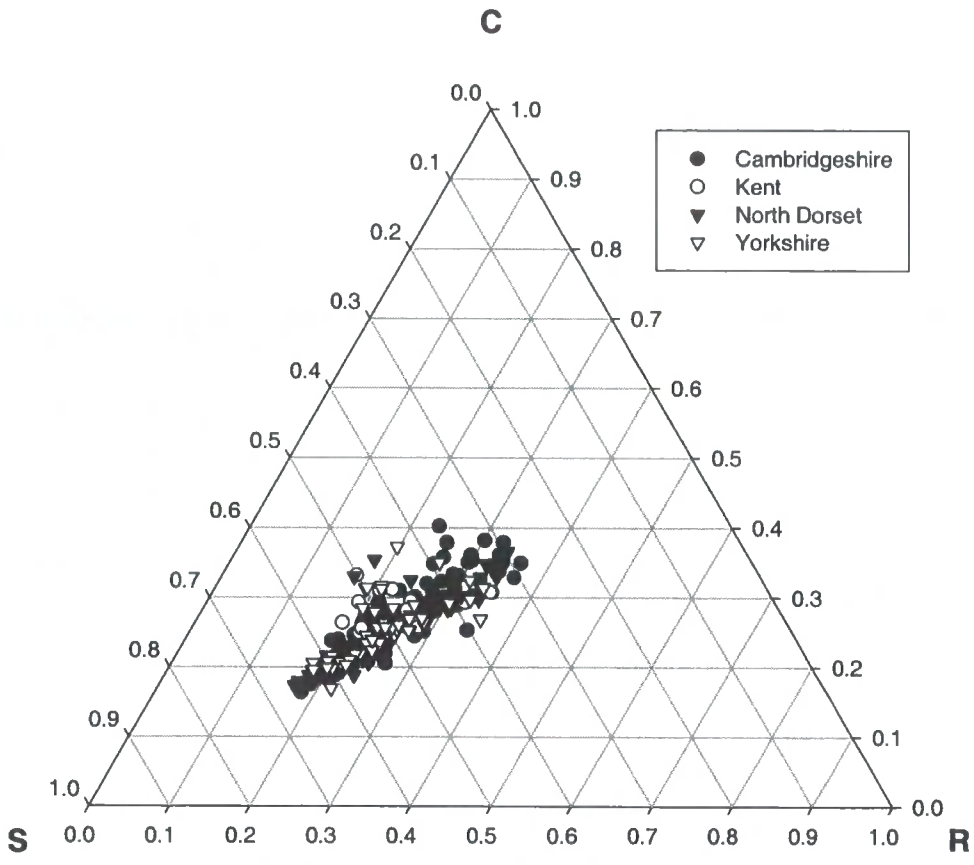

Figure 2.5: Triangular C-S-R plot of Grime's indices for each plot (rescaled from 0-1), coded by region.

Table 2.1: Spearman's Rank correlation coefficients between first two DCA axes and vegetation variables. n.s. – not significant, *- significant at p<0.05, **- significant at p<0.01. Significance adjusted using Bonferonni correction for multiple comparisons.

	Axis 1	Axis 2
Ellenberg L	n.s.	-0.249**
Ellenberg M	0.492**	-0.600**
Ellenberg R	-0.294**	0.661**
Ellenberg N	0.855**	0.277**
Grime's C	0.664**	0.534**
Grime's S	-0.730**	-0.508**
Grime's R	0.838**	n.s.
No. of species	n.s.	-0.470**
Vegetation height	n.s.	0.470**
Grazing index	n.s.	-0.338**
Rabbits	n.s.	-0.285**
Total rainfall	n.s.	-0.498**
Summer rainfall	n.s.	-0.436**
Max July temp	n.s.	0.291**
Ri(1)	-0.200**	n.s.
Ri(2)	-0.272**	n.s.
Ri(3)	-0.195**	n.s.
Slope	n.s.	n.s.
Soil depth	n.s.	n.s.
Organic (%)	n.s.	-0.271*
pH	n.s.	0.412**
Total carbonates (%)	-0.240**	0.307**
Ca	n.s.	n.s.
P	0.199*	n.s.
K	0.227*	n.s.
Stones (%)	n.s.	n.s.

2.3.3.3 General additive models

The derived models are summarised in table 2.2, and figures 2.6 to 2.11 show partial residual plots in order to visualise the relationships between the explanatory and response variables.

Table 2.2: Summary of GAMs for DCA axes 1 and 2 and frequency of selected species with explained deviance , change in degrees of freedom and list of explanatory variables.

	Null deviance	Percentage deviance explained	Change in df	Significant explanatory variables
Axis 1	1410921	25	9	Carbonates, organic matter, Ri3
Axis 2	751079	26	6	Carbonates, rabbits, grazing
Hippocrepis comosa	101	20	5	Julymax, grazing, Ri3
Asperula cynanchica	108	49	3	Julymax, grazing, rabbits
Sanguisorba minor	194	21	9	Carbonates, organic matter, rabbits
Plantago lanceolata	117	7	2	Grazing, rabbits
Holcus lanatus	112	17	2	Grazing, s(pH)

Axis 1 is best explained as a function of total carbonates, organic matter and radiation index. This is consistent with the interpretation of a soil/microclimate gradient; low axis 1 values are associated with higher radiation values and soils with high carbonate and organic matter content.

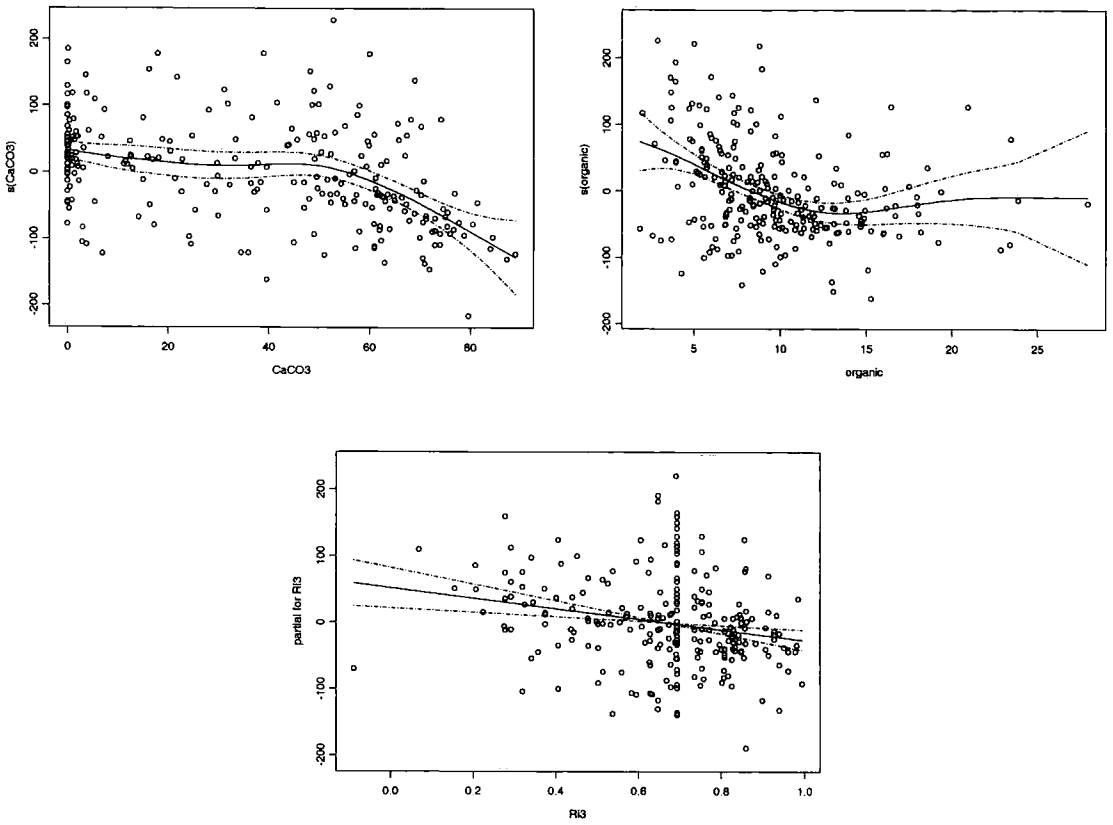

Figure 2.6: DCA axis 1 GAM partial residual plots for (a) total carbonates (b) organic matter (c) radiation index. Solid line - partial fit, dashed lines ± 1SD

Axis 2 is explained as a function of total carbonates, and the presence of rabbits and grazing. The latter two variables are consistent with the interpretation that it represents a gradient in grazing pressure/vegetation height; the relationship with total carbonates may be due to the confounding of grazing with region in the data set.

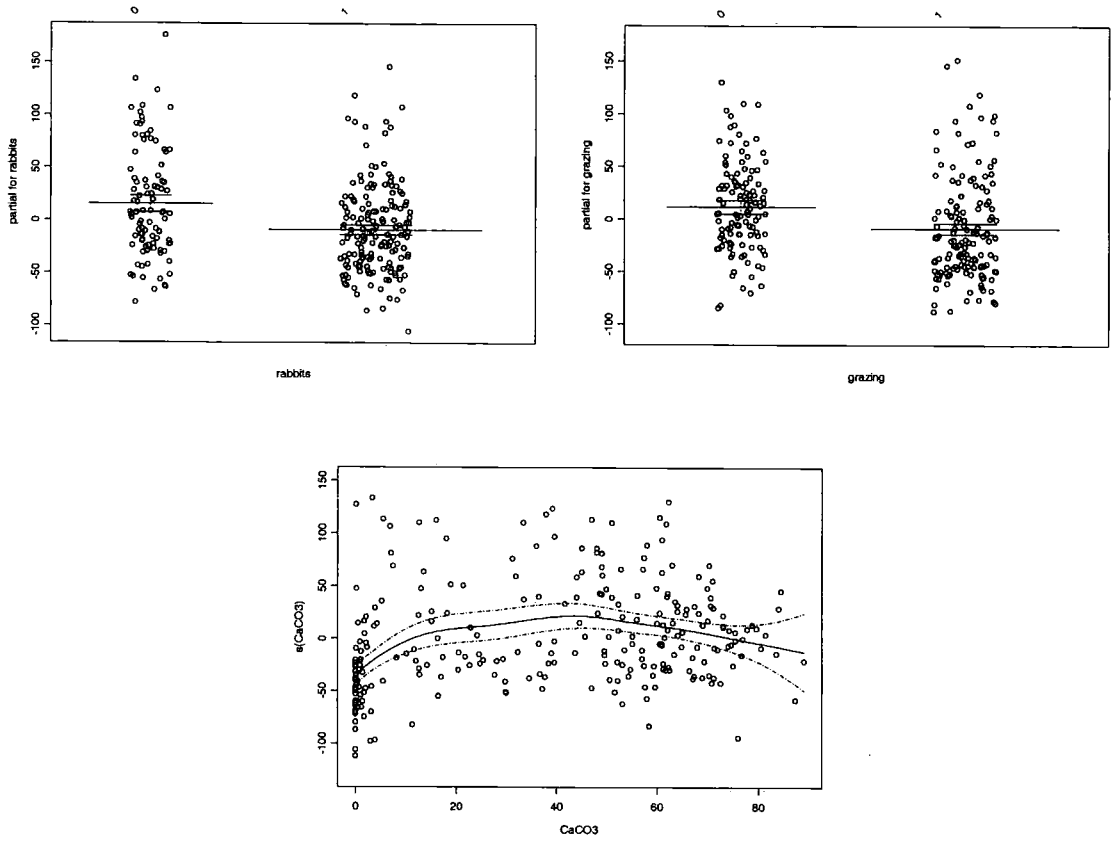

Figure 2.7: DCA axis 2 GAM partial residual plots for (a) rabbits (b) grazing (c) total carbonates. Solid line - partial fit, dashed lines ± 1SD

The model for *Hippocrepis comosa* consisted of functions for the variables July temperature, grazing and Ri(3) (August 1500h radiation index). The response to radiation index is similar to that obtained by Austin (2001), confirming that the effects of topography and soil are consistent through regions of different climate. Partial fit plots (fig 2.8) show the partial contribution of each variable to the model. It can be seen that the frequency of *Hippocrepis* tends to increase with summer temperature, solar radiation in the afternoon and with grazing.

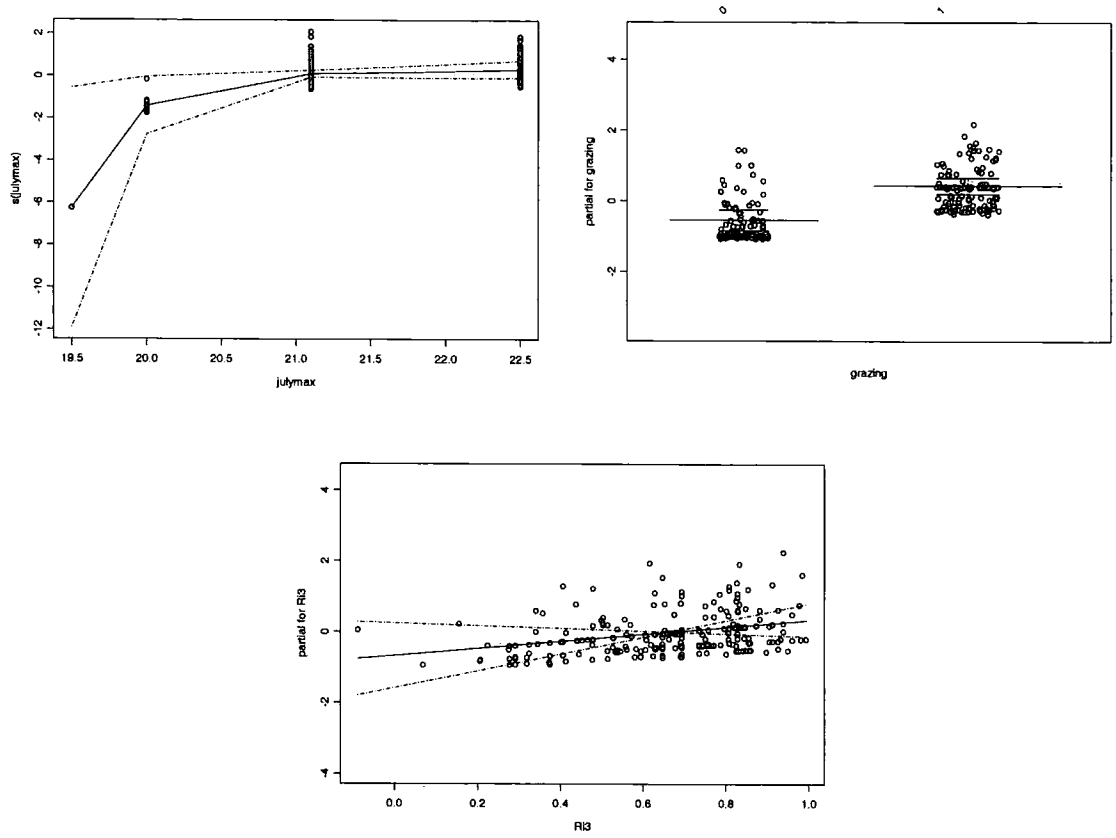

Figure 2.8 : *Hippocrepis comosa* GAM residual plots for (a) daily max July temperature (b) grazing presence/absence (c) radiation index. Solid line - partial fit, dashed lines ± 1SD

The model for *Asperula cynanchica* (figure 2.9) consists of smoothed functions of July temperature, presence of grazing and rabbits and vegetation height. The response of *Asperula* to summer is similar to that of *Hippocrepis*, although the lack of radiation index used in this model reflects the fact that *Asperula*'s topographic distribution is not as clearly skewed along a south-west axis.

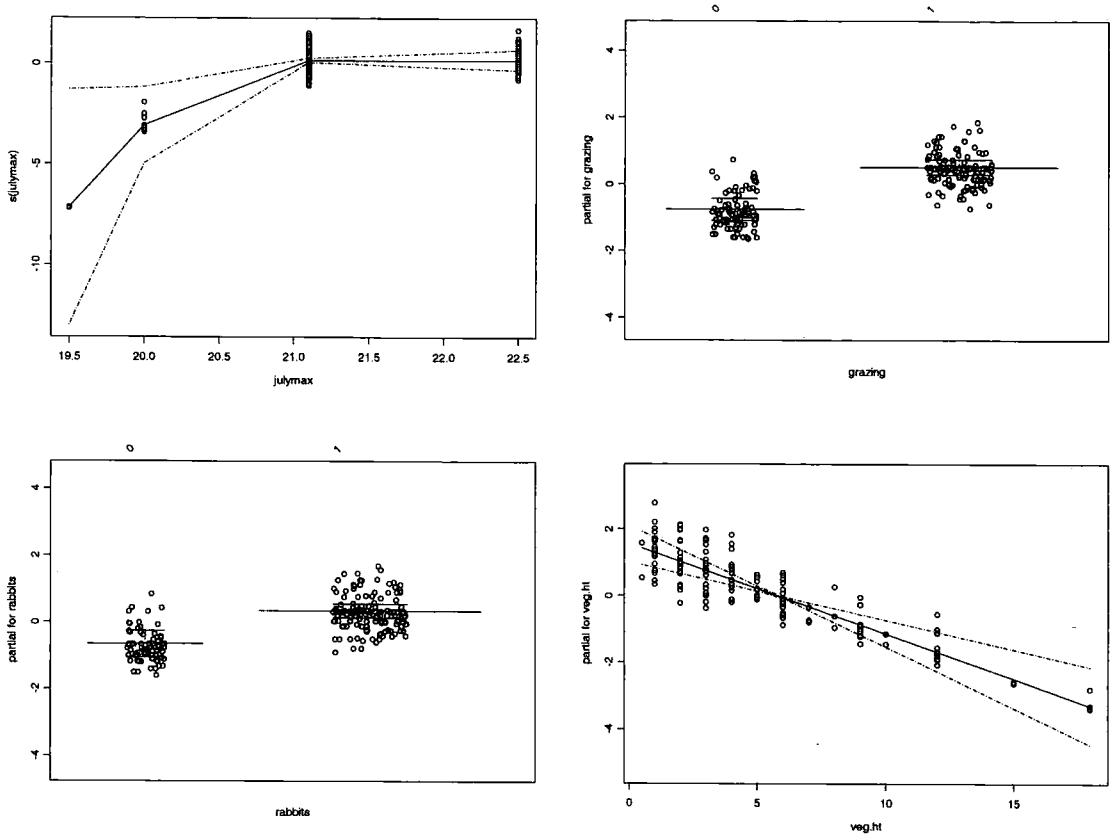

Figure 2.9: *Asperula cynanchica* GAM residual plots for (a) daily max July temperature (b) grazing presence/absence (c) rabbit presence/absence (d) mean vegetation height. Solid line - partial fit, dashed lines - ±1SD

The model for *Poterium sanguisorba* (figure 2.10) consists of smoothed functions of organic matter and total carbonates, similar to the functions describing DCA axis 1 (figure 2.6) and the presence of rabbits as a fixed factor.

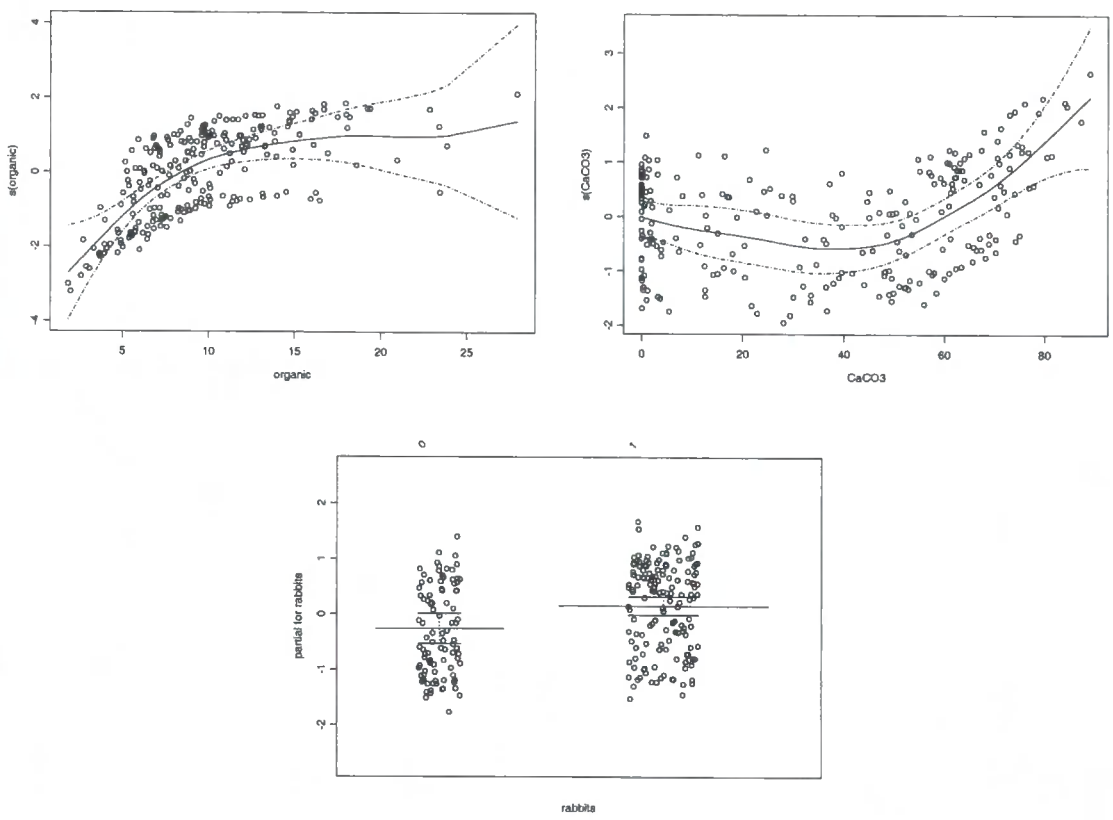

Figure 2.10: *Poterium sanguisorba* GAM residual plots for (a) organic matter (b) total carbonates (c) presence/absence of rabbits. Solid line - partial fit, dashed lines - ±1SD

The model for *Plantago lanceolata* (figure 2.11) consists of both grazing and rabbits as a fixed factor. Note that the explanatory power of this model is low (table 2.2)

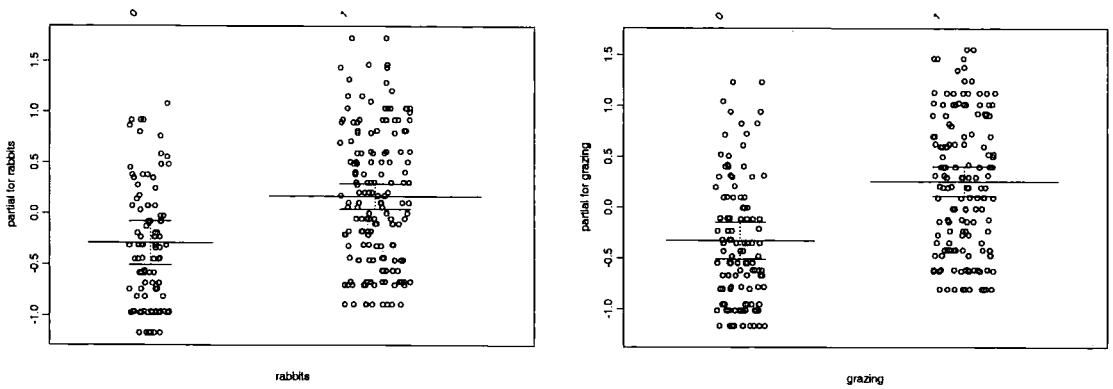

Figure 1.11: *Plantago lanceolata* GAM residual plots for (a) presence/absence of rabbits (b) presence/absence of grazing. Solid line - partial fit, dashed lines - ±1SD

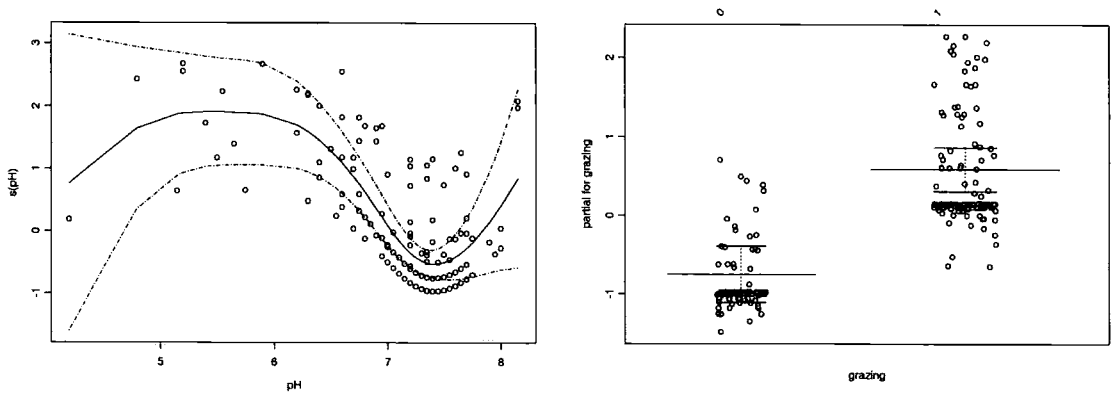

Figure 2.12: *Holcus lanatus* GAM residual plots for (a) soil pH (b) presence/absence of grazing. Solid line - partial fit, dashed lines - ±1SD

The model for *Holcus lanatus* (figure 2.12) consists of a curve fitted to pH and the presence/absence of grazing.

2.3.4 Discussion of analyses

2.3.4.1 DCA ordination

Interpretation of the DCA ordination suggests that the vegetation in chalk grassland is primarily influenced by two environmental gradients: a "stress tolerance" gradient associated with both edaphic and microclimatic factors, and a grazing/vegetation height gradient. This is broadly consistent with Perring's observation that soils and vegetation are associated with a gradient in humidity in British chalk grasslands

(represented here by the first DCA axis), and that this gradient is determined by an interaction between macroclimatic factors, and the effects of topography on microclimate. However the use of Ellenberg Indicator Values to interpret the ordination implies that axis 1 is strongly associated with moisture, but also equally strongly with soil reaction and fertility. The GAM approach also shows that soil organic content and total carbonates had the greatest explanatory power in predicting axis 1 scores. These variables may be distinguishing between soil types, as rendzina soils are typically characterised by high chalk and organic matter contents. While, in the long term, soil development may be driven in part by microclimatic conditions, it is clear that other factors also influence soil type. In particular topography (slope angle) has an effect independent of microclimate.

Previous ordinations of Atlantic European calcareous grasslands have recognised the importance of spatial variations in soil moisture on a landscape (topographic) scale (Austin, 1968) and on a regional (climatic) scale (Duckworth *et al.*, 2000c). This analysis confirms the importance of integrating macro- and micro-climatic factors, and of considering the apparently close interactions between drought, low nutrient availability and high soil pH and the stresses that they put on vegetation.

The second DCA axis was interpreted as representing grazing pressure from both livestock and rabbits, possibly obscured by the confounding effect of lack of grazing on the Cambridgeshire and Kent sites. The importance of both drought and grazing in influencing the vegetation composition of chalk grassland is well documented.

2.3.4.2 GAM analysis of species distribution

Generalised additive models of the distribution of five species, representative of Perring's classification of species with respect to their distribution along a climatic/topographic humidity gradient, proved to be a useful tool in determining the effects of a single variable independently of others. While the models produced varied in their explanatory power, they were often consistent with the known ecology of each of the species and with the distributions shown in Perring's

toposequence diagrams. For example, it has been previously observed that *Hippocrepis comosa* and *Asperula cynanchica* are among a group of species restricted to chalk grasslands where mean daily maximum temperatures in July exceed around 20° C (Rodwell, 1992), that *Hippocrepis* is more frequent on grazed slopes receiving afternoon sun (Fearn, 1973) and that *Asperula* is more frequent in short swards (Perring, 1956). These ecological preferences were clearly shown in the GAMs. The GAM for *Poterium sanguisorba* suggests a distribution influenced by soil type and rabbit grazing, while *Holcus lanatus* appears to be more frequent on grazed grassland with soil pH below around 7.

While the macro- and micro-scale gradients in vegetation associated with Perring's humidity gradient can be broadly considered as analogous to DCA axis 1 or the gradient from S to CR strategists, it is clear that the distribution of individual species along this gradient may be controlled by any of a number of related, but independent proximal variables including soil moisture, temperature, soil pH and soil fertility.

2.4 Summary of chapter 2

1. Studies on the effects of climate on plant distribution have been carried out at a range of spatial scales, from continental-scale correlations of climate and vegetation to experimental studies on physiological processes in individual plants.
2. Macroclimate interacts with topography to determine the microclimate in which plant physiological processes occur. In grasslands plant microclimate can vary considerably over small distances. Small-scale variations in microclimate therefore influence plant survival in the landscape, which in turn determines the micro- and macro-scale distributions of species and vegetation types.
3. The work of F. H. Perring on topographic and climatic gradients in chalk grassland shows links between plant distribution at macro- and micro-scales. Reanalysis of his original data using modern methods of exploratory analysis confirm some of his observations and can help to elucidate the

main factors determining vegetation composition in chalk grassland (gradients associated with microclimate/soil processes and grazing pressure) and individual species distribution (for example, July maximum temperature, topography and grazing for *Hippocrepis comosa*).

4. For the species associated with the wetter end of Perring's humidity gradient grazing and soil factors appear to be the most important factors determining their distribution; towards the drier end topography and climate appear to become more important.
5. To fully understand the interactions between climate and vegetation in calcareous grasslands, physical models of biologically relevant microclimatic variables that take into account the effects of both macroclimate and topography are required.

Chapter 3: Field sites and climate measurement

3.1 Introduction

Several previous studies have measured microclimatic variables on two contrasting slopes in the same vicinity and therefore under the same macroclimate (Påhlsson 1974; Rorison, Sutton and Hunt 1986; Oliver 1991). In the present study temperature and soil moisture measurements were taken from several points in complex landscapes under two contrasting regional climates, in order to investigate the interactions between macro- and microclimate.

This chapter introduces the two field sites used in this study, and summarises a series of macro- and micro-climatological measurements taken over the period June 2001 to 2002 at each site. Full AWS, data logger and soil moisture data sets collected during this study are presented on CD-ROM (appendix 5).

3.2 Methods

Two field sites, Hambledon Hill in North Dorset and Sylvan Dale in Millington Pastures, in the Yorkshire Wolds, were selected in contrasting regional climates, near the southern and northern limits of chalk grassland in the UK (figure 3.1). Both sites contain an area of grazed unimproved chalk grassland on a range of slopes and aspects, and Perring surveyed plots within each during 1952 and 1953 (Perring, 1959, 1960).

At each field site, an automatic weather station (AWS; CR10X Campbell Scientific, Shepstead, UK) was installed on a flat exposed site to record hourly synoptic climate data at a hilltop or plateau site. Forty vegetation plots, each measuring 7 m by 7 m were located at each site to represent as wide a range of slopes and aspects as was possible within the landscape, and their positions recorded by Geographical Positioning System (GPS; GPS 12XL, Garmin, Olathe, Kansas,

USA). The slope and aspect of each plot was measured in the field using compass and clinometer.

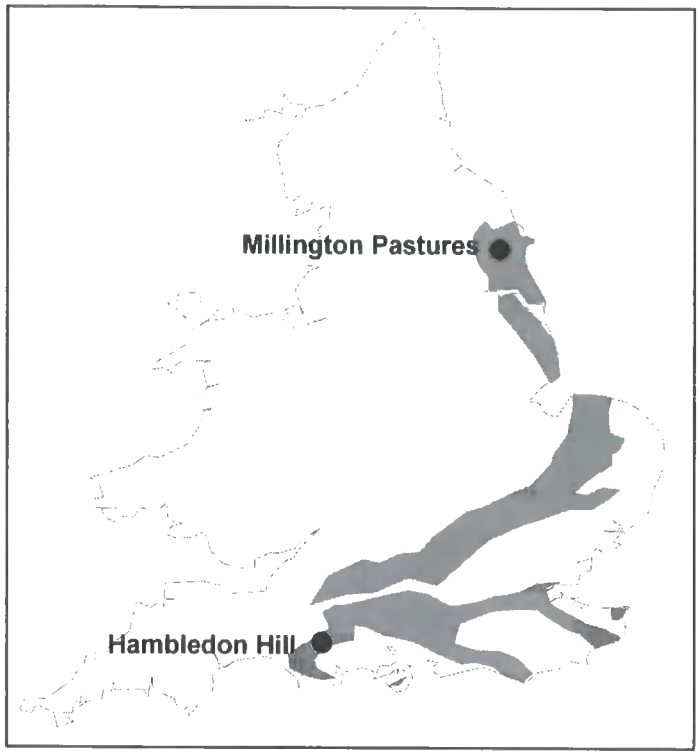

Figure 3.1: Location of field sites. Shading shows extent of underlying chalk geology in the UK

3.2.1 Hambledon Hill

Hambledon Hill (SE 84 12) is an outlier of the Wessex Downs, rising to 192 m above the flood plain of the River Stour (figure 3.2, plate 3.2). The site is on the Upper Chalk, and soils are mapped as shallow humic rendzinas of the Icknield series (Soil Survey of England and Wales, 1984), consisting of an organic-rich humose topsoil of up to 20 cm overlying broken chalk fragments or bedded chalk. Soils on the hilltop resemble calcareous brown earths. Large areas of the hill have been ploughed since 1950, and the remaining unimproved chalk grassland on the northern spur of the hill is designated a National Nature Reserve (NNR). The hilltop also includes considerable Iron Age Hill and Neolithic earthworks, increasing the topographic variation considerably. As the hill is the highest point in the surrounding area, there is little topographic obstruction to the outward facing

slopes of the hill. The vegetation at the sites is predominantly short, herb-rich *Festuca-Avenula* grassland on sloping ground, with less diverse, more mesotrophic grassland on flatter ground at the hilltop.

3.2.2. Sylvan Dale

Sylvan Dale is within Millington Pastures SSSI, an area of chalk grassland in the Yorkshire Wolds, encompassing a large dry valley system. The site is on the Middle Chalk, and soils in the area are strongly associated with topography. On the Wolds plateau, brown earths of the Pan Holes series form incorporating areas of aeolian drift; on shallow slopes these are replaced by brown rendzinas of the Andover series. On steeper slopes these are in turn replaced by humic rendzinas of the Icknield series. The valley bottoms are relatively deep colluvial brown calcareous earths of the Millington series (King and Bradley, 1987). The Wolds plateau has been ploughed or agriculturally improved up to the edge of the valley system in most parts; the remaining unimproved grassland on the slopes of the dales is designated a Site of Special Scientific Interest (SSSI). Sylvan Dale is an S-shaped dry dale running roughly east-west from the main valley (figure 3.3, plate 3.1). Soils on sloping ground within the study area are predominantly Icknield series humic rendzinas similar to those on Hambledon Hill. The study area also includes valley bottom brown calcareous earths and brown rendzinzas on shallow slopes. Patches of the unpalatable tussock forming grass *Brachypodium pinnatum* form a mosaic with short herb-rich *Festuca* turf on the slopes of the valley.

3.3 Acquisition of digital terrain models (DEM)

3.3.1 Hambledon Hill

A DEM of each site was obtained for solar radiation modelling. For Hambledon Hill, a DEM of the Stour Valley, covering most of the area of the field site, obtained by airborne light detection and ranging (LIDAR) was already available at CEH

Monks Wood. The horizontal resolution of this model is 1 m, the vertical resolution is 1 mm with an estimated accuracy of approximately ± 15 cm. The high resolution of this model allows the complex small-scale topography of the earthworks on Hambledon Hill to be visualised (figure 3.4). False surface elevation data due to the canopies of trees, animals or man-made structures is a feature of unprocessed LIDAR data; however, since the areas of interest in this study consisted of short grassland, no attempt was made to remo

3.3.2 Sylvan Dale

At Sylvan Dale, no previously existing DEM was available, so stereo aerial photography was acquired to create a suitable DEM. Stereo black and white diapositives were obtained for the field site (Cambridge University Aerial Photography Unit, Downing Place, Cambridge) at an approximate scale of 1:10 000, and professionally scanned using a flatbed photogrammetric scanner (greyscale, 1000 pixels/inch). Ground control positions (GCPs) were identified and matched in both the scanned images and the field and field positions were recorded by GPS; Elevation values for certain GCPs were derived from contour and spot heights on the relevant 1:10 000 OS maps (Ordnance Survey, Southampton, UK), other GCPs consisted of purely horizontal coordinates. Tie points, identified on both images but not referenced in the field, were also identified to improve the block triangulation process.

Block triangulation of the aerial photography was carried out using the Ortho*Max* module in Erdas Imagine v8.3 (ESRI Imaging Solutions: ESRI (UK) Ltd, Aylesbury, UK). GCPs and tie points were digitised manually between both aerial photographs, and camera parameters were entered manually. The "DEM-Tool" feature was used to extract a DEM at a horizontal resolution of 5 m and vertical resolution of 1 m.ve these effects.

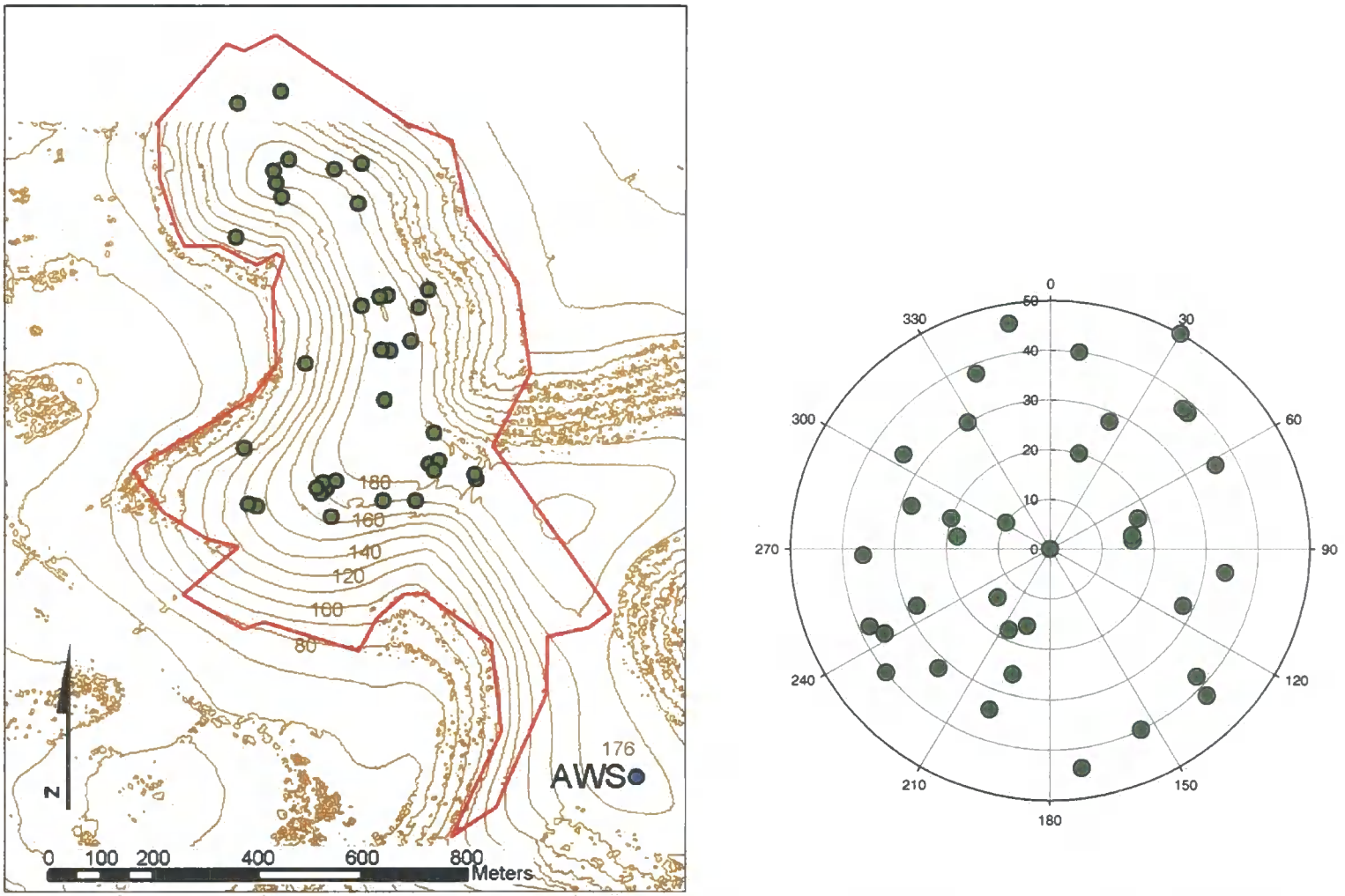

Figure 3.2: (a) Contour map derived from Hambledon Hill DEM. Red line shows boundary of NNR. Green circles show locations of vegetation plots. Blue circle shows location of AWS. (b) "Idealised hill diagram" showing distribution of vegetation plots with regard to topographic position: radial axes represent angle of slope, angular axis represents angle of aspect (degrees).

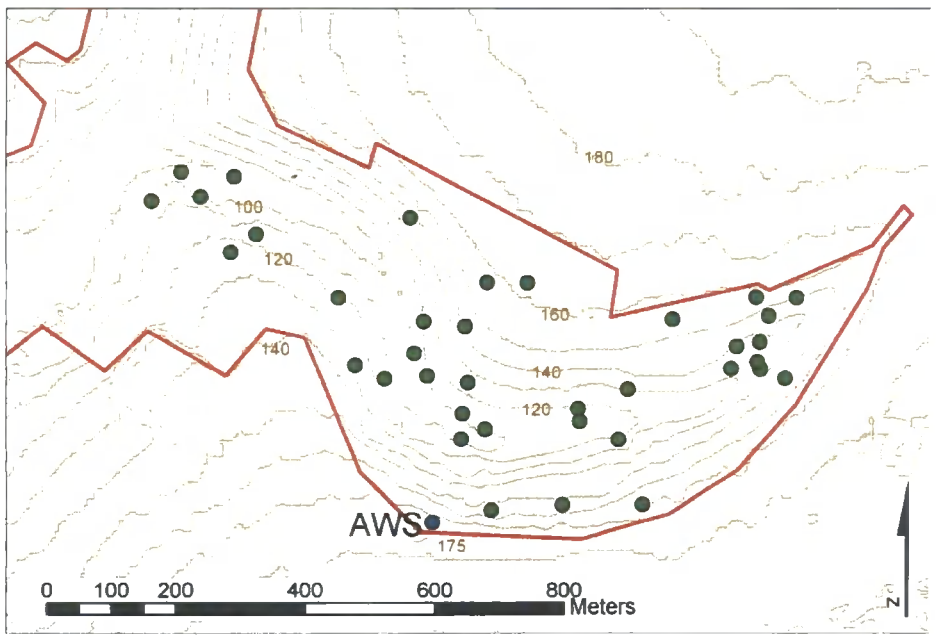

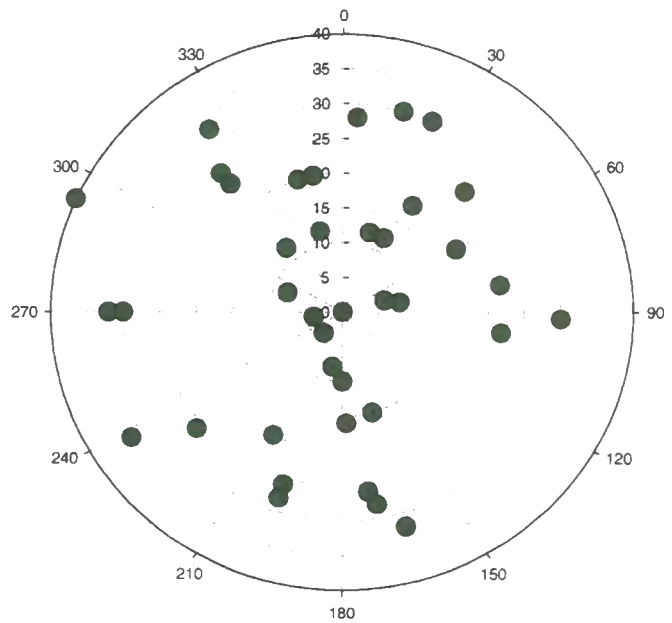

Figure 3.3: (a) Contour map derived from Sylvan Dale DEM. Red line shows boundary of Millington Pastures SSSI. Green circles show locations of vegetation plots. Blue circle shows location of AWS. (b) "Idealised hill diagram" showing distribution of vegetation plots with regard to topographic position: radial axes represent angle of slope, angular axis represents angle of aspect (degrees).

Plate 3.1: View of Sylvan Dale, facing west from near the AWS site.

Plate 3.2: View of North-western spur of Hambledon Hill, facing north.

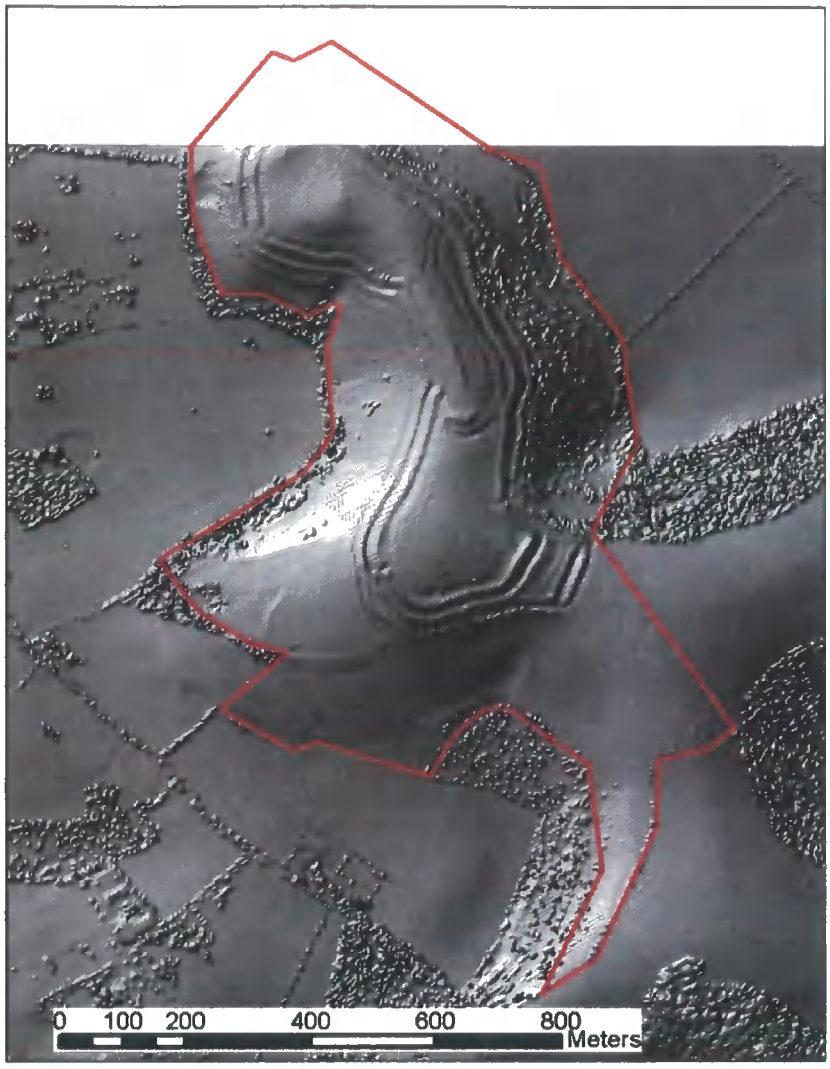

Figure 3.4: False shading image (produced with ArcGIS HILLSHADE command) of Hambledon Hill DEM. Red line shows boundary of NNR. The earthworks and areas of scrub, hedgerows and tree cover can be clearly seen.

Obvious errors in DEM extraction occurred in areas where the ground surface was homogenous or showed repeating patterns and errors were made in matching pixels from the images; ploughed fields on the plateau around the field site in particular caused several obvious "spikes" or "holes" in the DEM. Obvious errors were removed manually and noise was removed from the extracted DEM using editing tools in PCI ImageWorks v6.3 (PCI Geomatics: Henley on Thames, UK). Errors associated with the DEM extraction process, GPS accuracy and subsequent editing limit the accuracy of the extracted DEM (figure 3.5) – comparison with

1:10 000 OS contour maps suggested that a vertical accuracy of ± 5 m is a reasonable estimate.

The horizontal scale and vertical accuracy of a DEM will affect the accuracy of slope and aspect values derived from it. Since the two DEMs differ considerably in this regard, it was considered that slope and aspect measured in the field should be used in insolation modelling; the DEMs were used solely for modelling topographic shading. This ensured that slope and aspect measurements were comparable between sites and at a suitable scale for site-specific micoclimate models.

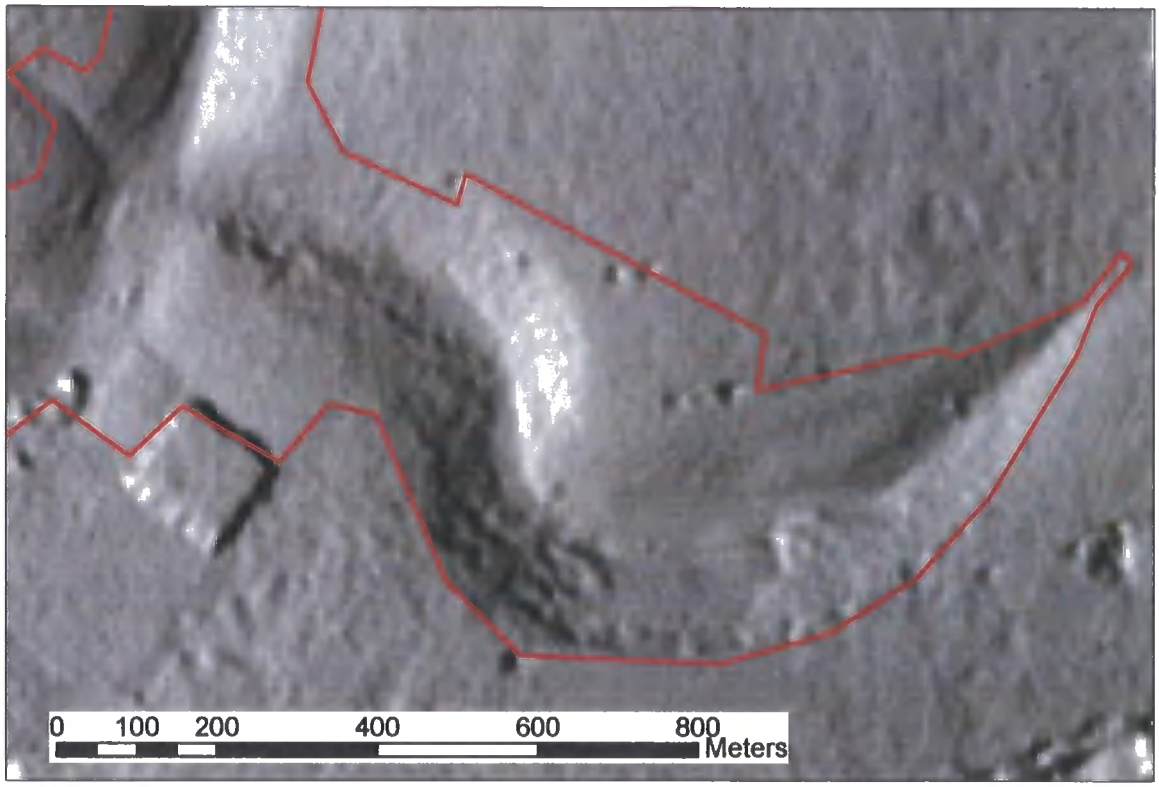

Figure 3.5: False shading image (produced with ArcGIS HILLSHADE command) of Sylvan Dale DEM. Red line shows boundary of SSSI. The raised square on left of image is a mixed conifer plantation.

3.4 Methods - Macro- and microclimate measurement

3.4.1 Measurements at AWS sites

Prior to deployment both AWS were erected within a meteorological enclosure at Moor House in the northern Pennines (NY 757328) for a period of six weeks and measurements were cross-validated between each AWS and against Meteorological Office data recorded at the site.
Each weather station measured the following variables at 10 minute intervals:

- Wet and dry bulb temperature at 1.5 m (H301 Psychrometer, Vector Instruments, Rhyl, UK)
- Soil temperature at 10 mm, 50 mm, 100 mm and 150 mm and shaded air temperature at 100 mm (107 Temperature probes, Campbell Scientific). Soil thermistors were buried horizontally, air thermistors were mounted on a stake and shielded from radiation by a white plastic shade.
- Net radiation (NR-Lite Net Radiometer, Kipp and Zonen, Delft, Netherlands)
- Solar radiation (SP1110 pyranometer, Skye Instruments, Llandrindod Wells, UK)
- PAR 400-700nm (SKP215 quantum sensor, Skye Instruments)
- Rainfall (ARG100 tipping bucket rainguage, Campbell Scientific)
- Wind speed at 2 m (A100R switching anemometer, Campbell Scientific)
- Wind direction (W200P potentiometer windvane, Campbell Scientific)
- Volumetric soil water content (CS616 water content reflectometer, Campbell Scientific)

Hourly mean values of all variables (hourly total for rainfall) were recorded from 1 June 2000 to 10 August 2002. Sporadic periods of missing or unreliable data for certain variables occurred due to low battery power, disturbance by livestock and lack of maintenance during access restrictions due to the outbreak of foot and mouth disease in the UK during 2001. Plate 3.3 shows the AWS after installation at Hambledon Hill.

3.4.2 Mobile dataloggers

Measurements of soil temperature at 50 and 100 mm depth, sward/air temperature at 100 mm height and solar radiation at the surface of sloping ground were made at different points in the landscape at Sylvan Dale. Pyranometers (SKS 1110, Skye Instruments) were mounted parallel to the ground surface at 50 mm height. 100 mm sward/air temperature was measured with a thermistor shielded from radiation with a white painted plastic shade; soil temperature thermistors were inserted horizontally into soil beneath short, unbroken turf (of approximately 10 cm height). Instruments were connected to two data loggers (Squirrel 1200, Grant Instruments, Cambridge, UK). Measurements were recorded at 10-minute intervals and converted into mean hourly values for analysis. Plate 3.4 shows a mobile data logger and sensors at Sylvan Dale. The two data loggers were initially deployed for periods of 25 to 140 days on contrasting slopes to provide validation data for temperature models, and also at plots used for experiments described in chapter 4.

3.4.3 Buried temperature loggers

Miniature data loggers with internal temperature sensors (Tinytalk II, Gemini Dataloggers, Chichester, UK) contained within a plastic canister (50 mm length, 35 mm diameter) were buried vertically in the top 50 mm of soil in experimental configurations designed to elucidate the factors affecting spatial variation in soil temperature for short periods at each site. Internal temperatures within the canister closely approximate the mean temperature of soil between 0 and 50 mm depth (J. Thomas, pers. comm.). Initially these were deployed at six vegetation plots at Sylvan Dale on contrasting slopes for the period 25th August – 19th September 2000. From 19th October to 20th November twelve loggers were deployed in pairs at six plots in the configuration shown in figure 3.6. Each pair consisted of one logger under short turf (50-100 mm height) and one logger under a tussock of *Brachypodium pinnatum* (200-500 mm height), not more than 1 m

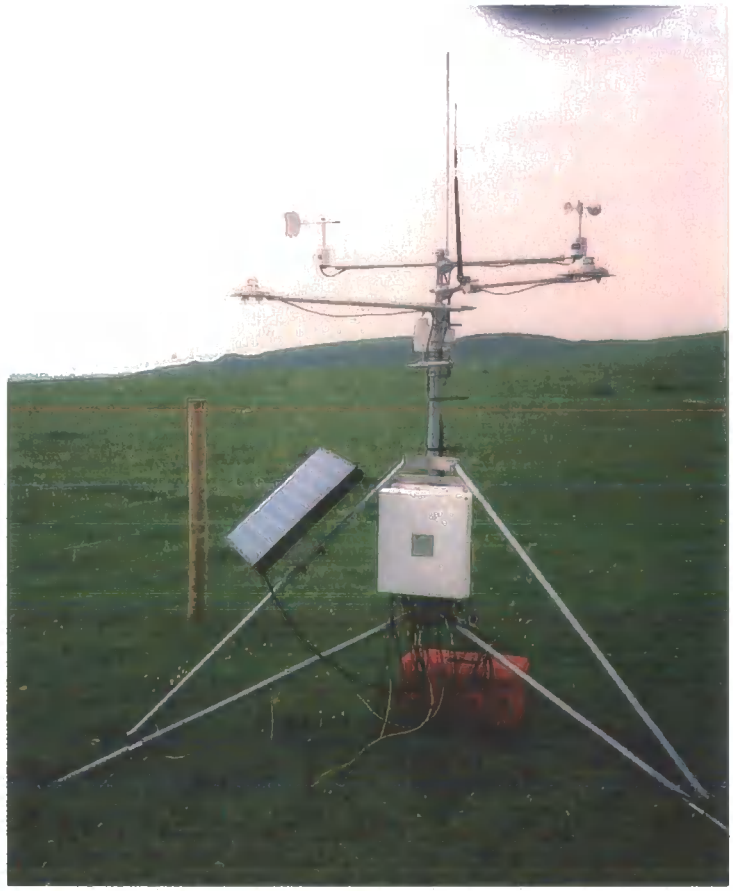

Plate 3.3: AWS installed at Hambledon Hill. Earthworks of the study site can be seen in the background.

Plate 3.4: Mobile data logger with pyranometer and buried and shaded thermistors on a north-facing slope at Sylvan Dale.

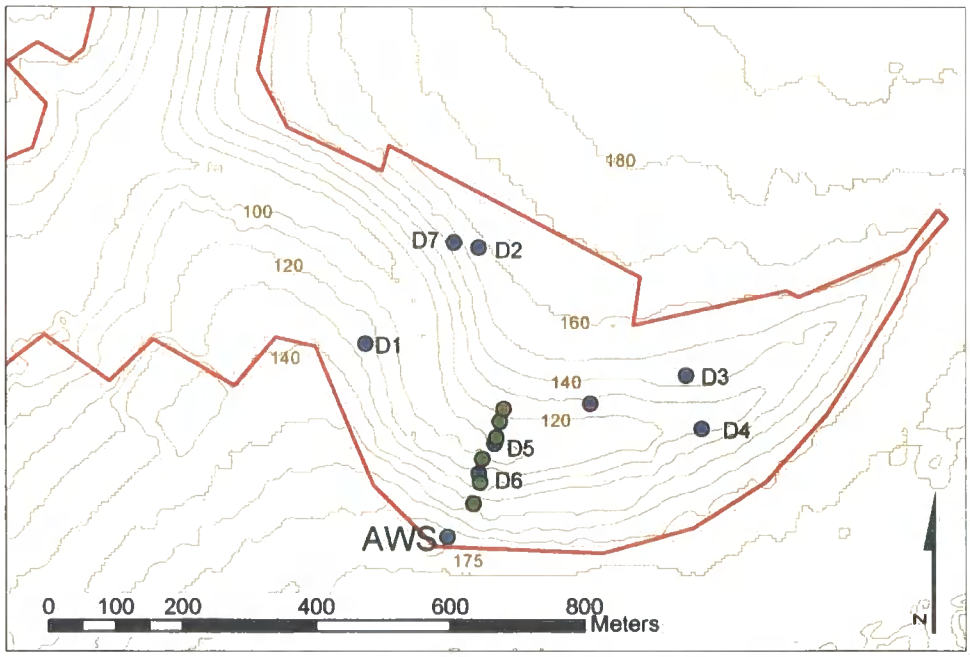

Figure 3.6: Contour map of Sylvan dale. Labelled blue circles show positions of mobile dataloggers; green circles show positions of buried tinytalk loggers in Autumn 2001.

apart. Plots were arranged in a transect across the valley from the AWS to incorporate both north- and south-facing plots and a range of heights up the valley slope.

Deploying data loggers at Hambledon Hill was problematic due to heavy recreational use of the site and restrictions on disturbance to the topsoil due to the status of the archaeological features as a Scheduled Monument. Scheduled Monument Consent was obtained in 2001 to bury miniature data loggers at the site, however due to access restrictions following the outbreak of foot and mouth disease in the UK during 2001, these were not deployed until summer 2002. Ten loggers were buried in the configuration shown in figure 3.7 consisting of a transect running roughly east-west over the hill and loggers on south, south-western and north-facing faces of the earthworks.

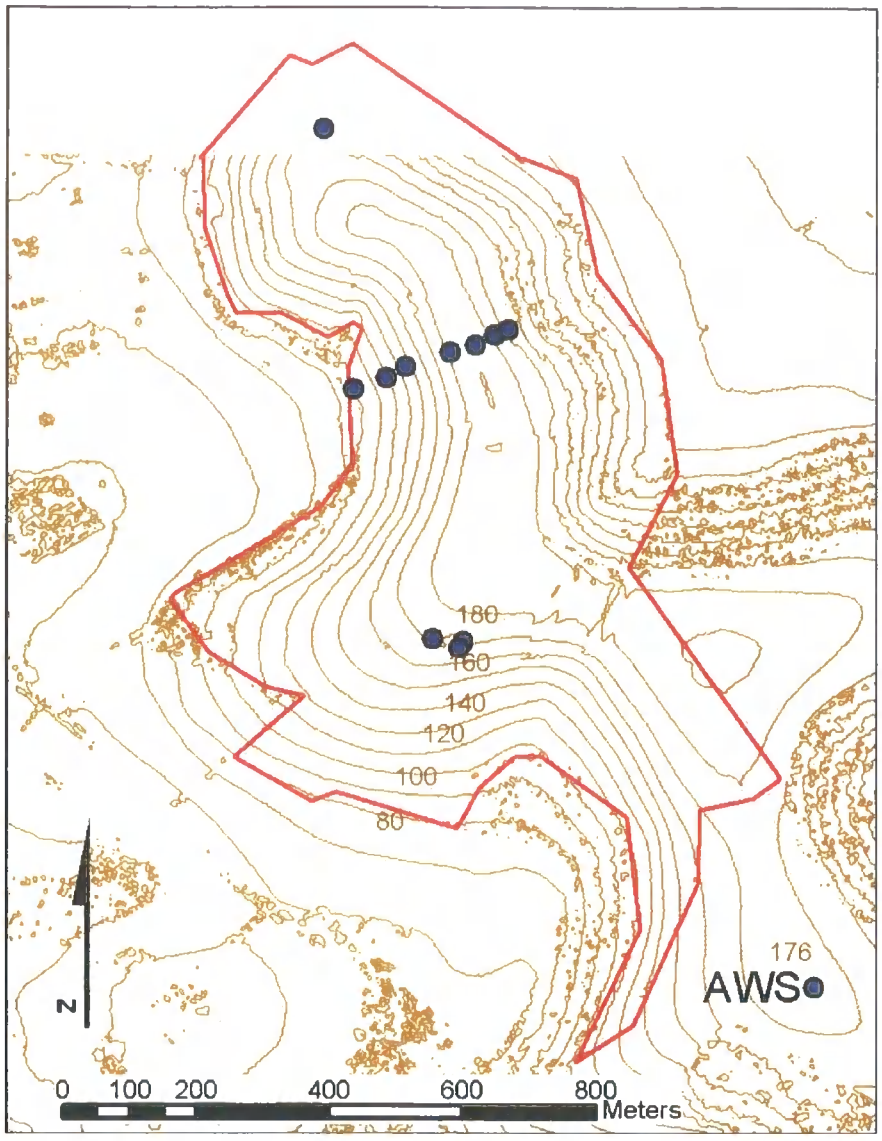

Figure 3.7: Contour map of Hambledon Hill. Blue circles show positions of buried tinytalk loggers in August 2002.

3.4.4 Soil moisture measurement

Soil moisture measurements were made with a hand-held volumetric soil moisture probe (Theta probe ML2, Delta-T Devices, Cambridge, UK) at each vegetation plot at both sites at approximately monthly intervals when possible throughout the study period. Ten replicate measurements were taken for each vegetation plot on each measurement date.

3.5 Climatic observations at field sites

3.5.1 Comparison of AWS climate between sites

Monthly mean screen air temperatures at the AWS at Hambledon Hill were higher than those at Sylvan Dale throughout the period of measurement by an average of 1.4 °C (figure 3.8).

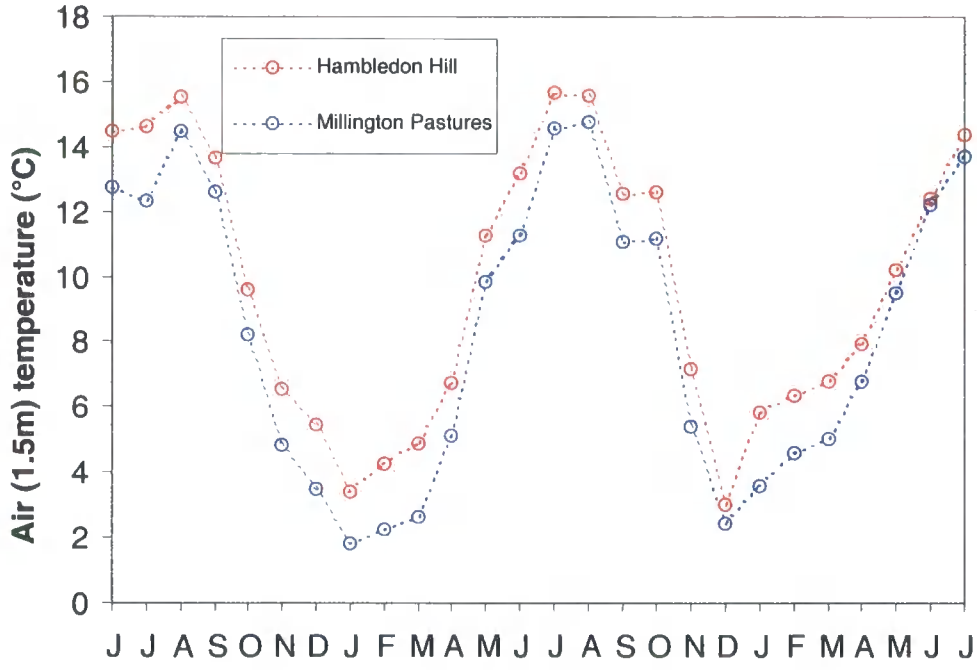

Figure 3.8: Mean monthly screen height air temperature at Hambledon Hill (red) and Millington Pastures (blue) at AWS sites, June 2000 to July 2002.

The Yorkshire Wolds lie in the Pennine rain shadow, and while rainfall was considerably higher at Hambledon Hill (figure 3.9) for much of the period where measurements are available, particularly the exceptionally wet autumn of 2000, in summer 2001 Sylvan Dale was wetter: annual totals for the period October 2000 to October 2001 are 1345 mm for Hambledon Hill and 880 mm for Sylvan Dale; for the six month period April to September 2001 totals are 263 mm and 394 mm respectively.

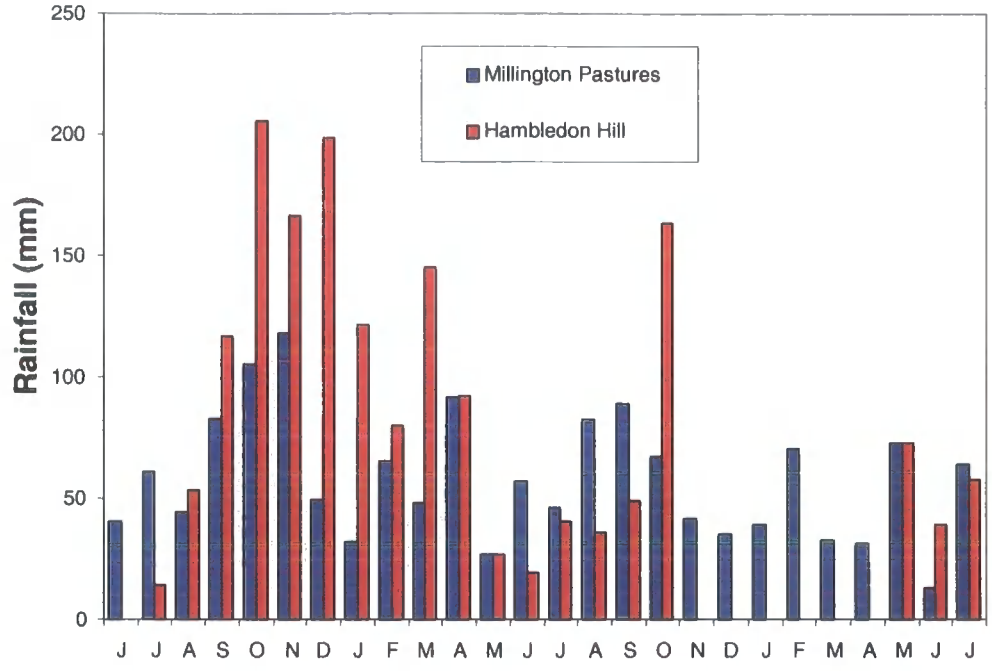

Figure 3.9: Total monthly rainfall at Hambledon Hill (red) and Millington Pastures (blue) Automatic Weather Stations, June 2000 to July 2002. Missing data from Hambledon Hill November 2001 to April 2002 due to equipment failure.

Despite the higher rainfall total at Hambledon Hill, relative humidity was on average lower at this site (figure 3.10), particularly in the spring/early summers of 2001 and 2002. Frequent incursions of mist and low cloud from the North Sea are a well-known feature of the Wolds climate (Furness *et al.*, 1981), and may explain the higher relative humidity at this site despite the lower rainfall.

Mean daily solar radiation was similar at both sites (figure 3.11), although slightly lower at Hambledon Hill in July 2000 and June 2001 suggesting greater summer cloudiness. No clear pattern emerges from the comparison of mean wind speeds in figure 3.12.

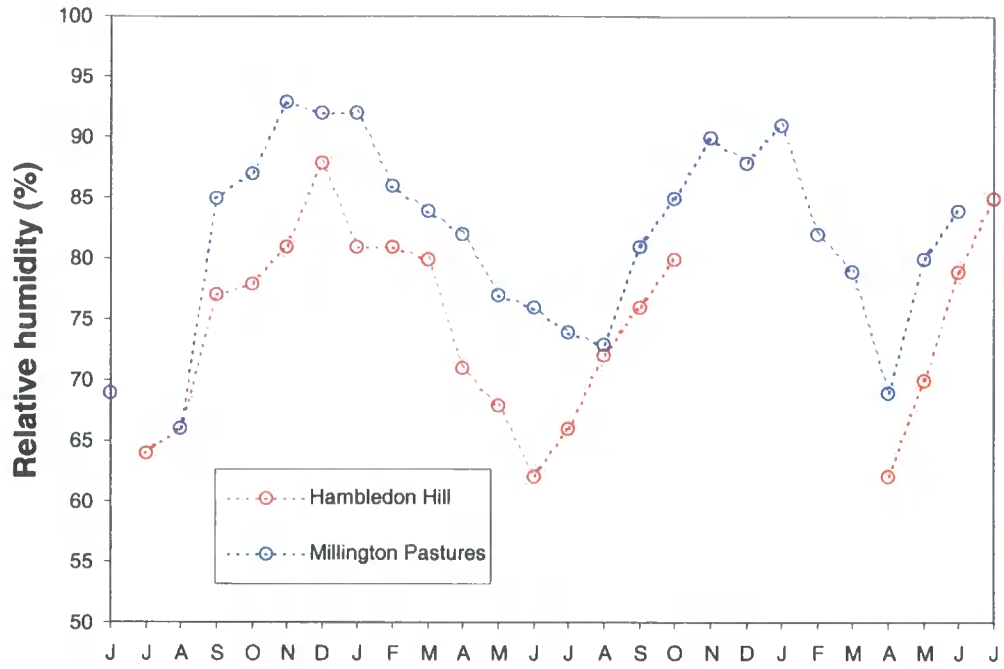

Figure 3.10: Mean monthly relative humidity at Hambledon Hill (red) and Millington Pastures (blue) Automatic Weather Stations, June 2000 to July 2002. Missing data from Hambledon Hill November 2001 to April 2002 due to equipment failure.

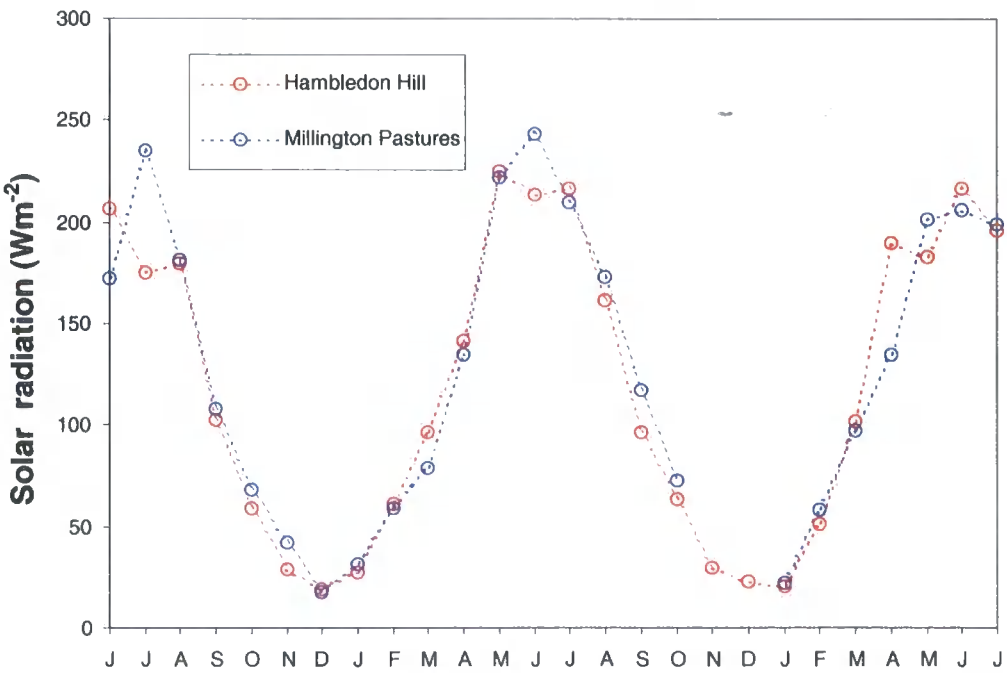

Figure 3.11: Monthly mean hourly solar insolation at Hambledon Hill (red) and Millington Pastures (blue) Automatic Weather Stations, June 2000 to July 2002. Missing data from Hambledon Hill due to equipment failure.

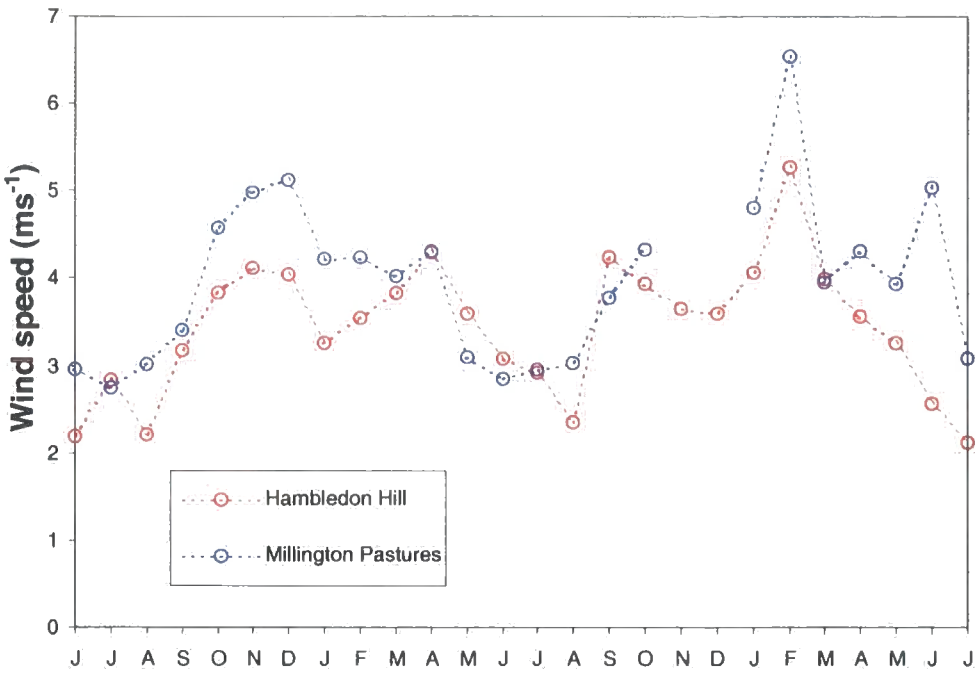

Figure 3.12: Monthly mean wind speed at Hambledon Hill (red) and Millington Pastures (blue) Automatic Weather Stations, June 2000 to July 2002.

A comparison of soil moisture time-series at the AWS sites (figure 3.13) shows that, while the soils at both sites have water contents of up to 60% during the winter months, the soil at Hambledon Hill dries out more rapidly around April to June and frequently had a water content below 25% during the summer months, while the soil at Sylvan Dale never fell below this point. The soil at the Hambledon AWS plot appears to switch fairly rapidly in spring 2001 from a saturated state to a dry state, while at Sylvan Dale it fluctuates between the two states.

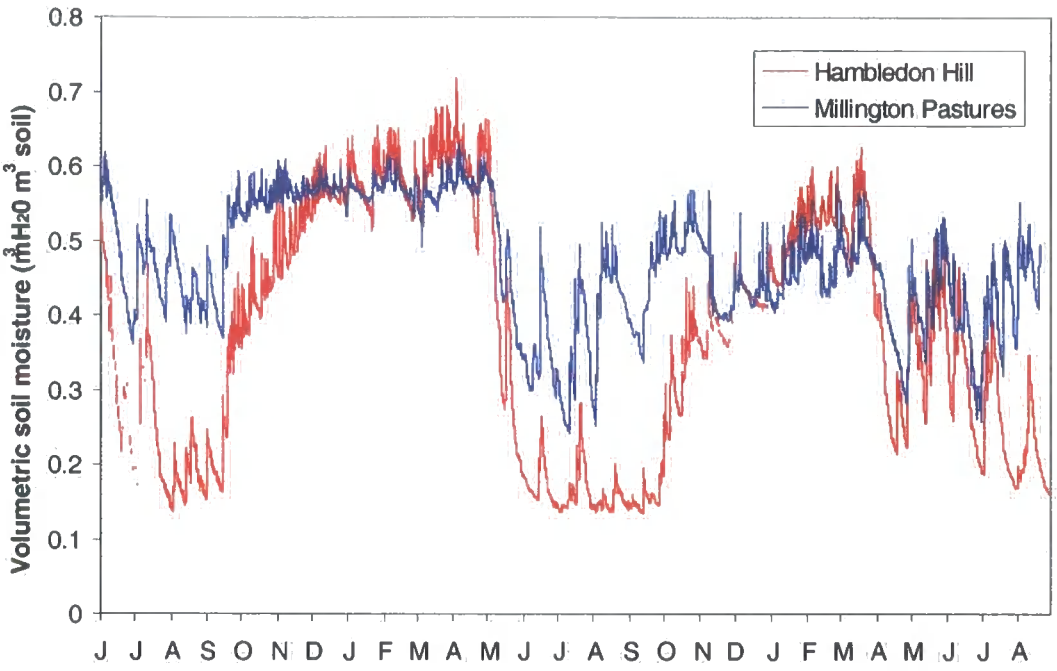

Figure 3.13: Daily mean soil moisture (0-5 cm depth) at Hambledon Hill (red) and Millington Pastures (blue) Automatic Weather Stations, June 2000 to July 2002.

3.5.2 Diurnal patterns in radiation and temperature

Figures 3.14 and 3.15 show the diurnal course of net radiation and temperature at screen height and near the surface on June 25th, 2001 at Hambledon Hill. The observed pattern is typical of similar measurements over short vegetation (Rorison *et al.*, 1986b; Oke, 1987; Geiger *et al.*, 1995). During periods of high solar radiation, the air temperature in the sward is up to 20 °C higher than air temperature measured at screen height. Soil temperatures show decreasing amplitude of oscillation about a mean with depth. At 10 cm depth the diurnal temperature oscillation shows considerable damping and time lag from that at the surface.

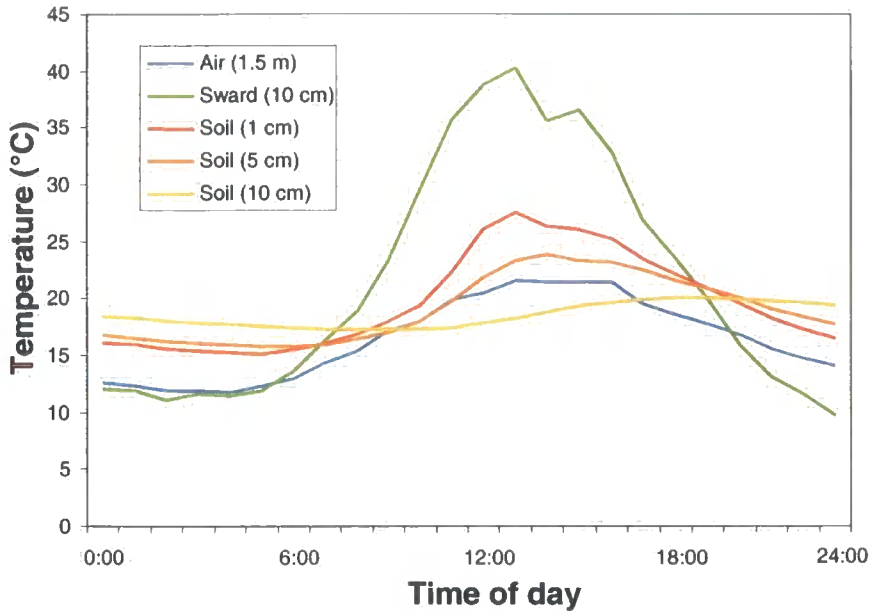

Figure 3.14: Hourly mean air (blue), sward (green) and soil temperature at 1, 5 and 10 cm depth (red, orange, yellow) for June 25th 2001 at Hambledon AWS.

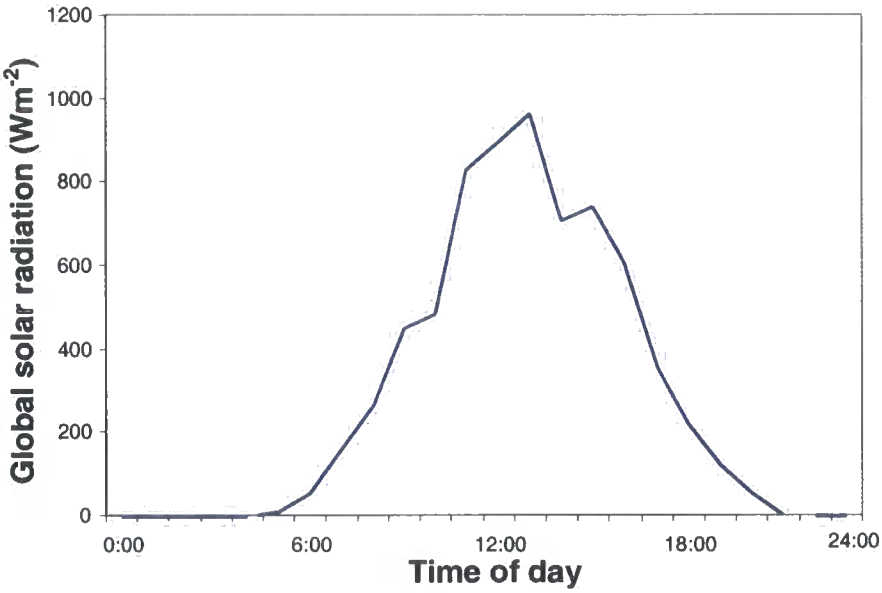

Figure 3.15: Hourly mean solar radiation at Hambledon AWS for June 25th 2001.

3.5.3 Temperature and altitude at Hambledon Hill

The nearest Meteorological Office weather station to the Hambledon Hill field site is at Fontmell Magna (ST865165) at an altitude of 90 m, approximately 5 km from the AWS at Hambledon Hill and 86 m lower in altitude. Daily maximum and minimum temperatures are measured at the site. A comparison of daily maximum and minimum temperatures at the Met Office station and AWS for the year 2001 is shown in figures 3.16 and 3.17. Minimum temperatures are, on average, similar, although there is considerable day-to day variation; maximum temperatures are consistently around 2 to 3 °C lower on the hilltop. Typical adiabatic lapse rates are approximately 0.6 °C per 100 m elevation (Linacre, 1992); the mean temperature difference (estimated as the average of the minimum and maximum) of 2.12 ° C over an altitude difference of just 86 m gives an unusually high apparent lapse rate of 2.47 °C per 100 m. This value may be better explained as due to the cooling effect of higher wind speeds on the exposed hill top AWS site than an adiabatic lapse rate.

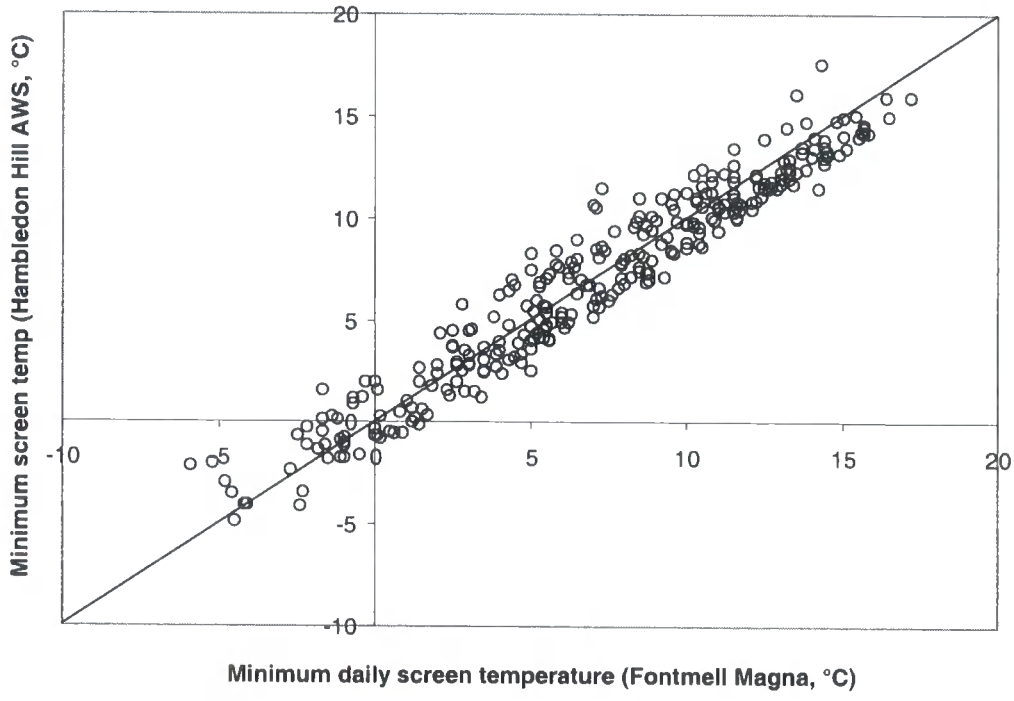

Figure 3.16: Daily minimum screen temperature measured at Hambledon AWS and Fontmell Magna Met Office station during 2001. Mean error = -0.007839.

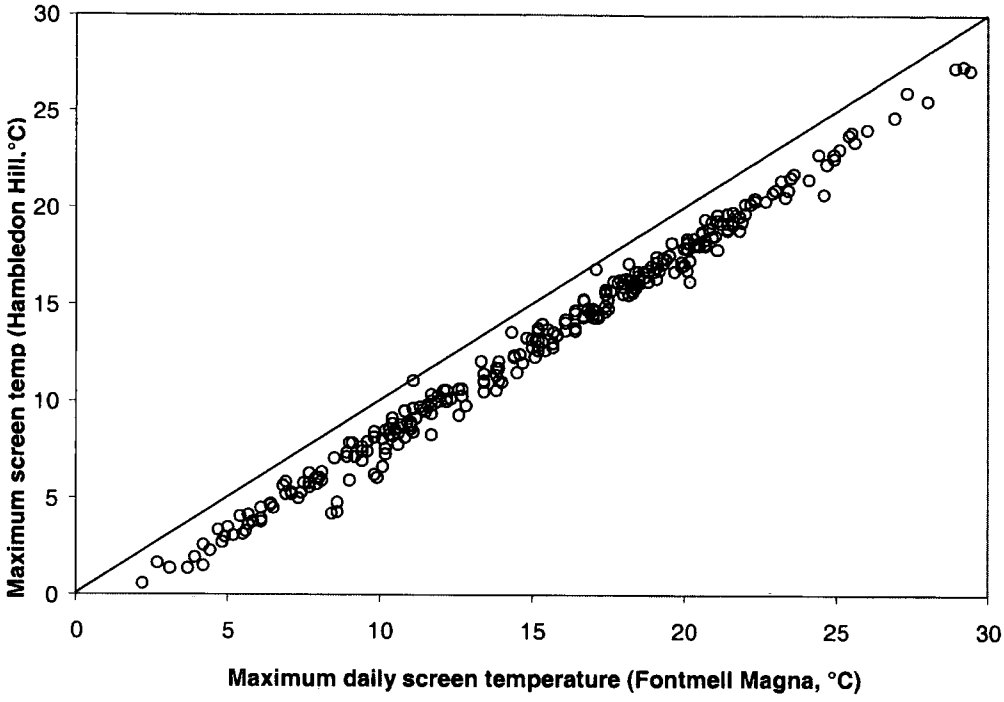

Figure 3.17: Daily maximum screen temperature measured at Hambledon AWS and Fontmell Magna Met Office station during 2001. Mean error = -2.12154.

3.5.4 "Frost hollow" effect at Sylvan Dale

Figure 3.18 shows hourly sward temperatures measured at the AWS at Sylvan Dale (altitude 175 m) and at datalogger site D5 at the bottom of the dale (110 m) for the period 24th February to 3rd April 2002. Surface temperatures at the valley bottom were up to 8 ° C lower than at the AWS during this period. This apparent temperature inversion coincided with a period of extremely clear skies; however, due to the low solar elevation at this time of year, north-facing slopes and the valley bottom received little or no direct solar radiation. Net radiation under these conditions is likely to be dominated by upwards long-wave radiation flux leading to heat loss from the surface to the atmosphere. Katabatic flow of cold air down slope accumulating in valley bottoms as a "frost hollow" is a well-known phenomenon (Geiger *et al.*, 1995; Oke, 1987), and has been previously referred to in the Yorkshire Wolds (Furness *et al.*, 1981). Cold temperatures at the valley bottom were also recorded on clear nights throughout the year on other data logger runs, with minimum temperatures up to 4° C lower at the valley bottom developing

shortly before dawn, however from April onwards these did not last beyond two hours after sunrise and no unexpected difference in daytime temperatures was observed.

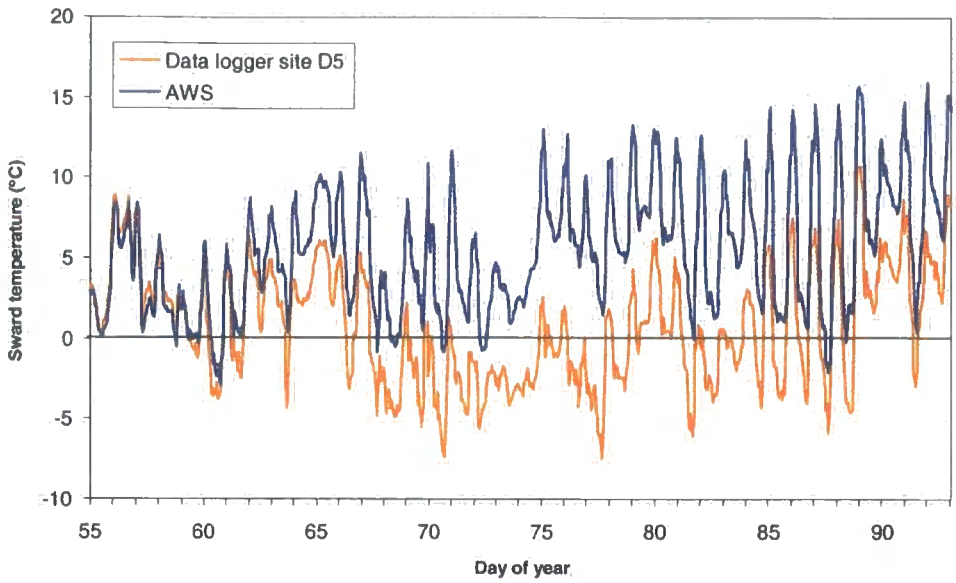

Figure 3.18: hourly sward temperature measured at Sylvan Dale AWS (plateau) and datalogger site D5 (N-facing, valley bottom) 24th February (day 55) to 3rd April (day 93) 2002.

3.5.5 Comparison of temperatures on different slopes

The patterns of temperature difference close to the ground on contrasting slopes has been described in detail elsewhere (Påhlsson, 1974; Rorison *et al.*, 1986a), and patterns recorded with mobile dataloggers at Sylvan Dale were qualitatively consistent with these previous observations. As an example of data collected from different slopes, figure 3.19 shows radiation and temperature differences at data logger sites D3 (north-facing) and D4 (south-facing) on three days in September. During the first two days, under relatively clear skies, there was considerable difference between radiation inputs on the slopes. On the third, overcast, day, there was little difference between slopes. This is reflected in higher sward temperatures on the first two days. In contrast to the data from the weather station in figure 3.15, at these sites 1 cm soil temperatures exceeded sward temperatures during the daytime. This suggests that at these sites the soil surface is heated

directly by solar radiation passing through the canopy, and not simply by

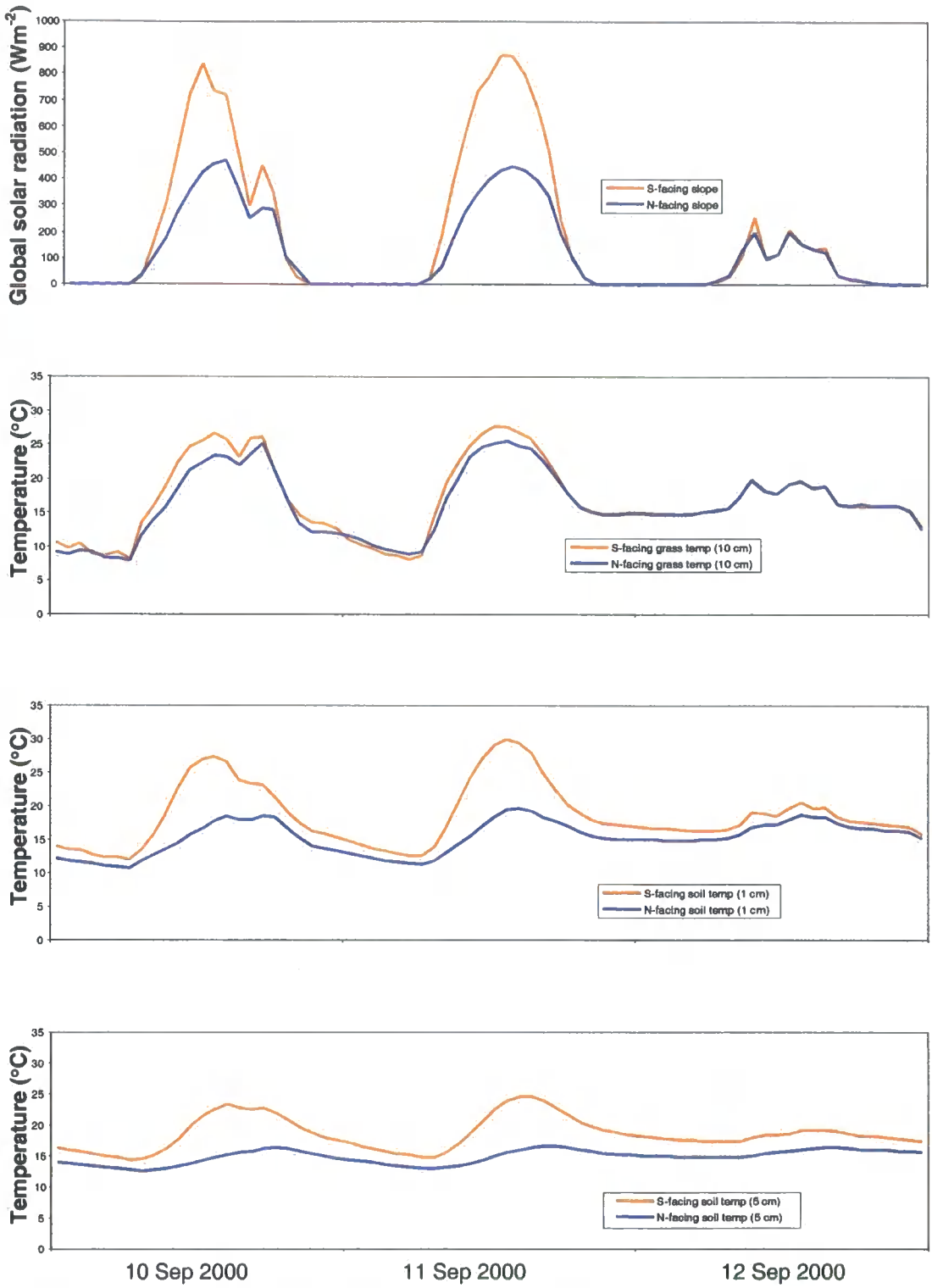

Figure 3.19: hourly mean (a) solar radiation (b) 10 cm sward temperature (c) 1 cm soil temperature (d) 5 cm soil temperature measured at datalogger sites D3 and D4, September 10 - 13 2000.

heat exchange with the vegetation surface above. The AWS site supported a relatively tall, dense sward (mean height 10-20 cm), without bare ground. This is untypical of grazed chalk grassland slopes, including the data logger sites, which typically support more varied sward with areas of thin canopy. There is spatial variation in vegetation characteristics with variation in vegetation height, density and distribution of bare ground, some sites (particularly North-facing slopes) supporting bryophyte cover, patches of tussock-forming grasses (*Brachypodium pinnatum* at Sylvandale) and "grazing-step" terraces on steeper slopes.

At 50 mm depth, the diurnal fluctuations in temperature are considerably dampened, but there is a consistent difference in soil temperature at this time of year, suggesting that cumulative differences in daily soil heat flux between slopes lead to differences in the long-term mean temperature.

3.5.6 Observed patterns in soil temperature

Data collected with the miniature buried data loggers showed three other factors affecting soil temperature in addition to slope orientation: vegetation structure and the frost hollow effect at Sylvan Dale and an altitudinal effect at Hambledon Hill.

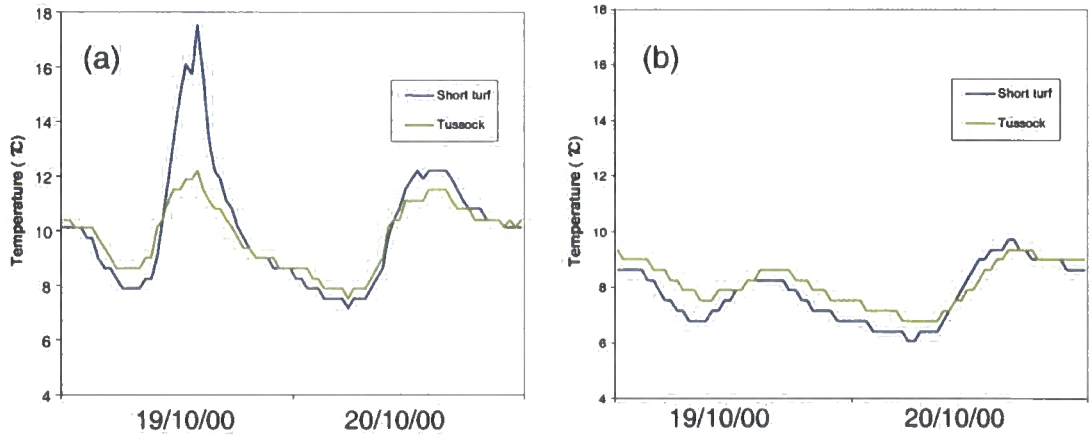

Figure 3.20: 30 min soil temperature (0-50 mm depth) under a short turf (blue) and *Brachypodium* tussock (green) for (a) south-facing and (b) north-facing slope for two representative days in October 2000.

3.5.6.1 Effects of vegetation

Figure 3.20 shows soil temperatures on opposing slopes at 120 m altitude under both a short sward and *Brachypodium* tussock for two example days. The effect of vegetation structure is more pronounced on the south-facing slope, where maximum daily soil temperatures are considerably higher under a short sward than under tussock. On both slopes the minimum temperatures under tussocks are slightly higher than under a short sward.

3.5.6.2 Frost hollow effect

Figure 3.21 shows soil temperatures recorded under short turf along the transect down the north-facing slope of Sylvan Dale for two days in October 2000. The night of the 21st October was particularly clear, and minimum temperatures decrease with altitude from the top to the bottom of the valley. This pattern suggests that the frost-hollow effect observed at the mobile dataloggers may have a systematic effect on long term soil temperatures.

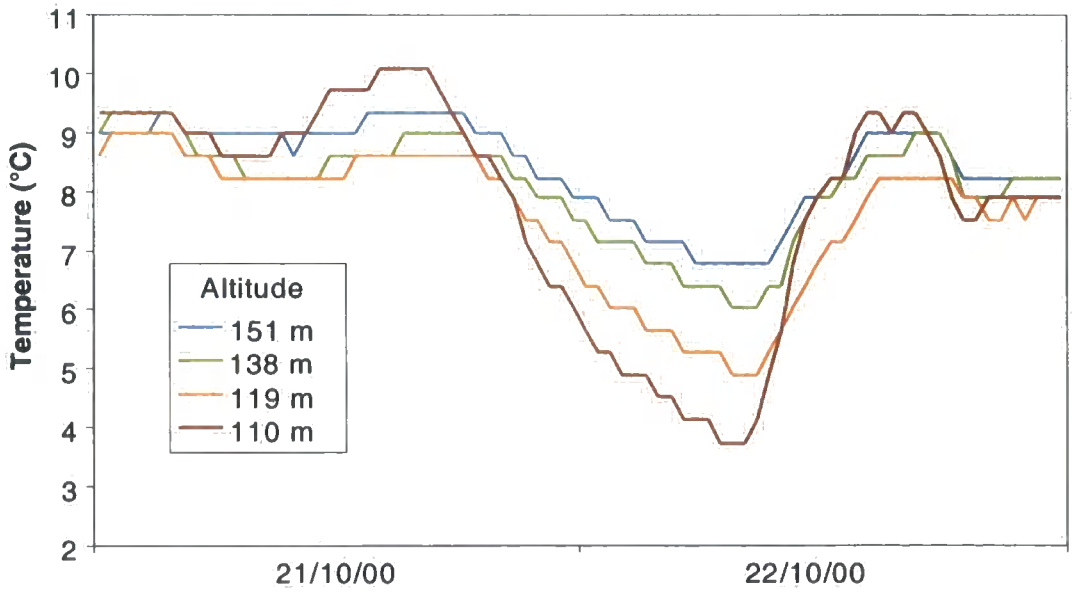

Figure 3.21: 30 min soil temperature (0-50 mm depth) at different heights down the north facing slope of Sylvan Dale during a night time temperature inversion, showing the decrease in soil temperature with height down the valley.

3.5.6.3 Altitude effect at Hambledon Hill

Figure 3.22 shows soil temperatures recorded on the altitudinal transect on west-facing slopes of approximately 30˚ measured by buried data loggers for eight days. The first four days were mostly overcast, while the following four days were clear and calm. An altitudinal gradient in soil temperature at this depth can clearly be identified during the overcast days and at night, consistent with the observations of an apparent lapse rate. However, this gradient is less pronounced on clear days when the diurnal course of soil temperature is dominated by the effects of solar radiation.

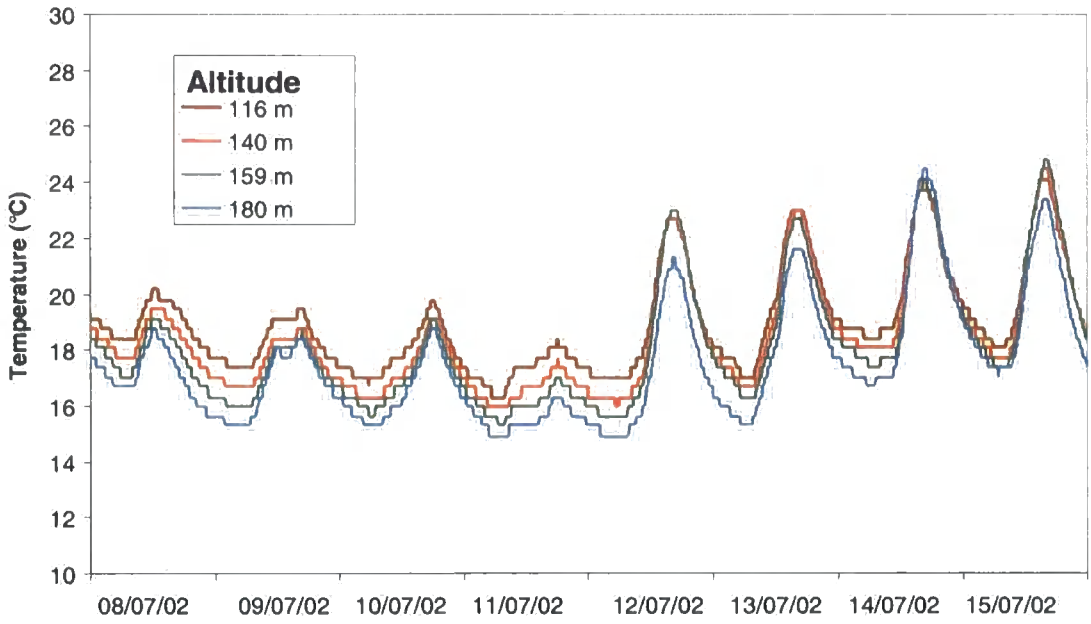

Figure 3.22: 30 min soil temperature (0-50 mm depth) at different heights down the west-facing slope of Hambledon Hill for four overcast followed by four clear days in August 2002.

3.5.7 Observed patterns in soil moisture

Time series of soil moisture, measured at each AWS, and mean soil moisture from 10 measurements at each vegetation plot, are shown in figure 3.23. At Sylvan Dale there is a clear distinction between soil moisture on slopes inclined towards

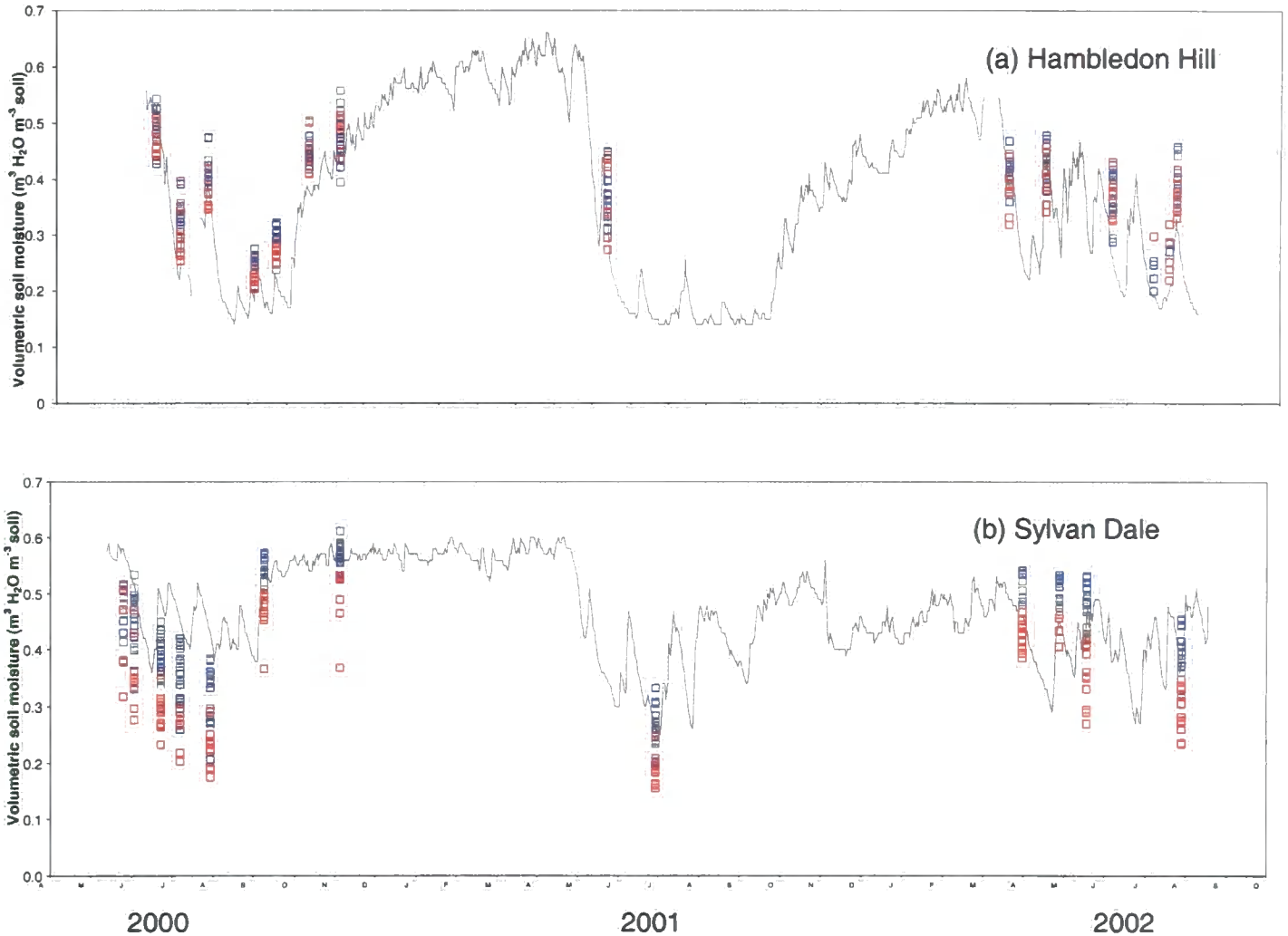

Figure 3.23: Soil moisture at (a) Hambledon Hill (b) Sylvan Dale. Grey line: daily mean measured at AWS. Squares: means of 10 measurements from vegetation plots. Red: sloping (>15°) ground facing south. Blue: sloping ground facing north. Grey: flat ground (<15°).

the south (shown in red), which tend to be drier than those inclined towards the north (blue). At Hambledon Hill this distinction is not clear. Variation in soil moisture about these mean values within plots is typically high (± 0.1 m^3m^{-3}) at both sites. At Hambledon Hill much of the variation in soil moisture appears to occur at the sub-plot spatial scale, and does not appear to be determined by slope aspect; while at Sylvan Dale slope aspect is clearly associated with soil moisture at this scale.

3.6 Summary of Chapter 3

1. Field sites were located at Hambledon Hill, North Dorset, and at Sylvan Dale in Millington Pastures, in the Yorkshire Wolds. These sites were selected near the southern and northern limits of chalk grassland in the UK.
2. An AWS was set up on at each site to record climatic variables on an hourly mean basis from June 2000 to August 2002, and a series of microclimatological measurements were taken from different points in the landscape throughout this period.
3. Over the study period, Hambledon Hill experienced a warmer, less humid climate as measured by the AWS than Sylvan Dale. Annual rainfall was higher at Hambledon Hill over the period, but also more seasonal – summer rainfall totals were lower. Soil moisture at Hambledon Hill AWS appeared to "switch" from a saturated state in winter to a dry state in summer, while this distinction was less clear at Sylvan Dale, and soil at the AWS did not appear to completely dry out at this site.
4. During early spring 2002, and on clear nights throughout the year a marked "frost hollow" effect was recorded at Sylvan Dale. At its maximum, valley bottom sward temperatures were up to 8 °C lower than those at the top of the valley. This magnitude of effect clearly contradicts the assumption that screen-height variables are constant across the site. At Hambledon Hill, maximum daily temperatures at the hilltop AWS were around 2 °C lower than those near the foot of the hill, suggesting that the cooling effect of wind is significant.

5. Clear effects of topography on sward and soil temperatures were observed, qualitatively consistent with previous studies. However, application of a general surface temperature model to different slopes is likely to be complicated by (a) sub-plot scale variation in vegetation structure, which has been shown to have a marked effect on both sward and soil temperature and (b) meso-scale variation in screen height climatic variables, particularly the observed frost-hollow effect at Sylvan Dale.
6. Soil moisture measurements at Sylvan Dale show that south-facing slopes are consistently drier than north-facing slopes. At Hambledon Hill, this pattern is not clear. It may be hypothesised that in a climate with relatively long dry summer periods, soil near the surface tends to become droughted in spring regardless of aspect. Given the high variability of soil moisture measured within plots, micro-scale factors such as small variations in soil depth, root density and distribution of chalk and flint and organic matter in the soil may be more important than aspect. In a more humid spring/summer climate, where intermittent drought/rewetting cycles are frequent, the rate of drying out of soil may become more important leading to a more consistent effect of slope and aspect on soil moisture.

Chapter 4: Modelling topographic microclimate

4.1 Introduction

Ecological studies have attempted to incorporate the effects of slope and aspect as meaningful environmental variables in several ways. The simplest approach is to select sites or transects from opposing aspects (Hutchings, 1983; Rorison *et al.*, 1986a; Rorison *et al.*, 1986b; Mark *et al.*, 2001) and make a comparison between factors of microclimate and/or vegetation from these sites. Other studies have quantified the effects of topographic variation in solar radiation by using transformed aspects (Lakhani and Davis, 1982) or topographic radiation indices derived from slope and aspect (Oke, 1987; McCune and Keon, 2002) as environmental variables. More recently, ecological studies have used models of solar geometry, coupled with a digital terrain model (DTM) to quantify potential clear-day direct solar radiation at the ground surface, integrated over a whole year or for a certain critical time period (Weiss et al., 1988). Such models may require adjustment by an empirical factor to allow for the frequently observed east-west asymmetry in vegetation distribution. One drawback with each of these approaches is that, while they allow comparisons between slopes in the same local or regional climate, they do not easily allow comparisons to be made between sites with different regional climate. In Perring's (1960) moisture gradient in chalk grassland, for example, it may be useful to directly compare the microclimate of a south-facing slope in the Yorkshire Wolds with a North-facing slope in North Dorset.

4.2 Approach to modelling topographic microclimate

4.2.1 Physical/empirical approaches

Any model involves simplification of the complexity of the real world (Krzanowski, 1998). To allow the topography-microclimate models described here to be

applicable to areas with different regional climates, they are designed to be based on physical processes, and to predict direct environmental gradients that are biologically relevant at the scale being studied. However, while complex physical-based energy and water flux models have been developed for both semi-natural systems (Flerchinger and Saxton, 1989a), they typically have high data requirements in terms of soil characteristics and vegetation canopy structure. The aim here is to produce "hybrid" models (Kang et al., 2000), based on physical processes, but incorporating robust simplifying empirical elements where necessary.

4.2.3 Landscape-scale variation in screen height climate

Spatial variation in microclimate due to variation in solar radiation is greatest at or near the boundary layer, and decreases with height above the ground (Geiger et al., 1995). Previous studies have found little or no consistent difference in air temperature and humidity at screen height (1.5 - 2 m) above short vegetation on different aspects (Påhlsson, 1974; Joyce, 2000). The models described here distinguish between such "macroclimatic" variables, as measured by conventional meteorological stations, which are considered to be spatially uniform across the landscape at the scale studied, and "microclimatic" variables such as surface temperature and soil moisture which vary over small distances due to the effects of topography. In reality, these divisions are two points along a continuum of scales at which spatial variation of climate occurs. A key initial assumption of the models described in this study is that several macroclimatic variables (air temperature, vapour pressure and wind speed measured at screen height, cloud cover and rainfall) are uniformly distributed across the landscape. However, it is noted that at a landscape scale both air temperature and vapour pressure are known to vary systematically with altitude and topographically-induced cold air drainage (Oke, 1987; Geiger et al., 1995; Joyce, 2000); rainfall and wind speed and direction are also influenced in complex ways by topography (Raupach and Finnigan, 1997). Spatially explicit modelling of these meso-scale processes is outside the scope of this study. Since the landscapes studied here measure less than 2 km across, and encompass a range of altitude of less than 100 m, systematic errors due to

landscape-scale variation in macroclimate under normal conditions are considered to be small. Where the data collected suggest that errors may be significant, and where suitable data are available, adjustments have been made to correct for the effect of altitude at and temperature inversions.

The approach to microclimate modelling adopted here can be summarised:

- Calculate hourly mean solar radiation flux perpendicular to the ground surface at different points in a landscape, incorporating the effects of slope, aspect and topographic shading.
- Using hourly mean solar, net and photosynthetically active radiation measured on a horizontal plane, adjust modelled solar radiation values for "real-time" cloud-conditions, and long-wave heat exchange.
- Derive simple models of surface temperature and soil moisture on a horizontal grassland surface from measured macroclimate data.
- Run soil moisture and surface temperature models using topographically corrected net radiation values.
- Validate models by comparison with measured soil moisture and temperatures on slopes.

4.3 Model development

4.3.1 Solar radiation

4.3.1.1 Clear-day solar radiation

Many previous studies have been produced on the subject of modelling potential (clear-sky conditions) global solar radiation on inclined surfaces, for a variety of end-uses including engineering, architecture, hydrology, agriculture and ecology (Isard, 1983; Hay and McKay, 1985; Nunez, 1980; Oliver, 1991; Varley et al., 1996; Olmo et al., 1999). Global solar radiation consists of both a direct beam and a diffuse component. The angle of incidence of direct beam radiation on a surface is a function of solar elevation and azimuth, slope angle and aspect. This can be

calculated for any combination of slope, aspect, latitude and time of year using trigonometric equations or tables such as those in Oke (1987). Approaches to quantifying clear-sky global radiation differ mainly in the way they quantify diffuse radiation. Models differ in the method of calculating the transmission and scattering of radiation through the atmosphere, and thus the proportion of direct beam and diffuse radiation, and in the assumption that the diffuse component of the radiation is isotropic (equal from all directions of the sky dome) or anisotropic (distributed depending on the position of the sun and the horizon). In mountainous or snow covered terrain the effect of reflected radiation from land surfaces may also be incorporated (Olyphant, 1986).

P. R. J. North (Department of Geography, University of Wales Swansea) supplied the modelled global solar insolation data used in this study. The insolation model (North, 1994) uses an assumption of anisotropic diffuse radiation and calculates atmospheric transmission from the model LOWTRAN (Kneizys et al., 1988). Hourly mean values of direct and diffuse radiation at a horizontal plane were calculated for the latitude of each field site under two sets of simulated atmospheric conditions: (a) clear sky and (b) low altostratus clouds. These scenarios were intended to represent likely maximum and minimum hourly values for solar insolation at each AWS. The clear sky modelled values give good agreement with measured AWS values on clear days throughout the year (figure 4.1).

For most days, however, measured irradiance values are characterised by deviations from the ideal clear-sky curve due to changing cloud conditions. Furthermore, on days with partial cloud cover, during time periods when the sun is not obscured by cloud, global irradiance may exceed the values predicted under clear-sky conditions, due to the increased diffuse component from a partially cloudy atmosphere.

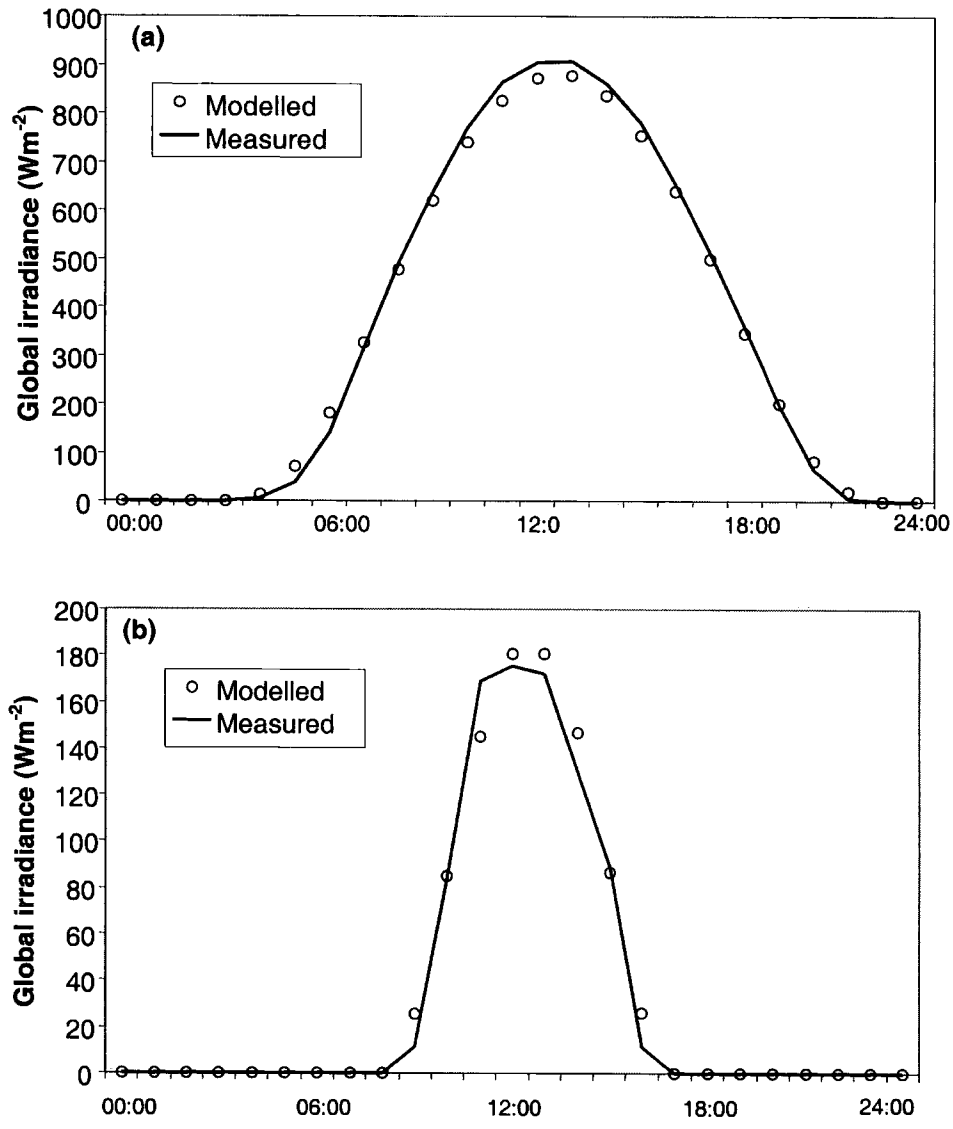

Figure 4.1: Example data comparing hourly mean modelled and measured solar radiation at Hambledon Hill AWS on days with clear skies at contrasting times of year: (a) July 5th and (b) December 27th 2001. Note different scales on y-axis.

4.3.1.2 Modelling variable cloudiness with AWS data

The LOWTRAN atmospheric model used in the insolation model can specify a range of atmospheric conditions other than the clear day and low altostratus scenarios modelled (Kneizys et al., 1988). However, sufficiently detailed calibration data on cloud conditions is not available from ground-based instruments, particularly on an hourly time scale. In this study no direct information

on cloud cover directly applicable to an atmospheric transmissivity was available. Empirical correlations between recorded cloud cover estimates and direct/diffuse radiation estimates have been used to estimate cloud-adjusted solar insolation integrated over longer time scales (Nunez, 1980), but are likely to be a considerable source of error in a model based on hourly data. Isard (1983) has described the use of a "clearness index" – the ratio of measured global to calculated maximum possible global radiation – as an empirical tool to predict the ratio of direct and diffuse radiation. A related approach is used here to derive a clearness index for each hour:

$$c = \frac{S\downarrow_{aws} - S\downarrow_{cloud}}{S\downarrow_{clear,aws} - S\downarrow_{cloud}} \qquad \textbf{Equation 4.1}$$

Where c is a clearness index, $S\downarrow_{aws}$ is measured global solar insolation at the AWS, $S\downarrow_{clear,aws}$ is modelled insolation under clear-sky scenario, $S\downarrow_{cloud}$ is modelled insolation under overcast scenario. Each hourly value of c may be considered as an index of average cloud conditions over that hour. A value of 0 represents fully overcast and 1 represents fully clear-sky conditions. Values over 1 are possible during the partially cloudy scenario outlined above.

Hourly clear-sky scenario global insolation values, $S\downarrow_{clear,\ plot}$, were calculated for all vegetation and datalogger plots by P. R. J. North, using the DTMs to simulate topographic shading and field-measured slope and aspect values.

Under overcast conditions insolation is virtually isotropic (North, 1994), so $S\downarrow_{cloud}$ is not modelled separately for each plot.

Clear-sky global solar insolation at each plot is adjusted to estimate real conditions of variable cloud using the equation:

$$S\downarrow_{plot} = S\downarrow_{cloud} + c(S\downarrow_{clear,plot} - S\downarrow_{cloud}) \qquad \textbf{Equation 4.2}$$

4.3.2 Photosynthetically active radiation (PAR)

Olseth and Skartveit (1997) have derived models of PAR over complex terrain, treating direct and diffuse radiation separately, and allowing for atmospheric water content, under the assumption that water vapour extinction of radiation occurs only at non-PAR wavelengths. However, when hourly mean PAR data from both weather stations (full data sets, n = 38876) were plotted against solar insolation (figure 3.25), the relationship was found to be surprisingly linear. Since these data represent a wide range of solar elevation angles and atmospheric conditions it was concluded that for the purpose of this study PAR above the canopy can be adequately modelled as a simple linear function of incoming solar radiation:

$$PAR = aS\downarrow \qquad \textbf{Equation 4.3}$$

Using linear regression on the data shown in figure 4.2, a value of a=0.184 was derived (R^2 = 0.998).

4.3.3 Net radiation

The net radiation flux, rather than the incoming solar insolation, is needed to resolve the heat and moisture balance of a surface. Net radiation can be approximated as a linear function of solar radiation (Oliver, 1991). Figure 4.3 shows solar radiation and net radiation for the same data set as figure 4.2.

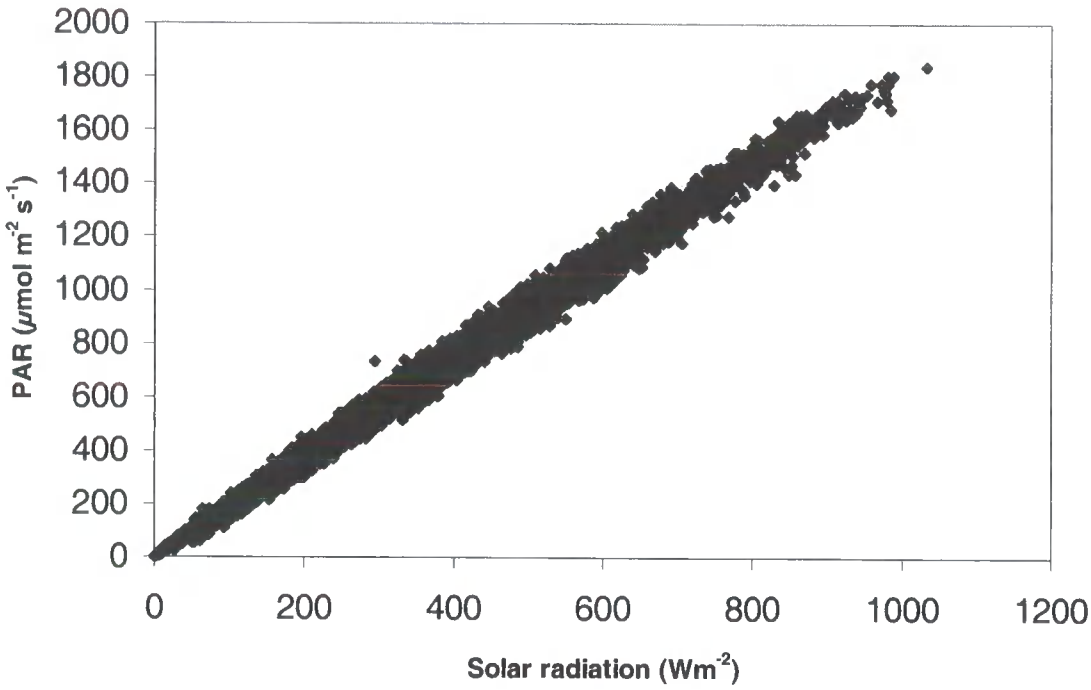

Figure 4.2: Hourly mean global solar radiation $S\downarrow$ vs PAR measured at both AWS sites.

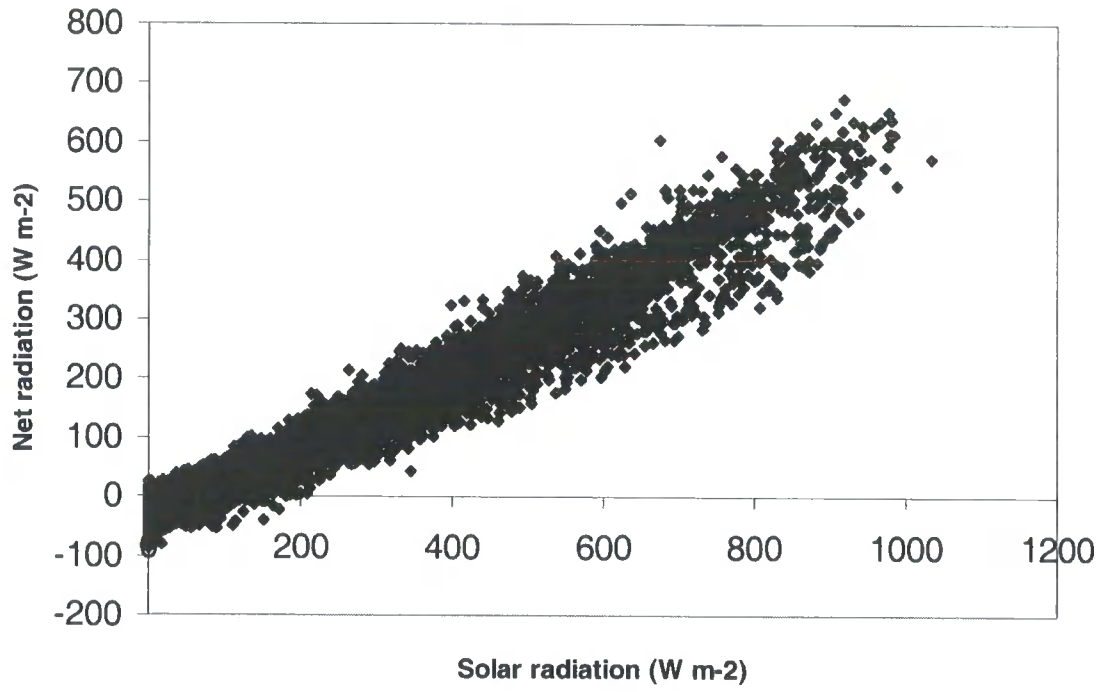

Figure 4.3: Hourly mean global solar radiation $S\downarrow$ vs net radiation R_n measured at both AWS sites.

However, a linear relationship does not apply when net radiation is negative and the hourly data shows considerable scatter when net radiation is positive. A more accurate estimate of hourly net radiation from solar radiation may be derived from considering short-wave and long-wave radiation separately. Net radiation is the sum of incoming solar (short-wave) radiation, outgoing (reflected short-wave) solar radiation, incoming long-wave radiation and outgoing long-wave radiation:

$$R_n = S\downarrow + S\uparrow + L\downarrow + L\uparrow \qquad \textbf{Equation 4.4}$$

Where R_n is net radiation, $S\uparrow$ is reflected radiation, $L\downarrow$ is incoming long-wave radiation, $L\uparrow$ is outgoing long-wave radiation. Reflected short-wave radiation depends on the albedo α of the surface:

$$S\uparrow = \alpha S\downarrow \qquad \textbf{Equation 4.5}$$

The albedo of a vegetated surface is largely dependent on its height, with short grass surfaces having a value of around 0.23 (Monteith and Unsworth, 1990). This value is used in the present study.

The long-wave radiation emitted by a surface is described by the Stefan-Bolzmann equation:

$$L\uparrow = \varepsilon\sigma T_k^{\,4} \qquad \textbf{Equation 4.6}$$

Where T_k is the surface temperature in Kelvin, ε is the emissivity of the surface, and σ is the Stefan-Bolzmann constant (equal to 5.67×10^{-8} W m^{-2} K^{-1}). Incoming long-wave radiation depends on atmospheric conditions, and is largely dependent on cloud-base temperature under cloudy conditions.

Empirical methods for estimating incoming daily or longer-term long-wave radiation from AWS data exist (Burman and Pochop, 1994). In this study, net long-wave exchange at the AWS is calculated from the total net radiation and global solar radiation by rearranging equation 4.4 and 4.5:

$$L_{n,aws} = L\downarrow_{aws} + L\uparrow_{aws} = R_{n,aws} - S\downarrow_{aws}(1-\alpha) \qquad \textbf{Equation 4.7}$$

Where $L_{n,aws}$ is net long-wave exchange at the AWS. Since $R_{n,\,aws}$ and $S\downarrow_{aws}$ are measured, and α is estimated at 0.23 for a grass surface, net long-wave exchange $L_{n,aws}$ at the AWS can be estimated. Extrapolating this value of L_n to other points in the landscape allows for temporal variation in long-wave radiation flux due to changes in the height and temperature of the cloud base. However, it also introduces a source of error into the model; incoming long-wave exchange varies spatially with the topographic sky-view of a plot, and outgoing long-wave radiation varies with surface temperature and surface emissivity according to equation 4.6. However, assuming an emissivity of 0.97 for a grass surface (Burman and Pochop, 1994), errors in R_n due to differences in surface temperature will be small (in the region of 6 Wm^{-2} per K, calculated using equation 3.6). Variation in sky-view is likely to be important only in areas of extreme relief. For the purposes of this study, therefore, long-wave radiation at all plots is considered to be equal to that at the AWS. The net radiation at a plot is therefore calculated as:

$$R_{n,plot} = S\downarrow_{plot}(1-\alpha) + L_{n,aws} \qquad \textbf{Equation 4.8}$$

The steps in modelling radiation on slopes are summarised in flow chart in figure 4.4. SITERAD, the FORTRAN 90 program used to calculate hourly time series of radiation on slopes is listed in full in appendix 1.

4.3.4 Near surface temperatures

The radiation model described here regards the ground-vegetation surface of grassland as a plane parallel to the slope of the land. In reality the vegetation-soil "surface", even in short grassland, is not a simple plane at all but consists of many layers of leaves and stems at different orientations, overlapping a heterogeneous soil surface. Miller (1971) showed that individual leaves within a canopy could vary considerably in their temperature depending on their orientation with respect to the sun. Energy absorbed by the vegetation is largely dispersed into the atmosphere through convection and radiation as sensible heat or converted to latent heat through evapotranspiration; in temperate climates and where a ground cover of vegetation or litter is continuous, the flux of heat downwards into the soil during

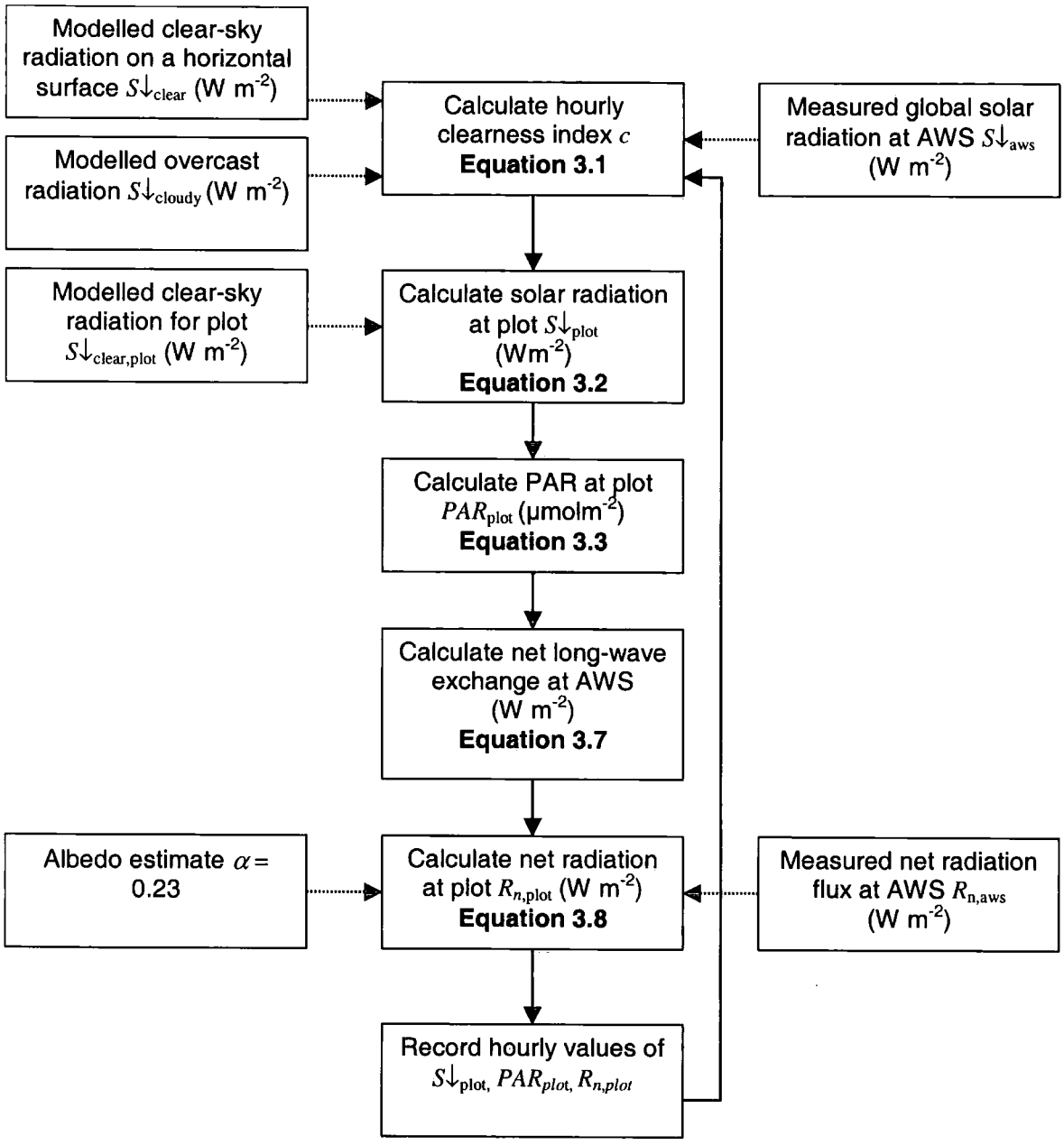

Figure 4.4: Model of radiation on slopes.

the day is low compared to the other components of the energy balance (Oliver et al., 1987). Under these conditions the soil surface temperature is determined by heat exchange with the overlying vegetation/air layer through convection, conduction and radiation. At patches of bare soil or where the canopy is thin or discontinuous, the soil surface is heated directly by radiation and soil surface temperature may exceed that of vegetation.

Soil temperature at any depth is determined by the heat flux at the soil surface (the upper boundary conditions) and the thermal properties of the soil itself (van Wijk and de Vries, 1963b). The thermal properties of soil may vary with depth, and as a function of water content; however, an assumption of a spatially and temporally homogenous soil is often used (de Vries, 1963). For a model of soil temperature close to the surface, this assumption is probably reasonable. A fundamental problem in modelling soil temperatures from meteorological data is in establishing the boundary conditions at the upper soil surface. The energy balance of the soil surface may be modelled explicitly if detailed information on the structure of the canopy, litter and soil are known (Flerchinger and Saxton, 1989a, b; Thunholm, 1990). Mathematical studies of heat transfer in soils have used harmonic temperature variations at the soil surface as an approximation of more complex diurnal or annual variations. However, in a complex landscape solar radiation may vary considerably both spatially and temporally due to the effects of topography, vegetation cover and cloudiness, and heat flux across the boundary layer may change rapidly. In order to quantify the differences between different sites in the landscape, more realistic boundary conditions are necessary. Thunholm (1990) compares two approaches; using air temperature as a boundary condition and explicitly calculating the energy balance at the soil surface. Other studies have derived empirical relationships between soil surface temperature and air temperature from long-term data sets (Campbell, 1985; Franko et al., 1995; Kang et al., 2000). This approach has the advantage that data are readily available; however, it is unsuitable for this study since it does not explicitly model the effects of radiation on surface temperature; any empirical correction factors are likely to be site specific and dependent on the time of year.

Since sensible heat exchange at the soil surface is likely to be with the layer of air/vegetation close to the ground, rather than screen height air temperature, it is assumed that some measure of sward temperature is likely to provide a better upper boundary condition for soil temperature than screen height air temperature. Following the meteorological practice of measuring grass minimum temperatures at 50 to 100 mm above the soil surface in a short grass sward, "sward

temperature" is here taken to be the air temperature measured by a shaded thermistor at 100 mm height. The actual temperatures of components of the vegetation or invertebrates at this height in the sward may differ from sward temperature depending on whether they are in sun or shade; sward temperature is assumed to be a representative average temperature of a layer of air and shaded vegetation at this height above the ground. Data from both AWS sites suggest that daily or longer-term mean soil temperatures would be more accurately modelled as a lagged and dampened response to sward temperatures than screen air temperatures (figure 4.5), particularly during the summer months when the effects of solar radiation are greatest.

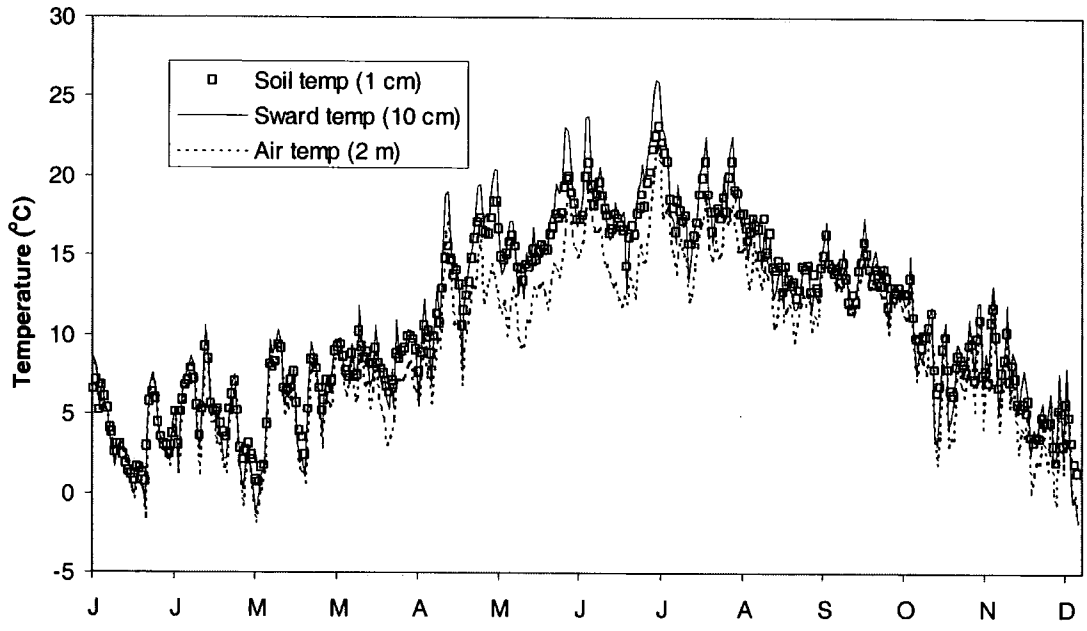

Figure 4.5: Hourly mean soil (squares) sward (solid line) and air (dashed line) temperatures at Hambledon Hill AWS, 2001.

4.3.4.1 Sward temperature

Sward temperature is modelled as both a potentially important environmental variable in its own right and useful as a boundary variable for a soil temperature model. The surface temperature model described here is a compromise between an explicit physical energy balance model and an empirical correlation of screen-

height meteorological variables and surface temperature. For the purposes of modelling hourly sward temperature several simplifying assumptions are made. It is assumed that the most important energy fluxes determining grass temperature are those due to radiation and convection that occur at the vegetation-atmosphere boundary; heat fluxes into the soil are smaller due to relatively poor coupling between vegetation and soil. Latent heat exchanges are also considered to be negligible. The heat capacity of the vegetation is considered to be small so that, compared to the hourly time scale of the model, surface temperature rapidly comes into equilibrium with environmental conditions and is considered to be at a steady state. The steady state heat balance for a hypothetical surface with negligible latent heat flux is (Monteith and Unsworth, 1990):

$$R_n = \rho c_p (T_0 - T) / r_{HR}$$
$$(T_o - T) = (r_{HR} / \rho c_p) R_n \qquad \textbf{Equation 4.9}$$

Where R_n is net radiation flux per unit area, T_0 is the surface (sward) temperature, T is air temperature, ρ is the density of air, c_p is the specific heat of air at constant pressure and r_{HR} is a resistance for the loss of sensible heat. The difference between the surface temperature and the ambient temperature is a linear function of net radiation R_{ni} with gradient $r_{HR}/\rho c_p$. This term is a measure of the thermal coupling of the surface to the atmosphere. If equation 4.9 is applied to sward temperature, assuming the vegetation to act like a surface, while both ρ and c_p are constant, r_{HR} varies as a function of both the structure of the vegetation and wind speed.

To test the validity of this approach and establish a relationship between $r_{HR}/\rho c_p$ and the wind speed at 2 m over a short grass surfaces, measured sward temperature data from the Hambledon Hill AWS was examined. All hourly data records from September 2000 to August 2001 were sorted into wind speed u_2 categories and for each category a linear regression of $(T_0 - T)$ against R_{ni} was carried out, with the regression line through the origin. From equation 4.9, the gradient of the line is equal to $r_{HR}/\rho c_p$.

Table 4.1: Values of $r_{HR}/\rho c_p$ derived from linear regression of R_n against (T_0-T) for hourly mean data from Hambledon Hill AWS, sorted by wind speed.

u_2 (ms^{-1})	$r_{HR}/\rho c_p$	R^2	p
0-1	0.0395	0.834	<0.001
1-2	0.0332	0.907	<0.001
2-3	0.0323	0.916	<0.001
3-4	0.0295	0.927	<0.001
4-5	0.0261	0.903	<0.001
5-6	0.0246	0.906	<0.001
6-7	0.0200	0.913	<0.001
7-8	0.0194	0.862	<0.001
8-9	0.0180	0.897	<0.001
9-10	0.0148	0.886	<0.001
10-11	0.0149	0.894	<0.001
11-12	0.0149	0.896	<0.001
12-13	0.0145	0.912	<0.001
13-14	0.0156	0.887	<0.001
14-15	0.0166	0.619	<0.001

For each wind speed category, the temperature difference between surface and screen height is linearly correlated with net radiation, but the slope of this relationship, depending on the coupling of the surface to the atmosphere, decreases with increasing wind speed. The surface temperature probe at Hambledon Hill was inside the grazing exclosure, in a sward dominated by the tussock-forming grass *Dactylis glomerata* at an average height of 250 mm in mid-summer. This sward height is significantly greater than that at much of the grazed areas at both field sites. The same process was repeated using data from the same period at the Sylvan Dale AWS and from March to August 2002 at datalogger site D7. Surface temperatures at both these sites were recorded in

Table 4.2: As table 4.1, data from Sylvan Dale AWS.

u_2 (ms^{-1})	$r_{HR}/\rho c_p$	R^2	p
0-1	0.0219	0.634	<0.001
1-2	0.0149	0.680	<0.001
2-3	0.0136	0.697	<0.001
3-4	0.0106	0.664	<0.001
4-5	0.0087	0.605	<0.001
5-6	0.0109	0.720	<0.001
6-7	0.0104	0.764	<0.001
7-8	0.0090	0.749	<0.001
8-9	0.0107	0.846	<0.001
9-10	0.0079	0.893	<0.001
10-11	0.0064	0.755	<0.001
11-12	0.0077	0.848	<0.001

Table 4.3: As table 4.1, data from Sylvan Dale datalogger plot D7, Feb-August 2002.

u_2 (ms^{-1})	$r_{HR}/\rho c_p$	R^2	p
0-1	0.0245	0.456	<0.001
1-2	0.0146	0.752	<0.001
2-3	0.0127	0.689	<0.001
3-4	0.0120	0.769	<0.001
4-5	0.0125	0.736	<0.001
5-6	0.0156	0.693	<0.001
6-7	0.0173	0.683	<0.001
7-8	0.0154	0.756	<0.001
8-9	0.0182	0.844	<0.001
9-10	0.0134	0.681	<0.001
10-11	0.0186	0.936	<0.001

grazed swards of average height 100 mm dominated by fine-leaved *Festuca* species, more typical of the sward structure of species-rich chalk grassland. For the datalogger site, values of T and u_2 were obtained from the Sylvan Dale AWS and net radiation was modelled as previously outlined. Tables 3.1 show the results of these regressions.

Figure 4.6 shows values of $r_{HR}/\rho c_p$ plotted against u_2 for each data set. At Hambledon, the data form a well-defined curve suggesting a clear relationship between wind speed and resistance for heat exchange. The two data sets from the Sylvan Dale show generally lower values of $r_{HR}/\rho c_p$ for equivalent values of u_2. This is consistent with the shorter turf height at both these sites. These two curves are generally similar, except at higher wind speeds. This may be due to errors associated with extrapolating wind speeds measured at the AWS to a site on a slope a considerable distance away.

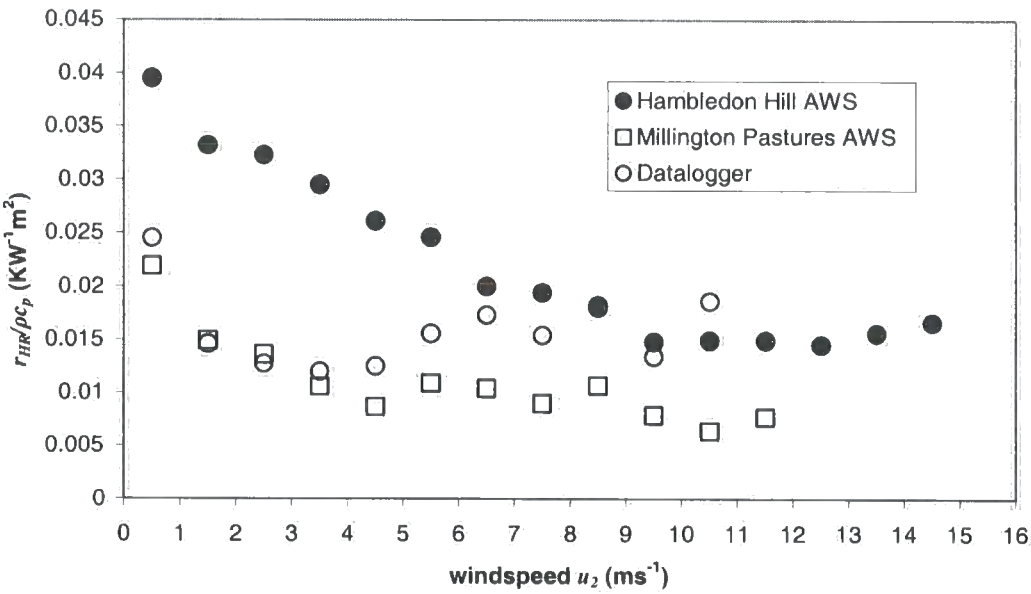

Figure 4.6: Values of $r_{HR}/\rho c_p$ from tables 4.1-4.2 plotted against mid-point windspeed.

Between wind speeds of 0 and 10 ms^{-1}, the points for Hambledon Hill approximate a straight line. Linear regression for these points gives an intercept of 0.0386 and slope of 0.00256 ($R^2 = 0.976$, $p < 0.001$). Applying these values to equation 4.9,

the following semi-empirical equation is derived for the surface temperature at the 20 cm sward at Hambledon Hill AWS:

$$T_0 = T + (0.0386 - 0.00256u_2)R_n \quad \textbf{Equation 4.10}$$

Due to the rather arbritrary nature of fitting a curve through the points of the short turf data from Millington AWS and the datalogger site, two separate equations were derived using estimates of $\rho c_p / r_{HR}$ for the cases where $u_2 < 1$ and $u_2 > 1$:

If $u_2 < 1$ $\quad T_0 = T + 0.022R_n$ **Equation 4.11**

If $u_2 > 1$ $\quad T_0 = T + 0.013R_n$ **Equation 4.12**

4.3.4.2 Soil temperatures

Assuming that, for a layer of soil from 0 to 50 mm depth, the energy flux at the soil surface through radiation is proportional to the surface net radiation (van Wijk and de Vries, 1963a):

$$Q_{rad} \propto R_n \quad \textbf{Equation 4.13}$$

Energy flux between soil and the air near the surface is proportional to the temperature difference between the soil and the air (Campbell, 1985):

$$Q_{air} \propto (T_{air} - T_{soil}) \quad \textbf{Equation 4.14}$$

Energy flux between the soil layer and the layer below is proportional to the temperature difference between layers:

$$Q_{soil} \propto (T_{soil1} - T_{soil2}) \quad \textbf{Equation 4.15}$$

The change in temperature of a layer of soil during a short period of time is proportional to the net heat flux of the layer, so can be expressed as:

$$\Delta T_s = aR_n + b(T_a\text{-}T_s) - c(T_s - T_{sx}) \qquad \textbf{Equation 4.16}$$

Where T_s is the mean soil temperature between 0 and 50 mm depth, T_a is the sward temperature, T_{sx} is the mean soil temperature in a soil layer below, and a, b and c are constants, functions of the thermal conductance, depth of soil layer, time period, heat capacity of the soil layers and canopy transmittance.

Assuming that the layer of soil beneath has no heat flux at its base, the change in temperature of this layer during the same time period can be expressed as:

$$\Delta T_{sx} = d(T_s - T_{sx}) \qquad \textbf{Equation 4.17}$$

Using suitable values for the constants, these equations may be used to estimate time series of mean daily temperatures for two soil layers, using a forward difference solution (Campbell, 1985). Data inputs are time series of mean daily sward temperature and net radiation. Using modeled net radiation and sward temperature data, the model was run for datalogger run D7, and values of a = 0.01, b = 0.5, c = 0.5, d = 0.5 were found to give reasonable results. Alternative values of b, c, and d of the same order of magnitude give similar results, suggesting that this model is relatively insensitive to soil properties.

The steps in modelling radiation on slopes are summarised in flow chart in figure 4.7. SITETEMP1 and SITETEMP2, the FORTRAN 90 programs used to calculate soil and surface on the slopes is listed in full in appendix 2.

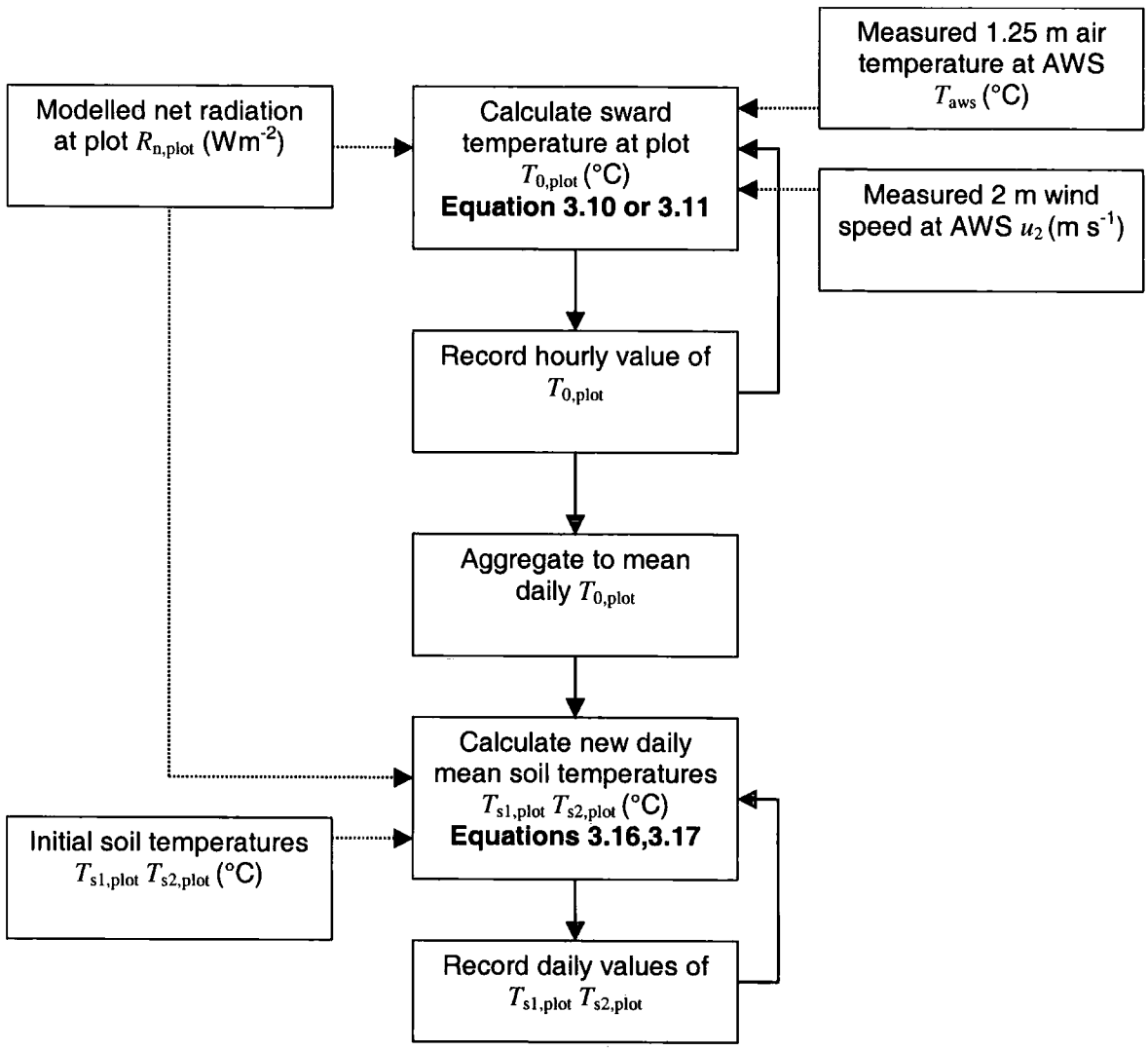

Figure 4.7: Model of hourly mean sward and daily mean soil temperature on slopes.

4.3.5 Soil moisture

4.3.5.1 Estimating evapotranspiration

Evapotranspiration from a vegetated surface can be calculated from hourly weather data using the FAO-56 method (Allen et al., 1998), based on the Penman-Monteith equation (Penman, 1948). The equation for a hypothetical short grass with a height of 0.12 mm, a surface resistance of 70 sm^{-1} and an albedo of 0.23 is (Allen et al., 1998):

$$ET_0 = \frac{0.4808\Delta(R_n - G) + \gamma \frac{37}{T + 273.2} u_2 \ (e_s - e_a)}{\Delta + \gamma(1 + 0.34u_2)}$$ **Equation 4.18**

Where

ET_o potential evapotranspiration

R_n net radiation (MJ $m^{-2}h^{-1}$)

G soil heat flux (MJ $m^{-2}h^{-1}$)

T air temperature (°C)

e_s saturation vapour pressure at air temperature (kPa)

e_a vapour pressure of air (kPa)

u_2 wind speed at 2 m (ms^{-1})

Δ slope of saturation vapour pressure curve at air temperature (kPa C^{-1})

γ psychrometer constant (kPa C^{-1})

The derivation of each of these terms from hourly AWS data, from Allen (1998) is described in appendix 4.

The FAO-56 version of the Penman Monteith equation is physically based, with empirical corrections for different surfaces; the form shown has been validated for short grass surfaces under a range of climatic conditions (Allen, 2000). The equation requires inputs of screen-height climatic variables, and so in theory it can be modified to estimate evapotranspiration on slopes, assuming a homogeneous climate at screen height and simply changing the value of R_n. The numerator of the equation can be split into two terms; a "radiation term", dependent on net radiation, and a "ventilation term" dependent on vapour pressure difference and wind speed. The ventilation term is assumed constant across the landscape, while the radiation term varies with topography.

4.3.5.2 Modelling soil moisture

Blyth (2002) has pointed out that most existing soil moisture models have been designed with either atmospheric or hydrological modelling as an end use, and that

modelled soil moisture parameters often "soak up" errors in the rest of the model to accurately reproduce the surface energy or water balance for these purposes. For ecological studies, an accurate model of absolute soil moisture over short timescales is desirable. Few soil moisture models are calculated to accurately predict soil moisture near the surface for ecological purposes. Naden *et al.* (2000 , 2001) have modelled soil moisture at a landscape scale at five sites of ecological interest, including one site on chalk at Purbeck, Dorset. The main process involved in distributing soil moisture in this model is assumed to be lateral movement of water down slope, and the basic unit of the model is a slope from the watershed boundary to stream. No account is taken of aspect of slope. However, while lateral movement of water is likely to be important in redistributing soil water on less permeable rocks, hydrological models of water movement on chalk soils emphasise vertical movement of water (Mahmood-ul-Hassan and Gregory, 2002; Ragab et al., 1997). The assumption that vertical movement of water dominates is perhaps reasonable for an ecological soil moisture model, since overland flow or surface water is rare on chalk. If lateral movement of water within the soil does occur, it is likely to occur only after a period of heavy rain when the soil and underlying chalk are close to saturation point and spatial variation in soil moisture is minimal. During ecologically critical periods of summer drought, vertical flow of water is likely to dominate.

Ragab et al, (1997) modelled soil moisture deficits accurately on sites on chalk and sandstone for the purposes of estimating groundwater recharge using a version of the Penman Monteith equation and a four root layer model (FRLM). In the FRLM model, the rooting zone is divided into four layers and vertical movement of water is modelled between these layers and the atmosphere. Evapotranspiration from the vegetation is extracted from each root layer according to a stress index for each layer based on its water content. A similar four-layer approach is used here, and the concept of a stress index is used, but the equations defining the stress index and governing water extraction by roots and flow between layers differ from Ragab's model. In the present study the depth of the top root layer corresponds to the depth of the organic soil layer, measured in the field as the depth a 3 mm diameter rod into the soil can be inserted before hitting solid chalk. Water is

preferentially extracted by plants from this layer, and only extracted from lower layers when this organic soil layer is stressed. The lower three layers are 100 mm, 200 mm and 300 mm thick respectively. A set of equations governs vertical water flow between layers at an hourly time step. If the top root layer is below saturation point θ_{sat}, the percolation into the top layer is considered to be equal to rainfall:

$$p_1 = P \qquad \textbf{Equation 4.19}$$

Where P is total hourly rainfall, p_i is percolation into root layer i.

If the water content θ_{i-1} in any root layer i-1 is above field capacity, and the layer below it has a lower water content, the excess water flows downwards to the lower soil layer at each hourly time step:

$$\text{If } \theta_{i-1} => \theta_i \qquad p_i = z_i(\theta_{i-1} - \theta_i) \qquad \textbf{Equation 4.20}$$

Where z_i is the depth of soil layer i.

If the water content in a root layer falls below the stress point θ_{sp}, the stress index s_i is defined as the proportion of free water between the stress and wilting point θ_{wp} (s_i is 1 when there is no soil moisture stress, 0 at wilting point):

$$s_i = (\theta_i - \theta_{wp})/(\theta_{sp} - \theta_{wp}) \qquad \textbf{Equation 4.21}$$

If the stress index of the top root layer is 1, then the water extracted from this layer at each time step is equal to E_t; if the stress index is less than 1, the proportion of E_t extracted from this layer e_i is equal to the stress index. The remaining E_t is extracted from the root layer below according to the stress index of this layer:

$$\begin{aligned} e_1 &= s_1 \\ e_2 &= s_2(1 - e_1) \\ e_3 &= s_3(1 - (e_1 + e_2)) \\ e_4 &= s_4(1 - (e_1 + e_2 + e_3)) \end{aligned} \qquad \textbf{Equations 4.22-4.25}$$

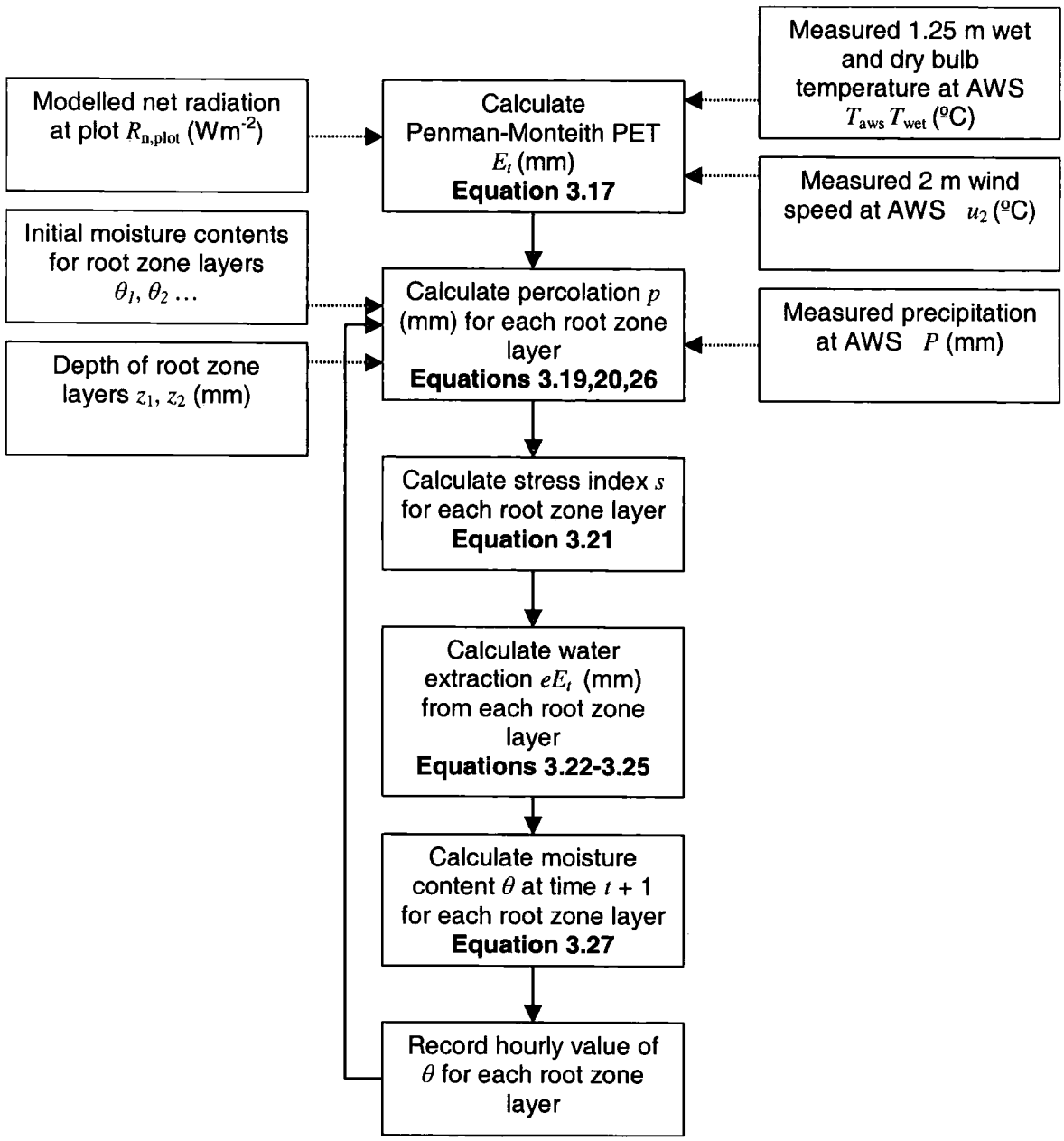

Figure 4.8: Model of hourly mean soil moisture on slopes.

The lower soil layer drains to field capacity at a rate defined by:

$$p_4 = d(\theta_4 - \theta_{fc}) / (\theta_{sat} - \theta_{fc}) \qquad \textbf{Equations 4.26}$$

Where d is a constant, θ_{fc} is field capacity.

At each time *t*, the new soil moisture of each layer is calculated by adding the percolation into the layer to the soil moisture at the previous time step *t-1* and subtracting evapotranspiration and percolation out of the layer:

$$\theta_{i,t+1} = \frac{\theta_{i,t} + p_i - (e_i Et) - p_{1+1}}{z_i} \qquad \textbf{Equations 4.27}$$

The steps in modelling soil moisture on slopes are summarised in flow chart in figure 3.31. SITEMOISTURE, the FORTRAN 90 programs used to calculate soil and surface on the slopes is listed in full in appendix 3.

4.4 Model testing and validation

Data collected from the mobile dataloggers at Sylvandale were used to test the models of solar insolation, sward and soil temperatures. Data sets used in model calibration were not used in the test.

4.4.1 Solar radiation

Figure 4.9 shows example time series of measured and modelled solar insolation on opposing N- and S- facing slopes for three days in September 2000. The model qualitatively predicts the differences between slopes on clear, overcast and mixed days. A quantitative measurement of error in the model over five datalogger runs is shown in table 4.4.

The positive mean errors suggest that the model consistently overestimates measured values. However, both mean errors and rms errors are small compared to the observed differences in insolation between slopes. A considerable portion of the error in this model might be attributed to discrepancies between the measurement of the angle of slope and aspect of the whole plot by clinometer and compass, and the angle at which the pyranometer was mounted, by sight parallel to the ground surface. The validation method would be improved if the precise slope and aspect of the pyranometer were used in the insolation model. An

unknown proportion of error may be attributed to the method for allowing for variable cloudiness.

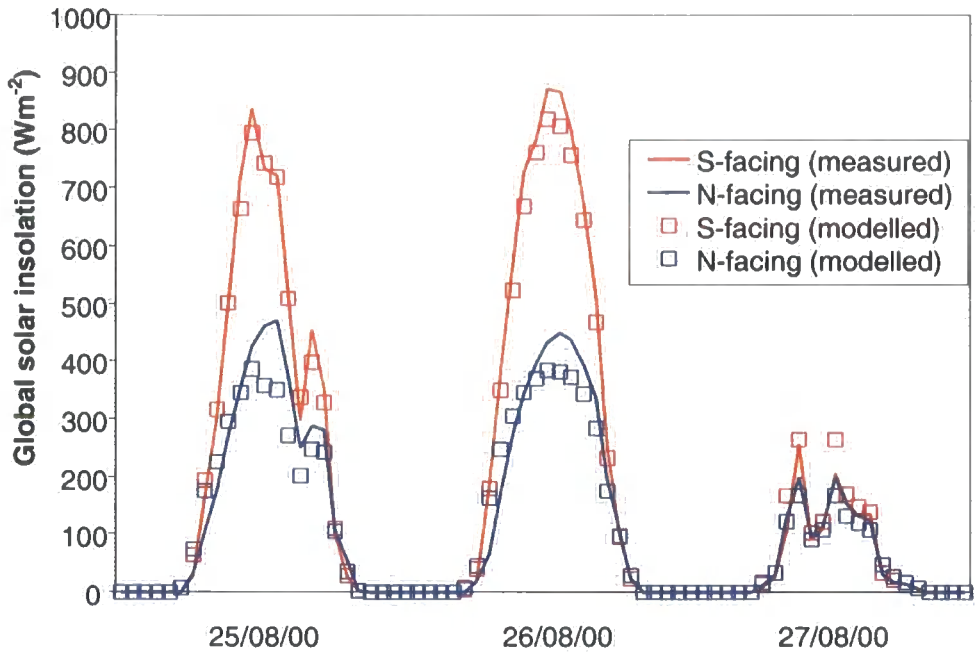

Figure 4.9: Example hourly mean modelled and measured solar radiation on slopes, 25th – 27th August 2000.

Table 4.4: Mean and rms errors of modelled vs. measured solar insolation from datalogger runs 2000-2002

Start date	End date	Days	Plot	Mean error (Wm^{-2})	RMS error (Wm^{-2})
25th Aug 00	19th Sep 00	25	D3	8.58	44.00
		25	D4	22.00	43.46
30th Nov 00	18th Jan 01	50	D8	2.81	12.61
15th Feb 01	11th Mar 01	24	D5	-2.43	33.13
11th May 01	13th Aug 01	85	D8	37.65	81.34
24th Feb 02	18th Aug 02	123	D7	6.75	74.35
		137	D5	39.17	114.76

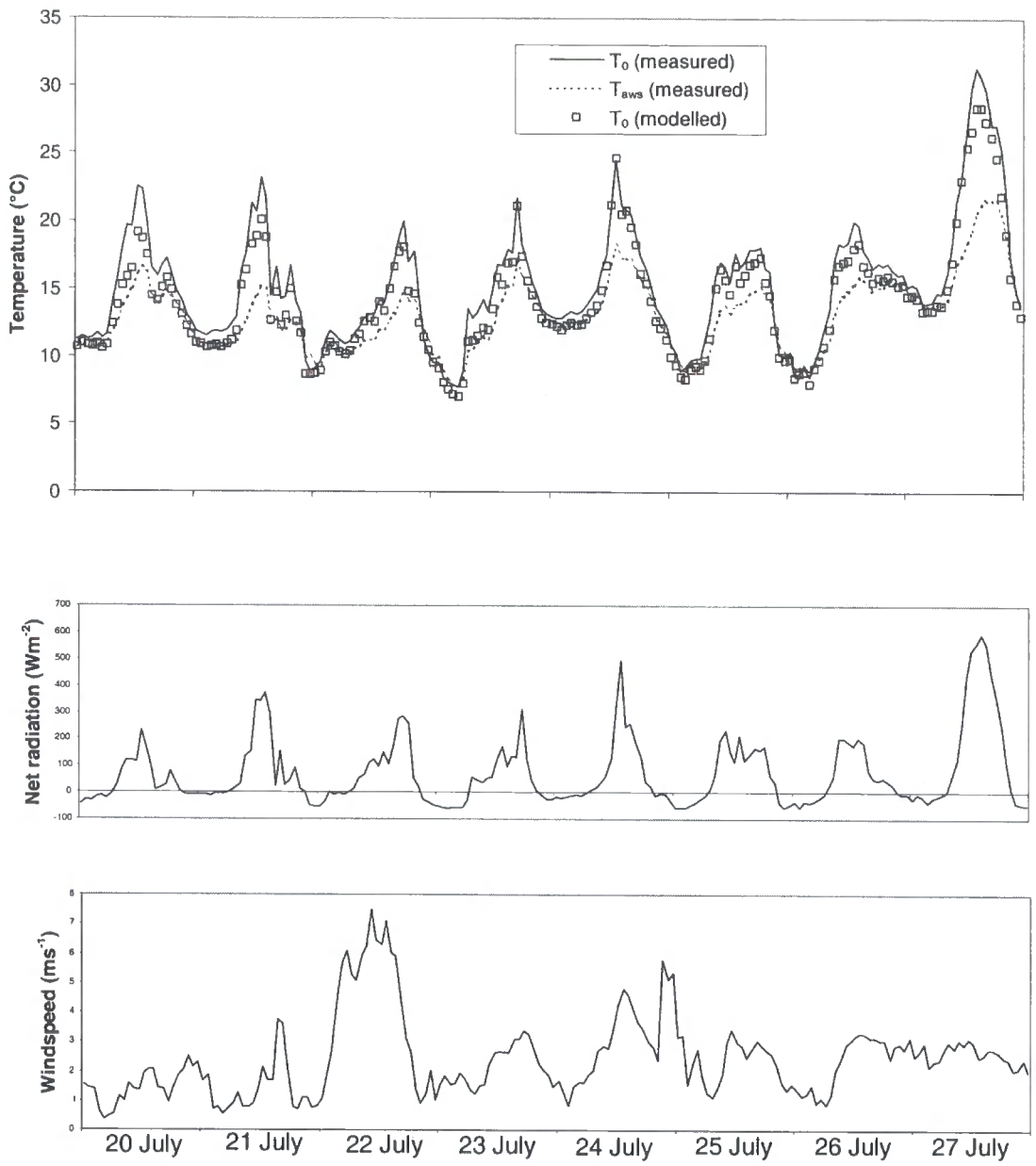

Figure 4.10: Hourly mean modelled and measured sward temperature (a), measured net radiation (b) and wind speed (c) for Sylvan Dale AWS, for the period 20th-27th July 2002.

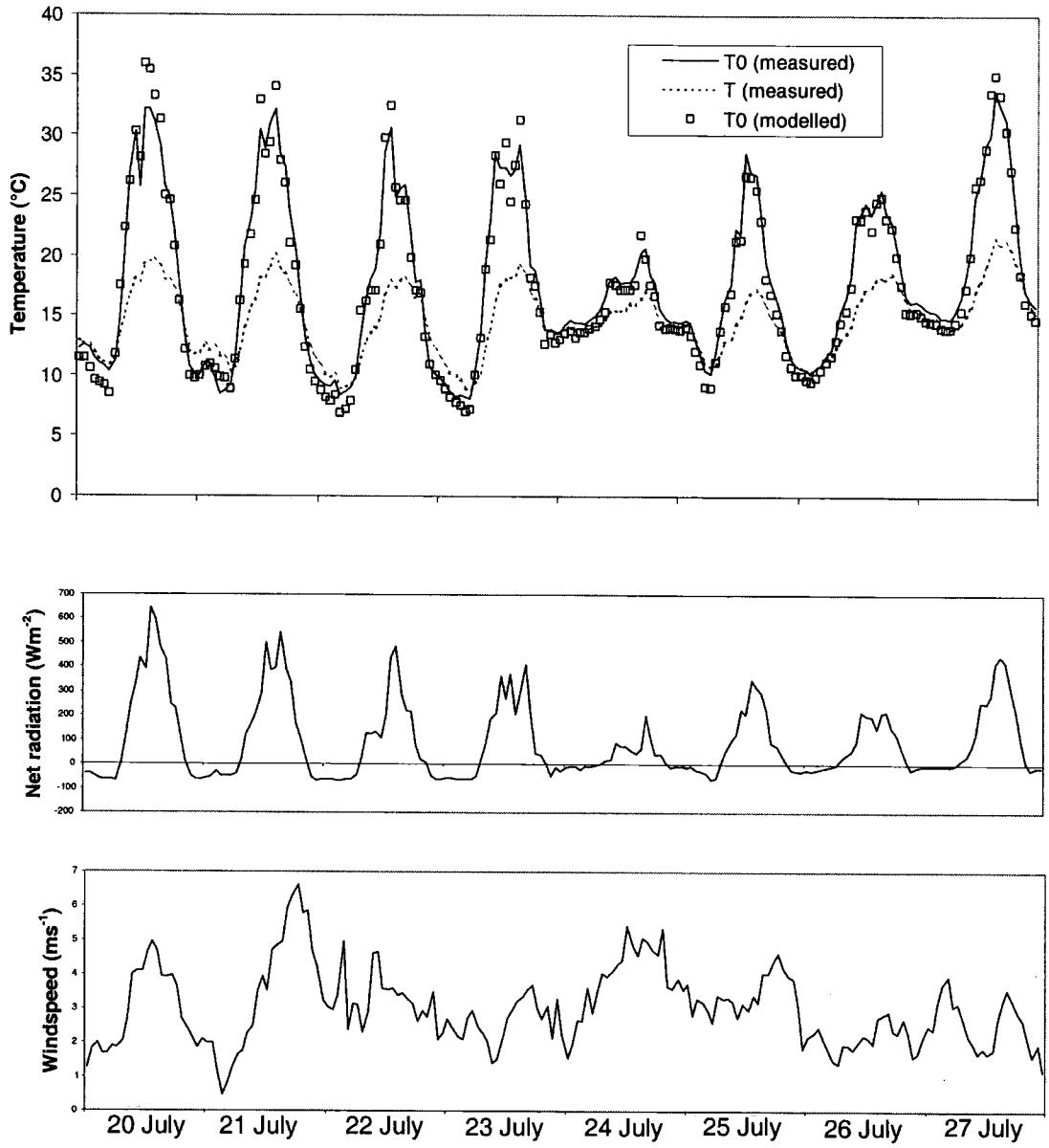

Figure 4.11: Hourly mean modelled and measured sward temperature (a), measured net radiation (b) and wind speed (c) for Hambledon Hill AWS, for the period 20th-27th July 2002.

4.4.2 Sward temperature

The sward temperature model equations were used to model hourly mean surface temperatures for the 12 months following the calibration period at both AWS sites (September 2000 – August 2001), using the site calibrations. Figures 4.10 and 4.11 show measured and modelled data for eight representative days. Table 4.5 shows the mean and root mean squared (RMS) errors for both sets of data.

Table 4.5: Mean and rms errors of modelled vs. measured sward temperature from AWS data June 2000 - August 2002

Start date	End date	Days	AWS	Mean error	RMS error
1st Jun 00	31st Aug 02	822	Hambledon	0.620 °C	1.328 °C
		822	Sylvan Dale	0.036 °C	0.987 °C

Overall these models perform acceptably for daytime (R_n positive) temperatures when calibrated for a given sward, although the model for Sylvan Dale AWS has a tendency to over estimate high temperatures. Calculations of hourly mean errors are influenced by nighttime temperatures, which are less accurately represented by the models; under stable conditions with the T_0 lower than T, convective heat fluxes are much smaller than during the day, and therefore the values of r_{HR} would be expected to be smaller. The model might be improved by deriving a different equation for surface temperature when R_n is negative.

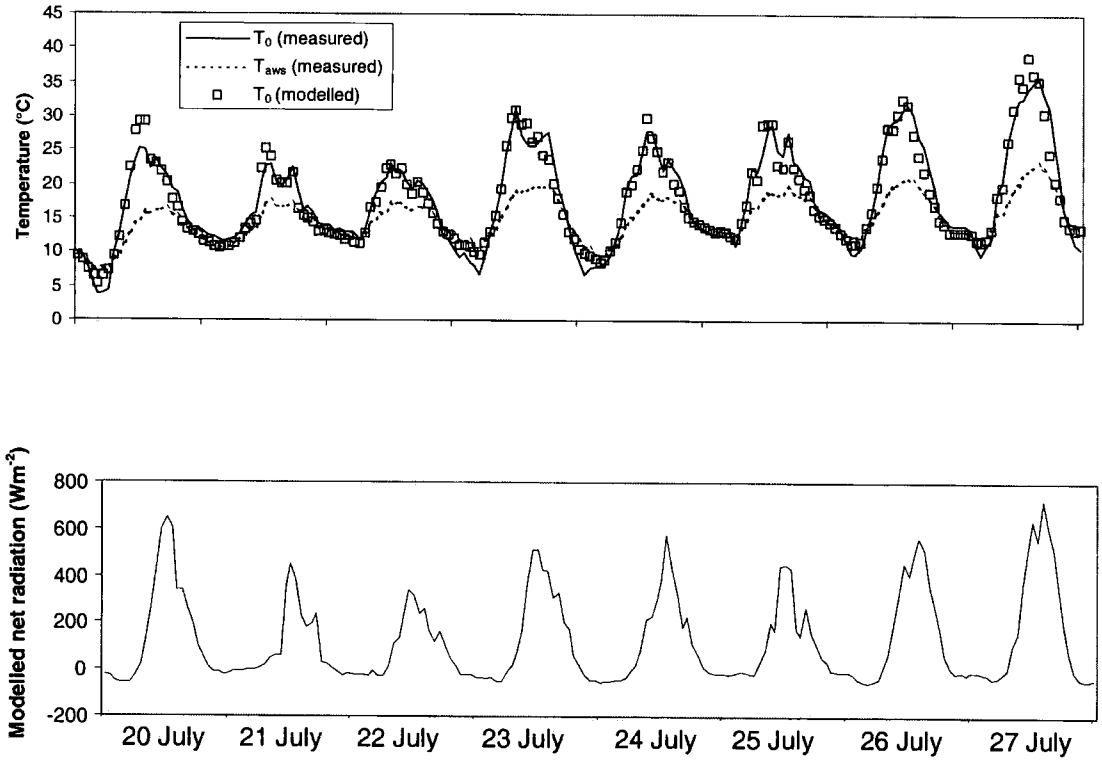

Figure 4.12: Hourly mean modelled and measured sward temperature (a), and modelled net radiation (b) for datalogger site D7 (S-facing) during the period July 20th-27th 2001.

To test the applicability of this type of model to a generalised short turf using data from a local AWS and modeled R_n values, modelled sward temperatures were compared to temperatures measured during datalogger runs, using equations 4.11 and 4.12. Figure 3.35 shows example modelled data for datalogger run D7, eight consecutive days.

Table 4.6: Mean and rms errors of modelled vs. measured sward temperature from datalogger runs 2000-2002

Start date	End date	Days	Plot	Mean error	RMS error
25th Aug 00	19th Sep 00	25	D3	0.077	1.42
		25	D4	0.39	1.20
30th Nov 00	18th Jan 01	50	D8	0.13	1.09
15th Feb 01	11th Mar 01	24	D5	-1.86	3.38
11th May 01	13th Aug 01	85	D8	0.55	1.87
24th Feb 02	18th Aug 02	137	D5	-2.11	3.44

The model performed poorly on the data logger runs for the valley bottom north-facing slope D5 during winter, with mean errors of around –2 °C suggesting that the sward temperature here was consistently lower than air temperature at the AWS. This is consistent with the observation of frost hollow development in the valleys at this time of year.

4.4.3 Soil temperature

The mean soil temperature on any one day in the model is dependent not only on the weather conditions on that day, but also on the temperature of the soil at a greater depth and the soil temperature of the previous day. Results from the model, in common with observed soil temperature, exhibits a lagged response to sward temperature and surface net radiation flux, reflecting the relative thermal inertia of the soil. Modelled soil temperatures for any day or period are therefore highly dependent on the initial starting conditions. There is also a high degree of temporal autocorrelation between measurements taken on consecutive days. For this reason, 10 day mean data collected from the tinytalk loggers at both

Hambledon Hill and Sylvan Dale, rather than time series data were used to test the soil temperature model.

Soil temperature was derived from mean daily sward temperature for each plot, starting each model run from 1st January with an initial soil temperature of 0 °C to minimise the effects of starting conditions. To allow for the effects of the lapse rate at Hambledon Hill, daily lapse rates were calculated from data from the difference between mean daily temperature at the AWS and the Meteorological Office weather station at Fontmell Magna. Assuming a linear response of temperature to altitude, mean daily sward temperatures were adjusted according to their altitude, and soil temperatures were calculated accordingly. No adjustment was made for the frost hollow effect at Sylvan Dale at this stage since calibration data from the valley bottom were not available for this period. For modelling temperature under *Brachypodium* tussocks, the model was adjusted to omit the radiation term in equation 4.16 as it was assumed negligible radiation reached the soil surface under a dense sward. Figures 4.13 to 4.15 show the modelled and measured soil temperature data for these data logger runs.

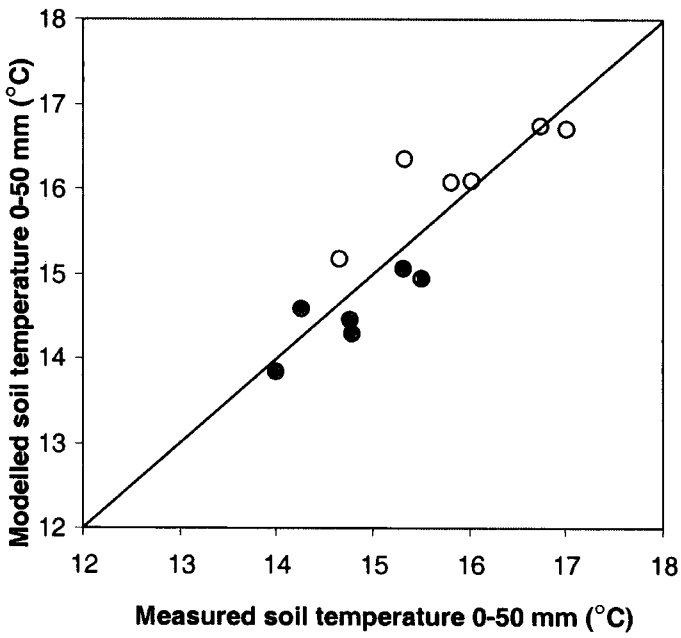

Figure 4.13: Ten day mean measured and modelled soil temperatures for tinytalk data loggers at Sylvan Dale for the period 25th August – 4th September 2000 (open circles) and 10th –19th September (filled circles).

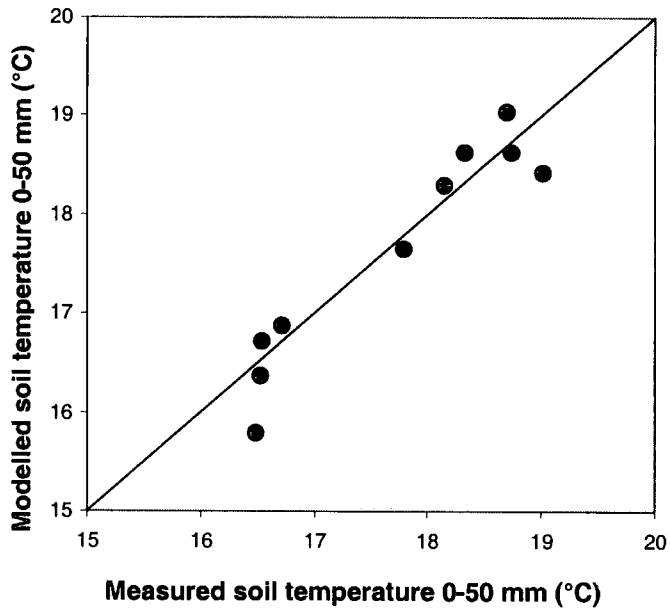

Figure 4.14: Ten day mean measured and modelled soil temperatures for tinytalk data loggers at Hambledon Hill for the period 7th – 16th August 2002.

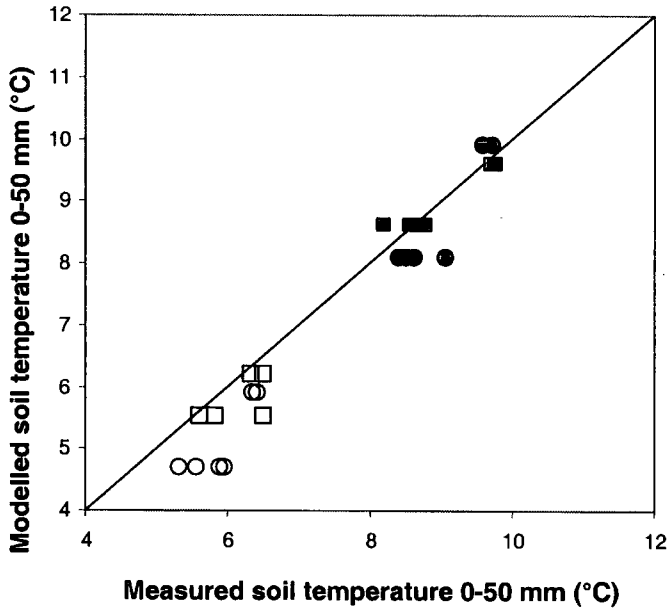

Figure 4.15: Ten day mean measured and modelled soil temperatures for tinytalk data loggers under short grass (circles) and tussocks (squares) at Sylvan Dale for the periods 19th - 29th October (filled symbols) and 3rd-12th November 2000(open symbols).

4.4.4 Soil Moisture

Empirical constants in the soil model were calibrated by running for the period July 2000 to October 2001 using climate data from Hambledon Hill AWS and soil depth measured at the site (80 mm), and initial water content at all root layers set to 0.4. The model was then run from February to August 2002 for the site (figure 4.16). The model, with the same constants except for soil depth (measured at 120 mm), was then run for the Sylvan Dale AWS (figure 4.17) for the same time period. Model performance was good for both AWS sites, capturing the difference in magnitude of fluctuations of soil moisture at both sites.

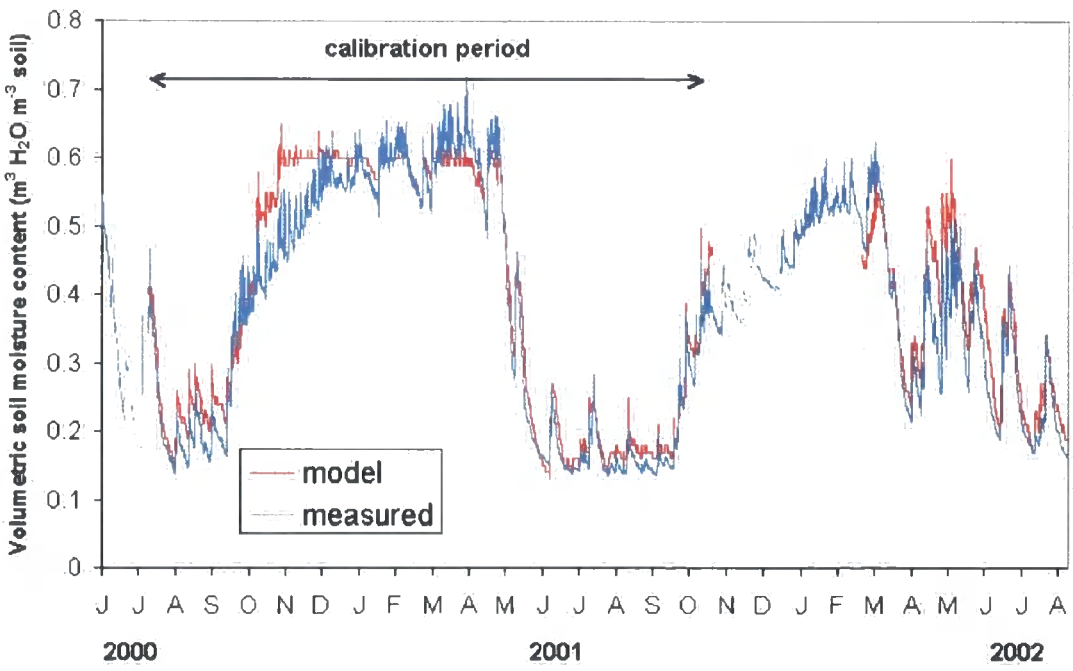

Figure 4.16: Modelled and measured soil moisture at Hambledon Hill AWS, June 2000 to August 2002. Mean error = -0.0465, Root Mean Squared Error = 0.00589. Soil moisture was not modelled during winter 2001-02 due to intermittent loss of data from the AWS.

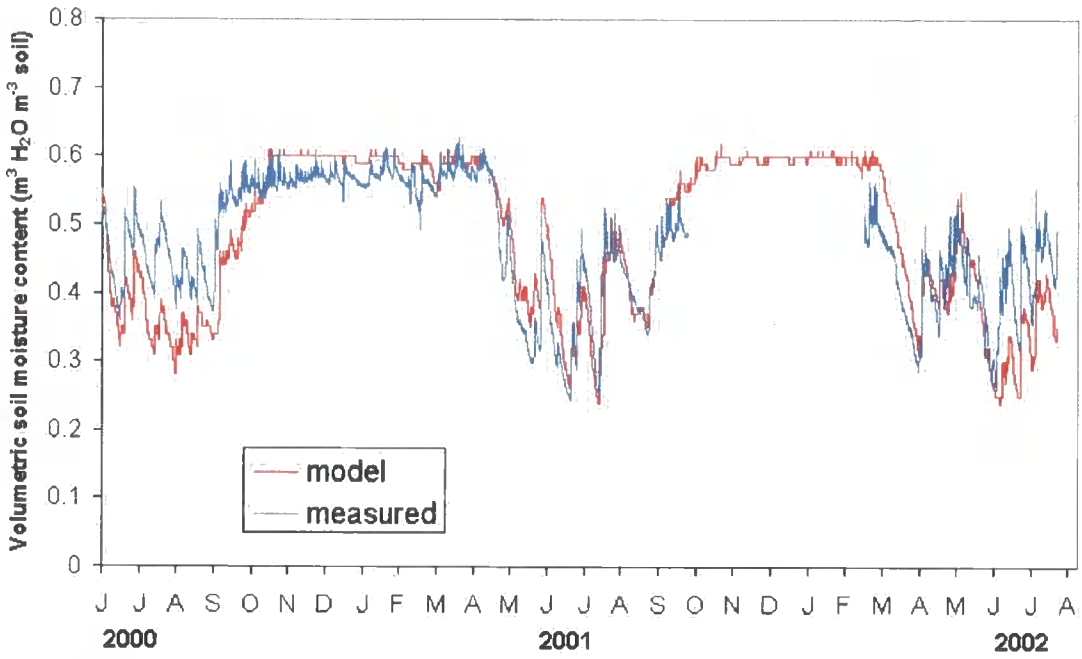

Figure 4.17: Modelled and measured soil moisture at Sylvan Dale AWS, June 2000 to August 2002. Mean error = -0.0210, Root Mean Squared Error = 0.0592. Soil moisture measurements are absent during winter 2001-02 due to equipment failure.

To assess the applicability of the soil moisture model across the landscape, the model was run for each of the vegetation plots at each measurement date. Modelled vs. measured results are shown in figures 4.18 and 4.19. Pearson's R^2 values, mean error and root mean errors for these model runs are shown in tables 4.7 and 4.8.

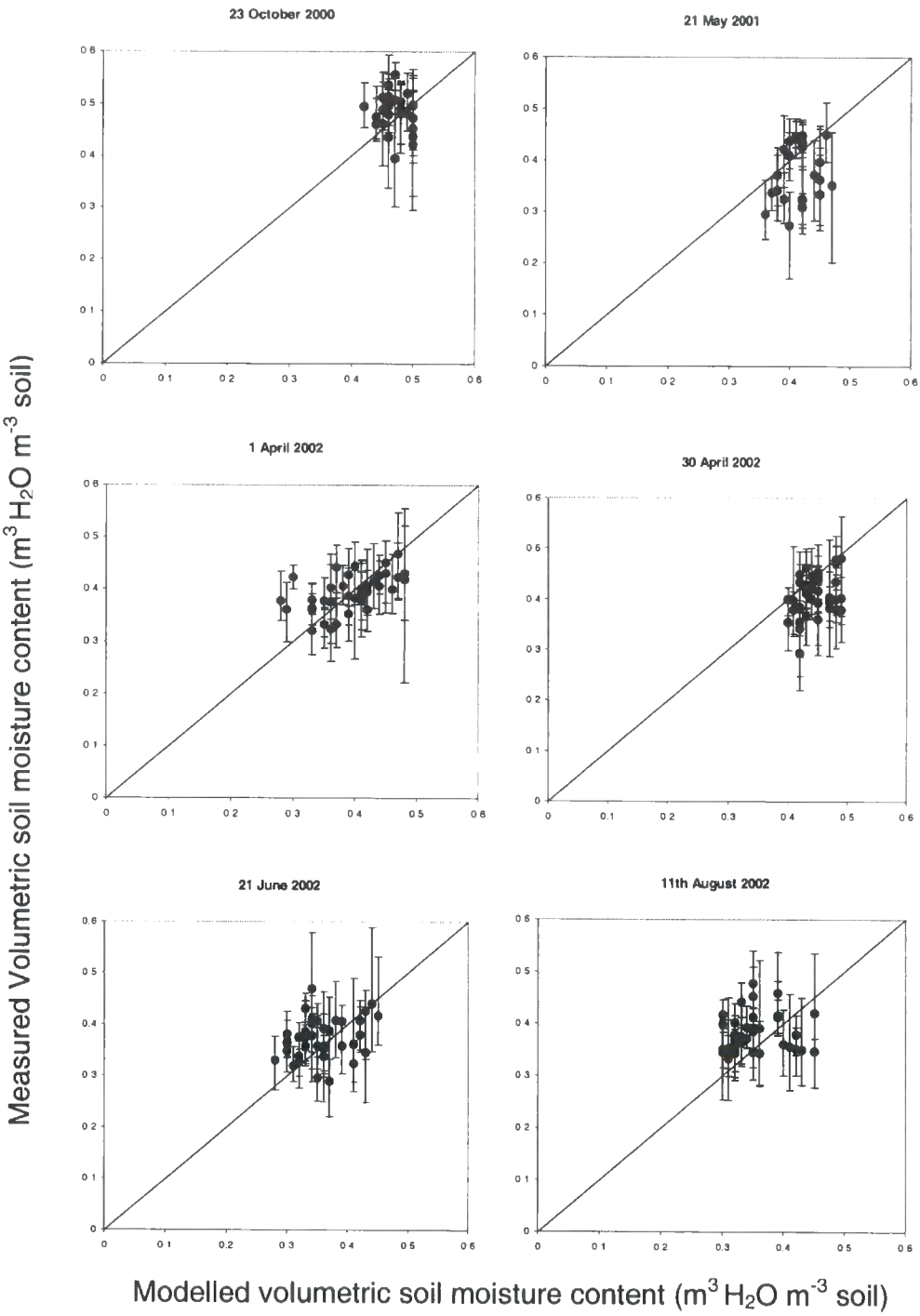

Figure 4.18: Modelled and measured soil moisture at vegetation pots at Hambledon Hill. Error bars show range of measured values at each plot. Diagonal line shows position of perfect concordance.

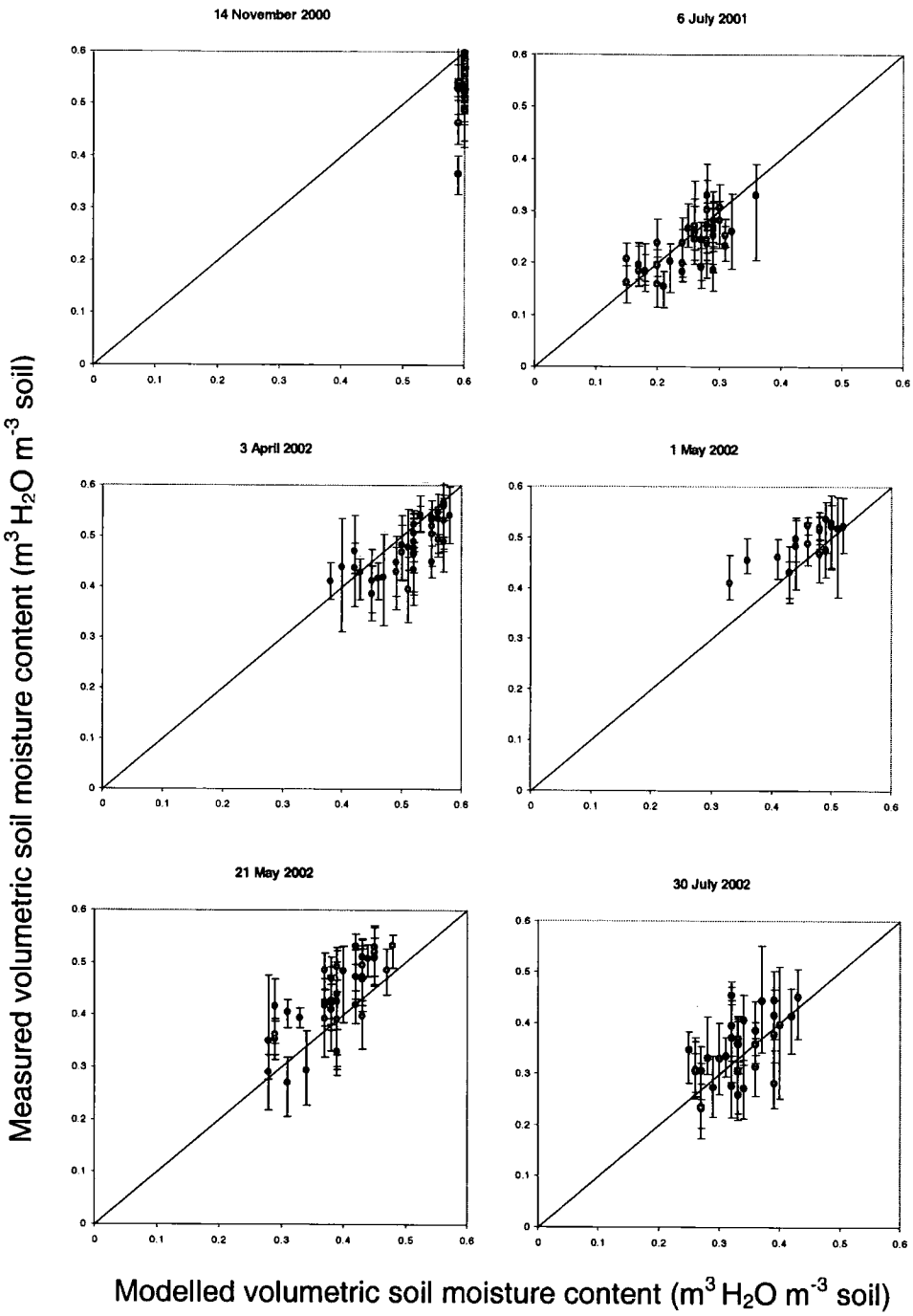

Figure 4.19: Modelled and measured soil moisture at vegetation pots at Sylvan Dale. Error bars show range of measured values at each plot. Diagonal line shows position of perfect concordance.

Table 4.7: Pearson's R^2, Mean and rms errors of modelled vs. measured soil moisture from datalogger runs 2000-2002.

Date	No. of plots	R^2	*p*	Mean error	RMS error
14th Nov 00	40	**0.567**	<0.000	-0.0495	0.0630
6th July 01	40	**0.592**	<0.000	-0.0144	0.0382
3rd April 02	49	**0.585**	<0.000	-0.0289	0.0457
1st May 02	40	**0.357**	0.026	-0.216	0.0328
21st May 02	40	**0.347**	0.030	0.0233	0.117
30th July 02	40	**0.356**	<0.000	0.0167	0.0538

Table 4.8: Pearson's R^2, Mean and rms errors of modelled vs. measured soil moisture from datalogger runs 2000-2002.

Date	No. of plots	R^2	*p*	Mean error	RMS error
23rd Oct 00	27	0.585	0.395	0.0110	0.0453
21st May 01	27	0.051	0.288	-0.0394	0.0674
1st April 02	40	**0.334**	<0.000	-0.000320	0.0434
30th April 02	40	0.127	0.125	-0.0370	0.125
21st June 02	40	0.073	0.102	0.0161	0.0521
11th Aug 02	40	0.009	0.590	0.0289	0.0616

4.5 Discussion

Models of solar radiation, PAR, sward temperature, and 0-50 mm soil temperature and moisture content on slopes are described and evaluated in this chapter. The radiation model was shown to adequately estimate hourly mean solar radiation at different points in the landscape from AWS data under variable cloud conditions, using slope and aspect measured in the field and a DTM to allow for topographic shading. Differences between the angle at which the pyranometers were mounted in the field and the recorded slope and aspect values for each site may be a source of error in this model. Neither net radiation nor PAR were directly measured on slopes, but the strong linear relationship between solar radiation and PAR found at

the AWS sites suggests that PAR at the top of the grass canopy can be modelled with a similar degree of accuracy. The validity of the assumptions regarding long-wave radiation cannot be assessed here, and will be an unknown source of error for temperature and moisture models based on net radiation estimates.

Hourly mean sward temperatures were modelled accurately using site-specific semi-empirical equations at the AWS sites as a function of air temperature, net radiation flux and wind speed at 2 m. However, different equations were needed for the ungrazed sward at Hambledon Hill than for the shorter sward at Millington, demonstrating the importance of sward structure on near-surface temperatures. The effect of the taller sward appears to be to reduce wind speed and reduce the rate of heat loss to the atmosphere. Short turf is characterized as a warm habitat (Thomas *et al.*, 1999) – however, this study shows that air temperatures at a height of 100 mm in short turf are typically lower than at an equivalent height in longer grass due to increased exposure to wind. The temperature of an individual plant or animal within the turf or at the soil surface under conditions of strong radiation, however, will be higher in short turf due to the reduced effect of shading. The effect of vegetation height on soil temperatures would appear to be complex, since tall grass both reduces the cooling effect of wind close to the ground and reduces the direct effect of radiative heating on the soil surface. Thus on north-facing slopes tall swards may be warmer than short ones, while on south-facing slopes they may be cooler.

Extrapolating the sward and soil temperature models to sloping ground using a generalized model gives reasonably accurate results, assuming a short sward with a similar aerodynamic resistance to that at the Sylvan Dale AWS, and allowing for some direct radiative heating of the soil surface. Again, the influence of vegetation structure is demonstrated; grazed chalk grassland on sloping ground tends to be composed of fine leaved grasses and herbs with canopy gaps and areas of bare earth on steeper slopes. Grassland on flatter land commonly consists of a denser sward of coarse grasses with little or no bare ground. At Sylvan Dale, the grass *Brachypodium pinnatum* forms dense tussocks and large quantities of litter in patches, creating a mosaic of short turf and tussock patches. Tussocks have been

shown to have a pronounced effect on soil temperature. The effect of a dense litter or bryophyte layer may also be effective in shading the soil surface. As bryophytes are more abundant on north-facing slopes, they may reinforce the cooler soil temperatures at these sites. While a general "short fine turf" temperature model may be applicable to many sites, it should be used with caution.

As with the sward temperature model, the site-specific soil moisture model proved accurate in predicting volumetric soil moisture, both at the Hambledon Hill AWS site following calibration, and at the Sylvan Dale AWS with no further calibration. The main differences in soil moisture between AWS sites were reproduced by the model, supporting the idea that observed patterns in soil moisture could be attributed to climate rather than any differences in the two soils. When extrapolated to sloping ground, however, the explanatory power of the model differed between sites. At both sites the range of soil moisture values measured within a single 7 m by 7 m plot on any one date was considerable, but at Sylvan Dale, a clear relationship existed between slope and aspect and mean soil moisture at a plot. The model therefore successfully predicted a significant proportion of the variation in mean soil moisture between sites. At Hambledon Hill, however, there was no such clear relationship, and only on one date did the model predict a significant proportion of the variation. This date was during a dry period in early spring, when the difference in radiation load between slopes is relatively large due to the low solar elevation, and the rate of soil drying from a winter saturated state would be critical in determining soil moisture. At other times of year slope and aspect may be less important in determining soil moisture at any point than smaller scale spatial variation. Possible causes of micro-scale variation in soil moisture include variation in soil depth, root and organic matter distribution, the distribution of chalk or flint fragments within the topsoil and differences in drainage rate of the underlying chalk.

Standard measurements of climate from meteorological networks are often not an accurate measure of the actual environment in which plants exist. They may be better understood as representative of a climatic "envelope" defining a range of possible microclimates. The models of microclimate described in this chapter

attempt to define more accurately the temperature and moisture regimes in which biological processes operate in chalk grassland. However, in validating these models with data collected at single points in space, considerable variation has been found to exist in temperature and soil moisture at scales smaller than the vegetation plots in this study. The microclimates described by the model output are perhaps better regarded as themselves microclimatic "envelopes" defining a range of possible temperature and moisture niches within a finely heterogeneous vegetation and soil structure.

4.6 Summary of chapter 4

1. An approach to modelling topographic microclimate was outlined in which climatic variables (as measured at screen height) are assumed to be spatially uniform across the landscape, and the microclimate close to the ground is assumed to be modified solely by spatial variation in direct solar radiation at the surface. Solar radiation at a point in the landscape is calculated using a model of clear-sky atmospheric transmission and solar geometry in conjunction with a DTM, and adjusted fro cloudiness using measured solar radiation on the horizontal.
2. Hourly mean solar radiation was modelled accurately at different points in the landscape using calculated direct solar radiation values for slopes adjusted for cloudiness using solar radiation data measured at an AWS. Net radiation at a point was modelled using measured net radiation at the AWS to estimate the long wave component of net radiation. The accuracy of this approach was not tested.
3. Process-based models of PAR, sward temperature and 0-50 mm soil temperature and moisture content, based on measured screen height climate data and modelled radiation were described.
4. Both temperature and soil moisture models performed well when tested against independent time series data at the AWS sites, using measured net radiation data. Using modelled net radiation data on sloping ground, the models were less accurate, but still gave generally good results.

5. Where the models failed to give adequate predictions, this could be attributed to either (a) medium scale spatial variation in climatic variables (for example the "frost-hollow effect" at Sylvan Dale) violating the assumption that most climatic variables are spatially uniform across the landscape except where modified close to the ground by solar radiation, or (b) variation in microclimate at a scale smaller than that of the vegetation plots considered (for example high variation in soil moisture within vegetation plots at Hambledon Hill).

Chapter 5: Field experiments and observations

5.1 Introduction

In chapter 2, the processes through which topographic microclimate influence the composition and spatial distribution of vegetation were discussed. In this chapter, three aspects of microclimate-vegetation interaction in chalk grassland are studied in more detail through field measurements and experiments – soil nutrient cycling, photosynthesis, and seed germination.

5.2 Nutrient cycling on contrasting slopes

5.2.1 Calcareous grassland soils

The soils underlying much of the "typical" chalk grassland communities of the south-east of England are rendzinas, consisting of a shallow organic A horizon, often with a high content of chalk fragments, directly above weathered chalk penetrated by root systems. These soils are rapidly draining, base-rich and oligotrophic (Rodwell, 1992). Under suitably humid conditions, and in the absence of disturbance, these soils may develop into deeper brown calcareous earths with a more developed leached B-horizon. Weathering of chalk soils was related to climate and topography by Perring (1954), who showed that total carbonates and pH increased towards the drier end of the rainfall/humidity gradient in Britain. A slight N-S difference was also noted, but the main topographic effect was associated with angle of slope more or less independent of aspect, with an increase in carbonates and pH at slopes above about 15°. This concurs with observations of soil catenas on slopes on limestone and chalk that mid-slopes are shallower, due to lateral movement down slope, and that brown calcareous earths develop on plateau or valley bottoms (Balme, 1953; Trudgill, 1976). Under drier conditions, soil development appears to be inhibited even on shallow slopes, due to less leaching of carbonates and possibly to increased physical erosion during drought conditions when ground cover is reduced.

5.2.2 Nutrient availability in chalk grassland

Calcareous grassland soils are often considered to be nutrient-poor, with low levels of nitrogen and phosphorus – however, the nutrient that constrains biomass production has been found to vary between sites studied by different authors, being nitrogen in English lowland ex-arable fields (Lloyd and Pigott, 1967; Uncovich *et al.*, 1998), P on sugar limestone grasslands in Teesdale (Jeffrey and Pigott, 1973) and Swedish alvar grasslands (Tyler, 1996) and N and P co-limitation in a calcareous site in the Peak District (Morecroft *et al.*, 1994) and Swiss limestone grasslands (Köhler *et al.*, 2001). Moreover, the limiting nutrient may vary between species; Grime and Curtis (1976) found that *Festuca ovina* seedlings in a Derbyshire grassland soil responded with increased growth to the addition of P, while *Arrhenatherum elatius* seedlings responded only to a combination of N and P. The availability of N and P, and interactions with water availability, are likely to differ.

5.2.2.1 Nitrogen

Soil temperature and moisture, and organic matter substrate quantity and quality (C:N ratio), have long been known to determine the rate of nitrogen mineralisation within the soil and therefore the availability of N to plants (Witkamp, 1966). Rodrigo *et al.* (1997) have assessed a range of different models of the temperature and moisture effects on C-N transformations in soil. Although models differ in the functions assigned to each variable, usually derived from laboratory incubations, all agree that the relative rate of N mineralisation increases with temperature over the range of typical soil temperature, and increases with soil moisture between permanent wilting point and field capacity.

On ex-arable chalk grassland at Wytham, Oxfordshire, Jamieson *et al.* (1999) found that gross rates of N mineralisation determined by isotope dilution were highest in spring and autumn, and lowest in summer, when soil moisture was low. They concluded that water availability was the main restraint on microbial

processes and plant growth. Uncovich *et al.* (1998) found that plant growth at this site increased substantially with liquid N fertiliser, and to a lesser extent the addition of water, suggesting that biomass production at the grassland was nitrogen-limited. Thus it was considered that nitrogen availability was constrained by soil water availability. However, in experimental plots at the site, winter warming and summer drought/enhanced rainfall treatments were applied using soil warming cables, automatic rain shelters and supplementary watering. In these plots, no treatment had the expected significant effect during the season in which it was applied – there was no significant difference in summer N mineralisation (measured using ^{15}N pool dilution) between droughted, control and supplementary rainfall plots. However, in the subsequent autumn and winter, the enhanced rainfall plots had significantly reduced N mineralisation compared to controls, while droughted plots had significantly increased N mineralisation. In the spring following the winter warming treatment, heated plots had increased N mineralisation rates (Jamieson *et al.*, 1998). It was concluded that the observed effects were due to the effects of temperature and drought on litter production (through plant growth and death), and thus soil organic C content, rather than direct effects of soil microclimate.

These studies suggest that nitrogen mineralisation in chalk grasslands may be limited by microclimate in two ways – by the short-term control of microbial processes by temperature and moisture content, and by longer-term control of litter production and soil organic matter. The observed low rates of N-mineralisation during the summer months may be due to either low soil moisture or to low availability of organic N for mineralisation.

5.2.2.2 Phosphorus

Several studies have shown empirical relationships between low available soil phosphate and high species diversity in grasslands (Critchley *et al.*, 2002; Janssens *et al.*, 1998). Calcareous soils are often associated with low levels of extractable P (Rorison, 1987; Tyler, 2002). At high pH phosphorus is bound as

apatite or apatite-like calcium compounds. Calcicole plants may solubilise these phosphates in their rooting zone by exuding oxalic and citric acids, and inability to solubilise them excludes many calcifuge plants from high pH soils (Tyler, 1994, 1996). Low available P is important in determining the characteristic diversity and calcicole species composition of chalk grassland, and may be the limiting or co-limiting nutrient for biomass production.

5.2.1 Methods

During the growing season (March to October) of 2002, field measurements of soil extractable N and P across macro- and microclimatic gradients were carried out. To investigate the dynamics behind these "snapshot" measurements of available nutrients, N mineralisation was measured using a buried bag *in situ* soil incubation method (Eno, 1960; Schaffers, 2000). To assess variation in rates of organic matter decomposition at the sites, weight loss from litter bags was used (Wieder and Lang, 1982).

5.2.1.1 Experimental plots

Measurements were taken from four experimental plots chosen to represent both macro- and microclimatic gradients. Plots were situated at the sites of the Automatic Weather Stations at Hambledon Hill and Millington Pastures (hereafter referred to as DAWS and YAWS respectively), at a valley-bottom N-facing site and a mid-slope SW-facing slope at Millington Pastures, both with slope angles of around 30° (referred to as YNF and YSF respectively). These correspond to datalogger positions D6 and D7 (figure 3.6). These positions were chosen to maximise the temperature difference between plots. Plot YSF experienced high daily maximum temperatures due to the increased solar radiation in the afternoon; plot YNF received low solar radiation input and low minimum temperatures during temperature inversions. Figure 5.1 shows the mean daily soil temperature at the plots over the two periods.

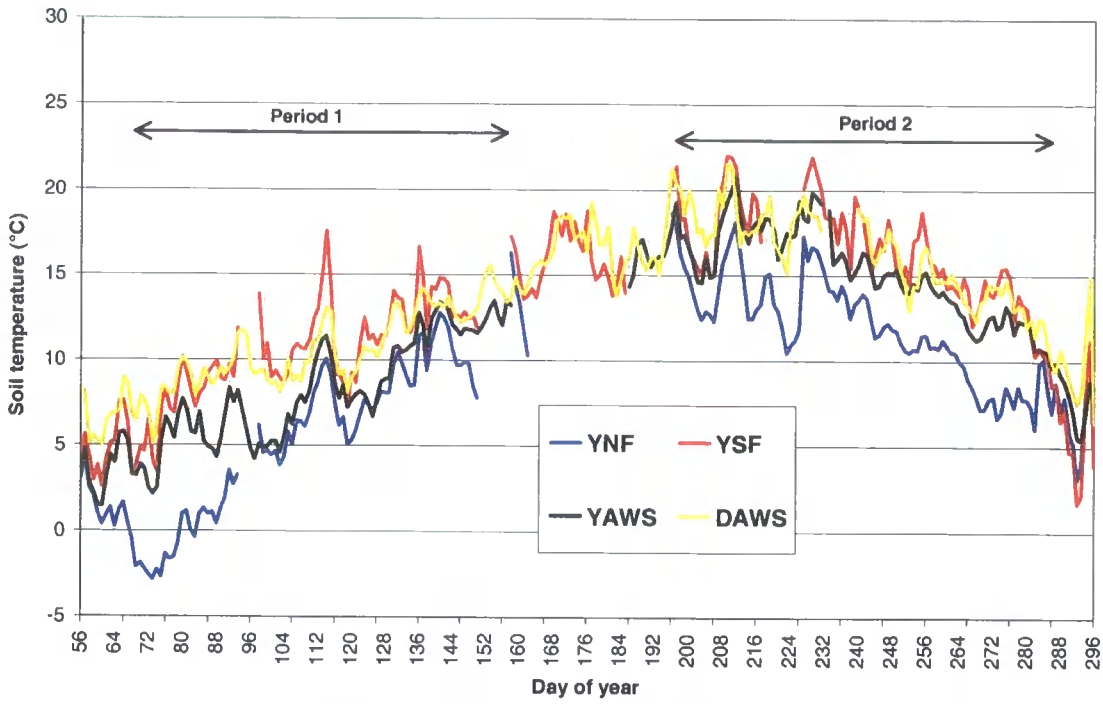

Figure 5.1: Mean daily soil temperature (10 mm depth) at experimental plots. Durations of soil incubation and litter bag experiments shown.

Mean soil temperature over both periods (table 5.1) differed between pairs of plots considerably. The Yorkshire south facing slope YSF had a very similar mean soil temperature to the hilltop site in Dorset DAWS.

Table 5.1. Mean soil temperature (10 mm depth) at each plot for the experimental periods.

	Mean soil temperature (°C)			
Period	**YSF**	**YNF**	**YAWS**	**DAWS**
1	10.4	5.5	8.1	10.5
2	16.3	12.0	15.2	16.2

5.2.1.2 Litter bags

Above ground leaf litter was collected from a S-facing slope in Millington Pasture in February 2002. By far the most abundant species in the litter was *Brachypodium pinnatum* (estimated at around 95%), which produces large quantities of litter around tussocks; the remainder was mostly *Festuca ovina* with small quantities of other grasses and forbs. The litter was air dried for 24 hours, mixed and cut into lengths of roughly 5 cm. Approximately 1.0 g of litter was sewn into each of 10 × 10 cm nylon bags (gauge 1 mm). The exact net and gross weight of each bag, was measured (to 0.001 g). Six litter bags were oven dried at 80° C to constant weight to calculate an oven/air dry ratio for the litter. Ten bags were fastened to the soil surface at each plot on the 5th or 6th March. On the slopes at Millington Pastures, all bags were in short *Festuca ovina* turf (50 - 100 mm). At the automatic weather stations at Millington Pastures and Hambledon Hill, five bags were placed in short mixed turf outside the grazing enclosure. The bags were retrieved after 90 days, carefully clipped open and any extraneous material removed (bryophytes, insects, fine grass shoots etc...), oven dried at 80° C and weighed. Weight loss for each bag was calculated.

The above procedure was repeated later in the year using litter collected from the same site in early July, and placed at the plots on July 14th and 15th. Due to disturbance by livestock, several of the litter bags were lost or split open during the second period, leading to smaller, and unequal, sample sizes.

5.2.1.3 Hypotheses

The litter bag experiment was designed to test the following hypotheses:

1. In spring, litter decomposition is temperature limited and therefore occurs more rapidly under the warmer micro- and macroclimates (YSF>YNF, DAWS>YAWS).
2. In summer, litter decomposition is moisture limited and therefore occurs more rapidly under moist conditions (YNF>YSF, YAWS>DAWS)

5.2.1.4 Soil measurements

At the beginning of each experimental period, on 5th/6th March, and 14th/15th July, six groups of three soil cores were extracted from each plot. Cores were of diameter 35 mm and depth 100 mm. Groups of three cores were extracted as close together as possible, at points selected at random from a grid of 4×4 possible locations spaced 20 cm apart. Cores were inserted into sealable polyethylene bags and labelled. One bagged core from each group of three was taken to the laboratory for immediate analysis, one was replaced into its original position, and the third was transplanted into a corresponding coring hole left on the contrasting slope or site. Cores were incubated in the field for 90 days under field conditions, and then removed for analysis. Polyethylene is permeable to air, but not to water; incubated cores were therefore aerated and exposed to field temperature variations but remained at constant water content. However, it should be noted that Abril *et al.*, (2001) found that microbial activity within polythene bags resulted in some oxygen depletion and the method therefore may tend to slightly underestimate gross field N mineralisation rates. The start date of the second incubation was selected after several days without rain, when there was a significant difference in soil moisture between the N and S-facing plots. After the second 90-day period, six new cores from each plot were taken for analysis.

Due to the archaeological status of Hambledon Hill soil samples could not be taken from the earthworks for a comparative soil incubation experiment. However, at the end of the second 90 day period, a single core was taken from each of two sites, a 30° SW facing slope and a 30° NW facing slope to the west of the scheduled ancient monument, in order to compare soil characteristics with those at the AWS and in Millington Pastures.

5.2.1.5 Soil analyses

All soil cores were transported and stored in sealed polythene bags at 5 °C. Extractions and pH measurement were carried out within 48 hours of removal from the field. The fresh soil cores were passed through a 2 mm mesh to remove large roots and stones.

Standard procedures of analysis of soils and extractions were used following Allen (1974) and automated analysis of extracted N and P was carried out following the methods in Skalar (1995).

Soil pH was measured by half filling a 50 ml beaker with fresh soil, and adding sufficient water to immerse the electrodes of a pH meter (Wissenschaftlich-technische 192, Germany).

Moisture content was determined by heating a weighed sample (approximately 1 g) of sieved soil in an air-circulation oven at 110° C for six hours, cooling in a dessicator and reweighing.

Loss on ignition (LOI) was determined by heating oven-dried samples in a crucible at 500° C in a muffle furnace for four hours, cooling and reweighing.
Available ammonium (NH_4^+) and nitrate (NO_3^-) was measured by potassium chloride (KCl) extraction. 5 g of soil was mixed with 50 ml of 1 M KCl and shaken mechanically for 1 hour. Samples were filtered over Whatman No. 2 filter paper and the extract stored at 5° C. Extracts were analysed for NH_4^+ and NO_3^- using a Skalar San-plus Segmented Flow Analyser (Skalar Ltd, Breda, Netherlands).

Available P in was measured by extraction with Olsen solution, suitable for calcareous soils (Allen 1974). 2.5 g of sample was mixed with 100 ml of Olsen solution (0.5 M $NaHCO_3$ adjusted to pH 8.5 with 1.0 M NaOH). Samples were shaken for 30 minutes and filtered through Whatman No. 2 filter paper. Before analysis, 4.5 ml of 0.5 M H_2SO_4 was added to 10 ml of extract to bring the pH to

5 ± 0.1. Extracts were analysed by the molybdenum blue procedure using a San-plus Segmented Flow Analyser (Skalar Ltd, Breda, the Netherlands).

5.2.1.6 Hypotheses

The N mineralisation experiment was designed to test the following hypotheses:

1. N mineralisation is temperature-limited and therefore occurs more rapidly under the warmer micro- and macroclimates for a given soil (YSF>YNF, DAWS>YAWS).
2. In summer, when soils are below field capacity, N mineralisation is moisture-limited and therefore occurs more rapidly under moist conditions under a given temperature regime (YNF>YSF, YAWS>DAWS).

5.2.1.7 Statistical analyses

Mass loss from litter bags, expressed as a proportion of the original weight, was transformed using the arcsine transformation and transformed distributions tested for normality using the Shapiro-Wilk statistic. Differences between plots were analysed using Analysis of Variance (ANOVA). Post hoc multiple comparisons were carried out using Tukey tests. N mineralisation was calculated by subtracting initial extracted N (NH_4^+ and NO_3^-) from extracted N after incubation. Soil measurements and N mineralisation were tested for normality using the Shapiro-Wilk statistic and, if normal, analysed using ANOVA with "source" of soil and "incubation plot" (treatment) as factors. All analyses were carried out using SPSS v.10.0.5 (SPSS Inc., Illinois, USA). Where data were not normally distributed, and could not be transformed using standard transformations, non-parametric two-way comparisons were carried out using the Scheirer-Ray-Hare test using two-way ANOVA in SPSS on ranked data as described by Dytham (1999).

5.2.2 Results

5.2.2.1 Litter bags

Figure 5.2 shows the percentage weight loss of litter bags at each plot over each 90 day period.

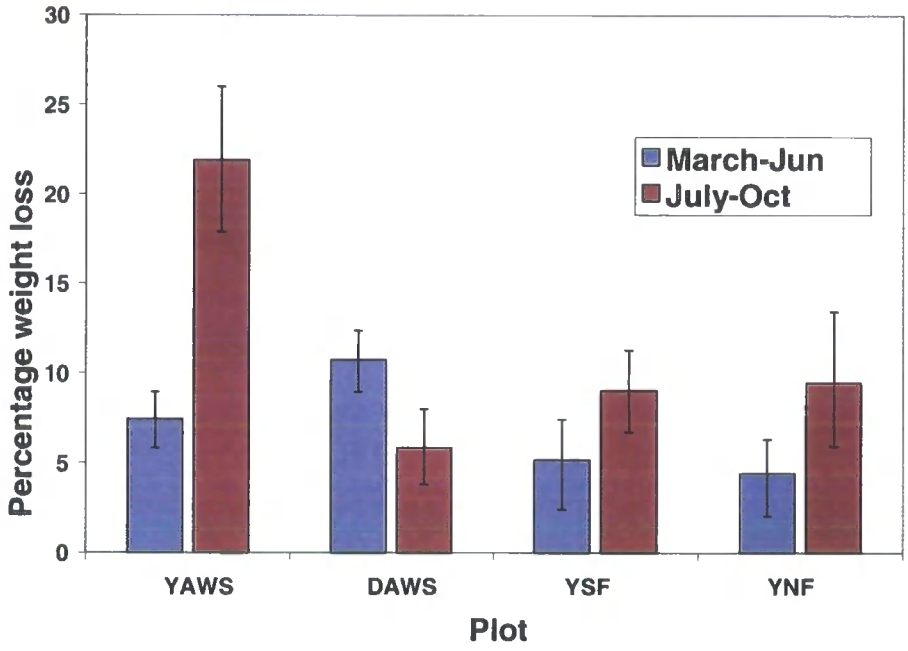

Figure 5.2: Percentage weight loss of litter bags at each plot over each 90 day period. Error bars show ± 95% confidence intervals (backtransformed).

Table 5.2: ANOVA results for litter bags

Source	SS	df	MS	F	Sig.
Model	0.398	7	0.057	7.715	0.000
Intercept	5.324	1	5.324	721.878	0.000
Season	0.133	1	0.133	17.999	0.000
Plot	0.129	3	0.043	5.841	0.001
Seasonxplot	0.162	3	0.054	7.336	0.000
Error	0.428	58	0.007		
Total	6.213	66			

During the spring period, mass loss from the three plots at Millington Pastures was relatively low and did not differ significantly between plots. During this period mass loss from the plot at Hambledon was significantly higher. This cannot be wholly attributed to higher mean temperatures as YSF had similarly high temperatures but not significantly different rates of mass loss from YNF. During the summer period, mass loss at the three Millington pastures plots was significantly higher than in spring, with particularly high values at the YAWS site. However, mass loss at DAWS was less during the summer.

A comparison between the two AWS sites is consistent with Hypotheses 1 and 2; however no significant difference between decomposition between YSF and YNF slopes was found. Furthermore, the differences in summer rates of decomposition at plots YSF, YNF and YOR, and spring rates between DOR and YSF cannot be fully explained by the effects of mean temperature and moisture.

5.2.2.2 Characterisation of soils

The soils at both AWS plots were shallow brown calcareous earths, with an identifiable B-horizon, grading into chalk at between 200 to 250 mm depth. Soils on the slopes YSF and YNF were shallow rendzinas (Avery 1980); consisting of an organic A-horizon containing chalk fragments with no sign of leaching grading into chalk bedrock at a variable depth of between 50 and 180 mm.

Table 5.3: Soil variables at experimental plots (n=6).

	Mean pH	Min pH	Max pH	Mean LOI	Min LOI	Max LOI
YAWS	**6.9**	6.7	7.3	**14%**	13%	16%
DAWS	**6.9**	6.5	7.2	**20%**	18%	21%
YSF	**7.5**	7.3	7.8	**20%**	18%	24%
YNF	**7.3**	6.9	7.5	**22%**	15%	30%

ANOVA and post hoc Tukey tests showed that the pH of YAWS and DAWS is significantly different to YSF and YNF ($F_{3,28}$ = 15.60, P<0.01). There was no significant difference between NF and SF slopes or between YAWS and DAWS.

Mean LOI values were around 20% at NF, SF slopes and at DAWS, but were significantly lower (14%) at YAWS (ANOVA $F_{3,28}$ = 15.45, P<0.01).

5.2.2.3 Seasonal variation in extractable N and P

NO_3^- availability at all sites was relatively low in March, following a period of cold weather, consistent with the hypothesis that N mineralisation and nitrification is limited by temperature during winter and early spring (figure 5.4). At this time there was no significant difference in extractable NO_3^- between the sites ($F_{3,28}$ = 2.63, P = 0.07). Mean NO_3^- availability was greater at all sites in July, although YSF has significantly lower values than the other plots ($F_{3,28}$ = 6.33, P < 0.01). This is consistent with increased summer temperatures allowing greater rates of N mineralisation, with low soil moisture on the south-facing slope becoming a limiting factor. In October, DAWS and YSF had higher mean extractable NO_3^- values, the only significant difference between plots being that values for YNF were higher than DAWS ($F_{3,28}$ = 6.70, P < 0.01).

In March, NH_3^+ availability was low at all sites except DAWS, where it was significantly greater (figure 5.4). It reached a peak at all sites in July and then declined. Total N generally followed the pattern of NO_3^-, which is usually the most common form of N in these soils (figure 5.5).

In comparison with available N, P is available in relatively constant amounts throughout the year – significantly higher at YAWS, with extremely low amounts on soils on the slopes. DAWS has intermediate P values throughout the year (figure 5.6).

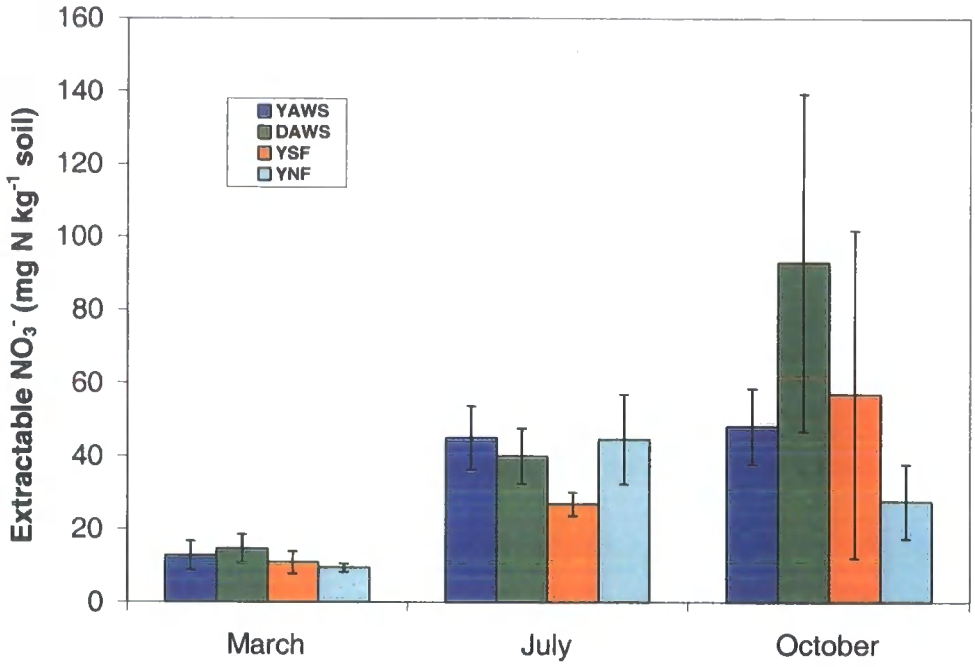

Figure 5.3: Extractable NO_3^- in cores at all sites. Error bars show ± 95% confidence intervals.

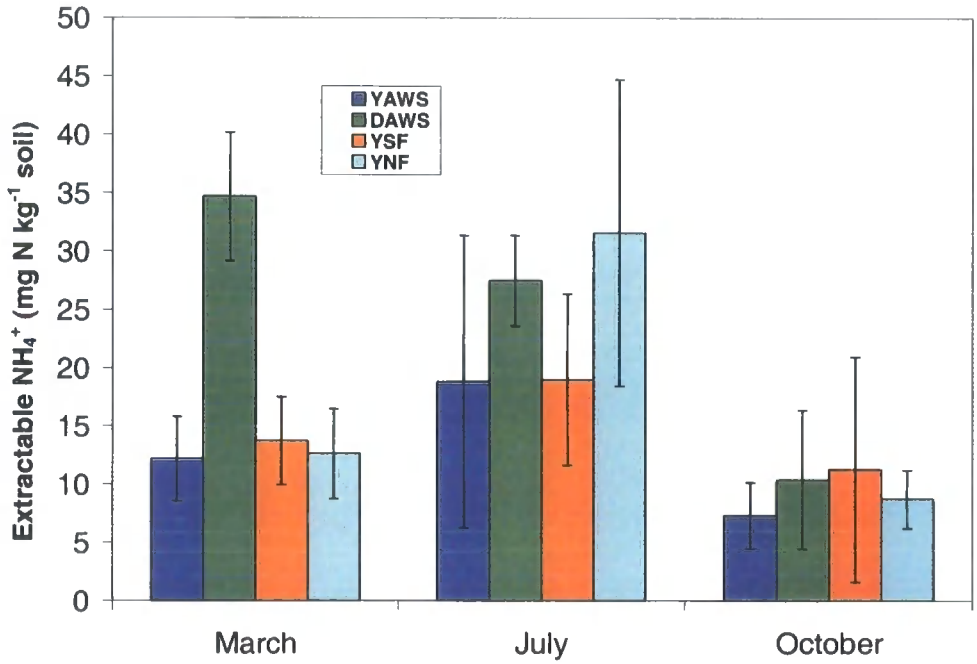

Figure 5.4: Extractable NH_4^+ in cores at all sites. Error bars show ± 95% confidence intervals.

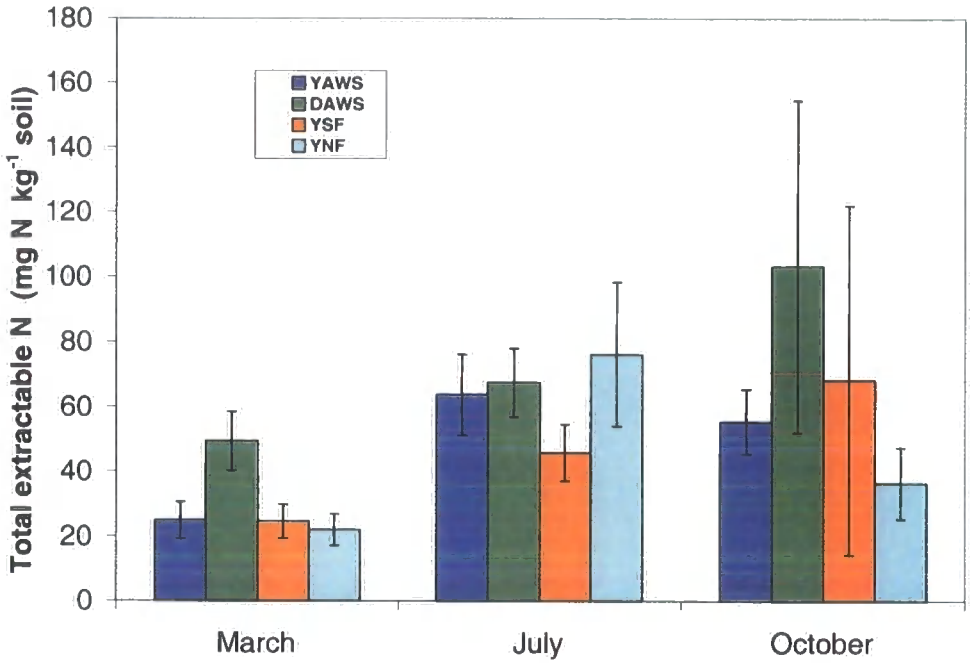

Figure 5.5: Extractable N in cores at all sites. Error bars show ± 95% confidence intervals.

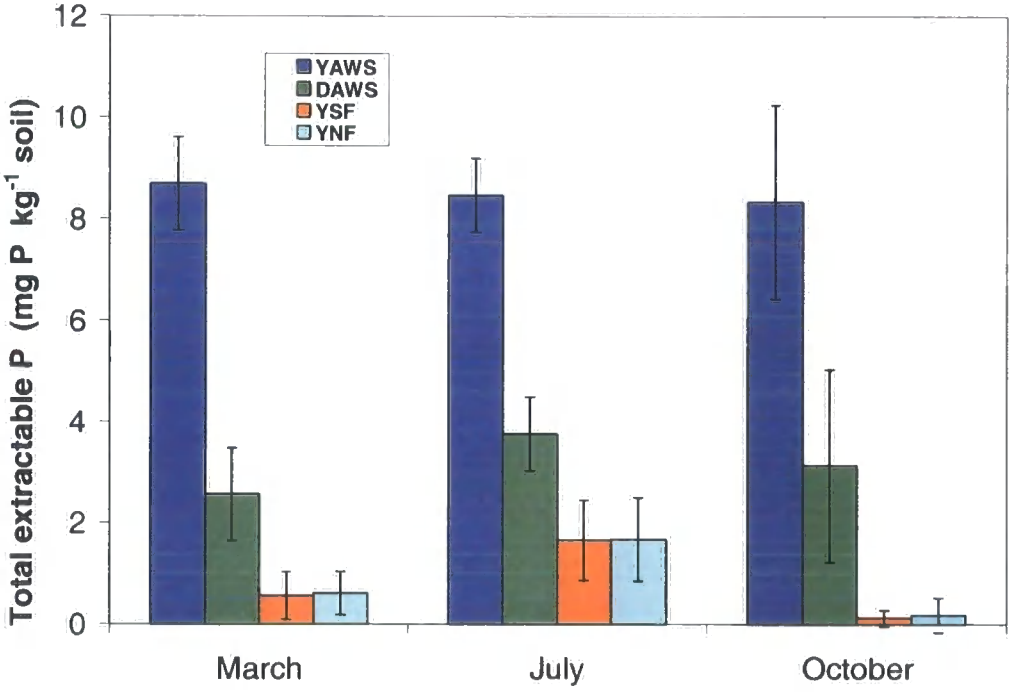

Figure 5.6: Total extractable P (as PO_4^{3-}) in cores at all sites. Error bars show ± 95% confidence intervals.

5.2.2.4 Analysis of soils on slopes of Hambledon Hill

Table 5.4: Soil measurements on slopes at Hambledon Hill, October 2002.

	pH	LOI	NO_3^- (mg kg^{-1})	NH_4^+ (mg kg^{-1})	Total N (mg kg^{-1})	P (mg kg^{-1})
SW-facing	7.5	21%	18.6	5.7	24.5	0.49
NW-facing	7.4	23%	15.9	7.2	22.9	0.48

The two cores taken from slopes of Hambledon Hill (table 5.4) show that these soils are similar to the shallow rendzinas on the slopes of Millington Pastures, having similar pH, LOI and extremely low available P.

5.2.2.5 N-mineralisation

March-June (experimental period 1)

Figures 5.7 to 5.9 show the distribution of gross N mineralisation distribution in the incubated soil cores for each pair of plots in period 1. Tables 5.5 and 5.6 show the results of ANOVA tests. During this period there was no significant effect of source of the soil or treatment plot, or any interaction effect, on mineralisation rates at the Automatic Weather Stations. On the Millington Pasture slopes there was no effect of soil source and no interaction but a significant effect of treatment plot ($p < 0.05$). Soil N mineralisation was higher in the YSF treatment (Tukey $p < 0.05$) than the YNF treatment, and was independent of soil type. This is in concordance with hypothesis 1.

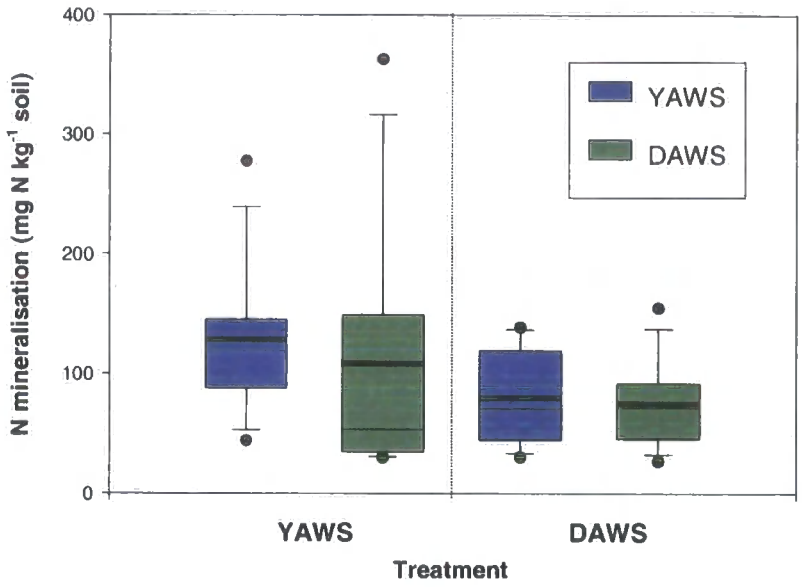

Figure 5.7: N mineralisation measured at automatic weather stations during experimental period 1. Thick line – mean value, thin line – median value, box – 1st and 4th quartiles, bar – 95% limits, points – outliers.

Table 5.5: N mineralisation ANOVA results for AWS during experimental period 1 (spring)

Source	SS	df	MS	F	*p*
Model	0.015	3	0.005	0.900	0.453
Intercept	0.307	1	0.307	55.012	0.000
Source	0.001	1	0.001	0.215	0.646
Plot	0.013	1	0.013	2.403	0.132
Source×plot	0.000	1	0.000	0.083	0.775
Error	0.156	28	0.006		
Total	0.478	32			

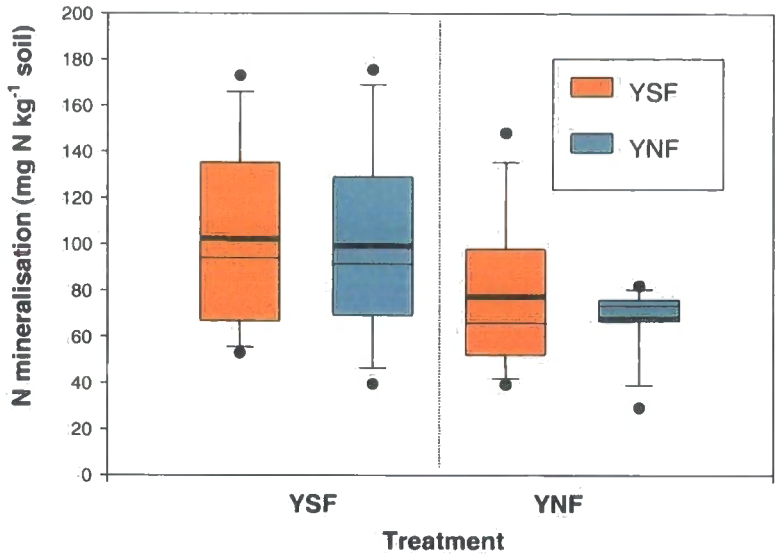

Figure 5.8: N mineralisation measured on slopes during experimental period 1. Explanation as in figure 5.7.

Table 5.6: N mineralisation ANOVA results for slopes during experimental period 1 (spring)

Source	SS	df	MS	F	Sig.
Model	0.007	3	0.002	1.640	0.203
Intercept	0.241	1	0.241	176.174	0.000
Source	0.000	1	0.000	0.222	0.641
Plot	0.006	1	0.006	4.635	0.040
Source*plot	0.000	1	0.000	0.061	0.807
Error	0.038	28	0.001		
Total	0.286	32			

July-Oct (experimental period 2)

Figures 5.9 and 5.10 show the distribution of gross N mineralisation in the plots during experimental period 2. Almost half of the cores show apparently low, or negative, mineralisation values (negative values are possible when mineralisation

rates are low compared to the spatial variation in initial available N, and final available N in the incubated core is lower than the initial value recorded in the adjacent core). The distributions of the data are therefore skewed and significantly differ from a normal distribution (Shapiro-Wilk test, $p < 0.05$). The data could not be made normal using standard transformations, so analysis was carried out using non-parametric Scheirer-Ray-Hare test. No significant effects of source, treatment or interactions were found for either data set, probably due to the wide variation in mineralisation rates within groups, and relatively low power of the test.

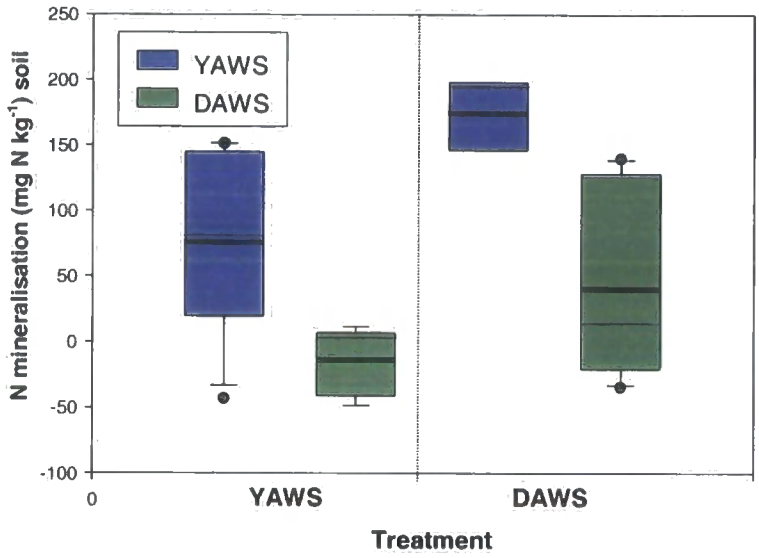

Figure 5.9: N mineralisation measured at automatic weather stations during experimental period 2. Explanation as in figure 5.7.

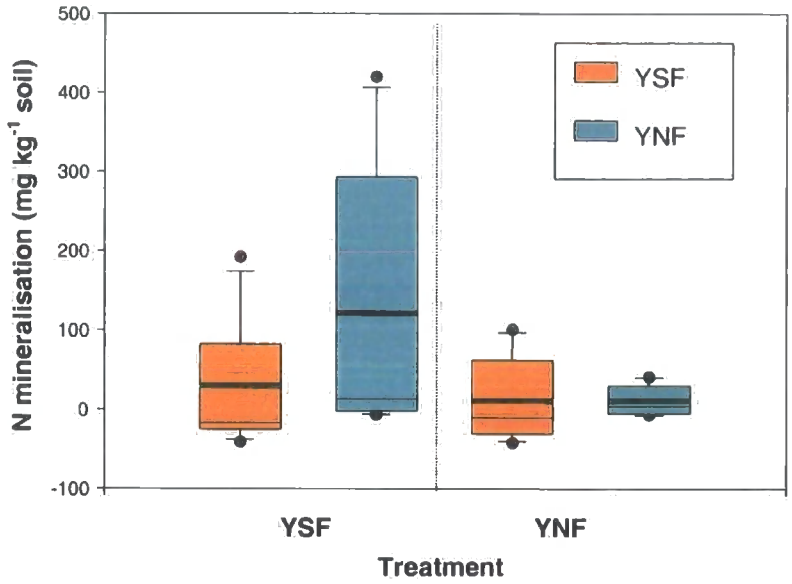

Figure 5.10: N mineralisation measured on slopes during experimental period 2. Explanation as in figure 5.7.

5.2.3 Conclusions

5.2.3.1 Above-ground biomass decomposition

The results for the litter bag experiment from the AWS sites along the macroclimatic gradient are consistent with hypotheses 1 and 2. However, no significant differences in mass loss between bags on the contrasting slopes (microclimatic gradient) were found. Since these plots had the greatest differences in microclimate, differences in mass loss cannot be ascribed to microclimate alone, and neither hypothesis 1 nor 2 can be accepted. Although both temperature and moisture are known to affect rates of organic matter decomposition (Heal *et al.*, 1978), other factors must explain the rates of mass loss observed in this study. Since the litter came from the same source and was well mixed, variations in litter C:N ratio between sites cannot explain the significant

effects. The most likely explanation is that the size and composition of the decomposer community (bacteria and fungi) varies between sites.

5.2.3.2 Soil analyses

Preliminary analysis of soil samples showed that the soils on the steep slopes of the dale at Millington Pastures have higher pH and considerably lower available P than those on the plateau. This concurs with the observations of Perring (1959) on the distribution of soil variables with respect to slope, and with observations on catenas in soils over limestone (Balme, 1953; Trudgill, 1976). These observations are consistent with thin soils with a high $CaCO_3$ content on steep slopes, as P is increasingly bound in the soil as apatite at higher pH and Ca^+ availability (Tyler, 2002). Soil cores taken at the hilltop AWS and two cores taken on slopes suggest that this pattern is repeated at Hambledon Hill. The soil organic content is lower at the AWS site at Millington Pastures than at Hambledon Hill, and available P higher; this may have a climatic explanation (Perring, 1960) or be due to the incorporation of drift material on the Wolds Plateau soils (Ellis and Newsome, 1991).

5.2.3.3 N mineralisation

Extractable N, measured from unincubated cores was relatively low in March, higher in July and October. Flushes of N mineralisation have been previously recorded in European dry grasslands in spring and autumn, when both temperatures and soil moisture are sufficiently high (Jamieson *et al.*, 1999; Schaffers, 2000). Significantly higher rates of N mineralisation on the 4.9° C warmer south-facing slope than on the north-facing slope, independent of soil source during the March-June incubation implies that there is sufficient quantity and quality of substrate for mineralisation in March but that mineralisation is limited by low temperature (hypothesis 1). No significant difference was found between soils incubated at the Millington and Hambledon AWS sites. The temperature difference here was smaller (2.4° C). It is also notable that cores at the north-facing slope in Millington would be frozen for two weeks in March (figure 5.2).

Despite significantly higher rates of N-mineralisation in the cores incubated from March-June on the south-facing slope, available N measured at this plot in July was significantly lower than at the other plots. This suggests that low soil moisture may have limited mineralisation in the field, while the incubated cores were kept at constant moisture content. However, no significant effects of either soil source or treatment plot were found in the July-October incubation. Hypothesis 2 is therefore rejected; soil moisture is not the primary factor limiting N mineralisation in summer. The high variability within groups – due to a large proportion of cores in which negligible mineralisation occurred during this incubation - hides any clear relationships between soil, treatment and N mineralisation in the data. Since this occurs with both wet and dry soils, at all sites and under temperature conditions suitable for mineralisation to occur (mean soil temperatures 12 – 16° C) this cannot be ascribed to the direct effects of microclimate. One plausible explanation is that following a pulse of mineralisation in spring, mineralisable organic nitrogen in these cores has been exhausted by mid-summer. This conclusion is consistent with the observations at Wytham, where a seasonal increase in C:N ratio was reported with maximum values in July, coinciding with minimum net mineralisation rates (Jamieson *et al.*, 1999), and summer rainfall manipulations had no direct effect on net mineralisation rates (Jamieson *et al.*, 1999). It should be noted that some incubated cores at in this experiment clearly did contain sufficient organic substrate to show high gross N mineralisation in summer, the highest rates being, as expected, the wettest soils (YNF) in the warmest environment (YSF). This suggests a patchy spatial distribution of organic substrate and/or C:N ratio within the soil in summer and fine-scale spatial heterogeneity in nitrogen mineralisation and therefore N availability at this site.

5.2.3.4 Topography and nutrient availability

The simple experiments and measurements described here, carried out on four plots over a single growing season, cannot give a full picture of nutrient cycling at these sites. However, they do provide insights about the ways in which

topography, microclimate and soil processes may influence nutrient availability. Nitrogen availability has been shown to be both spatially and temporally highly variable. A significant difference in nitrogen mineralisation rate between north- and south-facing slopes was shown, consistent with temperature limitation in early spring. In summer, mineralisation rates were much more variable, and variation within each plot was greater than variation between plots, consistent with a patchy distribution of organic nitrogen within the soil. In summer nitrogen availability appears to be dependent on the availability of a suitable organic substrate, at least over the 90-day timescale of these experiments. Periods of drought over the summer may affect short term N mineralisation by temporarily reducing microbial activity and in the long term increase the input of organic substrate through root and shoot death.

Phosphorus availability at both sites appears to be relatively stable over time and largely controlled by the effect of topography on soil physics and chemistry. Shallow rendzina soils on sloping ground have characteristically high pH and very low available P in comparison with the deeper calcareous brown earths formed on relatively stable flat areas.

5.3 Gas-exchange measurements in four chalk grassland species

5.3.1 Soil moisture, photosynthesis and water-use efficiency

Differences between the microclimate of contrasting slopes, particularly differences in soil moisture, are likely to affect the physiological performance of plants. During the extreme drought of 1995, Buckland *et al.* (1997) found that in a limestone dale at Buxton, Derbyshire, UK, the relative water content (RWC) of leaves of tap-rooted forbs on shallow soils was maintained at a higher level than that of shallow-rooted species. For species with a distribution centred on deeper soils, decreasing frequency of occurrence along a soil depth gradient was correlated with falling RWC values. Forseth *et al.* (2001) found that the reduction of soil moisture under shrubs reduced net CO_2 uptake, stomatal conductance,

transpiration and instantaneous water use efficiency (WUE), defined as the ratio of CO_2 and H_2O fluxes) of the herbaceous perennial *Cryptantha flava* in an arid system. Tsialtas *et al.* (2001) measured long-term water-use efficiency (defined by carbon isotope discrimination) in species of a water-limited grassland in Greece and found that water use efficiency was negatively correlated with biomass production. In a laboratory experiment, Ferris and Taylor (1995) found that in watered plots, the chalk grassland herbs *Sanguisorba minor* and *Anthyllis vulneraria* had higher rates of photosynthesis and transpiration, higher stomatal conductance and lower WUE than droughted plots. In a review of stomatal control of photosynthesis and transpiration, Jones (1998) considered that stomatal conductance may respond to both leaf and soil water status, with feedbacks due to water loss as transpiration. In this section gas-exchange measurements of leaves from four species are compared between north and south-facing slopes in mid-August 2002 to assess the influence that landscape position may have on carbon-gain and water-use efficiency.

5.3.2 Methods

5.3.2.1 Field measurements

Measurements were taken on four species; *Brachypodium pinnatum*, a tussock forming grass, *Carex flacca,* a sedge, *Lotus corniculatus*, a leguminous forb and *Thymus polytrichus*, a low mat-forming shrub. These species were selected as they all grow on both north- and south-facing slopes of the valley, to allow comparison between individuals growing on different aspects. Gas exchange measurements were taken on fifteen separate plants of each species from within an area of ca. 50 m^2 (7 m by 7 m). All measurements were made between 1100 and 1500h on the 14th, 15th and 16th of August 2002. During this period the solar zenith was sufficient that both slopes were exposed to direct irradiance, when clouds did not obscure the sun. Either a section of leaf (*Brachypodium* and *Carex*) or a section of stem and several leaves (*Thymus* and *Lotus*) were enclosed within the leaf chamber (area 4 cm^2). Gas exchange was measured using a portable

infrared gas analyser (LI-6400, Licor Inc., Nebraska, USA) at an air flow rate of 500 μmol s^{-1}.

Since it was not possible to manipulate light flux in the field with the equipment available, ambient irradiance levels were maintained, and photosynthetically active radiation between a wavelength of 400 and 700 nm (PAR) was measured inside the leaf chamber. Leaf temperature was maintained at 25 (± 1.5) °C. Recorded PAR values at the leaf chamber varied between 500 and 2200 μmol m^{-2} s^{-1}. Figure 5.11 shows hourly mean PAR and air temperature at 100 mm above the soil surface recorded at the Millington Pastures AWS over the three days. Instantaneous PAR measured within the leaf chamber frequently exceeded the hourly mean value measured at the AWS. Figure 5.12 shows the actual PAR measured at the leaf chamber for all species on different slopes. Measurements taken on south-facing slopes showed overall significantly higher PAR values (Two-way ANOVA, $F_{1,96} = 7.317$, $p = 0.08$) probably reflecting the orientation of leaves with respect to the sun; further variability in PAR is expected due to the position of the leaf within the canopy and atmospheric conditions at the time of measurement.

At each measurement, net photosynthesis rate per unit leaf area A_n (μmol m^{-2} s^{-1}), stomatal layer conductance to water vapour g_s (mmol m^{-2} s^{-1}) and transpiration rate E (mol m^{-2} s^{-1}) were recorded. Instantaneous water use efficiency (W) was calculated as the rate of photosynthesis divided by the rate of transpiration (A_n/E). After gas exchange measurements were made all material enclosed within the chamber was clipped and removed to the laboratory where it was scanned and photosynthetically active surface area (single surface projection) for each sample was calculated using image analysis software (Delta-T Scan v2.0, Delta-T Devices Ltd, Cambridge, UK).

Volumetric soil moisture (to 50 mm depth) was measured using a ThetaProbe (Delta-T Devices, Cambridge, UK) on August 15th 2002, using default settings for an organic soil. Ten replicates were taken on each slope. Mean soil moisture content on the south-facing slope was 36.8%, and 45.1% on the north-facing slope. The difference is highly significant (ANOVA, $F_{1,18} = 32.4$, $p < 0.01$).

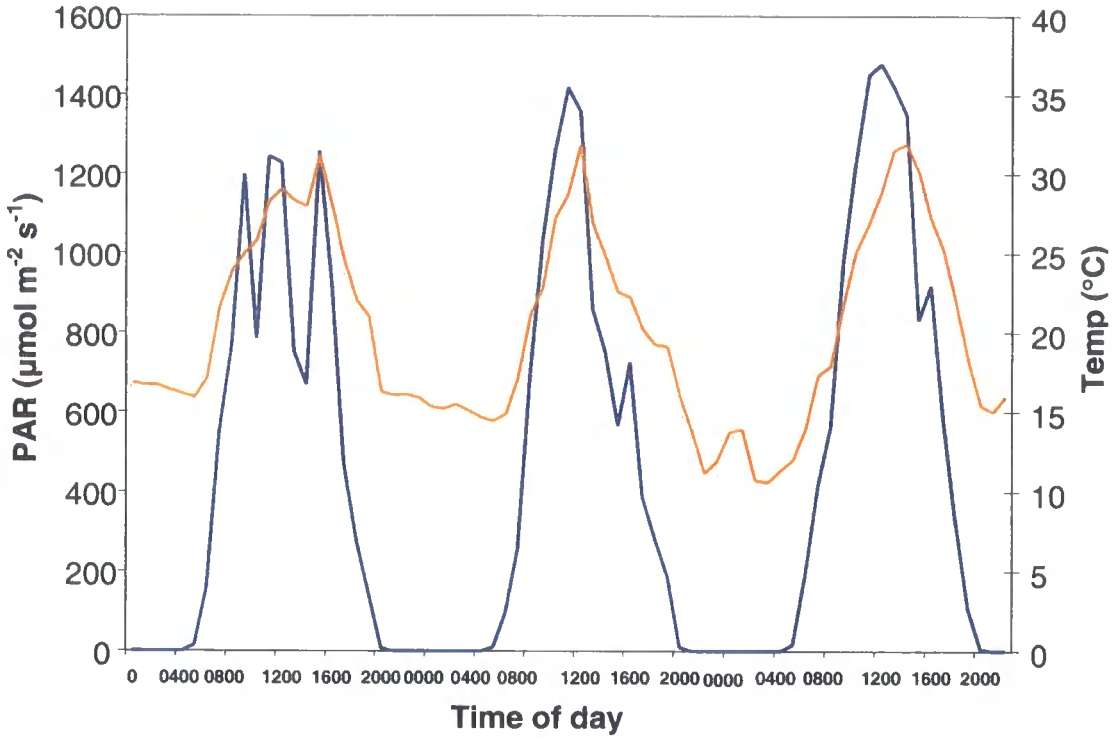

Figure 5.11: Hourly mean PAR (blue) and air temperature at 10 cm (orange) at Millington Pastures AWS, 14th-16th August.

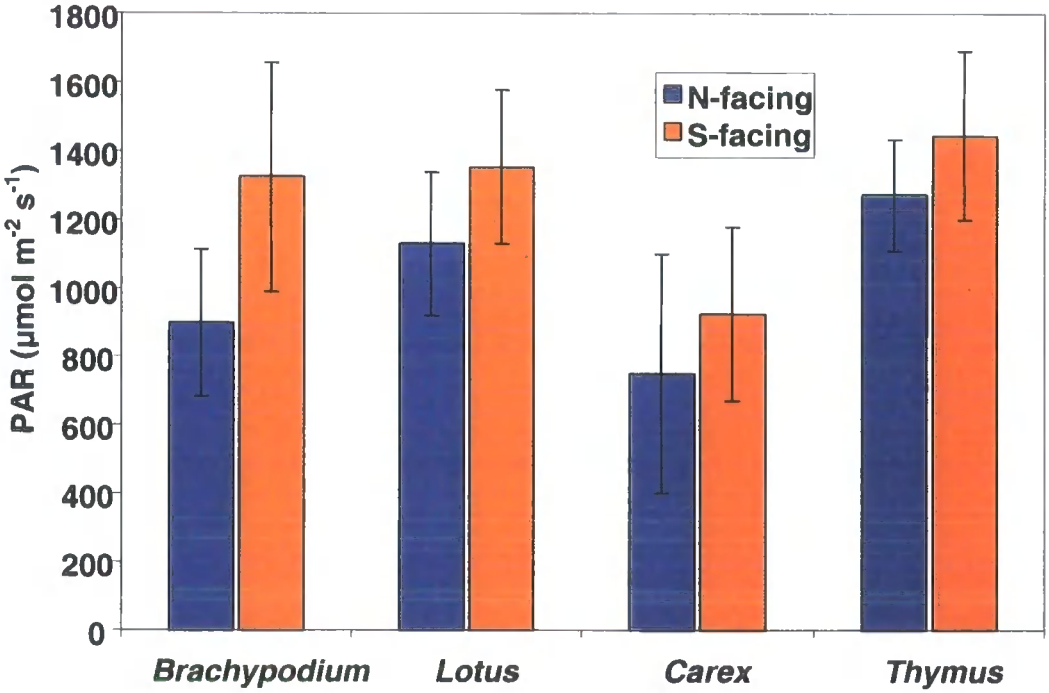

Figure 5.12: Instantaneous PAR measurements at the leaf chamber during gas-exchange measurements; error bars show 95% confidence intervals about the mean.

5.3.2.2 Data analysis

Data for transpiration rates, photosynthetic rates, stomatal conductance and water use efficiency for each species were tested for normality (Shapiro-Wilk test) and no transformation was required. Data were analysed using t-tests to test for difference between data from different slopes for each species.

5.3.3 Results

No significant difference in photosynthetic rate (figure 5.13) or transpiration rate (figure 5.14) between slopes was found for any species. However, both *Brachypodium pinnatum* and *Carex flacca* had significantly lower stomatal conductance (figure 5.15) and higher water use efficiency (figure 5.16) on south-facing slopes than on north facing slopes.

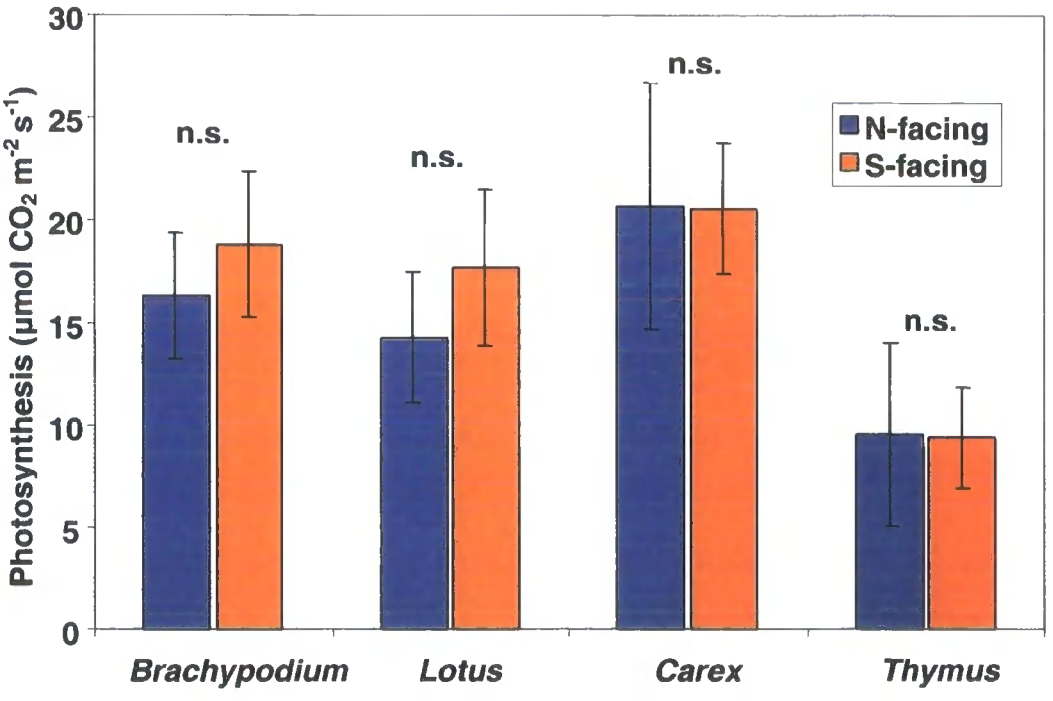

Figure 5.13: Leaf-level measurements of photosynthetic rate of four species growing on slopes of different aspect at Sylvan Dale. n = 15, n.s. – no significant difference between slopes.

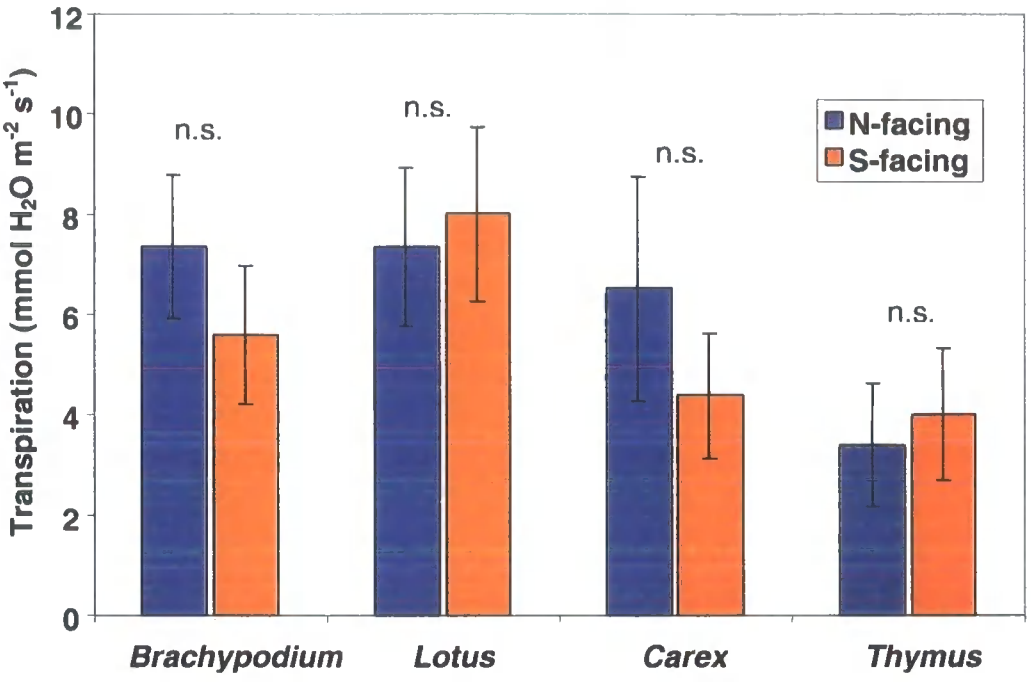

Figure 5.14: Leaf-level measurements of transpiration rate of four different growing on slopes of different aspect at Sylvan Dale. n = 15, n.s. – no significant difference between slopes.

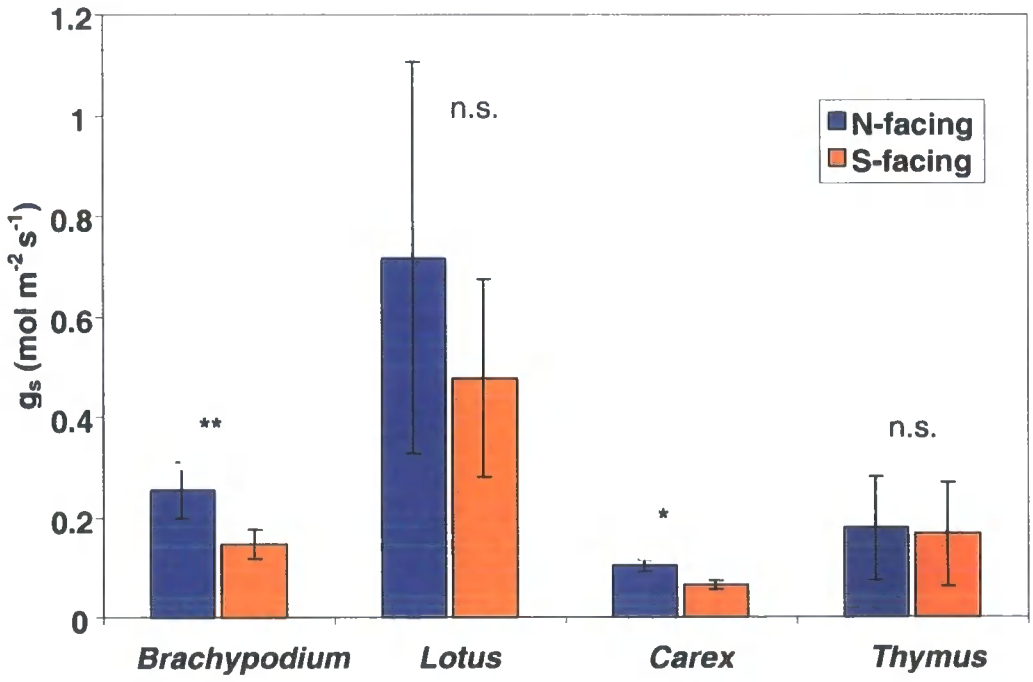

Figure 5.15: Leaf-level measurements of stomatal conductance (g_s) of four different growing on slopes of different aspect at Sylvan Dale. n = 15, n.s. – no significant difference between slopes, * = significant at $p < 0.05$, ** = significant at $p < 0.01$.

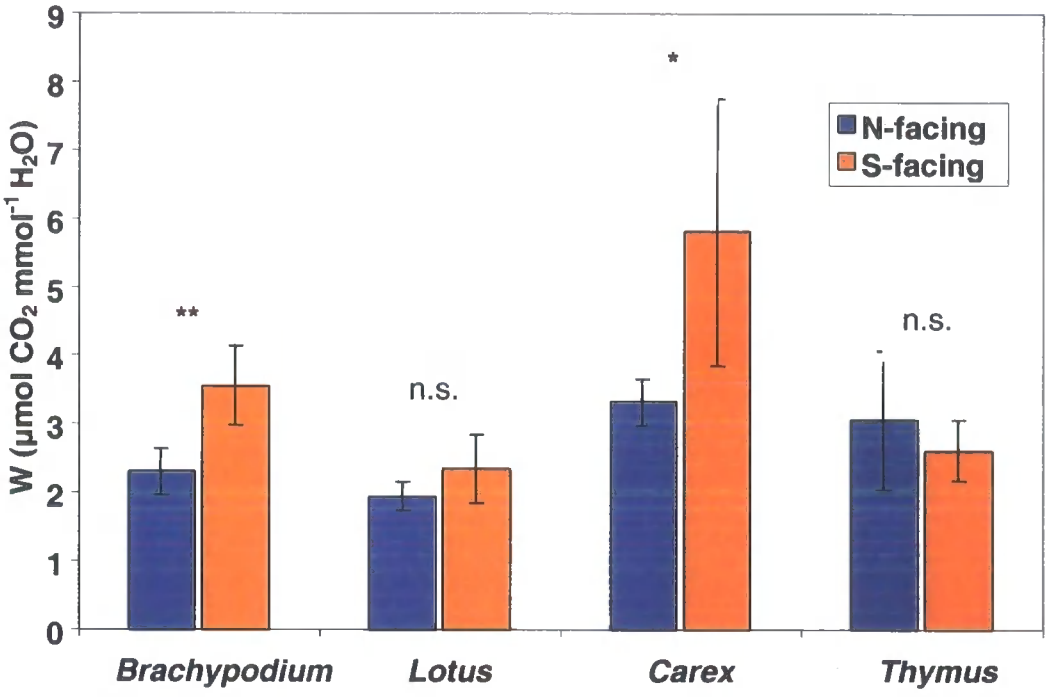

Figure 5.16: Leaf-level measurements of water use efficiency of four different growing on slopes of different aspect at Sylvan Dale. n = 15, n.s. – no significant difference between slopes, * = significant at $p < 0.05$, ** = significant at $p < 0.01$.

5.3.4 Conclusions

The differences in soil moisture between north and south facing slopes during this experiment were significant, however at 36.8% even the south-facing slope was only a little under field capacity. Water contents as low as 17% by volume were recorded at the south-facing slope during the previous summer. It is therefore not surprising that no significant effect of aspect on photosynthetic rate was recorded, as none of the plants would be expected to be under unusual drought stress at this time. Variation in PAR between and within sites was likely to be a more important control of both photosynthesis and transpiration for the time period of this study. In a review of stomatal control of photosynthesis and transpiration, Jones (1998) concluded that in under most conditions, the stomata play a relatively small role in determining the rate of photosynthesis. It is possible, however, that small differences in instantaneous photosynthetic rate, too small to be statistically

significant in this study, have a cumulative effect and are important in the long term. However, periods of more severe drought stress, leading to decreases in photosynthesis or even leaf death, are likely to be more important in reducing carbon assimilation on south facing slopes over a growing season, with a potential feedback to litter production and nutrient cycling.

Despite the lack of a significant response for photosynthesis or transpiration, and the relatively high water availability at both sites, stomatal conductance was significantly lower on the drier S-facing site for *Brachypodium* and *Carex*, and water use efficiency was significantly higher at this site for *Brachypodium* and *Carex*. This suggests that these species are responding to the lower soil water potential by limiting water loss through stomatal closure; in both these species, transpiration was lower on south-facing slopes, although this result is not statistically significant. Since the photosynthetic rate is unchanged, this results in increased water use efficiency. An alternative explanation is that plants growing on the south-facing slopes may undergo selection for high water-use efficiency.

Thymus polytrichus and *Lotus corniculatus* did not appear to respond to the lower soil moisture on south-facing slopes through increased water use efficiency. These species may have alternative strategies for dealing with low soil moisture. *Thymus* had the lowest rates of both photosynthesis and transpiration of all four species; its slow growth rate may be an adaptation to water stress (Pigott, 1955). Conversely *Lotus* has a long tap-root (Jones and Turkington, 1986) that may allow it to access soil water and maintain high transpiration rates.

5.4 Germination of selected chalk grassland species

5.4.1 Microclimate and germination

The effect of temperature, light and soil moisture on the germination of seeds is one process by which topography, and therefore microclimate, might be expected to influence vegetation composition. The reproductive niche is thought to be an important factor in determining the structure of chalk grasslands, and chalk grassland species have temperature and light requirements believed to control the

timing and micro-habitats in which their seeds germinate (van Tooren and Pons, 1988). Seed germination may respond to temperature fluctuations (Thompson, 1993), mean temperature (Arnold and Monteith, 1974; Thompson and Band, 1993) or thermal time (Trudgill *et al.*, 2000). Temperature responses to germination in Caryophyllaceae have been associated with distribution on a European scale (Thompson, 1970). However, Rorison and Sutton (1975) found that, while *Scabiosa columbaria* had a requirement of mean daily temperatures of 10 °C for germination which explained the timing of seedling emergence in an experiment on opposing sloes of Lathkill Dale, Derbyshire, this requirement did not explain its restriction to south-facing slopes at the site. The experimental design described here was designed to investigate the effects of manipulation of the radiation balance of the soil surface, using mirrors and shades, on germination of nine chalk grassland species, at two sites along a climatic gradient. Mirrors have previously been used to manipulate light as a treatment in established grassland plots (Eek and Zobel, 1997, 2001) but not apparently to manipulate soil microclimate. The treatments were designed to simulate the effect of microclimatic variation at contrasting climates near the northern limits, and near the core of the range of typical British chalk grassland communities. Since the southerly plot (at Monk's wood, Huntingdonshire) was damaged, only data from the northern plot at Durham is presented here.

5.4.2 Materials and Methods

5.4.2.1 Field sites

Sites with contrasting climates were selected for the experiment: Durham Botanic Gardens (grid reference NZ 274409), near the northern limit of lowland chalk grassland in the UK and the ranges of several of the species studied, and Monk's Wood Experimental Station, Huntingdonshire (TL 201797), in an area of the UK with close to continental climate. At Durham the experiment was carried out in an area of lawn, with no significant topographic obstruction above to the south; at Monk's Wood no area of grass was available, so the experiment was carried out

inside a metal tank of 1.5 by 2.5 metres filled with earth and surfaced with turf, to approximate a grassland surface.

5.4.2.2 Experimental design

At Durham nine seed trays (200 mm by 150 mm by 50 mm) were buried in gaps cut in turf in a lawn with the top of the tray level with the soil surface, in the layout shown in figure 5.16. At Monk's Wood the trays were buried in a metal tank of earth 1.5 by 2.5 metres with turfs planted around the trays. The trays were filled with soil removed from molehills at Millington Pastures. Two treatments were applied to trays. Shaded trays had a piece of plywood, 150 by 200 mm mounted in a vertical position to the south of the tray, with the side facing the tray painted matt black, shading the plot from direct sunlight for most of the day. Mirrored trays had a mirror, 150 by 200 mm mounted in a vertical position facing the tray, reflecting direct and diffuse radiation back towards the tray, and effectively doubling the direct radiation input onto the soil surface (figure 5.16). Each experimental plot had three mirrored trays, three control and three shaded plots (figure 5.17).

The effect of the treatments on soil temperature, measured using Tinytalk dataloggers buried in trays (Gemini Dataloggers, Chichester, UK), at ten-minute intervals over three days in July is shown in figure 5.19 On clear days (18/20 Jun) the shaded trays were up to 15 °C lower in temperature than the control trays. The mirror trays were up to 10 °C higher in temperature than controls. Night time temperatures were similar between plots.

Figure 5.20 shows the soil moisture, measured with a Theta-probe (Delta-T devices, Cambridge) twice daily for three days in July at Durham under different treatments, following watering to field capacity at 1200h on the first day.

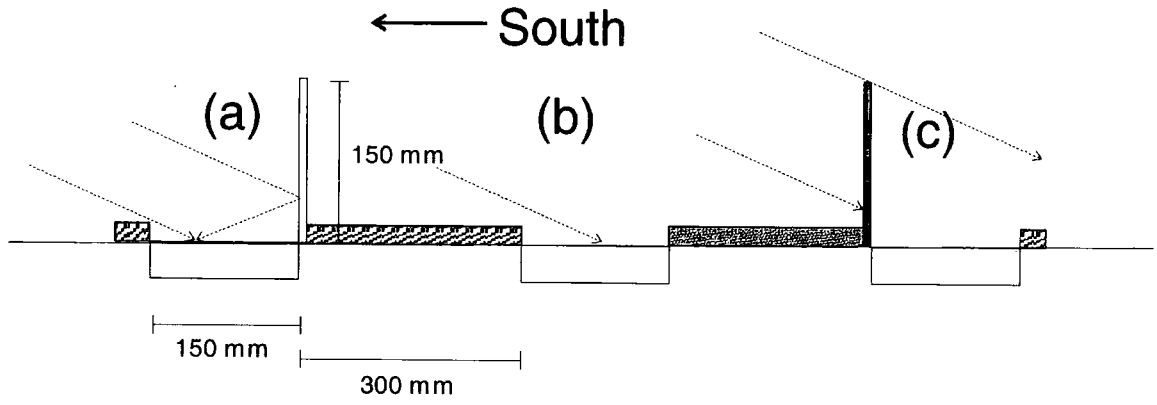

Figure 5.17: Side view of experimental set up (not to scale) showing a) mirrored treatment b) control c) shade treatment. Arrows represent hypothetical path of direct solar radiation.

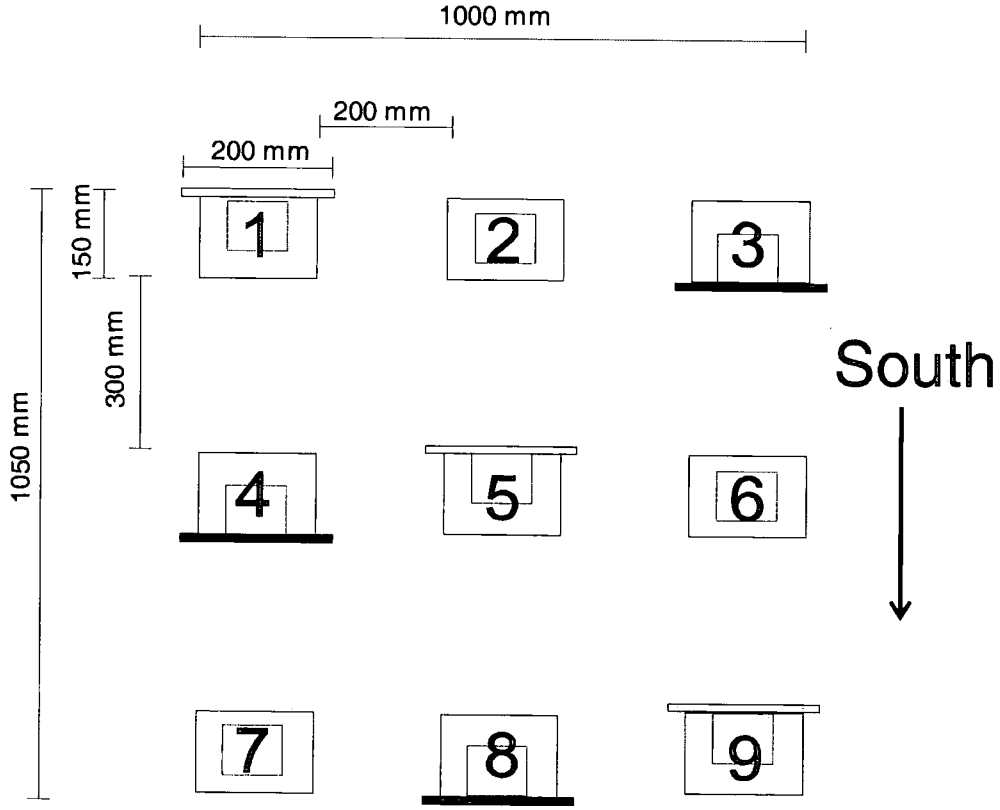

Figure 5.18: Plan view of experiment, showing numbered seed trays with mirrors (open rectangles) and shades (filled boxes).

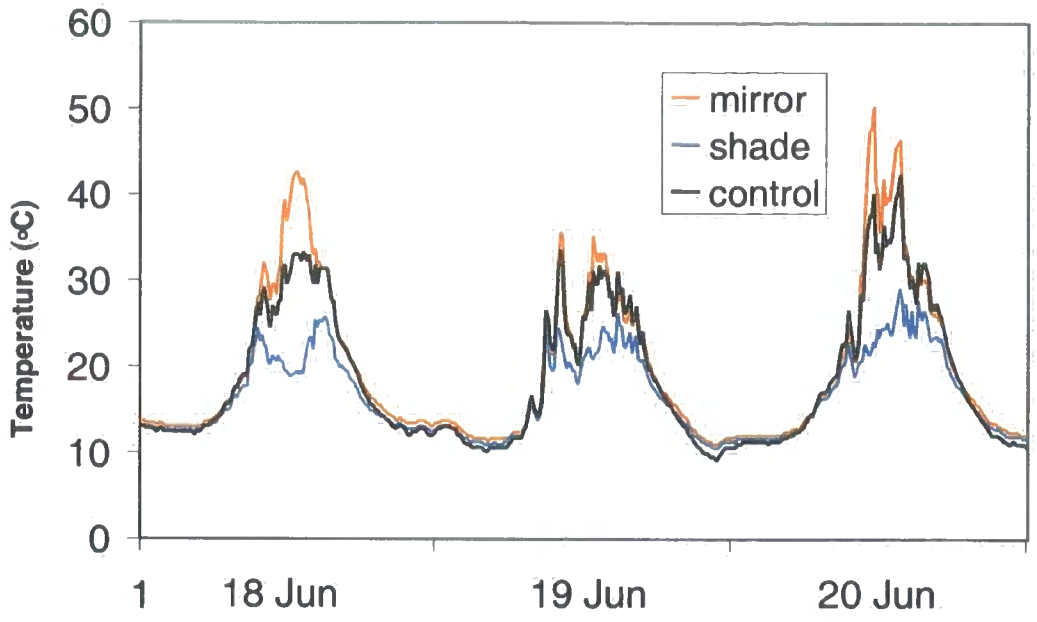

Figure 5.19: Soil temperature (0-50 mm depth) of experimental plots.

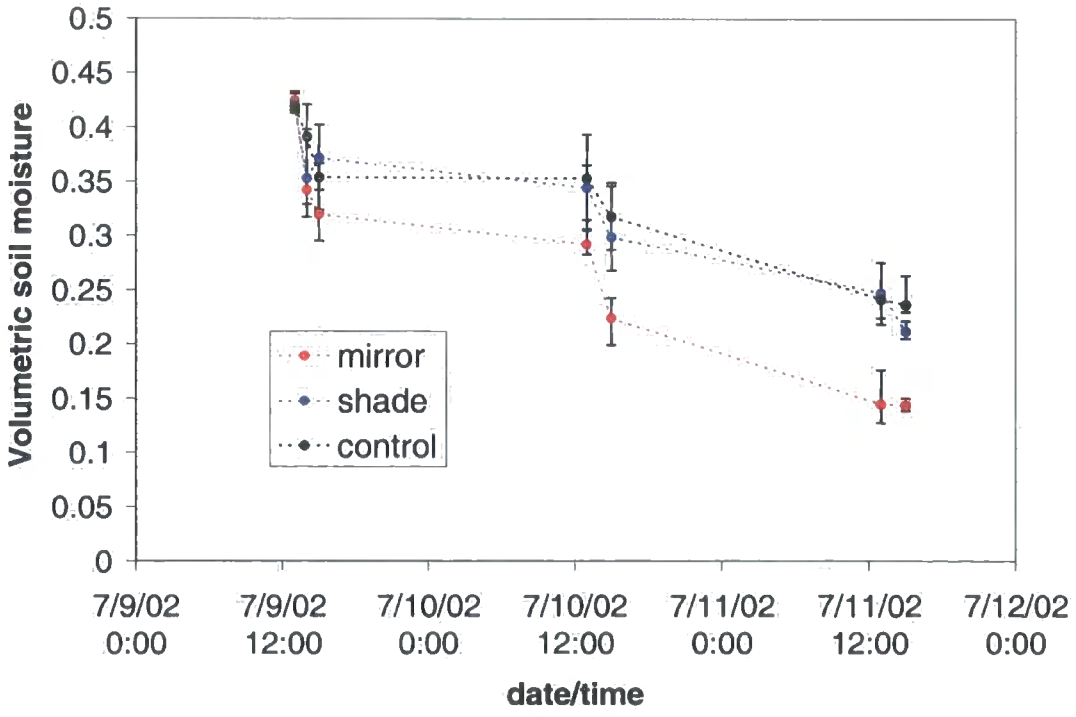

Figure 5.20: Volumetric soil moisture (0-50 mm) of experimental plots after watering. Bars show minimum/maximum values.

Seeds of nine species were collected from Hambledon Hill between 25 July and 10 October 2001. Seeds were stored in paper envelopes at room temperature prior to planting. Topsoil was collected from molehills at Millington Pastures in October and sieved through 4 mm mesh to remove roots and rhizomes. Prior to the experiment, 50 seeds of each species were tested for viability by germination on damp filter paper at a temperature regime of 16 h at 20° C, 8 h at 5°. All species tested achieved over 50% germination within a month, except *Hippocrepis comosa,* which achieved 20% germination and *Helianthemum nummularium*, in which no seeds germinated unless the seeds were scarified, in which case close 92% of the seeds germinated. Two separate samples of *Helianthemum* seeds were included in the experiment; one scarified and one non scarified.

Seeds were planted at 5 mm depth in the topsoil of each tray, in 100 mm single-species rows spaced 10 mm apart. The order of the rows in each tray was randomised. Seeds were planted on 25th April 2002 at Durham and 26th April at Monk's Wood. Trays were watered, when no rain had fallen, three times a week; however, observations and soil moisture measurements (figure 5.19) suggest that the high surface temperatures under the mirror treatment lead to more rapid soil drying.

Seedlings were counted at approximately weekly intervals for the first month of the experiment and fortnightly after the first month.

5.4.2.3 Data analysis

Data were analysed for differences between treatments on the date of maximum number of total seedlings. Data could not be assumed to be normal and so were analysed using a non-parametric single factor Kruskall - Wallis test using treatment as a factor, with three replicates for each factor.

5.4.3 Results

Disturbance by birds damaged the plots at Monks Wood after three weeks, and this part of the experiment had to be abandoned. Data are presented from the Durham experiment only. Figure 5.21 shows the mean number of seedlings recorded for each treatment for each recording date. Only one Kruskall - Wallis test showed a significant difference between treatments, probably due to the small number of replicates and low power of the test, rather than a lack of response to the treatments. *Cirsium acaule* showed a significant difference in treatment plots (χ^2 = 6.830, df = 2, $p<0.05$), with control plots showing a higher rate than either treatment. However, due to the effect of multiple comparisons, the chances of a Type II error are high and this result should be treated with caution.

5.4.4 Conclusions

The experimental treatments of shading and mirrors were shown to be a successful and cheap method of manipulating soil surface microclimate in a field experiment, demonstrating the critical effect of the radiation balance on temperature and soil moisture. One disadvantage of the method is that, even with regular watering, it was shown to be difficult to manipulate soil temperature independently of moisture. This is perhaps not a serious problem in an experiment designed to approximate realistic field conditions, where soil temperature and moisture are clearly not independent. A more serious problem is that, by effectively doubling direct radiation, mirrored treatments are exposed to higher radiation in the visible and photosynthetically active spectra than would be experienced under field conditions, even on south-facing slopes. The germination of some species is known to be inhibited by high light flux (Grime and Jarvis, 1975; Grime *et al.*, 1981). Mounting the mirrors at an angle tilted upwards, reducing the angle of incidence of reflected radiation, could moderate the extreme effect of the mirror plots.

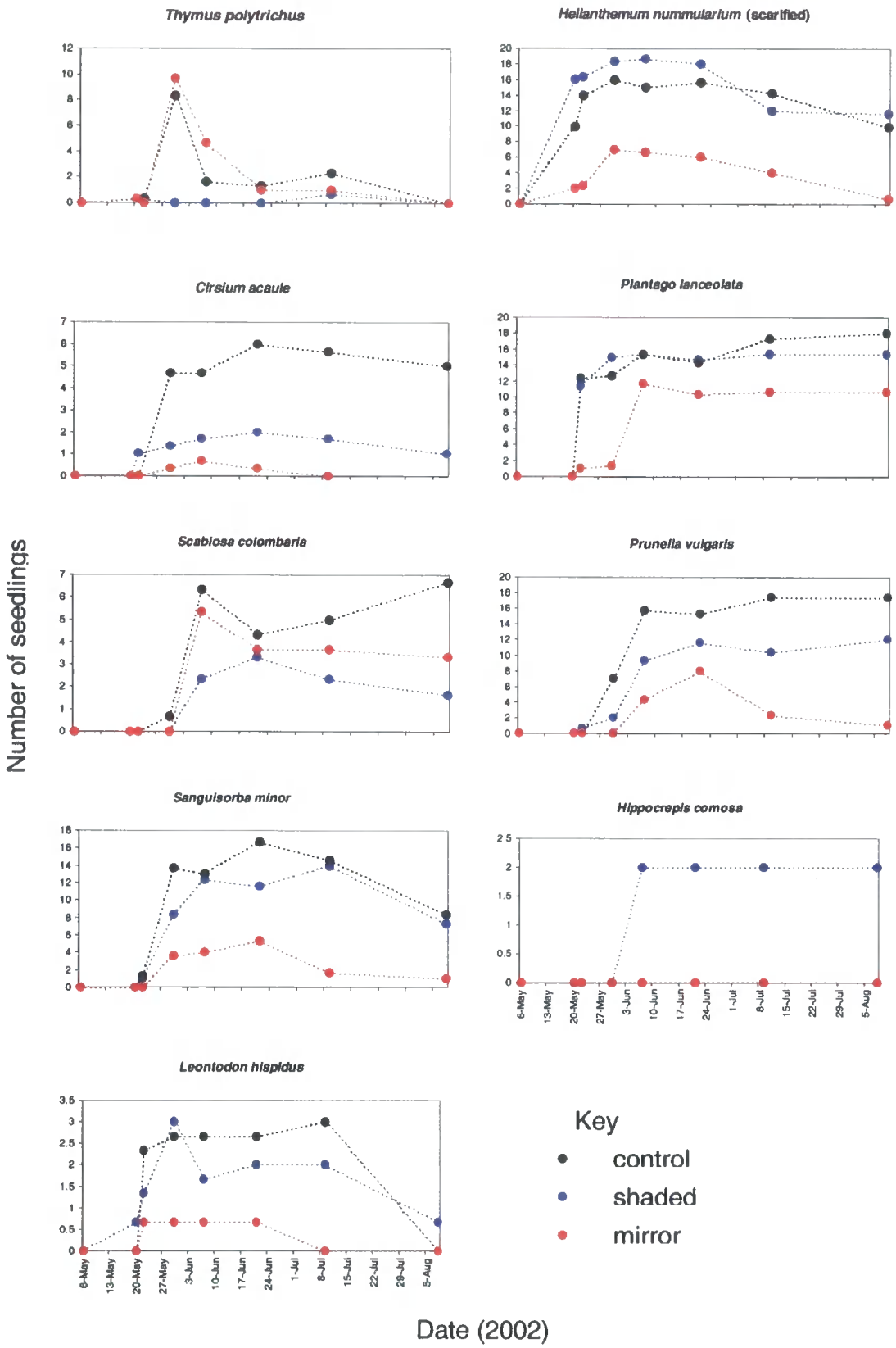

Figure 5.21: Mean number of seedlings of each species for each treatment. Black: control, blue: shaded plots, red: mirror plots. Note scales of y-axis vary.

The conclusions drawn from this experiment regarding the germination response to treatments are limited due to the failure of the Monk's Wood plots, and the lack of significant differences between treatments. However, it is notable that in almost all cases, seeds germinated as well, or better, in the shaded plots as in the control plots, and several species showed low rates of germination in the mirror plots. This suggests that those species tested here that are limited to south-facing slopes at the northern edge of their range are not limited by a high radiation/high temperature microclimate requirement for germination. For example, while only six seedlings of *Hippocrepis comosa* were recorded, all were in shaded trays. Other species more common in south/west facing slopes in Yorkshire, such as *Helianthemum nummularium* and *Sanguisorba minor* showed high rates of germination in shaded and control plots but lower rates in mirror plots. High mean temperatures and large diurnal fluctuations in temperature are typical of south-facing slopes. While several grassland species have a requirement for high or fluctuating temperatures for germination, Thompson and Grime (1983) consider that in many cases this is an adaptation to a ruderal habit, allowing species to make use of patches of open ground appearing at any time of the year. By contrast, survival in drought-prone environments may require germination in autumn or early spring, to allow seedlings to establish a viable root system before they are exposed to water stress. Thus Thompson (1970) found that species of Caryophyllaceae with a Mediterranean distribution had lower minimum temperature requirements for germination than Temperate species; Olff *et al.* (1994) regard autumn or winter germination a viable strategy for grassland plants when the risk of freezing in winter is lower than the risk of death in summer due to either competition or drought.

Oomes and Elbes (1976) have found that water availability in microsites was critical for the germination of a range of grassland species, including *Prunella vulgaris* and *Plantago lanceolata*. It seems likely that germination of most species in the mirrored plots were constrained by the rapid drying out of the soil after watering.

One exception to this pattern is *Thymus*, which showed high rates of germination in control and mirror plots, but low rates in the shade, consistent with a light/temperature requirement for germination. However most seedlings had died in these plots within two weeks, apparently due to water stress. *Cirsium* showed low rates of germination in the shaded plots, which was consistent with data presented by Grime *et al.* (1981) showing a comparatively high temperature requirement for germination. However, this species also showed low germination in the mirror plots, presumably due to low water availability.

The failure of non-scarified *Helianthemum* seeds to germinate, and the high rates of germination of scarified seeds suggests that breaking physical dormancy may be an important factor in the control of germination of this species. The low rates of germination of the *Hippocrepis* seeds also suggest physical dormancy. The role of low winter or high summer temperatures, diurnal temperature fluctuations and drying/rewetting cycles in breaking physical dormancy may be an important aspect of the control of germination of this species which has not been explored in this experiment.

5.5 Summary of chapter 5

1. Phosphorus availability at both sites appears to be relatively stable over time and largely controlled by the effect of topography, independently of microclimate, on soil physics and chemistry; unstable rendzinas on slopes were found to be extremely low in extractable phosphate at both sites. Plant growth is more likely to be phosphorus limited on slopes than on flat ground.
2. A significant difference in nitrogen mineralisation rate between north- and south-facing slopes at Sylvan Dale was found in early spring, consistent with temperature limitation at this time of year.
3. In summer nitrogen availability appears to be dependent on the patchy availability of a suitable organic substrate.

4. Short term nitrogen availability to plants may be limited by microclimate during the spring, when sufficient organic substrate for mineralisation is present; during the summer it is likely to be limited by the availability of substrate, which may vary on a small spatial scale. Long term nitrogen availability will therefore depend on feedbacks of organic matter to the soil.
5. No significant differences in litter decomposition rate were found between slopes; significant differences between flat sites could not be fully explained by the microclimatic variables measured.
6. No significant differences in photosynthetic rate or transpiration between north and south-facing slopes at Sylvan Dale were found in four chalk grassland species in August 2002. *Brachypodium pinnatum* and *Carex flacca* were found to have significantly lower stomatal conductance and higher water use efficiency on the drier south-facing slopes, suggesting that these species reduce water loss as soils dry out. No significant difference in these variables was found for *Lotus corniculatus* or *Thymus polytrichus*.
7. Of the seeds of nine chalk grassland species tested, all except *Cirsium acaule* germinated more often or equally well in shaded microsites in Durham than unshaded plots or those with increased radiation from mirrors. If microclimate requirements for germination plays a role in restricting species to south-facing slopes, it is more likely to be through breaking of physical dormancy of seeds with hard coatings (such as *Helianthemum nummularium* or *Hippocrepis comosa*) or in higher temperatures allowing earlier germination in spring, avoiding dessication later in the year. These processes would repay further investigation.

Chapter 6: Vegetation analysis

6.1 Introduction

In this chapter, gradients in vegetation composition at both field sites are examined. Detrended correspondence analysis (DCA) is used to examine differences in vegetation within and between field sites, and generalised additive models (GAMs) are used to investigate the relationships between microclimatic variables modelled using the methodology outlined in chapter 3, and the frequency of species within plots. Finally, 27 vegetation plots surveyed by Perring (1959) at Hambledon Hill in 1952 are compared with plots in equivalent positions in the landscape in 2000, to assess vegetation change in different landscape positions over the last 50 years.

Perring's study (1958; 1959; 1960) suggests that chalk grassland species are distributed on an environmental gradient from dry, calcareous grasslands with low soil moisture and high pH to neutral grasslands with more leached soils and more humid conditions. This environmental gradient is influenced by both macroclimate and microclimate; the gradient observed between sites from different climates is analogous to that between plots in different topographic positions in the same landscape.

Similar patterns have been observed in vegetation analysis of calcareous grasslands both within and between climatic regions. For example Gittens (1965a; 1965b; 1965c) used Bray and Curtis polar ordination to produce ordinations of both plots and species from a Carboniferous limestone grassland site in Anglesey. Almost all variation in the ordination was accounted for by a continuous gradient from "limestone" to "neutral" grassland (with two outliers representing "oligotrophic" plots associated with areas where sheep pastured overnight). This gradient was related to the environmental variables soil depth (assumed to be a proxy for available soil moisture) and available phosphate.

Over a much larger spatial scale, Duckworth *et al.* (2000a; 2000b) carried out DCA on calcareous grassland plots from a region of Atlantic Europe including Ireland, Southern England, France and Northern Spain. The first DCA axis extracted was assumed to represent a gradient from xerobromion to mesobromion grasslands, with a decrease in species with a Mediterranean and sub-Mediterranean distribution from SW France to N France, S England and Ireland.

In this chapter, a vegetation survey of 40 plots within each field site is described and the effect of topographic microclimate on the distribution of species and vegetation patterns is examined. Topographic microclimate variables are modelled using the methods developed in chapter 3. Detrended correspondence analysis (DCA) is used to investigate the main gradients of variation in the vegetation data. Generalised additive models (GAMs) are used to investigate the relationships between DCA axes, the frequency of individual species, and modelled variables. Modelled environmental variables are compared as predictors of vegetation and species distribution with topographic vegetation indices.

6.2 Methods

6.2.1 Vegetation survey

The vegetation survey methods of Perring (1959) were repeated as closely as possible to allow for comparisons between the present survey and his original data sets.

An area judged to be of relatively homogeneous vegetation (plot) of area 50 m^2 (approximately 7 x 7 m) was marked, and the slope and aspect of the plot were measured using a compass and clinometer. Within each plot twenty quadrats of area 10 cm x 10 cm were thrown at random. Within each quadrat, an estimate of cover for all vascular plants and bryophytes was recorded on a scale of 1 to 5, where a score of 1 represents 0-20% cover and 5 represents 80-100%. An estimate of total percentage cover for the plot was calculated as the sum of the

scores for all quadrats in the plot; a measure of percentage frequency was derived from the proportion of quadrats containing the species. Species present in the plots but not found in the quadrats were recorded but not used in the analysis. Vegetation survey took place during May to August 2000, August 2001 and May to August 2002. The relatively intensive survey method and small quadrat size meant that the majority of forbs and graminoids present in the quadrats were likely to have been positively identified from vegetative or flowering parts. However, inconspicuous or "difficult" groups are likely to have been under recorded or occasionally misidentified, particularly the less common bryophyte species.

6.2.1.1 Locating Perring's vegetation plots

At both field sites, attempts were made to locate Perring's original vegetation plots using site descriptions, grid references and maps. At both sites, large areas which had been under unimproved grassland at the time of Perring's survey had been converted to arable fields or ploughed and reseeded, particularly the southern flanks of Hambledon Hill (not included in the NNR) and the plateau top at Millington Pastures. At Hambledon Hill 27 out of 37 original plots were still under unimproved chalk grassland. These plots were resurveyed in 2000. The plots were unmarked, and so their precise locations were unknown; however, in many cases (for example where plots were located on earthworks with a given slope and aspect) it was possible to be confident that essentially the same area was being surveyed. In less distinct cases, the locations of plots surveyed in 2000 may not correspond exactly to that of the 1952 plots, but are in the close vicinity (in most cases probably within 10 metres), sharing the same slope and aspect. Only one of Perring's plots in the vicinity of Sylvan Dale survived as unimproved chalk grassland, and this was resurveyed in 2001.

6.2.1.2 Survey of additional vegetation plots

An additional 13 plots at Hambledon Hill were located to give a comprehensive coverage of all slopes and aspects represented at the site. At Sylvan Dale, where

only one of Perring's plots survived, an additional 39 plots were chosen to represent a comprehensive coverage of slope and aspect. A total of forty plots at each field site were therefore surveyed (figures 3.2 and 3.3).

6.2.1.3 Vegetation height

Following Perring (1954) a visual estimate of the minimum, mean and maximum vegetation height at each plot at the time of survey was recorded. Less apparently subjective methods of measuring sward height, the sward stick and drop disc, are reviewed by Stewart *et al.* (2001) and compared against the "direct" method of estimating by eye the level below which 80% of the vegetation is growing and measuring the height by ruler. The direct method was found to be more consistent, and a better predictor of soil temperature, particularly on short swards and on sloping ground.

6.2.1.4 Soil type and depth

Due to the archaeological status of the earthworks at Hambledon Hill, it was not possible to take soil samples or dig soil pits for each plot. Soil type for each plot was therefore subjectively classified on the basis of topography and examination of patches of disturbed earth within or near the plot. Soils were classified as rendzinas (Icknield series soil at both sites, usually on steeper slopes and consisting predominantly of organic matter and numerous chalk fragments), calcareous brown earths derived from chalk (on plateau at Millington Pastures and hilltops at Hambledon Hill) and colluvial brown earth (valley bottom at Millington Pastures and shallow lower slope at Hambledon Hill).

Measurement of soil depth in soils derived from chalk is subjective as organic soil frequently grades into chalk fragments with no clearly defined horizons; plant roots may penetrate several centimetres into the chalk bedrock itself. Depth to chalk was estimated by inserting a 5 mm diameter steel rod in to the soil until it met

resistance. Ten replicate measurements were taken for each plot and the mean value was recorded.

6.2.2 Microclimatic variables

Several microclimatic variables were modelled for each plot using the methodologies outlined in chapter 3. Ideally mean values for a period of several years prior to the vegetation survey should be modelled; for example, Silvertown *et al.* (2001) modelled soil moisture in lowland meadows using a hydrological model run for 15 years. However, sufficient input data from the field sites was only available for relatively short periods of time, so modelled variables for certain variables at key times of year over the study period were calculated, and considered to be representative of longer term climate.

6.2.2.1 Mean July maximum grass temperature (JMAX)

Mean hourly sward temperatures were calculated for each plot using input data from July 2002, using equations 4.11 and 4.12. Daily maximum temperatures were extracted from these data and a mean value calculated for the month. This variable was chosen as an indicator of the daily maximum temperature of the air layer close to the ground in summer. The effects of screen height temperature and net radiation flux on this variable are additive (assuming constant wind speed) and so highest values occur under warmer macroclimates and on steep southwest facing slopes where the maximum radiation flux coincides with maximum afternoon air temperatures at screen height.

6.2.2.2 March to May soil temperature sum above 5 °C (TSUM)

Hourly soil temperatures (at 50 mm depth) were calculated for each plot for the period March to May 2002. At Sylvan Dale, a mobile data logger was located at the valley bottom during this period; hourly data were corrected for the topographic drainage effect assuming a linear increase in sward temperature up slope from the

valley bottom to the plateau. This variable was selected to represent the temperature and timing of spring warming. This was shown to have an effect on nitrogen mineralisation in chapter 5; it is assumed that it also affects the phenology and growth rates of species. Highest values of this variable occur under a warm spring macroclimate and on steep south-facing slopes, at Sylvan Dale near the top of the valley, where the "frost hollow" effect is minimal. Due to the relatively low solar altitude at this time of year, topographic shading is also likely to have a significant effect. As this variable is a temperature sum, its topographic distribution would be expected to be symmetrical about a N-S axis.

6.2.2.3 Total annual PAR flux (AnnPAR)

Hourly PAR values during 2001 were calculated from the modelled insolation values for each plot using equation 4.3. The total annual incoming PAR flux above the canopy (mol m^{-2}) was calculated for the year. The topographic distribution of this variable is expected to be symmetrical about a N-S axis.

6.2.2.4 Spring/summer drought days (DR2002)

Daily mean volumetric soil moisture was calculated for each plot for the period 1 March to 15 August 2002. The number of days for which volumetric soil moisture fell below 30% was calculated for each plot. This variable was chosen to estimate the period of time under which plants may experience water stress; increased stomatal resistance in two species was shown to increase at a mean value of 37% soil water in chapter 5. Highest values would be expected to occur on steep south to southwest facing slopes with shallow soils under a dry macroclimate. Plots with a damp microclimate may have zero values for this variable; the upper limit for a regional climate tends towards the number of rain-free days during the period.

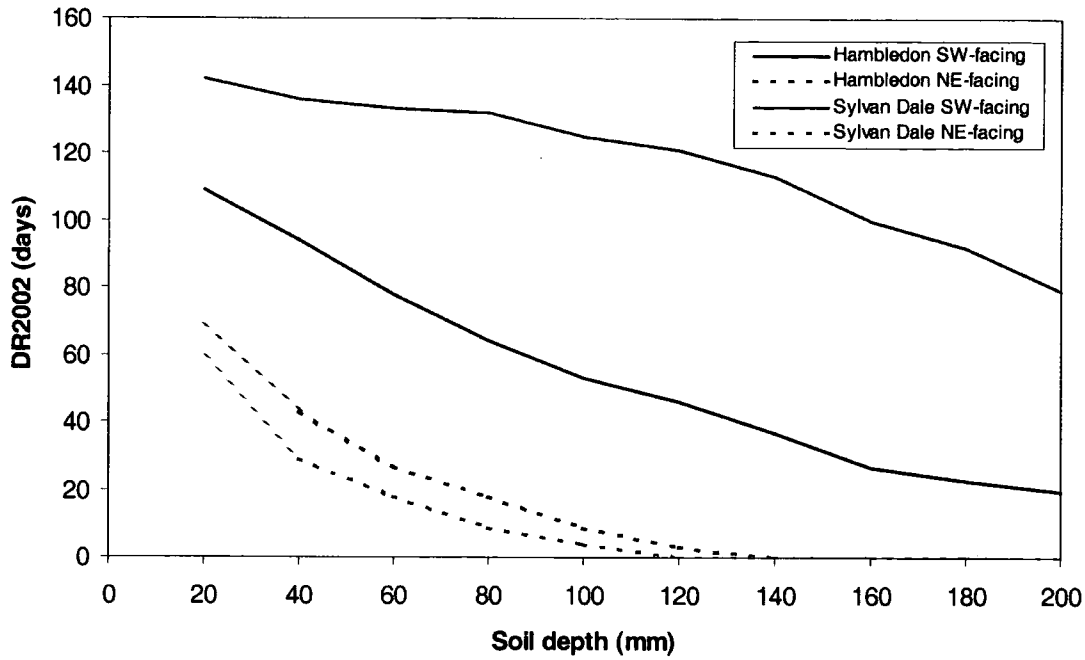

Figure 6.1: Modelled number of days where θ (m^3m^{-3}) < 0.3 during March – August 2002 (DR2002) for hypothetical 30°slopes facing due SW and NE under Hambledon Hill and Sylvan Dale climates.

As an example of the response of DR2002 to these factors, Figure 6.1 shows the results of running the soil moisture model to produce DR2002 values for hypothetical slopes of 30 ° facing SW and NE using climate data from each AWS, with different soil depth values. The interaction between macroclimate, soil depth and slope aspect can be clearly seen. Under all conditions, DR2002 decreases with increasing soil depth. During this period, the AWS at Hambledon Hill recorded higher vapour pressure deficit than that at Millington. The ventilation term of the Penman-Monteith equation was therefore relatively large. Under the more humid, less windy climate at Sylvan Dale, the radiation term is relatively more important, and thus there is a greater difference in DR2002 between slopes with different radiation fluxes. Despite the less humid climate, Hambledon Hill AWS recorded higher total, and more frequent, rainfall during this period. The period of drought is therefore shorter on south-facing slopes at Hambledon than Millington in this year.

6.2.3 Ellenberg and CSR scores

Ellenberg indicator scores and CSR scores were calculated for each plot using MAVIS plot analyser software (Stuart, 2000). Plot scores represent weighted mean species scores, from the Ellenberg indicator dataset extended to Great Britain (Hill *et al.*, 1999) and CSR scores for British species from Grime (1974; 1988). The Ellenberg indices are L (light), M (moisture), R (reaction) and N (nitrogen); the latter is probably best interpreted as a "productivity" indicator rather than a measure of nitrogen availability to plants (Hill and Carey, 1997; Schaffers and Sýkora, 2000). Grime's CSR scores represent the proportion to which a species is attributable to each of three strategies: S (stress tolerators), R (ruderals) or C (competitors). A high S score for a plot would indicate resource shortages that limit photosynthetic production such as drought, shade, or nutrient limitation; a high R score would indicate disturbance associated with destruction of biomass; and a high C score indicates the absence of these constraints on the accumulation of plant biomass. Plot scores were plotted on a triangular ordination. For descriptive purposes, sample plots were matched to NVC community (Rodwell, 1992) using MAVIS Plot analyser (Stuart, 2000).

6.2.4 Vegetation analysis

DCA was carried out on all data using the DECORANA FORTRAN program (Hill, 1979) using default values for all parameters and the default option of detrending by segments. Correlations between plot DCA scores on the first four axes and plot Ellenberg and CSR indicator values were calculated using non-parametric Spearman's Rank correlation coefficients using SPSS. To investigate possible non-linear relationships or interactions between environmental variables and the vegetation axes, the first DCA axis was modelled using a generalised additive model (GAM) (Hastie and Tibshirani, 1990) using S-PLUS v. 6.0. GAMs were also constructed for the frequency of several of the more abundant species to assess which variables best explained the distribution of both vegetation and species. For the species frequency data, the frequency scores were scaled between 0 (not present) and 1 (present in all quadrats in a plot). Scores were then used as the dependent variable with a logistic link function and binomial error term. Models

were constructed using a stepwise procedure. Explanatory variables were added firstly with a linear response function, then with a cubic smoothing spline. The change in residual deviance and degrees of freedom were examined using χ^2-tests, and terms were included if they significantly reduced the residual deviance of the model at $p < 0.05$. As the microclimate variables and radiation index were correlated, only one response function of this group of variables that gave the greatest reduction of deviance was included in the final model.

6.3 Results

6.3.1 Qualitative comparison between slopes

Representative vegetation data for plots on opposing slopes and flat sites for each field site are compared in tables 6.1 and 6.2.

Table 6.1 shows the cover and frequency scores for typical SW-, NE-facing and flat (valley bottom) plots at Sylvan Dale. Y37, the valley bottom plot, is mesotrophic grassland dominated by *Lolium perenne* and *Trifolium pratense,* and is clearly a very different community from the plots on the slopes. The dominant grasses in each of these are *Brachypodium pinnatum* and *Festuca ovina* and both are classified as NVC CG4 *Brachypodium pinnatum* grassland (Rodwell, 1992), the North-East facing slope approximating the *Holcus lanatus* sub-community, the South-west-facing slope the *Centaurea nigra-Leontodon hispidus* sub-community. Within the *Brachypodium-Festuca* matrix there are clear and consistent differences in the abundance of several species that are observed on contrasting slopes at this site. The North-facing slope has a high frequency of a group of species common in mesotrophic grassland and with a widespread geographical distribution in Britain, including *Achillea millefolium*, *Prunella vulgaris*, *Vicia sativa*, and *Ranunculus acris*. Several of these species are included in Perring's groups IV and V, being more common on flat ground or slopes between NW and E in North Dorset.

Table 6.1: Vegetation data from plots Y24, Y38 and Y37 at Sylvan Dale.

	Y24 (38° NE-facing)		Y38 (20° SW-facing)		Y37 (0° valley bottom)	
	cover (%)	frequency (%)	cover (%)	frequency (%)	cover (%)	frequency (%)
Forbs						
Achillea millefolium	3	10	0	0	2	5
Campanula rotundifolia	3	15	2	10	0	0
Centaurium erythraea	0	0	2	5	0	0
Cirsium arvense	0	0	0	0	3	5
Gentianella amarella	0	0	4	20	0	0
Helianthemum nummularium	0	0	8	20	0	0
Lathyrus pratensis	2	10	0	0	0	0
Leontodon hispidus	0	0	28	85	0	0
Linum catharticum	12	45	3	10	0	0
Lotus corniculatus	0	0	12	45	0	0
Pilosella officinarum	22	60	28	85	0	0
Pimpinella saxifraga	6	20	7	30	0	0
Polygala vulgaris	0	0	7	25	0	0
Potentilla erecta	2	5	1	5	0	0
Prunella vulgaris	22	50	3	10	0	0
Ranunculus acris	7	25	0	0	0	0
Ranunculus repens	0	0	0	0	5	20
Rumex acetosa	0	0	0	0	1	5
Stellaria media	0	0	0	0	1	5
Thymus polytrichus	0	0	65	100	0	0
Trifolium pratense	0	0	0	0	51	90
Urtica dioica	0	0	0	0	2	5
Veronica officinalis	3	10	0	0	1	5
Vicia sativa	2	5	0	0	0	0
Viola hirta	0	0	4	20	0	0
Viola riviniana	3	10	0	0	0	0
Grasses/sedges						
Agrostis capillaris	4	15	1	5	1	5
Brachypodium pinnatum	39	85	35	90	0	0
Briza media	7	30	15	40	0	0
Carex caryophylla	4	15	0	0	0	0
Carex flacca	14	35	35	95	0	0
Festuca ovina	67	100	40	100	0	0
Holcus lanatus	0	0	0	0	1	5
Koeleria macrantha	1	5	1	5	0	0
Lolium perenne	0	0	0	0	74	100
Luzula campestris	1	5	1	5	0	0
Phleum bertolonii	0	0	0	0	3	10
Bryophytes						
Calliergon cuspidatum	3	10	2	10	0	0
Campylium chrysophyllum	1	5	0	0	0	0
Dicranum scoparium	0	0	14	45	0	0
Plagiomnium undulatum	2	10	0	0	0	0
Pseudoscleropodium purum	14	45	4	15	0	0
Rhytidiadelphus squarossus	14	40	0	0	0	0

Table 6.2: Vegetation data from plots D24, D38 and D37 at Hambledon Hill.

	D15 (32° NE-facing)		D16 (30° SW-facing)		D37 (0° hilltop)	
	cover (%)	frequency (%)	cover (%)	frequency (%)	cover (%)	frequency (%)
Forbs						
Achillea millefolium	3	15	0	0	17	50
Asperula cynanchica	3	5	17	55	1	5
Cirsium acaule	1	5	0	0	0	0
Crepis capillaris	7	15	0	0	0	0
Euphrasia nemorosa	0	0	17	55	0	0
Galium verum	0	0	0	0	7	25
Gentianella amarella	0	0	1	5	0	0
Hippocrepis comosa	0	0	45	95	0	0
Leontodon hispidus	28	75	4	15	2	5
Linum catharticum	7	35	10	40	1	5
Lotus corniculatus	22	60	10	20	15	30
Odontites verna	0	0	0	0	1	5
Pilosella officinarum	3	10	7	20	0	0
Plantago lanceolata	22	70	20	55	26	65
Polygala calcarea	6	20	18	40	0	0
Sanguisorba minor	17	50	58	100	0	0
Prunella vulgaris	3	10	0	0	0	0
Ranunculus bulbosus	13	55	0	0	4	15
Rhinanthus minor	4	15	0	0	0	0
Rumex acetosa	2	5	0	0	4	15
Scabiosa columbaria	22	50	21	50	0	0
Senecio jacobaea	0	0	4	15	0	0
Thymus polytrichus	10	30	11	30	0	0
Trifolium pratense	0	0	1	5	0	0
Trifolium repens	7	30	0	0	16	45
Veronica chamaedrys	0	0	0	0	23	60
Grasses/sedges						
Agrostis vinealis	0	0	0	0	17	45
Agrostis capillaris	4	15	0	0	4	15
Arrhenatherum elatius	0	0	0	0	33	75
Avenula pratensis	6	15	3	10	0	0
Avenula pubescens	14	35	11	30	1	5
Brachypodium pinnatum	2	5	0	0	0	0
Briza media	10	35	13	50	0	0
Carex flacca	41	75	65	100	0	0
Carex caryophylla	0	0	1	5	0	0
Cynosurus cristatus	8	20	3	15	0	0
Dactylis glomerata	7	20	0	0	8	25
Festuca ovina	67	100	65	100	0	0
Festuca rubra	9	20	0	0	45	75
Holcus lanatus	0	0	0	0	26	60
Lolium perenne	0	0	0	0	10	30
Phleum bertolonii	1	5	0	0	11	40
Poa angustifolia	0	0	0	0	1	5
Bryophytes						
Calliergon cuspidatum	8	25	0	0	0	0
Homalothecium lutescens	10	30	8	25	8	25
Campylium chrysophyllum	0	0	0	0	7	25
Ctenidium molluscum	9	25	4	15	0	0
Hypnum cupressiforme	12	25	0	0	0	0
Neckera sp.	1	5	0	0	0	0
Pseudosceropodium purum	11	30	2	10	10	20
Rhytidiadelphus squarossus	8	25	0	0	0	0
Rhytidiadelphus triquetrus	3	10	0	0	2	10

The total bryophyte cover is higher on the NE facing slope, particularly *Rhytidiadelphus squarossus*, which is absent from the S-facing slope, while *Dicranum scoparium* is present only on the S-facing slope. *Pseudoscleropodium purum* is present in both plots, but more abundant on N-facing slopes at Sylvan Dale. Similar patterns for these three species have been observed in previous studies of bryophytes in chalk grassland in the Chilterns (Porley, 1999; Watson, 1960).

The south-facing slope has a higher proportion of several "typical" chalk grassland species species that are considered drought tolerant and/or calcicoles, including *Thymus polytrichus, Gentianella amarella, Helianthemum nummularium* and *Lotus corniculatus.*

A similar comparison for the Dorset sites is made in table 6.2. The NE- and SW-facing slopes are in this case two opposing sides of an earthwork near the hill summit, and the flat site is on the hill summit inside the earthworks. The hill top site is again essentially mesotrophic grassland, although here more diverse than the valley bottom site in Sylvan Dale. The vegetation on both slopes approximates CG2 *Festuca ovina – Avenula pratensis* vegetation (Rodwell, 1992), but again there are clear and consistent differences between slopes. The NE facing slope has several species of widespread distribution in mesotrophic grassland (*Achillea millefolium, Crepis capillaris, Prunella vulgaris, Trifolium repens, Festuca rubra*) which are absent or much reduced on the south-facing slope. The SW facing sward contains several calcicole species that have predominantly southern distributions in Britain, *Hippocrepis comosa, Polygala calcarea,* and *Asperula cynanchica,* recorded as having a preference for slopes between SE and W towards the north and western extent of their range (Perring, 1959). *Cirsium acaule,* is more abundant on south-west facing slopes at Hambledon, but in this example is recorded only from one quadrat on the NE facing slope. The bryophyte species *Calliergon cuspidatum, Homalothecium lutescens, Hypnum cupressiforme, Rhytidiadelphus squarrosus* and *R. triquetrus* are present on the NE-facing slope but not on the SW-facing slope; these species are recorded as having a

predominantly N-facing distribution in the Chilterns (Watson, 1960), although Porley (1999), records *Calliergon* as being more common on south-facing slopes.

6.3.2 DCA of sites at Sylvan Dale and Hambledon Hill

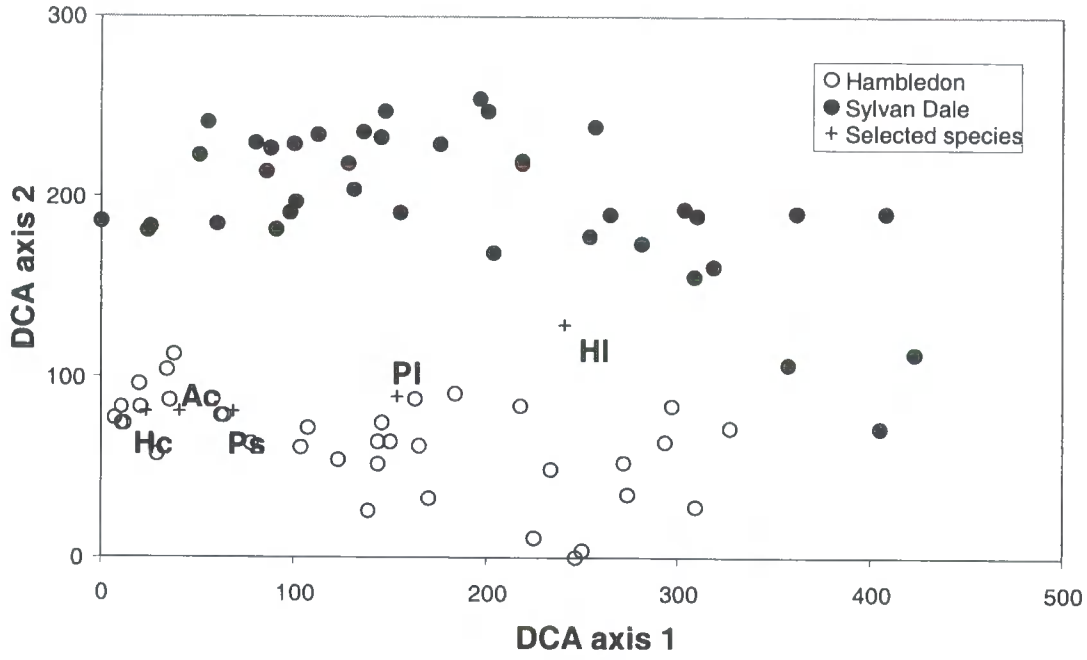

Figure 6.2: Ordination diagram of first two DCA axes of plots surveyed at both field sites. Eigenvalues of axes are are 0.542 and 0.346 respectively. Centroids of selected species: Hc *Hippocrepis comosa*, Ac *Asperula cynanchica*, Sm *Sanguisorba minor*, Pl *Plantago lanceolata*, Hl *Holcus lanatus*.

Detrended correspondence analysis was carried out using frequency data from all sites from the surveys of Hambledon Hill and Sylvan Dale from 2000-2002. The eigenvalues of the first four axes were 0.542, 0.346, 0.165 and 0.115 respectively. The plot scores along the first two axes are plotted in figure 6.2, with the species centroids (weighted mean plot scores) of the five species representative of Perring's groups plotted. Axis two clearly divides the plots between field sites. The clear division on the ordination is unsurprising, as there are several species that are abundant at one field site but absent or scarce at the other. There may be a climatic gradient responsible for the absence of several species from Sylvan Dale, particularly those with a southern distribution such as *Asperula cynanchica, Hippocrepis comosa, Cirsium acaule* and *Polygala calcarea*. Other differences

between sites are not as easy to interpret in climatic terms, such as the relative scarcity of *Brachypodium pinnatum* at Hambledon Hill, or of *Leucanthemum vulgare* at Sylvan Dale. Rather than representing a real environmental gradient, axis 2 may represent a number of species-specific climatic, environmental or historic factors, which lead to differences in the species pool at each site. The first axis, however, appears to represent a gradient which is more or less independent of the site. The centroids of selected species representing Perring's groups I to VI have been plotted on the ordination diagram. These are arranged along axis 1 in order of their degree of affinity to southwest facing slopes in Dorset. *Asperula* and *Hippocrepis* are absent from Sylvan Dale, and *Poterium* is infrequent, so these species centroids are towards the bottom left of the ordination. Figures 6.3 and 6.4 show the association of this axis with topography clearly; at both sites, the plots with low axis 1 scores are those on slopes of over 20° with aspects between E and NW.

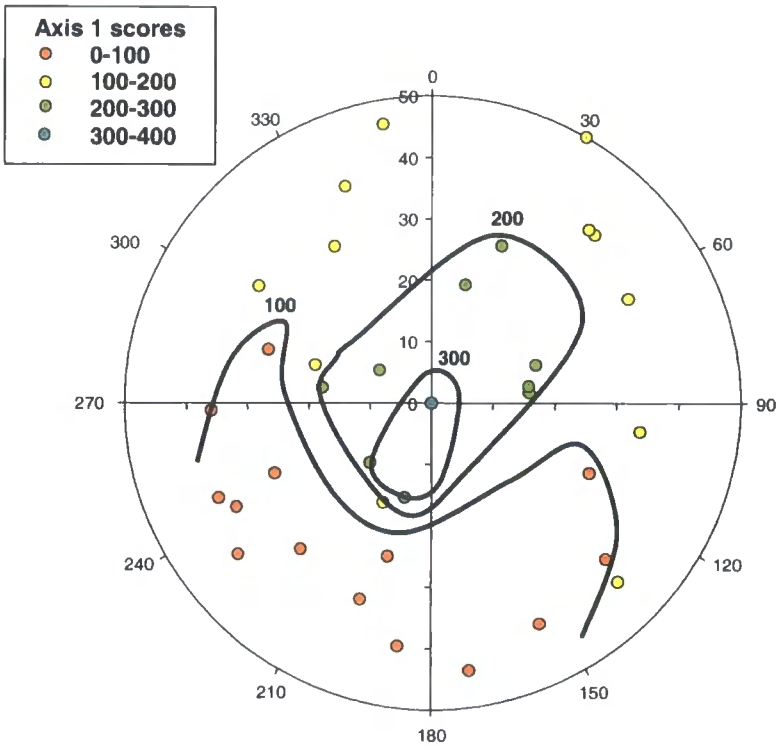

Figure 6.3: Contour plot of DCA axis 1 scores from plots at Hambledon Hill plotted on an "Idealised hill diagram": radial axis represents angle of slope, angular axis represents aspect (degrees). Circles show location of plots, coded as shown.

The highest values of axis 1 are located on flat or gently sloping plots. Low axis 1 values are therefore associated with warm and/or dry microclimates, however, the highest axis 1 values are apparently associated with developed plateau, hill top or valley bottom soils, rather than with the wettest or coolest microclimates on steep NE slopes. Although clearly associated with microclimate at one extreme, the gradient represented by the axis appears to be more strongly correlated with soil conditions at the other.

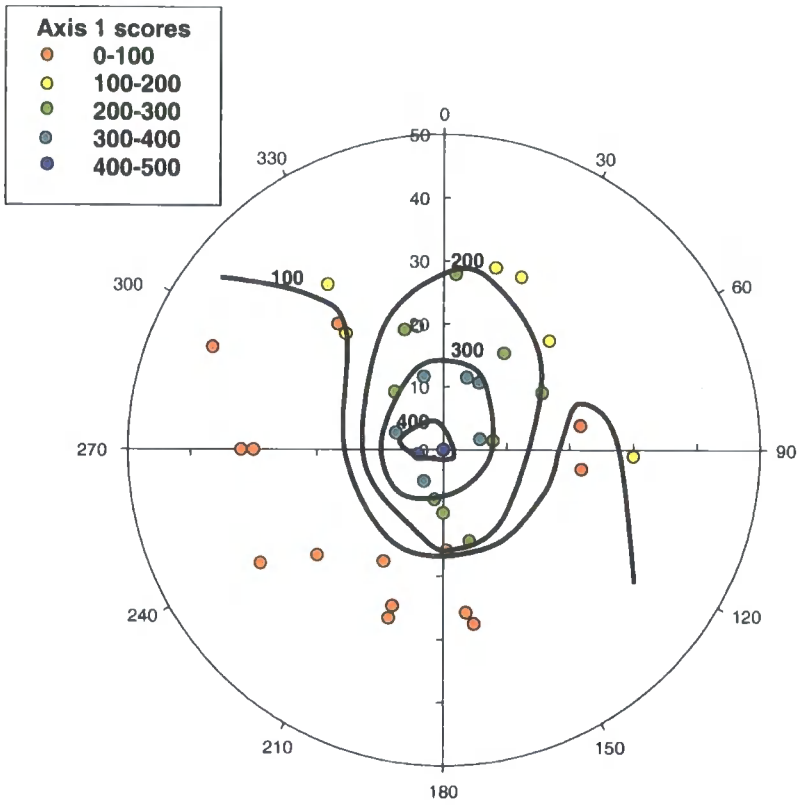

Figure 6.4: Contour plot of DCA axis 1 scores from plots at Sylvan Dale plotted on an "idealised hill diagram": radial axis represents angle of slope, angular axis represents aspect (degrees). Circles show location of plots, coded as shown.

Tables 6.3 to 6.5 show correlations between DCA axes and both modelled and measured variables. Axis 1 is significantly correlated with all four Ellenberg indicator values, particularly strongly with the fertility and moisture gradients, and with Grime's CSR values. Figure 6.5 shows a triangular plot of the CSR scores;

the plots are arranged in a gradient along the S axis. The strong correlation of axis 1 with slope is a reflection of the high axis scores on soils on flat or gently sloping ground shown clearly in figures 6.3 and 6.4. The rather weaker correlation with modelled microclimate values reflects the fact that these relationships are confounded by the relationship with slope independently of aspect. However, DR2002, PAR2001 and JMAX2001 are all more strongly correlated with axis 1 scores than the radiation index, suggesting that these physically modelled variables may be more effective measures of topographic microclimate than a geometric index alone.

Table 6.3: Spearman's Rank correlation coefficients between first four DCA axes and vegetation variables. n.s. – not significant, *- significant at p<0.05, **- significant at p<0.01

	Mean veg. height	Ellenberg L	Ellenberg M	Ellenberg R	Ellenberg N
Axis 1	0.274*	-0.472**	0.785**	-0.398**	0.958**
Axis 2	-0.372**	n.s.	n.s.	-0.249*	n.s.
Axis 3	0.421**	n.s.	-0.344**	0.173	n.s.
Axis 4	n.s.	n.s.	0.294**	-0.417**	n.s.

Table 6.4: Spearman's Rank correlation coefficients between first four DCA axes and climatic/topographic variables. n.s. – not significant, *- significant at p<0.05, **- significant at p<0.01

	DR2002	PAR2001	JMAX2001	TSUM2002	Ri	Slope
Axis 1	-0.325**	-0.239*	-0.279*	n.s.	n.s.	-0.667**
Axis 2	n.s.	-0.483**	n.s.	-0.814**	n.s.	n.s.
Axis 3	.297**	0.015	n.s.	n.s.	n.s.	n.s.
Axis 4	-0.374**	-0.609	-0.573**	-0.339**	-0.567**	n.s.

Table 6.5: Spearman's Rank correlation coefficients between first four DCA axes and soil variables/grazing index. n.s. – not significant, *- significant at p<0.05, **- significant at p<0.01

	Soil depth	Grime C	Grime S	Grime R
Axis 1	n.s.	0.955**	-0.980**	0.966**
Axis 2	n.s.	n.s.	n.s.	n.s.
Axis 3	n.s.	n.s.	n.s.	n.s.
Axis 4	n.s.	n.s.	n.s.	n.s.

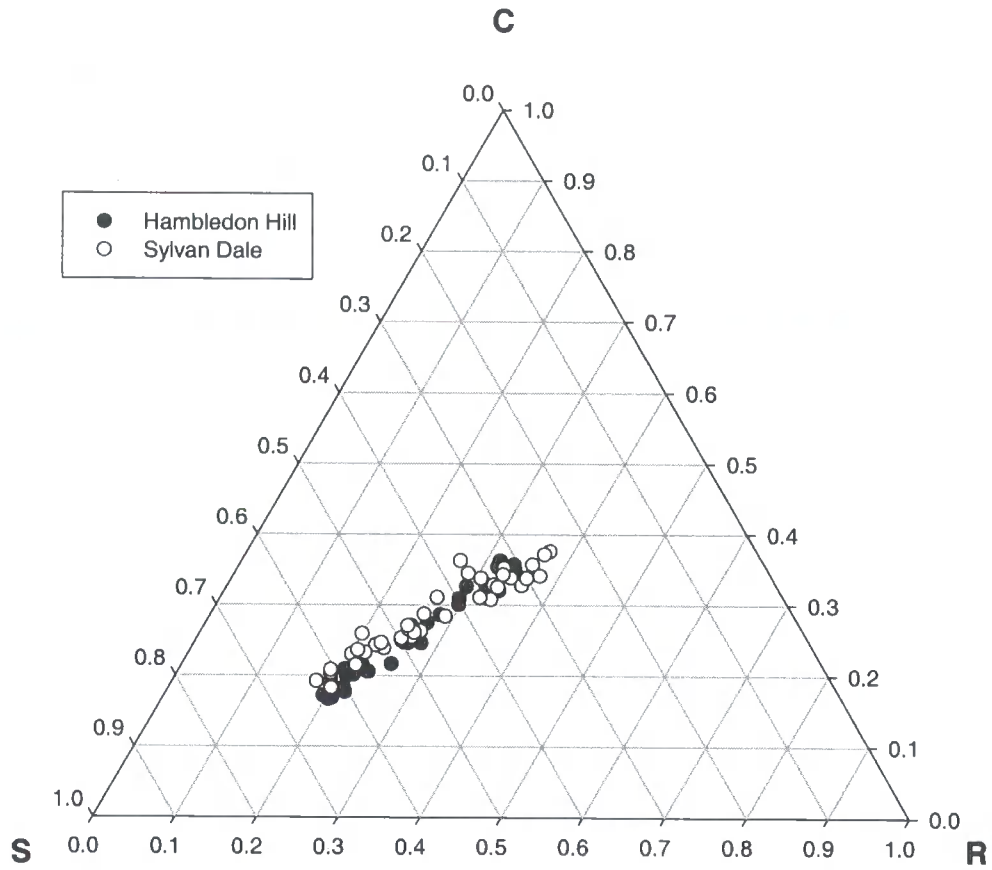

Figure 6.5: Triangular plot of CSR scores for each vegetation plot at Hambledon Hill (filled circles) and Sylvan Dale (clear circles).

6.3.3 GAMs of DCA axis 1 and species frequency

DCA axis 1 and eight of the seventeen most frequent species in the vegetation plots could be modelled using GAMs, with between 33 and 74% of the deviance explained by the model (table 6.6).

Table 6.6: Summary of GAMs for DCA axis 1 and selected species with explained deviance , change in degrees of freedom and list of explanatory variables. Variables separated by a colon represent an interaction term.

	Null deviance	Percentage deviance explained	Change in df	Explanatory variables
Axis 1	926000	74	7	Soil type:DR2002, slope
Asperula cynanchica	17.0	50	1	PAR
Carex flacca	61.1	44	2	Soil type
Brachypodium pinnatum	69.6	68	1	TSUM2002
Briza media	-	-	-	-
Cynosurus cristatus	-	-	-	-
Dactylis glomerata	-	-	-	-
Festuca ovina	80.6	33	2	Soil type
Hippocrepis comosa	27.4	72	3	Soil type:PAR
Holcus lanatus	-	-	-	-
Leontodon hispidus	-	-	-	-
Lolium perenne	45.4	37	2	Soil type
Pilosella officinarum	-	-	-	-
Plantago lanceolata	-	-	-	-
Sanguisorba minor	-	-	-	-
Pseudoscleropodium purum	-	-	-	-
Rhytidiadelphus squarrosus	25.8	39	1	DR2002
Thymus polytrichus	40.0	59	3	Soil type:DR2002

DCA axis 1 was modelled fairly accurately (74% of deviance explained) using a GAM using a cubic spline fitted to slope and an interaction between the factor soil type and a linear function of the variable DR2002 as independent variables (table 6.6). On the brown earth soils, axis 1 scores decrease with increasing slope and with increasing values of DR2002. These soils were not found on slopes of over 20°, so no values above this are plotted. On the rendzina soils, the pattern is similar, although scores are lower for any given slope and drought value. The effect of slope appears to decrease at angles over around 25°. Lowest axis 1 values are expected on droughted, steeply sloping plots.

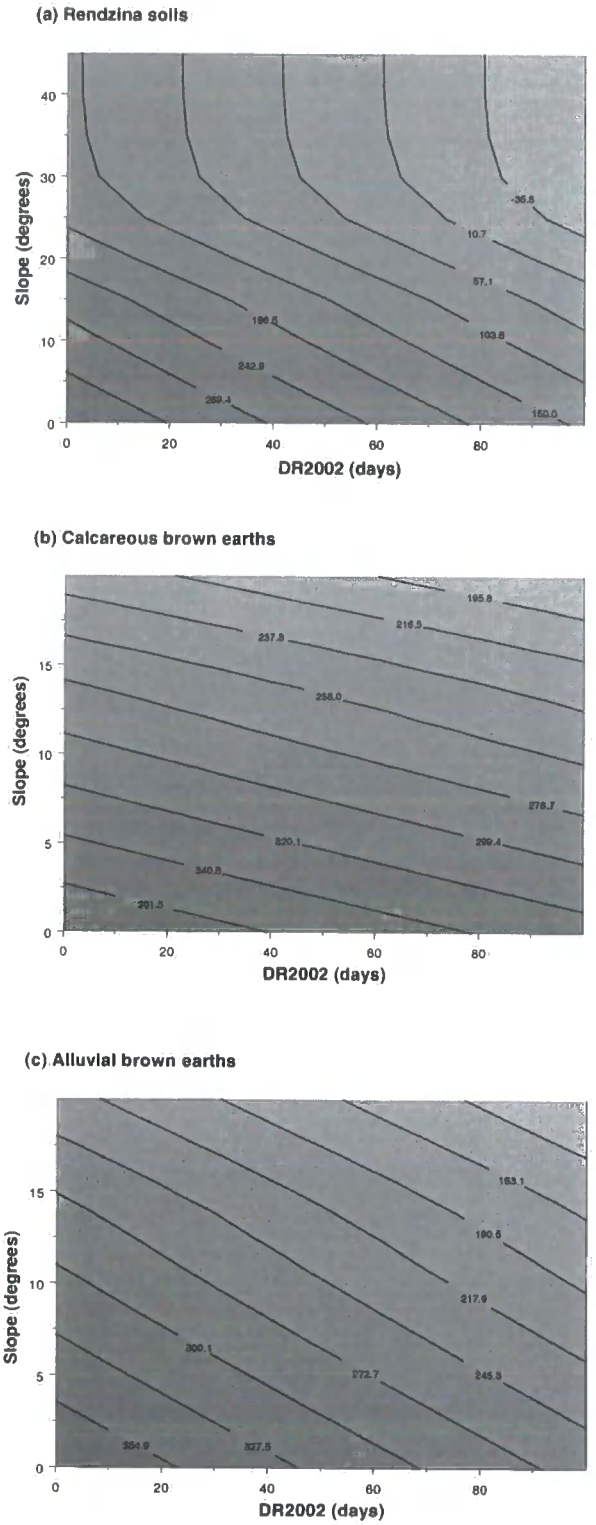

Figure 6.6: Response surfaces generated from GAM of DCA axis 1 plot scores, showing response of plot scores to angle of slope and DR2002 for each of three soil types (a) rendzinas (b) calcareous brown earth (c) alluvial brown earth. Note different y-axis scales for (b) and (c).

Where GAMs are used to model species frequency in this data set, linear functions were found to have as much explanatory power as nonparametric functions in all cases; under these conditions the GAM is essentially equivalent to a GLM or logistic regression. Care should be taken in interpreting species models; while *Brachypodium pinnatum* is correlated with low TSUM2002 values, this reflects its abundance at Millington Pastures and scarcity at Hambledon Hill, - but this may not imply a causal relationship with temperature. Equally, as several of the topographic microclimatic variables used are correlated, the inclusion of a significant term in the model does not imply a causal relationship with any particular variable. However, in most cases the models make intuitive sense when compared to the known biology of the species.

Asperula cynanchica is modelled by a linear function of PAR, reflecting its restriction to high light environments (figure 6.7).

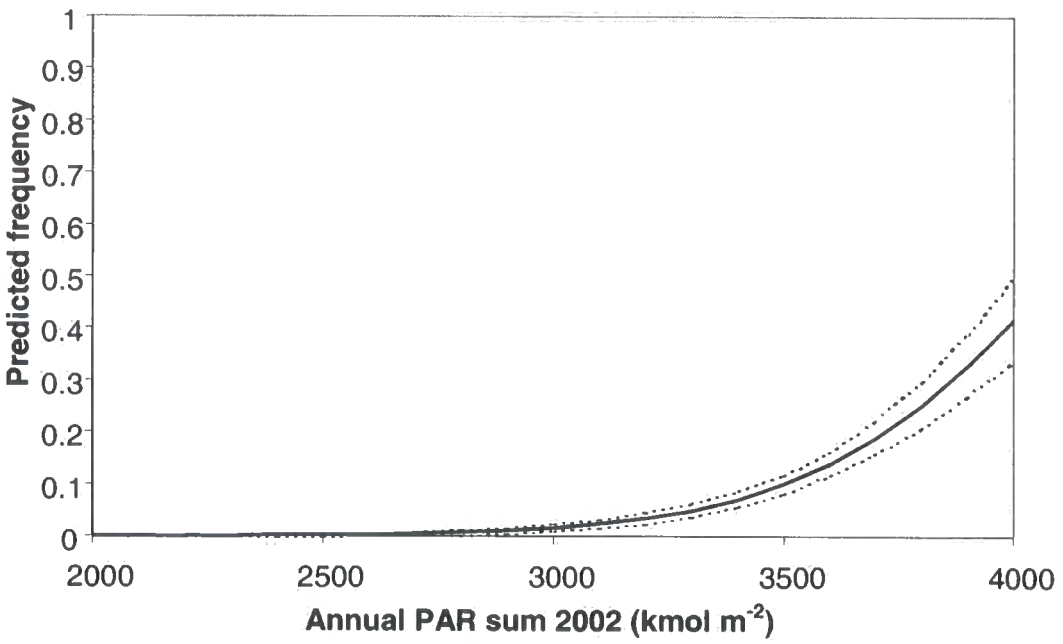

Figure 6.7: Response curve generated from GAM of PAR sum 2002 against predicted frequency of *Asperula cynanchica*. Dashed lines ± 1 s.e.

Three species distributions are described best purely by soil type; *Carex flacca* and *Festuca ovina* are significantly more frequent on rendzinas, and the competitive

grass *Lolium perenne* is more frequently present and sometimes dominant on the brown earth soils but absent from rendzina soils.

Hippocrepis comosa is modelled by an interaction in terms between soil type and PAR sum. This species is absent from the brown earth soils at both sites, but on rendzina soils shows a similar pattern to that of *Asperula cynanchica* (figure 6.8).

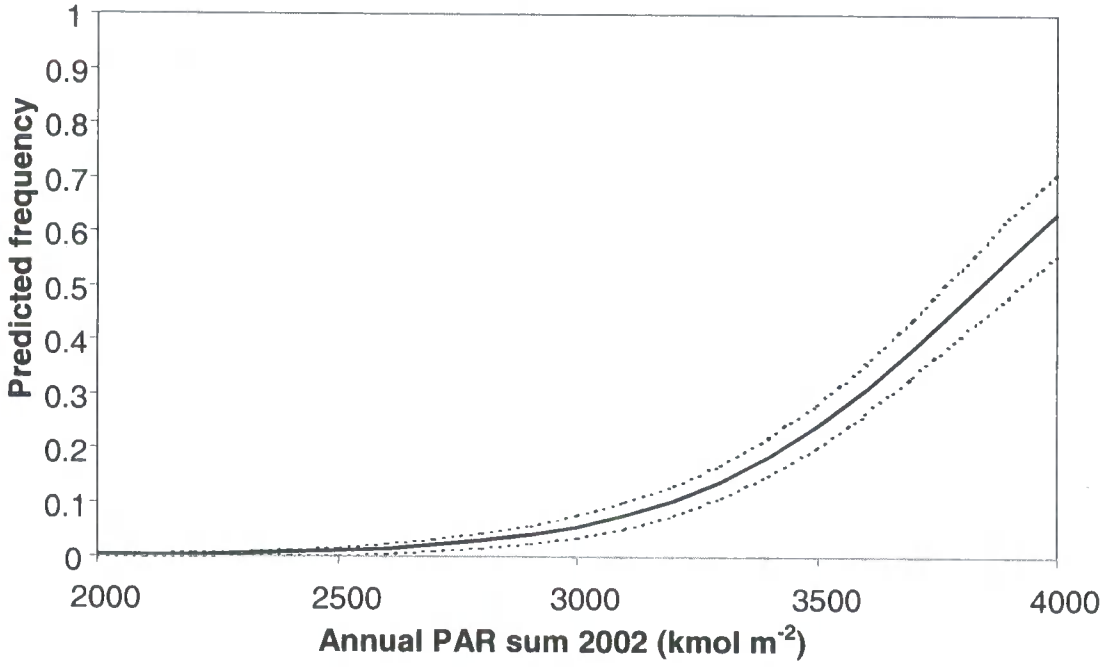

Figure 6.8: Response curve generated from GAM of PAR sum 2002 against predicted frequency of *Hippocrepis comosa* for Rendzina soils. Dashed lines ± 1 s.e.

The bryophyte *Rhytidiadelphus squarrosus* is modelled by a linear function of DR2002, reflecting its preference for a relatively damp microclimate (figure 6.9).

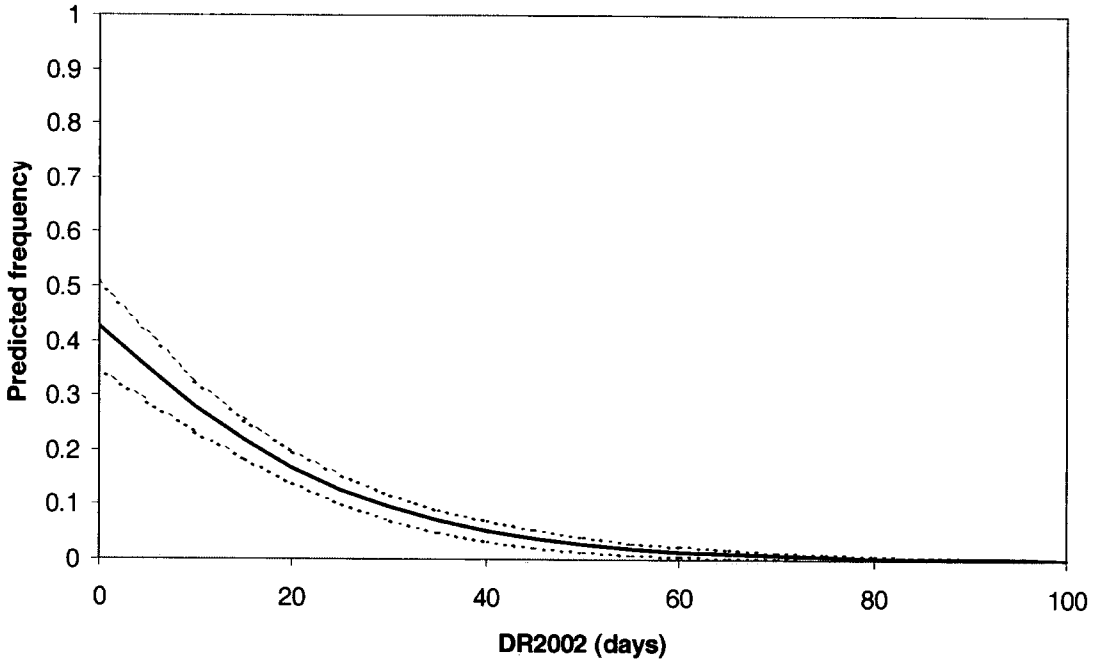

Figure 6.9: Response curve generated from GAM of DR2002 against predicted frequency of *Rhytidiadelphus squarrosus*. Dashed lines ± 1 s.e.

Thymus polytrichus is modelled by an interaction between soil type and a linear function of DR2002. On rendzina soils it reaches close to 100% frequency on droughted plots; on calcareous brown earths it has a consistently low frequency; and on alluvial brown earths it has an intermediate distribution (figure 6.10).

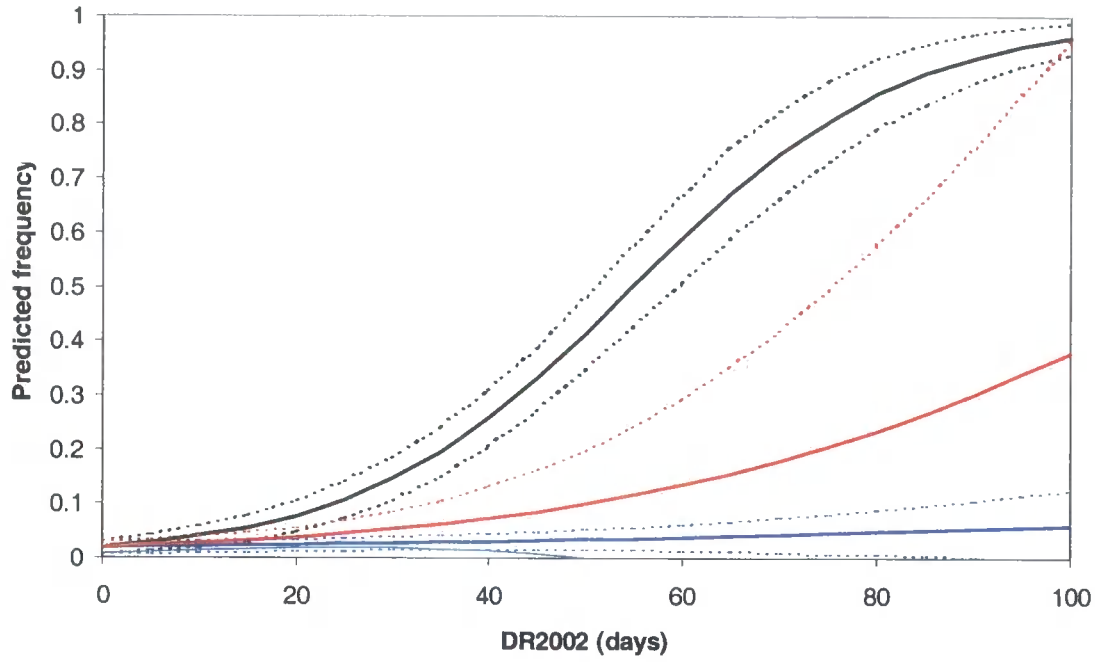

Figure 6.10: Response curve generated from GAM of DR2002 against predicted frequency of *Thymus polytrichus*. Black: Rendzina soils. Blue: calcareous brown earth. Red: alluvial brown earth. Dashed lines ± 1 s.e.

6.3.4 Vegetation change and topography at Hambledon Hill 1952-2000

To assess the difference in vegetation between the 2000 survey and Perring's 1952 survey, plots at Hambledon Hill were split into three "topographic" groups: flat or gentle slopes (less than 20°), "SW-facing slopes" (slopes of over 20° with aspect between 136° and 270°) and "NE-facing slopes" (slopes of over 20° with aspects between 271 and 135°), and two "management" groups: grazed by cattle and ungrazed in 1952. By 2000 the 27 plots within the NNR were grazed by cattle at the same stocking rate.

Tables 6.7 and 6.8 list all species that increased or decreased in frequency by more than 5% over all plots. Percentage increases and decreases are given for each group of plots. The significance of the changes was tested using paired t-tests in each case.

Table 6.7: Change in percentage frequency for species showing more than 5% overall decrease in frequency 1952-2000. roman numerals indicate groups of affinity to SW-facing slopes (Perring, 1958). Figures in bold show significant increases on south-facing slopes. n.s. = not significant; all other values significant at $p < 0.01$.

Species	Topography			Management 1952	
	<20° (n=7)	>20° S (n=10)	>20° N (n=10)	Ungrazed (n=9)	Grazed (n=18)
Grasses/sedges					
Koeleria macrantha **iii**	-56	-62	-56	-48	-66
Festuca ovina **iii**	-42	-16	-18	n.s.	-34
Briza media **iii**	-41	-39	-20	-29	-35
Helictotrichon pratensis **iii**	-33	-15	-20	-12	-28
Agrostis stolonifera **iv**	n.s.	-7	-18	n.s.	-21
Trisetum flavescens **iv**	-12	n.s.	-8	n.s.	-9
Carex flacca **iii**	-24	**+19**	-14	-11	n.s.
Forbs/shrubs					
Thymus polytrichus **iii**	-39	-15	-28	-31	-25
Sanguisorba minor **iii**	-38	**+8**	n.s.	-13	n.s.
Pilosella officinarum **ii**	-21	-14	-12	-9	-19
Cirsium acaule **iii**	-25	-11	-15	-32	-9
Campanula rotundifolia **iv**	-15	-10	-10	-10	-13
Asperula cynanchica **ii**	-15	n.s.	-10	n.s.	n.s.
Polygala calcarea **ii**	-12	n.s.	-8	n.s.	-10
Hippocrepis comosa **i**	-10	n.s.	-7	n.s.	n.s.
Mosses/liverworts					
Pseudoscleropodium purum **iv**	-39	-7	-20	-10	-26
Rhytidiadelphus squarrosus **v**	n.s.	n.s.	-21	n.s.	-24
Rhytidiadelphus triquetris **iv**	-14	n.s.	n.s.	n.s.	n.s.

Several species were considerably less frequent in 2000 than 1952, particularly drought tolerant and calcicole species typical of chalk grassland. Despite these large declines in frequency, all of the species listed are still quite common at Hambledon Hill, and several (*Festuca ovina, Carex flacca, Sanguisorba minor*) are matrix forming species that cover significant areas. Many of the less frequent species were not found in sufficient quadrats in either survey to draw conclusions on any change. Two species of particular conservation interest due to their restricted distributions in Britain, *Carex humilis* and *Gentianella anglica*, were found

in two or less quadrats in 1952 and none in 2000; however, they were found to be present at the site. Other notable changes that could not be tested for significance were the apparent extinction of *Danthonia decumbens* from the site and the loss of *Helianthemum nummularium* from flat and NE-facing slopes. The grasses and sedges declining at Hambledon Hill are all from Perring's groups iii (widespread, with maximum cover on slopes between W and SE) and iv (widespread with maximum cover on the flat top). The decreasing forbs and shrubs are from groups i (largely restricted to steep SW-facing slopes), ii (ii (maximum cover on steep SW-facing slopes), iii and iv. Two drought-tolerant species, *Sanguisorba minor* and *Carex flacca* have decreased in frequency on gentle slopes and NE-facing slopes, but increased in frequency on SW-facing slopes; the southern species *Asperula cynanchica, Polygala calcarea* and *Hippocrepis comosa* have significantly decreased on NE and flat slopes but experienced no significant change on SW facing slopes. The pleurocarpous mosses *Pseudoscleropodium purum, Rhytidiadelphus squarrosus* and *R. triquetrus* have all decreased on the slopes on which they were most abundant in 1952.

Table 6.8: Change in percentage frequency for species showing more than 5% overall increase in frequency 1952-2000. Roman numerals indicate groups of affinity to SW-facing slopes (Perring, 1958). n.s. = not significant; all other values significant at $p < 0.01$.

Species	Topography			Management 1952	
	<20° (n=7)	>20° S (n=10)	>20° N (n=10)	Ungrazed (n=9)	Grazed (n=18)
Grasses/sedges					
Phleum bertolonii -	+32	+6	+22	+29	+15
Dactylis glomerata **v**	+23	n.s.	n.s.	+9	+13
Arrhenatherum elatius **v**	+11	n.s.	n.s.	n.s.	+11
Helictotrichon pubescens **iv**	+6	+18	n.s.	+18	+8
Cynosurus cristatus **iv**	+24	+11	+6	+14	+12
Lolium perenne -	+20	n.s.	n.s.	+7	+4
Forbs/shrubs					
Plantago lanceolata **iv**	+24	+20	+6	+11	+18
Euphrasia nemorosa **ii**	n.s.	+28	+6	+16	n.s.
Scabiosa columbaria **ii**	n.s.	+36	+13	+20	+20
Mosses/liverworts					
Calliergon cuspidatum **iv**	n.s.	n.s.	+13	n.s.	n.s.

Those species increasing between 1952 and 2000 are predominantly in Perring's groups iv (maximum cover on flat top and NE facing slopes) and v (maximum cover on NE slopes). The exceptions are the group ii forbs *Scabiosa columbaria* and *Euphrasia nemorosa*, both of which have increased mainly on SW-facing slopes. The other species are typical of mesotrophic grassland and have a widespread distribution. The increases are generally greatest on flat slopes, with the moss *Calliergon cuspidatum* increasing on NE-facing slopes.

Other notable increases include *Holcus lanatus* and *Veronica chamaedrys*, absent from these plots in 1952 but now present on flat and NE-facing slopes.

6.3.5 Change in vegetation plot scores 1952-2000

Plot scores on DCA axis 1 were significantly greater in 2000 than 1952 on the grazed group of plots and on flat plots (figures 6.11 and 6.12).

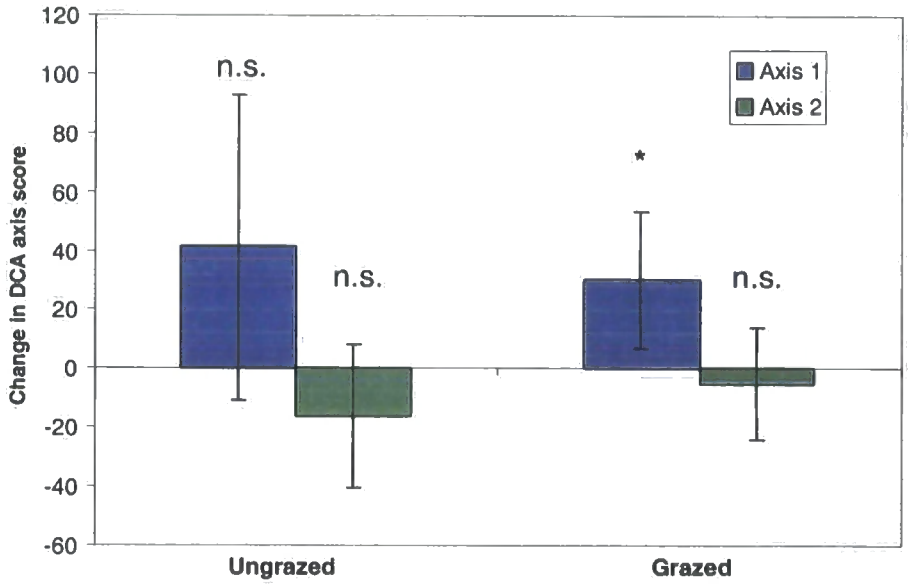

Figure 6.11: Change in DCA axis 1 and 2 sample scores, from 1952 to 2000 for management groups of plots at Hambledon Hill. Paired t-tests: n.s. not significant, * significant at $p < 0.05$, ** significant at $p < 0.01$. Error bars show 95% confidence limits about the mean.

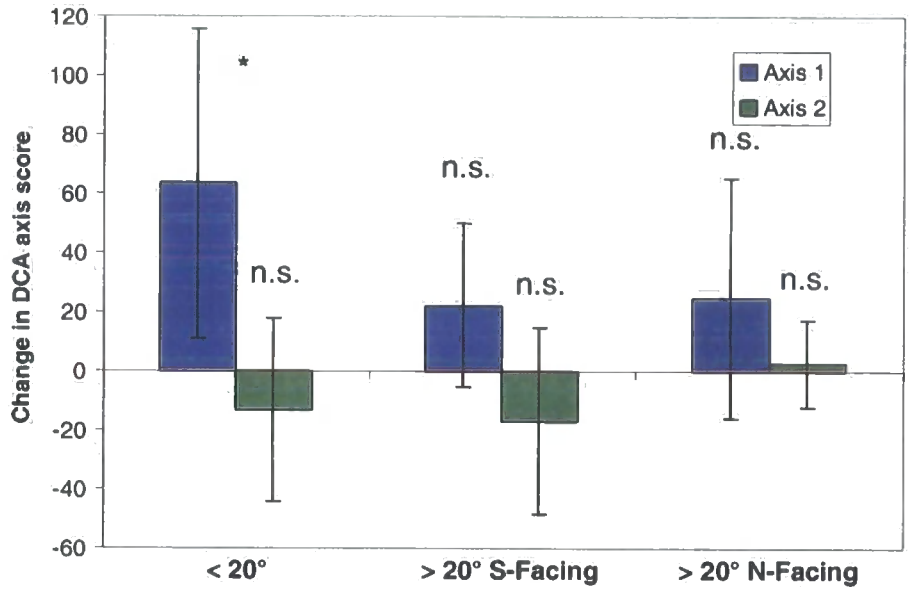

Figure 6.12: Change in DCA axis 1 and 2 sample scores, from 1952 to 2000 for topographic groups of plots at Hambledon Hill. Paired t-tests: n.s. not significant, * significant at $p < 0.05$, ** significant at $p < 0.01$. Error bars show 95% confidence limits about the mean.

CSR plot scores (figures 6.13 and 6.14) generally show slightly decreasing S scores, and increasing C and R scores across all groups; however, this effect is only significant for increased C and R scores for grazed and flat plots.

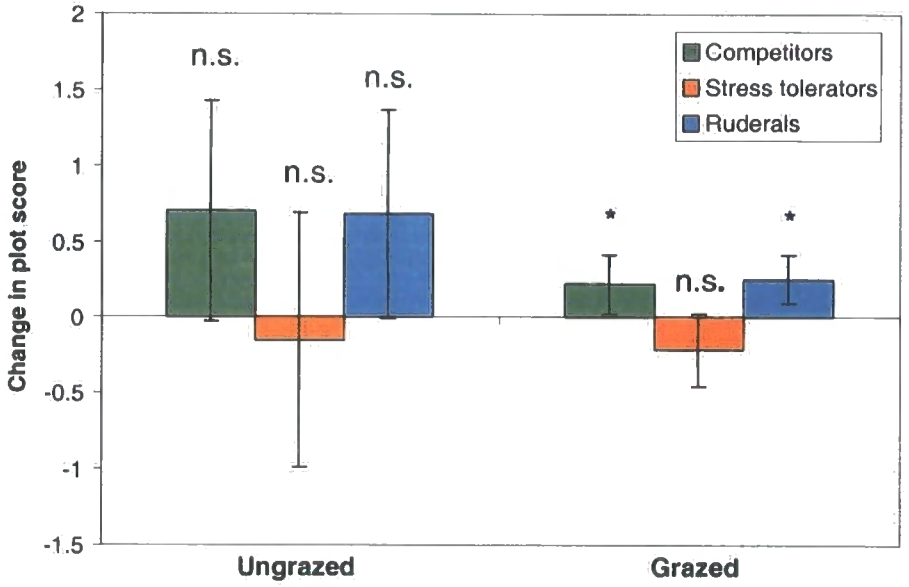

Figure 6.13: Change in CSR plot score, from 1952 to 2000 for management groups of plots at Hambledon Hill. Paired t-tests: n.s. not significant, * significant at $p < 0.05$, ** significant at $p < 0.01$. Error bars show 95% confidence limits about the mean.

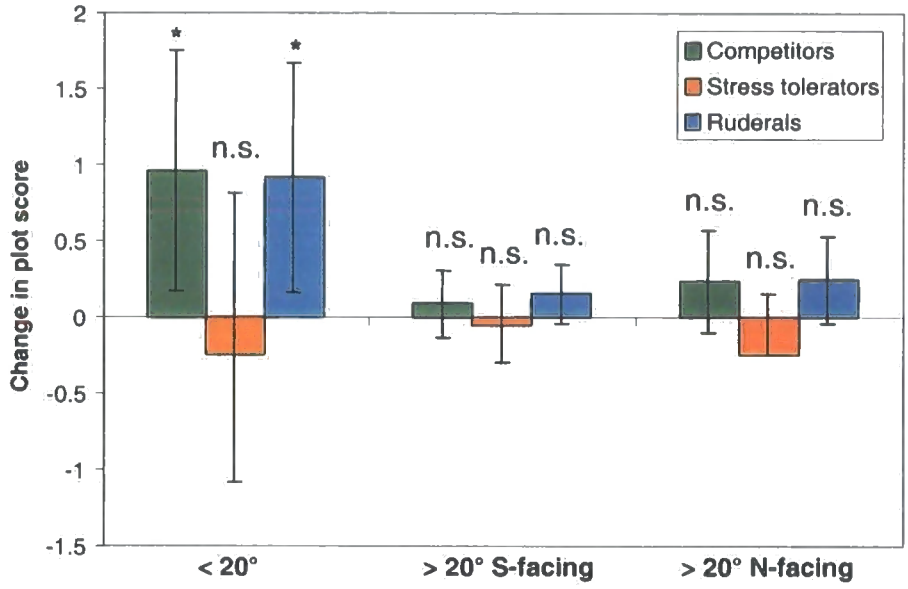

Figure 6.14: Change in CSR plot score, from 1952 to 2000 for topographic groups of plots at Hambledon Hill. Paired t-tests: n.s. not significant, * significant at $p < 0.05$, ** significant at $p < 0.01$. Error bars show 95% confidence limits about the mean.

Ellenberg plot scores show significantly increased N values and decreased L values for all groups except SW facing plots in 2000. R values are significantly lower for grazed and north-facing plots. It should be noted that the magnitude of change of these scores is not necessarily a guide to their relative importance. All species scores are on a scale from 1 to 9, and plants in well-drained chalk grasslands by definition occupy a restricted range of L, F, and R values; none will be restricted to acid, waterlogged or deeply shaded environments. Since a wide range of soil fertility occurs in these habitats, the range of potential plot scores for this index is higher.

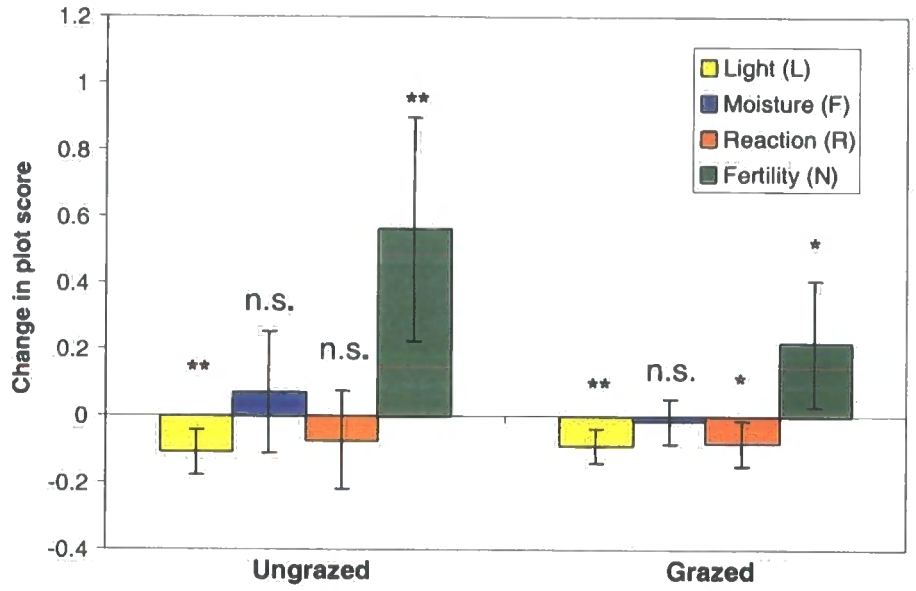

Figure 6.15: Change in Ellenberg indicator plot score, from 1952 to 2000 for management groups of plots at Hambledon Hill. Paired t-tests: n.s. not significant, * significant at $p < 0.05$, ** significant at $p < 0.01$. Error bars show 95% confidence limits about the mean.

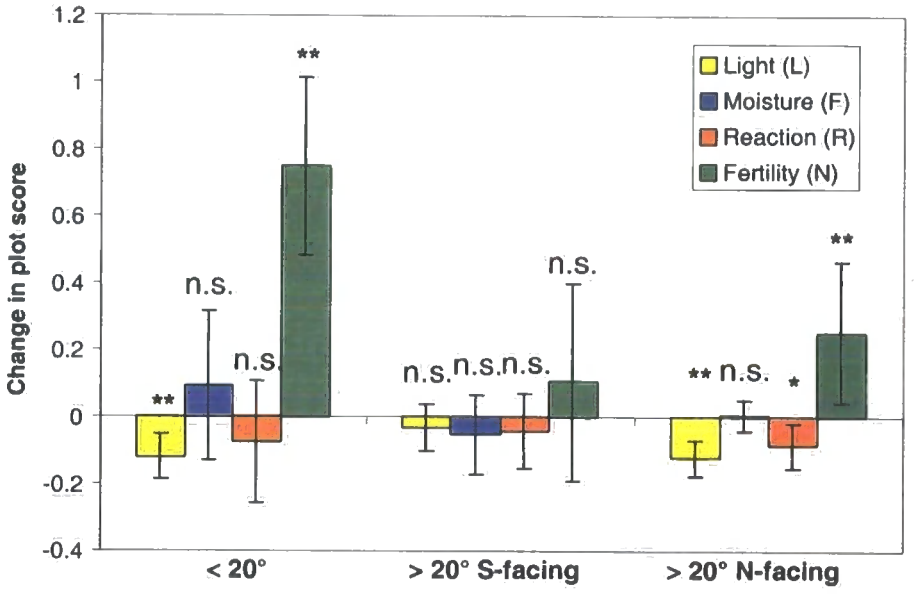

Figure 6.16: Change in Ellenberg indicator plot score, from 1952 to 2000 for topographic groups of plots at Hambledon Hill. Paired t-tests: n.s. not significant, * significant at $p < 0.05$, ** significant at $p < 0.01$. Error bars show 95% confidence limits about the mean.

6.4 Discussion

6.4.1 Topography, microclimate and vegetation at Hambledon Hill and Sylvan Dale

DCA of vegetation plots from Hambledon Hill and Sylvan Dale yields a first axis that represents a gradient from dry calcareous to mesotrophic grassland. This result is similar to the gradient identified in DCA of grasslands from different regions in chapter 2, and to previous ordinations of calcareous grasslands at different spatial scales (Gittens, 1965a; Duckworth *et al.*, 2000b). The gradient is strongly correlated with Grime's stress and Ellenberg N (fertility) indices. While axis scores show a correlation with modelled topographic microclimatic variables, the relationship is complicated by other factors. Plots on steep south to south-west facing slopes with shallow soils contain the driest microsites, and have the lowest axis 1 scores; however, the wettest microsites are on pockets of deep soils on steep north to north-east facing slopes, but these plots do not have the highest axis 1 scores; these occur on the leached, more developed calcareous or alluvial brown earths on flatter sites. The vegetation gradient revealed by DCA is not caused by a single environmental factor, but by a complex of factors. The GAM of axis 1 describes it as a function of soil type, slope and drought index. The proximal variables controlling the vegetation appear to be drought and some aspect of soil fertility; these are determined by the distal factors of climate, pH and topography.

South-facing slopes contain higher frequencies of drought-tolerators, drought–avoiders and calcicoles, while north-facing and flat sites contain increasing frequencies of more competitive mesotrophic species. Many of the stress tolerant species present on south-facing slopes at both sites have a relatively widespread distribution in Britain, occurring to varying degrees on limestones, sand dunes, thin soils and other dry habitats. Examples of these are *Thymus polytrichus, Carex flacca* and *Sanguisorba minor.* In addition, at Hambledon Hill there are several species absent from northern and western Britain; *Cirsium acaule, Polygala calcarea, Hippocrepis comosa* and *Asperula cynanchica* are the most abundant examples. These species, from Perring's groups I and ii, tend to be more markedly restricted to south-facing slopes in Dorset. The distribution of *Asperula* and

Hippocrepis is best modelled as a function of insolation (PAR); as with *Cirsium acaule* (Pigott, 1975), it is likely that temperature limits part of the life cycle of these species.

Pleurocarpous moss species in chalk grassland typically have little contact with the substrate through rhizoids (Watson, 1960). They therefore rely on a damp sward environment to maintain cell turgor and for reproduction. North-facing slopes have both higher total bryophyte cover and a greater number of species. The GAM of *Rhytidiadelphus squarrosus* frequency as a function of DR2002 is probably typical of most mosses, becoming less frequent in drier microsites.

6.4.2 Vegetation change at Hambledon Hill 1952-2000

The comparison of vegetation data collected at Hambledon Hill in 2000 provides an interesting indicator of change at the site over half a century. It is not clear, however, to what extent the observed changes in vegetation represent long term trends, abrupt changes or year-to-year variation; in the absence of disturbance, calcareous grasslands, dominated by long-lived perennials, are often considered resistant to change, and species turnover may take decades (Buckland *et al.*, 2001). However, the importance of annual climatic variation, particularly extreme drought events, in determining species abundance and in "resetting" plant distributions, has also been stressed (Hopkins, 1978; Watt, 1981; Buckland *et al.*, 1997). By using frequency, rather than cover, data in the analyses, the amount of subjectivity in the data was reduced; however, the replication of quadrats in the plots allowed quite small, but statistically significant changes to be quantified, particularly when analysed with respect to topographic position. Few of the observed changes in frequency would have been observed simply by comparing species lists from each date.

The analysis of indicator values shows a clear overall increase in the frequency of competitive/ruderal strategy species at the expense of stress tolerators, a decrease in frequency of species with high light requirements and an increase in frequency of species with high soil fertility requirements. These changes are larger in

magnitude and more statistically significant in plots on flat or gentle slopes, and smaller and generally non-significant in steep SW-facing slopes. Steep N-facing slopes are somewhat intermediate between the two groups. These patterns are reflected in a shift to higher scores on DCA axis 1. The pattern clearly suggests a shift towards a more mesotrophic grassland community, in which south-facing slopes have been less affected. A number of factors may have been responsible for this change over the intervening years. Likely causes of change are outlined below, with reference to observed changes in species frequency.

6.4.2.1 Decline in rabbit populations

The importance of rabbit grazing in shaping the vegetation in chalk grassland was reported from early observations and exclosure experiments (Tansley and Adamson, 1925, 1926; Hope-Simpson, 1941). The outbreak of myxomatosis in Britain during 1954 drastically reduced rabbit populations across the country. Since the outbreak, rabbit populations have recovered and fluctuated but only locally reached pre-1954 levels. The effects of this decline on rabbit-grazed vegetation on several chalk sites were recorded along fixed transects during the outbreak and as rabbit populations began to recover (Thomas, 1960, 1963). Initially, most species responded positively, with increased flowering and growth; after the first year ruderal species such as *Senecio jacobea,* which depended on disturbance around burrows, declined significantly. Longer term (after 7 years) changes included declines in less competitive species such as *Thymus polytrichus* as more competitive species, particularly ranker grasses such as *Arrhenatherum elatius* and *Dactylis glomerata,* became more frequent.

Many of the observed changes between 1952 and 2000 are consistent with these observations. Although there was no significant difference in minimum, mean or maximum recorded vegetation height between either grazed or ungrazed plots, there is some evidence of changes in vegetation structure; bare ground was frequently recorded in Perring's data sheets and minimum vegetation heights were on average 6cm lower, although this observation fell just short of statistical significance ($p = 0.06$). Contemporary aerial photographs (Perring, 1956) show an

apparently much more closely grazed sward than that observed today, with patches of bare chalk clearly visible, particularly on the slopes. The observed decrease in light demanding species and increase in competitive species is consistent with this. Several of the species that have decreased in frequency have been recorded as declining in the absence of rabbit grazing, including *Thymus polytrichus, Agrostis stolonifera* (Thomas, 1963), *Pilosella officinarum* (Watt, 1981), *Carex flacca* (Tansley and Adamson, 1925), and most pleurocarpous moss species (Tansley and Adamson, 1925; Watson, 1960). *Helianthemum nummularium* is associated with disturbance, particularly in more humid areas, and was reported from anthills on NE slopes of Hambledon Hill by Proctor (1958); in the present study it was not present in quadrats on NE or flat slopes. However, contrary to observations at Hambledon Hill, grass species such as *Koeleria macrantha, Avenula pratensis* and *Festuca ovina* have been recorded as becoming more vigorous in the absence of rabbits (Thomas, 1960; Watt, 1981). It is possible that under a humid climate, this increase in vigour is temporary as release from rabbit grazing allows invasion from more competitive mesic grasses such as *Dactylis glomerata, Arrhenatherum elatius* and *Holcus lanatus* increase.

6.4.2.2 Nitrogen deposition

Atmospheric nitrogen deposition has been implicated as a cause of vegetation change in nutrient-poor grassland ecosystems, including invasion by alien annual grasses in serpentine grasslands in the San Francisco Bay area (Weiss, 1999) and *Brachypodium pinnatum* dominance in chalk grasslands in the Netherlands (Bobbink, 1987). Experimental studies on calcareous grasslands in the UK have shown limited short-term responses to artificially enhanced N deposition (Morecroft *et al.*, 1994; Wilson *et al.*, 1995). Both authors conclude that phosphorus, or joint phosphorus and nitrogen, limitation in UK calcareous grasslands prevents a marked short term response in species composition to additional N in UK chalk grasslands. In study on a chalk grassland in Belgium (Jacquemyn *et al.*, 2003), however, a marked short term response to increased nitrogen treatments was shown, including an increase in competitive grass species, decrease in light penetration into the sward, and decrease in species richness. Shade intolerant-

species in particular were shown to decrease. Grazing was shown to counteract the effects of nitrogen additions to some extent, but did not prevent competitive species (tall forbs and grasses and rosette plants) from becoming dominant.

Although atmospheric N inputs in the UK over the last 50 years are thought to be considerably lower than those in the Netherlands (Wilson *et al.*, 1995), annual deposition was shown to exceed mineralisation as a source of N in Derbyshire grasslands (Morecroft *et al.*, 1994). Despite the apparent lack of short-term response in cover or species composition to N treatments, Carroll *et al.* (2003) record significant long-term trends, attributed to direct effects of tissue nitrogen accumulation, or secondary effects resulting from soil processes, markedly the acidification of nitrogen treated plots.

At Hambledon Hill the observed increase in frequency of plants with high Ellenberg N indices, and of competitors and ruderals at the expense of stress tolerators and shade-intolerant species, is consistent with an increase in the fertility of the system. Soils on sloping ground at Sylvan Dale and Hambledon Hill have been shown to have extremely low extractable P values on both N and S facing aspects, while P availability on the tops is higher, although still fairly low. If low P availability buffers calcareous grasslands from the effects of N fertilisation, then any effects of N deposition would be expected to be greater on the hilltop. This is the observed pattern.

6.4.2.3 Changes in management

All of the plots surveyed in 2000 at Hambledon Hill lie within the NNR and are currently grazed by cattle (and occasionally horses) by the landowner, in consultation with English Nature. In 1952 eighteen of these plots were grazed by cattle, nine were ungrazed. However, the observed patterns of change are similar in both groups of plots, and there is no significant decrease in sward height in plots ungrazed in 1952 and grazed in 2000. This suggests that rabbit grazing, recorded from all plots at the site, was more important in determining species composition and sward height in 1952 than grazing regime. However, *Arrhenatherum elatius,* a

tall grass typical of ungrazed grassland, has increased significantly only in those plots that were ungrazed in 1952.

While changes in the vegetation directly due to grazing practices may be difficult to discern due to the effects of rabbit grazing, and lack of information on stocking densities, other aspects of stock management may have had an effect on the vegetation. Grazing by stock generally represents a net loss of nutrients from the system, but if supplementary feeding is provided in winter, this may represent a significant input of nutrients. While rabbit droppings are generally distributed in patches close to their burrows, cattle typically congregate on the hilltop and shallow slopes; these species would be expected to cause different patterns of redistribution of nutrients in the landscape.

6.4.2.4 Topography and vegetation change

The surveys described in this chapter represent "snapshots" of the vegetation 48 years apart. There has been a considerable and significant change in frequency of several species over this period, and the direction of this change is consistent with that expected as a result of decreased rabbit populations, fertilisation through atmospheric nitrogen deposition and/or changing agricultural practices. Increasing values of Ellenberg N, and decreasing L values have been recorded for a wide range of habitats (although not calcareous grasslands) in the Countryside Surveys (Smart *et al.*, 2003), suggesting that the observed patterns may be part of a national trend. However, the relative contribution of any general or site-specific factors to the observed changes is impossible to determine from this study alone. Resurvey of more of Perring's original sites, including those where rabbits were not recorded at the time of his survey, may yield more information and allow more confidence to be placed in these possible causes and effects.

6.5 Summary of chapter 6

1. Vegetation surveys of the field sites showed that south facing slopes at both sites have higher frequencies of drought tolerant and calcicole plants than equivalent north-facing slopes. At Hambledon Hill south/south west facing slopes support several species with a predominantly southern distribution in Britain.
2. Detrended correspondence analysis of vegetation plots from both field sites produced a first axis that was independent of site, analogous to the gradient found in Perring's data in chapter 2, and probably equivalent to Perring's "humidity" gradient.
3. This gradient can be represented as a gradient in plant strategy from S to CSR species, or from dry calcareous to mesotrophic grassland.
4. The gradient is a complex gradient of several covarying variables that may influence plant growth and survival. GAM of species distributions suggest that the distribution of species or groups of species along the gradient may be a response to different "direct" variables. Species at the mesotrophic end of the gradient may be excluded from other sites primarily by factors related to soil fertility; those near the middle may be reacting to soil moisture; and those at the dry calcareous grassland end by other microclimatic variables such as light and temperature.
5. Comparison of plots at Hambledon Hill surveyed by Perring in 1953 and during this study in 2000 show a clear trend towards more mesotrophic sites, with higher Ellenberg N and lower Ellenberg L indices, and higher C and R and lower S indices for most plots. These changes may be attributable to several factors including reduced rabbit populations, atmospheric N deposition or changes in management.
6. These changes are considerably smaller in magnitude on slopes, particularly south-facing slopes, than on flat ground. This provides some evidence that these sites are buffered against change towards more mesotrophic vegetation by phosphate and water limitation.

Chapter 7: General discussion

7.1 Introduction

This chapter draws on the findings of this study and on the published literature to discuss the effects of slope and aspect on microclimate, soils and vegetation in chalk grassland. The wider relevance of these effects is examined with reference to environmental change and suggestions are made for future research.

7.2 Microclimatic gradients

7.2.1 Predicted and observed patterns

The observed patterns of radiation, temperature and soil moisture at both field sites, as summarised in chapter 3, were found to be generally consistent with previous studies of microclimate on contrasting slopes in grasslands (Oliver, 1991; Påhlsson, 1974; Radcliffe and Lefever, 1981; Rorison *et al.*, 1986b). The models of topographic microclimate developed in chapter 4 were consistent with these patterns and, when tested against independent data, had good predictive power, comparing favourably with other process-based models of temperature and soil moisture, including more complex heat and water flux models (Blyth, 2002; Flerchinger and Pierson, 1997; Naden *et al.*, 2000; Ragab *et al.*, 1997). They also have the advantage over empirical topographic radiation indices (McCune and Keon, 2002) that they can be used to compare topographic microclimates under different regional climates.

Another advantage of using physically-based, rather than purely empirical models is that the model may be used to explain, as well as predict, observed patterns, and to develop hypotheses. For example it was observed in chapter 3 (figure 3.23) that at Sylvan Dale there was a consistent and marked difference between measurements of soil moisture on "dry" south facing plots and "wet" north-facing plots, but that at Hambledon Hill any differences between plots were less

consistent over time and generally smaller compared to the variation in measurements within plots. Examination of the Penman-Monteith evapotranspiration term of the soil moisture model suggests an explanation for this pattern. The "radiation" term in the equation is relatively more important under a sheltered, cooler and more humid climate, while under a dry, warm and windy climate the "ventilation" term is dominant. Therefore, a greater difference in evapotranspiration rate between slopes, and greater divergence in soil moisture, is expected in climates with high atmospheric humidity and in sheltered valley locations than under dry and exposed sites (assuming a similar rainfall regime). Summer rainfall events, assuming that rain is equally distributed across the landscape, also act to reduce the divergence between slopes, bringing all sites closer to field capacity. This suggests to the hypothesis that under the climate of the Wolds (cooler and more humid, but with a lower summer rainfall than that of North Dorset), slope and aspect have a greater influence over soil moisture (see figure 6.1). Marked differences in vegetation community between opposing slopes of east-west running valleys have been observed in several calcareous regions in the North of England including the Derbyshire Dales (Anderson, 1965; Grime, 1963) and County Durham Magnesian limestone (Doody, 1980), as well as the Yorkshire Wolds (Perring, 1959). The hypothesis suggests that this could be due to a greater divergence of soil moisture at these northern sites rather than an abrupt shift in communities at this point along a microclimatic gradient.

Another hypothesis that could be tested using physical models is that the apparent south-west (rather than due south) facing distribution of many species is attributable to warmer ambient air temperatures in the afternoon, when south-west facing slopes receive the most radiation (Oke, 1987; Geiger *et al.*, 1995). If the assumptions of the temperature model are valid, and assuming cloud cover and wind speed do not vary systematically with the time of day, summer maximum daily sward temperatures are highest on slopes facing around south west. The deflection of the angle of symmetry from due south is reduced during winter, when maximum air temperatures occur closer to midday, and so maximum temperatures occur on slopes facing closer to due south. However, since south-east facing slopes receive the same net radiation flux as equivalent south-west facing slopes,

and the effect of radiation on temperature is linear under constant wind speed, mean daily temperatures, and temperature sums when the threshold is relatively low are predicted symmetrically around due south. Soil moisture, as calculated by the Penman Monteith equation, is likely to be only slightly asymmetrical around due south. Lakhani and Davis (1982) have empirically determined the optimum aspect for the distribution of *Helianthemum nummularium*. If a process is identified such as seed production in *Cirsium acaule* (Pigott, 1970) that limits the distribution of a species, and a temperature response can be determined experimentally, then the deflection of the species distribution from due south may well be explained by modelling maximum temperatures or temperature sum above a high threshold. Processes dependent on high temperature thresholds may include those that are limited by damage by moulds or rusts under cooler or damper conditions. Other species may be limited in their distribution by heat injury on south-west facing slopes, particularly if high temperatures coincide with periods of drought stress.

7.2.3 Limitations of models

Several factors have been identified that limit the accuracy of these models. The assumption that climatic variables at screen height are constant across the landscape, and that the radiation flux is the only cause of spatial variation is not satisfactory in landscapes where meso-scale atmospheric processes, such as altitudinal lapse rates and temperature inversions, are important. Ideally, a surface model could be "nested" in a spatial model of meso-scale temperature variation incorporating lapse rates and katabatic flow of cold air, such as that developed by Joyce (2000). Other relevant variables, such as wind speed, rainfall and vapour pressure deficit, are likely to vary spatially and might be modelled using a DTM (Raupach and Finnigan, 1997) but are outside the scope of this study.

Using the model as it stands, without incorporating any effects of meso-scale temperature variation, the most reliable temperature estimates are likely to be those of daytime sward temperature during the summer months, when the air at screen height is well mixed and radiation flux is the most important factor influencing surface temperature. Similarly since most evapotranspiration occurs

during the day, and low soil moisture is generally limited to the summer months, soil moisture is also likely to be more dependent on radiation flux. Slope and aspect are not good predictors of minimum or mean temperatures, or of soil temperatures if other landscape-scale variations exist. For example at Sylvan Dale minimum sward temperatures during early spring were shown to be predominantly determined by cold air drainage within the valley. In real landscapes, the biologically relevant variables that vary most consistently with slope and aspect are likely to be those associated directly with radiation flux, high summer temperatures and evapotranspiration rates. Since both the highest maximum daily temperature values and lowest soil moisture are predicted to occur around south or south-west facing aspects, it is unsurprising that this pattern is frequently observed in vegetation.

Another assumption of the models is that the plot being modelled is homogeneous. Validation measurements from the AWS sites and mobile data loggers are taken from a single point in space. However, the vegetation plots for which data were modelled were 50 m^2 in area, and soil moisture measurements were sampled from these areas. Within plot spatial variation in soil moisture was found to be considerable, probably due to variation in soil depth, texture and composition, the subsurface distribution of roots, chalk fragments and flints, and variations in vegetation structure, for example leaf area index. In the sward temperature model, different models were created for short turf and for a "tussock" sward but in reality canopy structure also varies on a sub-plot scale. Predictions of soil moisture or temperature might therefore be better expressed as probability distributions, rather than absolute values.

7.3 Soil gradients

7.3.1 Spatial heterogeneity

The results of the *in-situ* soil incubation suggested that nitrogen mineralisation in chalk grassland is limited by low temperatures in spring but was patchy and limited by lack of available substrate in summer. The distribution of available organic substrate, and hence available nitrogen, was found to be patchy on a small (sub-

plot) scale, particularly on the sloping plots. The effects of small-scale spatial heterogeneity in nutrient availability on competition in experimental plots have been studied (e.g. Day *et al.*, 2003) but the combined effects of small scale spatial and temporal variation in N supply in this system is difficult to quantify. Phosphorus availability was consistently very low in the samples from sloping ground at both sites. It seems likely that, overall, available N and P are both constrained by the amount and quality of available organic substrate in the soil, being released mainly as pulses in spring and autumn, but that the availability of P to plants is further constrained on the sloping plots, probably in part due to the high chalk content of the rendzina soils, leading to a high pH of the soil solution and fixing of P into less available forms. Studies of calcareous grasslands established on land that was previously under cultivation have shown that once P levels have been raised, they tend to remain higher than on undisturbed grassland and are a major barrier to the reestablishment of chalk grassland communities even when soil pH is high (Lloyd and Pigott, 1967; Uncovich *et al.*, 1998). On sloping ground, however, mass movement of soil downslope prevents the build up of P in the system, and maintains a high chalk content within the soil, with a high pH and maintains low P availability to plants. Sloping ground may therefore be buffered to some extent from P fertilisation, as well as from the natural development of rendzinas to calcareous brown earths.

7.3.2 Microclimate and soils

In the short-term, microclimate (both temperature and soil moisture) probably controls the timing of pulses of mineralisation of organic matter in the soil during spring and hence the availability of N. Soil moisture also apparently interacts directly with nutrient uptake in some plants, possibly by reducing diffusion pathways in the soil (Grime and Curtis, 1976; Rorison *et al.*, 1986a; Misra and Tyler, 1999, 2000). In the long term, however, nutrient availability is further limited by the availability and quality of substrate within the soil. This will be determined by feedbacks of plant production and decomposition, themselves influenced by microclimate and nutrient availability. Microclimate therefore affects nutrient

availability at different timescales. For example the immediate effect of a severe drought may be to reduce the uptake of nutrients in certain species, and to reduce rates of mineralisation of organic matter within the soil. If the drought is severe enough to cause plant death, however, a quantity of organic matter will be returned to the system as above and below ground litter. This input of substrate may cause a pulse of decomposition/mineralisation, and therefore higher nutrient availability, into the system in the following season (Jamieson *et al.*, 1998; Jamieson *et al.*, 1999). In the long term, however, a drought event may cause a reduction in the annual productivity of the vegetation, and a "bottleneck" in the carbon cycle, reducing the net quantity of organic matter returned to the soil, and reducing soil fertility. The removal (or redistribution) of organic matter by grazing animals may also be an important factor, involving long-term feedbacks to the carbon cycle.

7.3.3 Topography and soils

Despite these effects of microclimate on nutrient cycling and availability, the most striking differences in measured soil characteristics, particularly P availability, was not between wet north-facing and dry south-facing plots, nor between flat sites under different climates, but between the plots on slopes and those on the plateau/hilltop sites. This is consistent with Perring's observations that soil characteristics typically varied with slope and were more or less independent of aspect (Perring, 1959), and observations of soil catenas on chalk and limestone (Balme, 1953). On flat sites, rendzinas forming over chalk are expected to develop into calcareous brown earths, as the sub-surface chalk weathers and leaching of the topsoil forms distinct horizons. On sloping ground, mass movement of the soil downslope and the continuous exposure of chalk maintain unstable rendzinas. P is likely to be less available to most plants in rendzina soils on slopes soils due to their higher chalk content and higher pH. pH/P availability is probably responsible for the marked change in vegetation from mesotrophic communities to calcareous grassland between flat sites and slopes over around 15° observed at both field sites.

7.4 Vegetation gradients

The primary DCA axes of both Perring's original data set and data collected from the field site at this study identified a gradient in species composition in chalk grassland at the sites that was associated with a gradient in plots with predominantly stress tolerant species to plots dominated by competitive-ruderals. This vegetation gradient was also strongly correlated with Ellenberg indices, particularly those indicating fertility and moisture. This gradient in vegetation is interpreted as being due to a "compound" environmental gradient associated with both soil fertility and soil moisture.

One problem in determining the mechanisms by which soil moisture affects vegetation composition in calcareous grasslands is the association of "calcicole" behaviour in plants of chalk grassland with nutrient-poor environments, drought tolerance or drought avoidance. Considering the clear gradient observed in chalk grassland plots from those dominated by S to CR strategists may be useful here. Certain physiological traits shared by stress tolerant species may be advantageous for survival in conditions of both high soil pH, low available nutrients and low water content. Unravelling microclimatic from edaphic effects is complicated further as the calcium carbonate content of soils, and hence the pH of their soil solution, is a function of the rate of leaching and the rate of weathering of the underlying substrate. Under a more humid microclimate, leaching would be expected to occur more rapidly. Thus Perring (1960) assumed that vegetation and soil developed together as a function of climate, geology and topography. However, several problems emerge with this approach. Firstly, there is a clear effect of topography on soils that is independent of microclimate, as outlined above. Secondly, soils and vegetation may react to microclimate on different timescales. Finally, vegetation is more likely to respond to soil moisture during drought in the growing season, while leaching is more likely to occur during winter when the soil moisture may be above field capacity, and water flows vertically through the soil.

Perring (1960) showed that species with a high degree of exclusivity to chalk grassland in Dorset that exist on all slopes in Cambridgeshire become increasingly

restricted to south-facing slopes under the more humid climate of the Yorkshire Wolds. It was hypothesised in this study that the effect of slope and aspect on soil moisture is greater in calcareous grasslands in the humid north and west in the UK, and that this divergence between slopes is ecologically highly significant as it defines sites where frequent drought is an important factor in structuring the vegetation composition, and sites where drought is a rare occurrence. The relative importance of extreme climatic events, and average climatic conditions in determining vegetation composition in calcareous grasslands has been discussed elsewhere (Buckland *et al.*, 1997). Given sufficient input data over several years, models of topographic microclimate could be used to assess both the frequency and magnitude of drought events experienced at individual plots over long time periods.

7.4.1 The effect of soil moisture on vegetation

In chapter 4, water-use efficiency, transpiration rates and stomatal conductance were shown to be lower for certain species on south-facing slopes at a volumetric water content of 37% than on north-facing slopes at a volumetric water content of 45%, but no significant difference in photosynthetic rate was found. While soil moisture is often associated with stomatal resistance, it has been noted that stomatal resistance only accounts for a small part of the variation in carbon assimilation (Jones, 1998). Similarly Buckland, Grime *et al* (1997) found that even during the extreme drought of 1995, low leaf relative water content (taken to indicate drought stress) was rare except in plants in shallow soils and near rock outcrops at Buxton. They concluded that, while in average years, drought stress in plants was low, unusually dry years acted as a "resetting" mechanism, restricting expansion of drought-sensitive species onto shallower soils. It is feasible that extreme drought events (possibly in conjunction with heat stress due to high maximum daily temperatures) similarly restrict expansion onto south- or south-west-facing slopes, while on average years there is little or no effect of soil moisture. Additionally, dry soil conditions may restrict growth by limiting nutrient uptake in the short term, by reducing the long term quality and quantity of organic matter in the soil, or by maintaining high soil pH by reducing leaching of carbonates.

7.4.2 Species response to microclimate

Perring showed that species could be divided into groups on the basis of their climatic and topographic distributions, and that those species restricted to broadly warm/dry microclimates in Britain tended to be those with a high degree of exclusivity to chalk grasslands. Some suggestions can be made on the mechanisms determining the distribution of these species.

A group of Mesobromion species with a Continental (Matthews, 1955) or Temperate/Southern temperate (Preston and Hill, 1997) distribution in Europe are shown by Rodwell (1992) to be present in British *Festuca-Avenula* grasslands where August maximum daily (screen height) temperatures exceed 20° C. These species include *Cirsium acaule, Hippocrepis comosa, Polygala calcarea and Asperula cynanchica.* The species may be considered as equivalent to Perring's groups I and II, with some overlap to group III. The occurrence of species from this group within a sward defines typical "chalk" (as opposed to other limestone) grassland communities; the chalk outcrop in south-eastern England roughly follows the 20° C August maximum daily isotherm. However, these species are absent from Sylvan Dale and generally rather scarce or absent on chalk in the Yorkshire Wolds, suggesting a climatic, rather than geological explanation for their distribution. In *Cirsium acaule* this distribution has been shown to be attributable to a dependence on high summer temperatures in order to produce viable seed (Pigott, 1975). GAMs in this study for *Hippocrepis comosa* and *Asperula cynanchica* have shown that the distribution of these species is associated with high temperatures and a short sward height. It seems likely that several other species in groups I to III are limited in their distribution directly by low summer daytime temperatures at some stage in their life cycle, rather than by available soil moisture or other edaphic factors. Distributions centred on south-west, rather than south-facing slopes are consistent with this interpretation due to the maximum sward temperatures occurring on these slopes. It is notable that, while maximum sward temperatures are expected to show this asymmetry, mean temperatures and temperature sums ("thermal time") are not. The limit to their realised niche would therefore represent a physiological limit of the species, and would tend to be

sharply defined and might be determined experimentally. The germination experiment in this study did not show that shading restricted germination in any of the species studied. A temperature limit for fertilisation and viable seed production, dependent on maximum daily temperatures or with a non-linear response to temperature sum may be a more likely mechanism for this group of species, although the mechanism may vary between individual species.

In contrast with these species, many of the species in Perring's group III are often more frequent on south or south-west facing slopes on chalk, but are widely distributed in northern Britain on limestone and other free-draining soils. These are often matrix-forming species; *Sanguisorba minor, Thymus polytrichus and Carex flacca* are typical examples, along with the grasses *Festuca ovina* and *Koeleria macrantha.* It is unlikely that these species are excluded from north-facing slopes by low temperature given their wider distribution. They are, broadly speaking, stress tolerant species, adapted to drought and low nutrient availability (and interactions between the two) but not exclusively limited to chalk or even to calcareous soils. The distribution of *Thymus polytrichus* was best modelled as a function of drought duration using GAM; it seems likely that the distribution of this group of species is due to their competitive exclusion from sites of higher nutrient and/or soil moisture status.

Since the predominant vegetation gradient at both sites is related to drought, pH and nutrient stress, with north-facing slopes intermediate between south-facing and flat sites, few species are strictly limited to north- or north-east facing slopes in the landscape. The common bryophyte species *Pseudoscleropodium purum, Rhytidiadelphus squarrosus* and *R. triquetrus.* are exceptions, being more common on north-facing slopes at both field sites, as noted in previous studies (Hope-Simpson, 1941; Porley, 1999; Watson, 1960) and apparently respond predominantly to moisture. Perring's groups IV and V are predominantly the CSR/CR strategy species typical of mesotrophic grasslands that tend to have a distribution centred on flat sites. At Sylvan Dale, and in the Yorkshire Wolds generally, the calcifuge species *Potentilla erecta* and *Deschampsia cespitosa* are more abundant on north-facing slopes but often excluded from flat sites. These

species are presumably able to persist in unleached chalk rendzina soils in wet microclimates, but are excluded from mesotrophic grassland on the flatter sites by more competitive species.

7.7 Topography and vegetation change

7.7.1 Vegetation change at Hambledon Hill 1952-2000

The changes in vegetation observed at Hambledon Hill over the last 50 years showed a distinct trend towards a more mesotrophic community, with a decrease in stress tolerant, light demanding species. As discussed in chapter 6, the differences in vegetation between years could be attributed to a number of causal factors, including the decline in rabbit population after myxomatosis, atmospheric nitrogen deposition, and changes in management. Similar increases in Ellenberg N indices were found in a range of British plant communities over the period 1990 to 1998 (Smart *et al.*, 2003), although not in calcareous grasslands.

The relative lack of change in vegetation on south-facing slopes was interesting as it suggests that these areas may be providing refuge for stress-tolerant calcicoles from chalk grasslands. Pollen sequences suggest that chalk grassland species such as *Sanguisorba minor* persisted in lowland England throughout the Holocene, and it has been suggested that steep slopes provided a refuge for these species in a predominantly wooded landscape (Waller and Hamilton, 2000). Over the much shorter timescales of this study, low P availability, more frequent and severe drought events and high maximum temperatures may buffer south-facing slopes from change. Further resurvey of Perring's sites throughout the UK will help to identify whether the trends at Hambledon Hill are widespread, particularly as the dataset includes sites that are both grazed and ungrazed (at the time of survey), and with and without recorded rabbit populations.

7.7.2 Topography and future vegetation change

Current climate change scenarios for the UK suggest that mean temperatures will increase by between 1 and 3.5° C by 2050, summers will become substantially warmer and drier and winters will become wetter. Both extreme drought events and extreme high rainfall events are expected in increase in frequency (Hulme *et al.,* 2002). The topographic microclimate models developed in this study could provide a useful method for bridging the gap from these large-scale climatic predictions from global circulation models to small-scale predictions of biologically relevant variables. A model for a field site could be run using real climatic time series data from another region, or existing data could be adjusted to simulate, for example, the effects of higher temperature and vapour pressure deficit or different rainfall patterns, to provide quantitative predictions of topographic microclimate under future climates. The GAM approach to modelling species niches could be used to investigate the effect on species distribution.

In qualitative terms, the following changes in chalk grassland might be expected under a future climate scenario: an increase in the topographic range of those species currently restricted to south-west facing slopes by low summer temperatures; an increase in frequency of stress-tolerant species on all slopes; and long term effects on soil development due to changes in rainfall. Since most of the species currently of highest conservation importance in chalk grasslands are in those groups currently with a southern geographical distribution and often "south-facing" topographical distribution, these species may benefit from future climate change. However, factors other than climate, such as those implicated in the changes over the last 50 years at Hambledon Hill, are likely to continue to influence the species composition of chalk grasslands. Perhaps the most striking change in chalk grassland notable from Perring's data has been the loss of so many chalk grassland sites to intensive agriculture, forestry or the growth of scrub. Habitat fragmentation has been identified as a barrier to the northward expansion of species under future climate change in the UK (Hill *et al.,* 2002). The fragmentation of remaining sites is likely to prove a serious barrier to any northward expansion of chalk grassland species, in the absence of artificial

introductions. At sites where suitable grazing regimes are maintained, however, future climate change may lead to changes in the topographic distribution of species expanding from south-facing slopes.

References

Abril, A., Caucas, V., and Bucher, E.H. (2001) Reliability of the *in situ* incubation methods used to assess nitrogen mineralization: a microbiological perspective. *Applied Soil Ecology*, **17**, 125-130.

Alberdi, M. and Corcuera, L.J. (1991) Cold acclimation in plants. *Phytochemistry*, **30**, 3177-3184.

Allen, R. (2000) Using the FAO-56 dual crop coefficient method over an irrigated region as part of an evapotranspiration intercomparison study. *Journal of Hydrology*, **229.**

Allen, R., Pereira, L., Raes, D., and Smith, M. (1998). *Crop evapotranspiration: guidelines for computing crop requirements.* FAO Irrigation and Drainage paper no. 56. FAO, Rome.

Allen, S.E. (1974) *Chemical analysis of ecological materials* Blackwell Scientific Publications, Oxford.

Anderson, D.J. (1965) Studies on structure in plant communities: I. An analysis of limestone grassland in Monk's Dale, Derbyshire. *Journal of Ecology*, 53, 97-107.

Arnold, S.M. and Monteith, J.L. (1974) Plant development and mean temperature in a Teesdale habitat. *Journal of Ecology,* **62**, 711-720.

Austin, M.P. (1968) An ordination study of a chalk grassland community. *Journal of Ecology*, **56**, 739-757.

Austin, M.P. and Smith, T.M. (1989) A new model for the continuum concept. *Vegetatio*, **83,** 35-47.

Austin, M.P. (2002) Spatial prediction of species distribution: an interface between ecological theory and statistical modelling. *Ecological Modelling*, **157** (2-3), 101-118.

Avery, B.W. (1980) *Soil classification for England and Wales* Soil Survey, Harpendon.

Balme, O.E. (1953) Edaphic and vegetational zoning on the Carboniferous limestone of the Derbyshire Dales. *Journal of Ecology*, **41**, 331-344.

Beerling, J. (1993) The impact of temperature on the northern distribution limits of the introduced species *Fallopia japonica* and *Impatiens glandulifera* in north-west Europe. *Journal of Biogeography*, **20,** 45-53.

Blyth, E. (2002) Modelling soil moisture for a grassland and a woodland site in south-east England. *Hydrology and Earth System Sciences*, **6,** 39-47.

Bobbink, R. (1987) Increasing dominance of *Brachypodium pinnatum* (L.) Beav. in chalk grasslands: a threat to a species-rich ecosystem. *Biological Conservation*, **40**, 301-314.

Box, E.O. (1996) Plant functional types and climate change at the global scale. *Journal of Vegetation Science,* **7**, 309-320.

Boyko, H. (1947) On the role of plants as quantitative climate indicators and the geo-ecological law of distribution. *Journal of Ecology,* **35**, 138-157.

Buckland, S.M., Grime, J.P., Hodgson, J.G., and Thompson, K. (1997) A comparison of plant responses to the extreme drought of 1995 in northern England. *Journal of Ecology*, **85,** 875-882.

Buckland, S.M., Thompson, K., Hodgson, J.G., and Grime, J.P. (2001) Grassland invasions: effects of manipulations of climate and management. *Journal of Applied Ecology*, **38,** 301-309.

Buffo, J., Fritschen, L.J., and Murhy, J.L. (1972). *Direct solar radiation on various slopes from 0 to 60 degrees north latitude.* USDA Forest Service Research Paper PNW-142, Portland, Oregon.

Burman, R. and Pochop, L.O. (1994) *Evaporation, evapotranspiration and climatic data.* Elsevier, Amsterdam.

Burnside, N.G., Smith, R.F., and Waite, S. (2002) Habitat suitability modelling for calcareous grassland restoration on the South Downs, United Kingdom. *Journal of Environmental Management,* **65,** 209-221.

Campbell, G.S. (1985) *Soil physics with BASIC.* Elsevier, Amsterdam.

Carroll, J.A., Caporn, S.J.M., D., J., Morecroft, M.D., and Lee, J.A. (2003) The interactions between plant growth, vegetation structure and soil processes in semi-natural acidic and calcareous grasslands recieving long-term inputs of simulated pollutant nitrogen deposition. *Environmental Pollution*, **121**, 363-376

Criddle, R.S., Breidenbach, R.W., Fontana, A.J., Henry, J.-M., Smith, B.N., and Hansen, L.D. (1996) Plant respiration responses to climate determine geographic distribution. *Russian Journal of Plant Physiology*, **43**, 813-820.

Critchley, C.N.R., Chambers, B.J., Fowbert, J.A., Sanderson, R.A., Bhogal, A., and Rose, S.C. (2002) Association between lowland grassland plant communities and soil properties. *Biological Conservation,* **105,** 199-215.

Dahl, E. (1997) *The Phytogeography of Northern Europe (British Isles, Fennoscandia and adjacent areas).* Cambridge University Press, Cambridge.

Dargie, T.C.D. (1987) An ordination analysis of vegetation patterns on topoclimate gradients in south-east Spain. *Journal of Biogeography,* **14,** 197-211.

Davy, A.J. (1974) Seasonal patterns of nitrogen availability in contrasting soils in the Chiltern Hills. *Journal of Ecology,* **62,** 793-807.

Day, K.J., Hutchings, M.J., & John, E.A. (2003) The effects of spatial pattern of nutrient supply on yield, structure and mortality in plant populations. *Journal of Ecology*, 91, 541-553.

Doody, J.P. (1980). Grassland. In The Magnesian Limestone of Durham County (ed T.C. Dunn). Durham County Conservation Trust, Houghton-le-Spring.

Duckworth, J.C., Bunce, R.G.H., and Malloch, A.J.C. (2000a) Modelling the potential effects of climate change on calcareous grasslands in Atlantic Europe. *Journal of Biogeography,* **27**, 347-358.

Duckworth, J.C., Bunce, R.G.H., and Malloch, A.J.C. (2000b) Vegetation gradients in Atlantic Europe: the use of existing phytosociological data in preliminary investigations on the potential effects of climate change on British vegetation. *Global Ecology and Biogeography,* **9**, 187-199.

Duckworth, J.C., Bunce, R.G.H., and Malloch, A.J.C. (2000c) Vegetation-environment relationships in Atlantic European calcareous grasslands. *Journal of Vegetation Science*, **11**, 15-22.

Dytham, C. (1999) *Choosing and Using Statistics. A Biologists Guide* Blackwell Science Ltd, Oxford.

Eek, L. and Zobel, K. (1997) Effects of additional illumination and fertilization on seasonal changes in fine-scale grassland community structure. *Journal of Vegetation Science*, **8,** 225-234.

Eek, L. and Zobel, K. (2001) Structure and diversity of a species-rich grassland community, treated with additional illumination, fertilization and mowing. *Ecography,* **24**, 157-164.

Ellis, S. and Newsome, D. (1991) Chalkland soil formation and erosion on the Yorkshire Wolds, northern England. *Geoderma,* **48**, 59-72.

Eno, C.F. (1960) Nitrate production in the field by incubating the soil in polythene bags. *Proceedings of the Soil Science Society of America,* **24**, 277-279.

Erschbamer, B., Grabherr, G., and Reisigl, H. (1983) Spatial pattern in dry grassland communities of the Central Alps and its ecophysiological significance. *Vegetatio,* **54,** 143-151.

Fearn, G.M. (1973) Biological Flora of the British Isles. *Hippocrepis comosa* L. *Journal of Ecology*, **61**, 915-926.

Ferris, R. and Taylor, G. (1995) Contrasting effects of elevated CO_2 and water deficit on two native herbs. *New Phytologist*, 131, 491-501.

Flerchinger, G.N. and Pierson, F.B. (1997) Modelling plant canopy effects on variability of soil temperature and water: model calibration and validation. Journal of Arid Environments, **35**, 641-653.

Flerchinger, G.N. and Saxton, K.E. (1989a) Simultaeous heat and water model of a freezing snow-residue-soil system I. Theory and development. *Transactions of the American Society of Agricultural Engineers*, **32,** 565-571.

Flerchinger, G.N. and Saxton, K.E. (1989b) Simultaneous heat and water model of a freezing snow-residue-soil system II. Field verification. *Transactions of the American Society of Agricultural Engineers*, **32**, 573-578.

Forseth, I.N., Wait, D.A., and Casper, B.B. (2001) Shading by shrubs in a desert system reduces the physiological and demographic performance of an associated herbacious perennial. *Journal of Ecology*, **89,** 507-710.

Franklin, J. (1995) Predictive vegetation mapping: geographic modelling of biospatial patterns in relation to environmental gradients. Progress in Physical *Geography,* **19,** 474-499.

Franklin, J. (1998) Predicting the distribution of shrub species in southern California from climate and terrain-derived variables. *Journal of Vegetation Science,* **9,** 733-748.

Franklin, J., McCullough, P., and Gray, C. (2000). Terrain variables used for predictive mapping of vegetation communities in Southern California. In *Terrain Analysis* (eds J.P. Wilson and J.C. Gallant), pp. 331-354. John Wiley and Sons, New York.

Franko, U., Oelschlägel, B., and Schenk, S. (1995) Simulation of temperature-, water- and nitrogen dynamics using the model CANDY. *Ecological Modelling*, **81**, 213-222.

Furness, R.R., Jarvis, R.A., and King, S.J. (1981). Soils and Land use in the Yorkshire Wolds. *In Proceedings of the North of England Soils Discussion Group No. 18.* North of England soils Discussion Group.

Gauslaa, Y. (1984) Heat resistance and energy budget in different Scandinavian plants. *Holarctic Ecology*, **7,** 1-78.

Geiger, R., Aron, R.H., and Todhunter, P. (1995) *The climate near the ground,* 5th edn. Vieweg, Braunschweig.

Gittens, R. (1965a) Multivariate approaches to a limestone grassland community: I. A stand ordination. *Journal of Ecology,* **53,** 385-401.

Gittens, R. (1965b) Multivariate approaches to a limestone grassland community: III. A Comparative study of ordination and association-analysis. *Journal of Ecology*, **53,** 411-425.

Gittens, R. (1965c) Multivariate approaches to a limestone grassland community: III. A direct species ordination. *Journal of Ecology*, **53,** 403-409.

Gottfried, M., Pauli, H., and Grabherr, G. (1998) Prediction of vegetation patterns at the limits of plant life: a new view of the alpine-nival ecotone. *Arctic and Alpine Research*, **30,** 207-221.

Grace, J. (1981). Some effects of wind on plants. In *Plants and their atmospheric environment* (eds J. Grace, E.D. Ford and P.G. Jarvis), pp. 31-56. Blackwell, Oxford.

Grace, J. (1987) Climatic tolerance and the distribution of plants. *New Phytologist*, **106,** 113-130.

Grace, J. (1988). Temperature as a determinant of plant productivity. In *Plants and Temperature* (eds S.P. Long and F.I. Woodward), pp. 91-108. The Company of Biologists Ltd., Cambridge.

Grace, J., Allen, S.J., and Wilson, C. (1989) Climate and the meristem temperatures of plant communities near the tree-line. *Oecologia*, **79,** 198-204.

Graves, J.D. and Taylor, K. (1986) A comparative study of *Geum rivale* L. and *G. urbanum* L. to determine those factors controlling their altitudinal distribution I. Growth in controlled environments. *New Phytologist*, **104,** 681-691.

Grime, J.P. (1963) An ecological investigation at a junction between two plant communities in Coombsdale on the Derbyshire limestone. *Journal of Ecology*, **51**, 391-402.

Grime, J.P. (1974) Vegetation classification by reference to strategies. *Nature,* **250,** 26-31.

Grime, J.P. (1988) *Comparative Plant Ecology* Unwin Hyman, London.

Grime, J.P. and Curtis, A.V. (1976) The interaction of drought and mineral nutrient stress in calcareous grassland. *Journal of Ecology*, **64**, 975-988.

Grime, J.P. and Jarvis, B.C. (1975). Shade avoidance and shade tolerance in flowering plants II. Effects of light on the germination of species of contrasted ecology. In *Light as an ecological factor* (eds G.C. Evans, R. Bainbridge and O. Rackham), Vol. II, pp. 525-532. Blackwell, Oxford.

Grime, J.P., Mason, G., Curtis, A.V., Rodman, J., and Band, S.R. (1981) A comparative study of germination characteristics in a local flora. *Journal of Ecology*, **69,** 1017-1059.

Grubb, P.J. (1977) The maintenance of species-richness in plant communities: the role of the regeneration niche. *Biological Review*, **52,** 107-145.

Guisan, A., Weiss, S.B., and Weiss, A.D. (1999) GLM versus CCA spatial modeling of plant distribution. *Plant Ecology,* **143,** 107-222.

Hay, J.E. and McKay, D.C. (1985) Estimating solar irradiance on inclined surfaces: a review and assessment of methodologies. *International Journal of Solar Energy,* **3,** 203-240.

Hall, J.B. (1971) Pattern in a chalk grassland community. *Journal of Ecology,* **59**, 749-762.

Hardegree, S.P. and Vactor, S.S.V. (1999a) Germination and emergence of primed grass seeds under field and simulated-field temperature regimes. *Annals of Botany*, **85,** 379-390.

Hardegree, S.P. and Vactor, S.S.V. (1999b) Predicting germination response of four cool-season range grasses to field-variable temperature regimes. *Environmental and Experimental Botany*, **41**, 209-217.

Hastie, T.J. and Tibshirani, R.J. (1990) *Generalized Additive Models* Chapman and Hall, London.

Heal, O.W., Latter, P.M., and Howson, G. (1978). A study of the rates of decomposiiton of organic matter. *In Production Ecology of British Moors and Montane Grasslands* (eds O.W. Heal and D.F. Perkins), pp. 136-159. Springer-Verlag, Berlin.

Hill, J.K., Thomas, C.D., Fox, R., Telfer, M.G., Willis, S.G., Asher, J., and Huntley, B. (2002) Responses of butterflies to twentieth century climate warming: implications for future ranges. Proceedings of the Royal Society of London Series B: Biological Sciences, **269**, 2163-2171.

Hill, M.O. (1979) *DECORANA - a FORTRAN program for detrended correspondence analysis and reciprocal averaging.* Ithaca, New York.

Hill, M.O. and Carey, P.D. (1997) Prediction of yield in the Rothamstead Park Grass experiment by Ellenberg indicator values. *Journal of Vegetation Science,* **8,** 574-579.

Hill, M.O. and Gauch, H.G. (1980) Detrended correspondence analysis, an improved ordination technique. *Vegetatio*, **42,** 47-58.

Hill, M.O., Mountford, J.O., Roy, D.B., and Bunce, R.G.H. (1999) *Ellenburg's indicator values for British plants* Institute of Terrestrial Ecology, Huntingdon, UK.

Hogenbirk, J.C. and Reader, R.J. (1989) Biotic versus abiotic control of plant density: studies of *Medicago lupulina* L. on a topographic gradient. *Journal of Biogeography*, **16,** 269-277.

Hope-Simpson, J.F. (1941) Studies of the vegetation of the English chalk: VIII. A second survey of the chalk grasslands of the South Downs. *Journal of Ecology*, **29**, 217-267.

Hopkins, B. (1978) The effects of the 1976 drought on chalk grassland in Sussex, England. *Biological Conservation*, **14,** 1-12.

Howard, J.K. and Higgins, C.G. (1987) Dimensions of grazing-step terraces and their significance. In *International Geomorphology 1986: Proceedings of the first conference, Vol. 2*, pp. 545-568.

Hulme, M., Jenkins, G.J., Turnpenny, J.R., Mitchell, T.D., Jones, R.G., Lowe, J., Murphy, J.M., Hassell, D., Boorman, P., McDonald, R., and Hill, S. (2002). Climate change scenarios for the United Kingdom: the UKCIP02 scientific report. Tyndall Centre for Climate Change Research, School of Environmental Sciences, University of East Anglia, Norwich.

Hunt, R. and Neal, A.M. (1993). Fluctuating temperature and drought. In *Methods in comparative plant ecology* (eds G.A.F. Hendry and J.P. Grime), pp. 95-98. Chapman and Hall, London.

Huntley, B. (1991) How plants respond to climate change: migration rates, individualism and the consequences for plant communities. *Annals of Botany*, **67**, 15-22.

Huntley, B., Bartlein, P.J., and Prentice, I.C. (1989) Climatic control of the distribution and abundance of beech (*Fagus* L.) in Europe and North America. *Journal of Biogeography*, **16,** 551-560.

Huntley, B., Berry, P.M., Cramer, W., and McDonald, A.P. (1995) Modelling present and potential future ranges of some European higher plants using climate response surfaces. *Journal of Biogeography*, **22**, 967-1001.

Hutchings, M.J. (1983) Plant diversity in four chalk grassland sites with different aspects. *Vegetatio*, **53**, 179-189.

Isard, S.A. (1983) Estimating potential direct insolation to alpine terrain. *Arctic and Alpine Research*, **15**, 77-89.

Isard, S.A. and Belding, M.J. (1989) Evapotranspiration from the alpine tundra of Colorado. *Arctic and Alpine Research*, **21**, 71-82.

Jacquemyn, H., Brys, R., and Hermy, M. (2003) Short-term effects of different management regimes on the response of calcareous grassland vegetation to increased nitrogen. *Biological Conservation*, **111**, 137-147.

Jamieson, N., Barraclough, D., Unkovich, M., and Monaghan, R. (1998) Soil N dynamics in a natural calcareous grassland under a changing climate. *Biology and Fertility of Soils*, **27**, 267-273.

Jamieson, N., Monaghan, R., and Barraclough, D. (1999) Seasonal trends of gross mineralisation in a natural calcareous grassland. *Global Change Biology*, **5**, 423-431.

Janssens, F., Peeters, A., Tallowin, J.R.B., Bekker, J.P., Bekker, R.M., Fillat, F., and Oomes, M.J.M. (1998) Relationship between soil chemical factors and grassland diversity. *Plant and Soil*, **202**, 69-78.

Jenny, H. (1941) *Factors of soil formation.* McGraw Hill, New York.

Jeffrey, D.W. and Pigott, C.D. (1973) The response of grasslands on sugar-limestone in Teesdale to application of phosphorus and nitrogen. *Journal of Ecology*, **61**, 85-92.

Jones, D.A. and Turkington, R. (1986) Biological Flora of the British Isles. *Lotus corniculatus* L. *Journal of Ecology*, 74, 1085-1212.

Jones, H.G. (1992) *Plants and Microclimate,* 2nd edn. Cambridge University Press, Cambridge.

Jones, H.G. (1998) Stomatal control of photosynthesis and transpiration. *Journal of Experimental Botany,* 49, 387-398.

Joyce, A.N. (2000) *Modelling surface climate over complex terrain for landscape ecology,* Ph.D. thesis, University of Durham, Durham.

Kent, M. and Coker, P. (1994) *Vegetation Description and Analysis*: A Practical Approach, 2 edn. John Wiley and Sons, Chichester.

Kang, S., Kim, S., Oh, S., and Lee, D. (2000) Predicting spatial and temporal patterns of soil temperature based on topography, surface cover and air temperature. *Forest Ecology and Management*, **136,** 173-184.

King, S.J. and Bradley, R.I. (1987) *Soils of the Market Weighton District.* Soil Survey of England and Wales, Harpenden.

Köhler, B., Ryser, P., Güsewell, S., and Gigon, A. (2001) Nutrient availability and limitation in traditionally mown and in abandoned limestone grasslands: a bioassay experiment. *Plant and Soil*, **230**, 323-332.

Körner, C. (1999). Alpine plants: stressed or adapted? In *Physiological Plant Ecology* (eds M.C. Press, J.D. Scholes and M.G. Barker), pp. 297-311. Blackwell Science, Oxford.

Körner, C. (2003) Carbon limitation in trees. *Journal of Ecology*, **91,** 4-17.

Körner, C. and Diemer, M. (1987) *In situ* photosynthetic responses to light, temperature and carbon dioxide in herbaceous plants from low and high altitude. *Functional Ecology*, **1,** 179-194.

Kneizys, F.X., Shettle, E.P., Gallery, W.O., Chetwynd Jr., J.H., Abreu, L.W., Selby, J.E.A., Clough, S.A., and Fenn, R.W. (1988). *Atmospheric transmittance/radiance: Computer code LOWTRAN7.* US Department of Defense, Air Force Geophysics Laboratory, Optical Physics Division.

Krzanowski, W.J. (1998) *An Introduction to Statistical Modelling.* Arnold, London.

Lakhani, K.H. and Davis, B.N.K. (1982) Multiple regression models of the distribution of *Helianthemum chamaecistus* in relation to aspect and slope at Barnack, England. *Journal of Applied Ecology*, **19,** 621-629.

Larcher, W. (1995) *Physiological Plant Ecology*, 3rd edn. Springer-Verlag, New York.

Linacre, E. (1992) *Climate data and resources.* Routledge, London.

Lloyd, P.S. and Pigott, C.D., (1967) The influence of soil conditions on the course of succession on the chalk of southern England. *Journal of Ecology*, **55**, 137-146.

Mahmood-ul-Hassan, M. and Gregory, P.J. (2002) Dyamics of water movement on Chalkland. *Journal of Hydrology,* **257,** 27-41.

Mark, A.F., Dickinson, K.J.M., Allen, J., Smith, R., and West, C.J. (2001) Vegetation patterns, plant distribution and life forms across the alpine zone in southern Tierra del Fuego, Argentina. *Austral Ecology,* **26,** 423-440.

Matthews, J.R. (1955) *Origin and Distribution of the British Flora*, 1st edn. Hutchinson, London.

McCune, B. and Keon, D. (2002) Equations for potential annual direct incident radiation and heat load. *Journal of Vegetation Science,* **13,** 603-606.

Miller, P.C. (1971) Sampling to estimate mean leaf temperatures and transpiration rates in vegetation canopies. *Ecology,* **52,** 885-889.

Misra, A. and Tyler, G. (1999) Influence of soil moisture on soil solution chemistry and concentrations of minerals in the calcicoles *Phleum phleoides* and *Veronica spicata* grown on a limestone soil. *Annals of Botany,* **84,** 401-410.

Misra, A. and Tyler, G. (2000) Effect of wet and dry cycles in calcareous soil on mineral nutrient uptake of two grasses, *Agrostis stolonifers* L. and *Festuca ovina* L. Plant and Soil, **224,** 297-303.

Monteith, J.L. (1981). Coupling of plants to the atmosphere. In *Plants and their atmospheric environment* (eds J. Grace, E.D. Ford and P.G. Jarvis), pp. 1-29. Blackwell, Oxford.

Monteith, J.L. and Unsworth, M.H. (1990) *Principles of environmental physics*, 2 edn. Edward Arnold, London.

Morecroft, M.D., Sellers, E.K., and Lee, J.A. (1994) An experimental investigation into the effects of atmospheric nitrogen deposition on two semi-natural grasslands. *Journal of Ecology*, **82,** 475-483.

Murdoch, A.J., Roberts, E.H., and Goedert, C.O. (1989) A model for germination responses to alternating temperatures. *Annals of Botany*, **63**, 97-111.

Naden, P.S., Blyth, E.M., Broadhurst, P., Watts, C.D., and Wright, I.R. (2000) Modelling the spatial variation in soil moisture at the landscape scale:

an application to five areas of ecological interest in the UK. *Hydrological Processes*, **14,** 785-809.

Naden, P.S. and Watts, C.D. (2001) Estimating climate-induced change in soil moisture at the landscape scale: an application to five areas of ecological interest in the UK. *Climatic Change*, **49,** 411-440.

North, P.R.J. (1994). Chapter 8: Estimation of annual solar insolation for mountainous terrain. In *Effects of rapid climate change on plant diversity in boreal and montane ecosystems.* Report for 2nd year: 1994. CEC Programme "Environment".

Nunez, M. (1980) The calculation of solar and net radiation in mountainous terrain. *Journal of Biogeography,* **7**, 173-186.

Oke, T.R. (1987) *Boundary Layer Climates*, 2nd Edition edn. Methuen, London.

Olff, H., Pegtel, D.M., Groenendael, J.M.V., and Bakker, J.P. (1994) Germination strategies during grassland succession. *Journal of Ecology*, **82,** 69-77.

Oliver, H.R. (1991) Studies of surface energy balance of sloping terrain. *International Journal of Climatology*, **12,** 55-68.

Oliver, S.A., Oliver, H.R., Wallace, J.S., and Roberts, A.M. (1987) Soil heat flux and temperature variation with vegetation, soil type and climate. *Agricultural and Forest Meteorology*, **39**, 257-269.

Olmo, F.J., Vida, J., Foyo, I., Castro-Diez, Y., and Alados-Arboledas, L. (1999) Prediction of global irradiance on inclined surfaces from horizontal global irradiance. *Energy,* **24**, 689-704.

Olseth, J.A. and Skartveit, A. (1997) Spatial distribution of photosynthetically active radiation over complex topography. *Agricultural and Forest Meteorology,* **86,** 205-214.

Olyphant, G.A. (1986) The components of incoming radiation within a mid-latitude alpine watershed during the snowmelt season. *Arctic and Alpine Research*, **18**, 163-169.

Oomes, M.J.M. and Elberse, W.T. (1976) Germination of six grassland herbs in microsites with different water contents. *Journal of Ecology*, **64,** 745-755.

Osmond, C.B., Austin, M.P., Berry, J.A., Billings, W.D., Boyer, J.S., Dacey, J.W.H., Nobel, P.S., Smith, S.D., and Winner, W.E. (1987) Stress physiology and the distribution of plants. *BioScience,* **37**, 38-48.

Påhlsson, L. (1974) Relationship of soil, microclimate and vegetation on a sandy hill. *Oikos*, **25,** 21-34.

Penman, H.L. (1948) Evaporation from open water, bare soil and grass. *Proceedings of the Royal Society of London Series A: Mathematical, Physical and Engineering Sciences*, **193**, 120-146.

Perring, F.H. (1956) *Climatic and edaphic gradients of chalk grassland.* Ph.D. thesis, Queens College, Cambridge.

Perring, F. H. (1958) A theoretical approach to the study of chalk grassland. *Journal of Ecology,* **46**, 665-679.

Perring, F. H. (1959) Topographical gradients of chalk grassland. *Journal of Ecology*, **47,** 447-481.

Perring, F. H. (1960) Climatic gradients of chalk grassland. *Journal of Ecology*, **48,** 415-442.

Pigott, C.D. (1955) Biological Flora of the British Isles. *Thymus* L. *Journal of Ecology*, **43**, 365-387.

Pigott, C.D. (1970). The response of plants to climate and climate change. In *The Flora of a Changing Britain* (ed F.H. Perring), pp. 32-34. Classey, Faringdon.

Pigott, C.D. (1975) Experimental studies on the influence of climate on the geographical distribution of plants. *Weather*, **30**, 82-90.

Pigott, C.D. and Huntley, J.P. (1978) Factors controlling the distribution of *Tilia cordata* at the northern limits of its geographical range I. Distribution in north-west England. *New Phytologist*, **81,** 429-441.

Pigott, C.D. and Huntley, J.P. (1980) Factors controlling the distribution of *Tilia cordata* at the northern limits of its geographical range II. History in north-west England. *New Phytologist,* **84,** 145-164.

Pigott, C.D. and Huntley, J.P. (1981) Factors controlling the distribution of *Tilia cordata* at the northern limits of its geographical range III. Nature and causes of seed sterility. *New Phytologist,* **84**, 145-164.

Pigott, C.D. and Pigott, S. (1993) Water as a determinant of the distribution of trees at the boundary of the Mediterranean zone. *Journal of Ecology*, **81,** 557-566.

Pollock, C.J. and Eagles, C.F. (1988). Low temperature and the growth of plants. In *Plants and Temperature* (eds S.P. Long and F.I. Woodward), pp. 157-180. The Company of Biologists, Cambridge.

Pons, T.J. (1991) Dormancy, germination and mortality of seeds in a chalk grassland flora. *Journal of Ecology,* **79,** 765-780.

Porley, R.D. (1999) Bryophytes of chalk grassland in the Chiltern Hills, England. *Journal of Bryology*, **21**, 55-66.

Preston, C.D. and Hill, M.O. (1997) The geographical relationships of British and Irish vascular plants. *Botanical Journal of the Linnean Society*, **124**, 1-120.

Prince, S.D. and Carter, R.N. (1985) The geographical distribution of prickly lettuce (*Lactuca serriola*). III. Its performance in transplant sites beyond its distribution limit in Britain. *Journal of Ecology,* **73,** 49-64.

Proctor, M.C.F. (1958) Ecological and Historical Factors in the Distributions of the British Helianthemum Species. *Journal of Ecology,* **46**, 349-371.

Radcliffe, J.E. and Lefever, K.R. (1981) Aspect influences on pasture microclimate at Coopers Creek, North Canterbury. *New Zealand Journal of Agricultural Research*, **24,** 55-66.

Ragab, R., Finch, J., and Harding, R. (1997) Estimation of groundwater recharge to chalk and sandstone aquifers using simple soil models. *Journal of Hydrology,* **190,** 19-41.

Raupach, M.R. and Finnigan, J.J. (1997) The influence of topography on meteorological variables and surface-atmosphere interactions. *Journal of Hydrology*, **190,** 182-313.

Rich, P.M. and Fu, P. (2000) Topoclimatic Habitat Models. In *4th International Conference on Integrating GIS and Environmental Modeling (GIS/EM4): Problems, Prospects and Research Needs*, Banff, Alberta, Canada.

Roberts, E.H. (1988). Temperature and seed germination. *In Plants and Temperature* (eds S.P. Long and F.I. Woodward), pp. 109-132. The company of Biologists Ltd., Cambridge.

Rodrigo, A., Recous, S., Neel, C., and Mary, B. (1997) Modelling temperature and moisture effects on C-N transformations in soils: comparison of nine models. *Ecological Modelling*, **102**, 325-339.

Rodwell, J.S., ed. (1992) *British plant communities: Grasslands and montane communities.* Vol. 3. CUP, Cambridge.

Rorison, I.H. (1981). Plant growth in response to variations in temperature: field and laboratory studies. In *Plants and their atmospheric environment* (eds J. Grace, E.D. Ford and P.G. Jarvis). Blackwell, Oxford.

Rorison, I.H., Gupta, P.L., and Hunt, R. (1986a) Local climate, topography and plant growth in Lathkill Dale NNR. II. growth and nutrient uptake within a single season. *Plant, Cell and Environment*, **9**, 57-64.

Rorison, I.H. (1987) Mineral nutrition in time and space. *New Phytologist*, **106** (Suppl.), 79-92.

Rorison, I.H. and Sutton, F. (1975). Climate, topography and germination. In *Light as an ecological factor* (eds G.C. Evans, R. Bainbridge and O. Rackham), Vol. II, pp. 361-383. Blackwell, Oxford.

Rorison, I.H., Sutton, F., and Hunt, R. (1986a) Local climate, topography and plant growth in Lathkill Dale NNR. I. A twelve-year summary of solar radiation and temperature. *Plant, Cell and Environment,* **9**, 49-56.

Rorison, I.H., Gupta, P.L., and Hunt, R. (1986b) Local climate, topography and plant growth in Lathkill Dale NNR. II. growth and nutrient uptake within a single season. Plant, Cell and Environment, **9**, 57-64.

Sætersdal, M., Birks, H.J.B., and Peglar, S.M. (1998) Predicting changes in Fennoscandian vascular-plant species richness as a result of future climatic change. *Journal of Biogeography*, **25,** 111-122.

Salisbury, F.B. and Spomer, S.G. (1964) Leaf temperatures of alpine plants in the field. *Planta,* **60,** 497-505.

Schaffers, A.P. (2000) *In situ* annual nitrogen mineralization predicted by simple soil properties and short-period field incubation. *Plant and Soil*, **221**, 205-219.

Schaffers, A.P. and Sýkora, K.V. (2000) Reliability of Ellenberg indicator values for moisture, nitrogen and soil reaction: a comparison with field measurements. *Journal of Vegetation Science*, **11**, 225-244.

Smith, T.M., Shugart, H.H., Bonan, G.B., and Smith, J.B. (1992) Modeling the potential response of vegetation to global climate change. *Advances in ecological research,* **22,** 93-116.

Soil Survey of England and Wales (1984) *1:250 000 Soil Maps of England and Wales: South-West England.* Silsoe.

Silvertown, J., Dodd, M., and Gowing, D. (2001) Phylogeny and the niche structure of meadow plant communities. *Journal of Ecology,* 89, 428-435.

Smart, S.M., Bunce, R.G.H., Firbank, L.G., and Coward, P. (2002) Do field boundaries act as refugia for grassland plant species diversity in intensively managed agricultural landscapes in Britain? *Agriculture, Ecosystems and Environment,* 91, 73-87.

Smart, S.M., Clarke, R.T., van de Poll, H.M., Robertson, E.J., Shield, E.R., Bunce, R.G.H., and Maskell, L.C. (2003) National-scale vegetation change across Britain; an analysis of sample-based surveillance data from the Countryside Surveys of 1990 and 1998. *Journal of Environmental Management*, 67, 239-254.

Smith, A.J.E. (1980) *The Moss Flora of Britain and Ireland.* Cambridge University Press, Cambridge.
Stace, C. (1997) *New Flora of the British Isles*, 2nd edn. Cambridge University Press, Cambridge.

Stephenson, N.J. (1990) Climatic control of vegetation distribution: the role of the water balance. *The American Naturalist,* **135,** 649-670.

Stephenson, N.J. (1998) Actual evapotranspiration and deficit: biologically meaningful correlates of vegetation distribution across spatial scales. *Journal of Biogeography,* **25,** 855-870.

Stewart, K.E.J., Bourn, N.A.D., and Thomas, J.A. (2001) An evaluation of three quick methods commonly used to assess sward height in ecology. *Journal of Applied Ecology*, **38**, 1148-1154.

Stuart, S. (2000) *MAVIS Plot Analyser.* CEH Merlewood, Grange-over-sands, Cumbria.

Summerfield, R.J. (1975) Factors affecting the germination and seedling establishment of *Narthecium ossifragum* on mire ecosystems. *Journal of Ecology*, **63**, 642-656.

Tansley, A.G. and Adamson, R.S. (1925) Studies of the vegetation of the English chalk: III. the chalk grasslands of the Hampshire-Sussex border. *Journal of Ecology,* **13**.

Tansley, A.G. and Adamson, R.S. (1926) Studies of the vegetation of the English chalk: IV. A preliminary survey of the chalk grasslands of the Sussex Downs. *Journal of Ecology,* **14**, 1-32.

Thomas, A.S. (1960) Changes in vegetation since the advant of myxomatosis. *Journal of Ecology,* **48**, 287-306.

Thomas, A.S. (1963) Further changes in vegetation since the advent of myxomatosis. *Journal of Ecology,* **51**, 151-186.

Thomas, C.D., Bodsworth, E.J., Wilson, R.J., Simmons, A.D., Davies, Z.G., Musche, M., and Conradt, L. (2001) Ecological and evolutionary processes at expanding range margins. *Nature,* **411,** 577-581.

Thomas, J.A., Rose, R.J., Clarke, R.T., Thomas, C.D., and Webb, N.R. (1999) Intraspecific variation in habitat availability among endothermic animals near their climatic limits and their centres of range. *Functional Ecology,* **13,** 55-64.

Thompson, K. (1993). Germination at alternating temperatures. In *Methods in Comparative Plant Ecology* (eds G.A.F. Hendry and J.P. Grime), pp. 183-185. Chapman and Hall, london.

Thompson, K. and Band, S.R. (1993). Germination at a range of constant temperatures. In *Methods in Comparative Plant Ecology* (eds G.A.F. Hendry and J.P. Grime), pp. 185-187. Chapman and Hall, London.

Thompson, K. and Grime, J.P. (1983) A comparative study of germination responses to diurnally-fluctuating temperatures. *Journal of Applied Ecology,* **20**, 141-156.

Thompson, K., Hillier, S.H., Grime, J.P., Bossard, C.c., and Band, S.R. (1996) A functional analysis of a limestone grassland community. *Journal of Vegetation Science,* **7,** 371-380.

Thompson, P.A. (1970) Germination of species of Caryophyllaceae in relation to their geographical distribution in Europe. *Annals of Botany,* **34**, 427-449.

Thorpe, P.C., Hendry, G.A.F., and Duran, M.V. (1993). Plant responses to low temperature. In *Methods in Comparative Plant Ecology* (eds G.A.F. Hendry and J.P. Grime), pp. 61-63. Chapman and Hall, London.

Thunholm, B. (1990) A comparison of measured and simulated soil temperature using air temperature and soil surface energy balance as boundary conditions. *Agricultural and Forest Meteorology*, **53,** 59-72.

van Tooren, B.F. and Pons, T.L. (1988) Effects of temperature and light on the germination in chalk grassland species. *Functional Ecology*, **2.**

Trudgill, D.L., Squire, G.R., and Thompson, K. (2000) A thermal time basis for comparing the germination requirements of some British herbaceous plants. *New Phytologist,* **145,** 107-114.

Trudgill, S.T. (1976) The erosion of limestones under soil and the long term stability of soil-vegetation systems on limestone. *Earth surface processes*, **1**, 31-41.

Tsialtas, J.T., Handley, L.L., Kassioumi, M.T., Veresoglou, D.S., and Gagianas, A.A. (2001) Interspecific variation in potential water-use efficiency and its relation to plat species abudace in a water-limited grassland. *Functional Ecology*, **15,** 605-614.

Tyler, G. (1994) A new approach to understanding the calcifuge habit of plants. *Annals of Botany,* **73**, 327-330.

Tyler, G. (1996) Mineral nutrient limitations of calcifuge plants in phosphate sufficient limestone soil. *Annals of Botany,* **77**, 649-656.

Tyler, G. (2002) Phosphorus fractions in grassland soils. *Chemosphere,* **48**, 343-349.

Uncovich, M., Jamieson, N., Managhan, R., and Barraclough, D. (1998) Nitrogen mineralisation and plant nitrogen acquisition in a nitrogen-limited calcareous grassland. *Environmental and Experimental Botany,* **40**, 209-219.

Varley, M.J., Beven, K.J., and Oliver, H.R. (1996) Modelling solar radiation in steeply sloping terrain. *International Journal of Climatology*, **16**, 93-106.

de Vries, D.A. (1963). Thermal properties of soils. In *Physics of the Plant Environment* (ed W.R. van Wijk), pp. 210-235. North-Holland, Amsterdam.

Waller, M.P. and Hamilton, S. (2000) Vegetation history of the English chalklands: a mid-Holocene pollen sequence from the Caburn, East Sussex. Journal of Quaternary Science, **15**, 253-272.

Watson, E.V. (1960) A quantitative study of the bryophytes of chalk grassland. *Journal of Ecology*, **48,** 397-414.

Watt, A.S. (1981) Further observations on the effects of excluding rabbits from grassland A in East Anglian Breckland: the pattern of change and factors affecting it (1936-73). *Journal of Ecology,* **69**, 509-536.

Weiss, S.B., Murphy, D.D., and White, R.R. (1988) Sun, slope and butterflies: topographic determinants of habitat quality for *Euphydryas editha. Ecology*, **69**, 1486-1496.

Wieder, R.K. and Lang, G.E. (1982) A critique of the analytical methods used in examining decomposition data obtained from litter bags. *Ecology,* **63**, 1636-1642.

Williams, E.D. (1983) Effects of temperature, light, nitrate and pre-chilling on seed germination of grassland plants. *Annals of Applied Biology,* **103,** 161-172.

Wilson, E.J., Wells, T.C.E., and Sparks, T.H. (1995) Are calcareous grasslands in the UK under threat from nitrogen deposition? An experimental determination of a critical load. *Journal of Ecology,* **83**, 823-832

Witkamp, M. (1966) Decomposition of leaf litter in relation to environment, microflora and microbial respiration. *Ecology,* **47**, 194-201.

van Wijk, W.R. and de Vries, D.A. (1963a). The atmosphere and the soil. In *Physics of the Plant Environment* (ed W.R. van Wijk). North-Holland, Amsterdam.

van Wijk, W.R. and de Vries, D.A. (1963b). Periodic temperature variations in a homogenous soil. In *Physics of the Plant Environment* (ed W.R. van Wijk), pp. 102-140. North-Holland, Amsterdam.

Woodward, F.I. (1987) *Climate and Plant Distribution.* Cambridge University Press, Cambridge.

Woodward, F.I. (1988). Temperature and the distribution of plant species and vegetation. In *Plants and Temperature* (eds S.P. Long and F.I. Woodward), pp. 59-76. The Company of Biologists Ltd, Cambridge.

Woodward, F.I. (1997) Life at the edge: a 14-year study of a *Verbena officinalis* population's interactions with climate. *Journal of Ecology*, 85, 899-906.

Woodward, F.I. and Jones, N. (1984) Growth studies of selected plant species with well-defined European distributions. *Journal of Ecology,* **72,** 1019-1030.

Woodward, F.I., Korner, C., and Crabtree, R.C. (1986) The dynamics of leaf extension in plants with diverse altitudinal ranges. *Oecologia,* **70,** 222-226.

Woodward, F.I. and Pigott, C.D. (1975) The climatic control of the altitudinal distribution of *Sedum rosea* (L.) Scop. and *Sedum telephium* L. I. Field observations. *New Phytologist*, **74**, 323-334.

Yee, T.W. and Mitchell, N.D. (1991) Generalized additive models in plant ecology. *Journal of Vegetation Science*, **2**, 587-602.

Young, K.L., Woo, M., and Edlund, S.A. (1997) Influence of local topography, soils, and vegetation on microclimate and hydrology at a high arctic site, Ellesmere Island, Canada. *Arctic and Alpine Research*, **29**, 270-284.

Zimmermann, N.E. and Kienast, F. (1999) Predictive mapping of alpine grasslands in Switzerland: Species versus community approach. *Journal of Vegetation Science*, **10**, 469-482.

Appendix 1

Listing for SITERAD, FORTRAN 90 program to calculate solar radiation, PAR and net radiation at a plot

```
program SITERAD
    integer:: day,time
    real:: sclear,scloudy,scplot,saws,raws,c,splot,sAWS,netAWS,lAWS,PARplot,netplot
    OPEN (1,FILE='sclear.prn',STATUS='OLD')
    OPEN (2,FILE='scloudy.prn',STATUS='OLD')
    OPEN (3,FILE='sclplot.prn',STATUS='OLD')
    OPEN (4,FILE='sAWS.prn',STATUS='OLD')
    OPEN (5,FILE='netAWS.prn',STATUS='OLD')
    OPEN (6,FILE='siterad.txt',STATUS='UNKNOWN') !open files
400   format(2i8,f8.3)
402   format(2i8,3f8.3)
    albedo = 0.25
    DO N=1,8760 !hourly time step
        READ(1,400) day,time,sclear
        READ(2,400) day,time,scloudy
        READ(3,400) day,time,sclplot
        READ(4,400) day,time,sAWS
        if (scloud.gt.0) then
         c=(sAWS-scloud)/(sclear-scloud) ! calculate clearness index
         else
         c = 1
        end if
     splot = scloud + (c*(sclear-scloud)) !calculate S at plot
        PARplot = 0.184*splot !calculate PAR at plot
     lAWS = netAWS-sAWS*(1-albedo) !estimate lw radiation at AWS
     netplot = splot*(1-albedo)+lAWS !calculate net radiation at plot
    WRITE(6,402) day,time,splot,PARplot,lAWS !write to file
    END DO
    STOP
    END PROGRAM SITERAD
```

Appendix 2

Listing for SITETEMP1 and SITETEMP2, FORTRAN 90 programs to calculate soil and sward temperature at a plot

```
    PROGRAM SITETEMP1

    INTEGER year,time,day
    REAL netrad,solrad,par,ts50,ts10,ta150,ts150,tmp,wet,v1,v2,theta&
   &,wind,wdir,wstdev,rain,volts,To
    OPEN (1,FILE='aws.txt',STATUS='OLD')
    OPEN (2,FILE='temp.txt',STATUS='UNKNOWN')
    OPEN (3,FILE='siterad.txt',STATUS='OLD')
400   format(3i8,2f9.2,9f8.2,4f8.3,2f8.2)
401   format(2i8,3f8.3)
402   format(2i8,3f8.3)

    DO N=1,8760 ! hourly time step
      READ(1,400) year,day,time,netrad,solrad,par,ts50,ts10,ta150,ts150,tmp,wet&
     &v1,v2,theta,wind,wdir,wstdev,rain,volts
      READ(3,401) day,time,splot,PARplot,netplot !read modelled radiation file
      To = tmp + (0.0386-0.00256*wind)*netplot ! calculate sward temperature
     write(2,401) year,day,time,To !write hourly sward temperature
    END DO
    STOP
    END PROGRAM SITETEMP1


PROGRAM SITETEMP2

    INTEGER year,day
    REAL To,netplot,Ts,Tsx
    OPEN (1,FILE='dailytemp.txt',STATUS='OLD')
    OPEN (2,FILE='dailynet.txt',STATUS='OLD')  !DAILY mean temp/radiation files
    OPEN (3,FILE='soiltemp.txt',STATUS='UNKNOWN')
400   format(2i,1f8.3)
401   format(2i8,3f8.3)

   write(*,*)'enter initial Ts'
    read(*,*)Ts
    write(*,*)'enter initial Tsx'
    read(*,*)Tsx   !enter boundary conditions

    DO N=1,365 ! hourly time step
      READ(1,400) year,day,To
      READ(2,400) year,day,netplot
      Ts=Ts+0.01*netplot+0.5*(To-Ts)-0.5*(Ts-Tsx) !calculate 0-50mm soil temp
      Tsx=Tsx+0.5*(Ts-Tsx) !calculate soil temp below 50mm
      WRITE(3,401) year,day,T0,Ts,Tsx
    END DO
    STOP
    END PROGRAM SITETEMP1
```

Appendix 3

Listing for SITEMOISTURE, FORTRAN 90 program to calculate soil moisture at a plot

```
      PROGRAM SITEMOISTURE

      INTEGER year,time,day
      REAL netrad,solrad,par,ts50,ts10,ta150,ts150,tmp,wet,v1,v2,theta&
     &,wind,wdir,wstdev,rain,volts,clearrad,cloudrad,clearm,netradm,solradm,&
     &es,eswet,ea,delta,psych,z2,z3,z4,wp,fc,sp,satp,t1,t2,t3,t4
      real,dimension(20)::clearm,netradm,solradm,Et,G,Rn,theta1,theta2,&
     &theta3,theta4,perc1,perc2,perc3,perc4,perc5,stress1,stress2,&
     &stress3,stress4,evap1,evap2,evap3,evap4,aet,runoff,z1
      OPEN (1,FILE='aws.txt',STATUS='OLD')
      OPEN (2,FILE='soilout.txt',STATUS='UNKNOWN')
      OPEN (3,FILE='radmod.txt',STATUS='OLD')
      OPEN (4,FILE='dsite.txt',STATUS='OLD')
      OPEN (5,FILE='sdepth.txt',STATUS='OLD')

      write(*,*)'enter theta1'
      read(*,*)t1
      write(*,*)'enter theta2'
      read(*,*)t2
      write(*,*)'enter theta3'
      read(*,*)t3
      write(*,*)'enter theta4' !boundary conditions
      read(*,*)t4
      theta1=t1
      theta2=t2
      theta3=t3
      theta4=t4
      READ(5,404) z1
      z2=100 !depth of four root zone layers
      z3=200
      z4=200
      wp=0.03 !wilting point
      fc=0.14 !field capacity
      sp=0.4 !stress point
      satp=0.5 !saturation point

      DO N=1,n
      READ(1,400) year,day,time,netrad,solrad,par,t1,t2,t3,t4,tmp,wet,v1&
     &,v2,theta,wind,wdir,wstdev,rain,volts
      READ(3,402) clearrad,cloudrad
      READ(4,403) clearm
      if (n.eq.11416) then
      theta1=0.45
      theta2=0.45
      theta3=0.45
      theta4=0.45
      end if
      WRITE(*,*) day,time
400    format(3i8,11f8.2,4f8.3,2f8.2)
401    format(3i8,20f6.3)
402    format(2f8.3)
403    format(20f8.2)
404    format(20f8.2)
       if (cloudrad.gt.0) then
       cloud = (solrad-cloudrad)/(clearrad-cloudrad)
```

```
 else
 cloud = 1
 end if
 solradm = cloudrad+(cloud*(clearm-cloudrad)) !estimate short-wave
 Rlaws = (netrad-(0.8*solrad))
 netradm = (solradm*0.8)+Rlaws

 es = 0.61084*exp(17.27*tmp/(tmp+237.3)) !saturation vapour pressure, kPa
 eswet = 0.61084*exp(17.27*wet/(wet+237.3)) !wet bulb temp sat vap pressure, kPa
 delta = es*((17.269)/(237.3+tmp))*(1-(tmp/(237.3+tmp))) !Murray, 1967
 psych = 0.067 !Approximation for 100-200m above sea level
 ea = es-psych*(tmp-wet) !actual vapour pressure, kPa

 DO M=1,20
 Rn(M)=0.0036*netradm(M)
 if (netradm(M).lt.0) then
  G(M)=0.5*Rn(M)
  else
  G(M)=0.1*Rn(M)
 end if
 END DO

 Et=(0.408*delta*(Rn-G)+(psych*37*wind*(es-ea))/(tmp+273.2))/(delta&
&+psych*(1+0.34*wind))  !FAO Penman-Monteith eqtn

DO M=1,20
 if (theta1(M).gt.satp) then
  runoff(M)=rain
  else
  runoff(M)=0
 end if

 perc1(M)=(rain-runoff(M))

 if (theta1(M).gt.fc) then
  if (theta1(M).gt.theta2(M)) then
   perc2(M)=z1(M)*(theta1(M)-theta2(M))
   else
   perc2(M)=0
  end if
 else
  if (theta1(M).lt.theta2(M)) then
   perc2(M)=0.1*z1(M)*(theta1(M)-theta2(M))
  end if
 end if

 if (theta2(M).gt.fc) then
  if (theta2(M).gt.theta3(M)) then
   perc3(M)=z2*(theta2(M)-theta3(M))
   else
   perc3(M)=0
  end if
 else
  if (theta2(M).lt.theta3(M)) then
   perc3(M)=0.1*z2*(theta2(M)-theta3(M))
  end if
 end if

if (theta3(M).gt.fc) then
  if (theta3(M).gt.theta4(M)) then
   perc4(M)=z3*(theta3(M)-theta4(M))
   else
   perc4(M)=0
```

```
  end if
 else
  if (theta3(M).lt.theta4(M)) then
   perc4(M)=0.1*z3*(theta3(M)-theta4(M))
  end if
end if

if (theta4(M).gt.fc) then
 perc5(M)=0.035*((theta4(M)-fc)/(sp-fc))
 else
 perc5(M)=0
end if

if ((theta1(M)-wp)/(sp-wp).gt.1) then
 stress1(M)=1
 else
 stress1(M)=(theta1(M)-wp)/(sp-wp)
end if

if ((theta2(M)-wp)/(sp-wp).gt.1) then
 stress2(M)=1
 else
 stress2(M)=(theta2(M)-wp)/(sp-wp)
end if

if ((theta3(M)-wp)/(sp-wp).gt.1) then
 stress3(M)=1
 else
 stress3(M)=(theta3(M)-wp)/(sp-wp)
end if

if ((theta4(M)-wp)/(sp-wp).gt.1) then
 stress4(M)=1
 else
 stress4(M)=(theta4(M)-wp)/(sp-wp)
end if
END DO

evap1=stress1
evap2=stress2*(1-evap1)
evap3=stress3*(1-(evap1+evap2))
evap4=stress4*(1-(evap1+evap2+evap3))

theta1=theta1+perc1/z1-(Et*evap1)/z1-perc2/z1
theta2=theta2+perc2/z2-(Et*evap2)/z2-perc3/z2
theta3=theta3+perc3/z3-(Et*evap3)/z3-perc4/z3
theta4=theta4+perc4/z4-(Et*evap4)/z4-perc5/z4
aet = Et*evap1 + Et*evap2 + Et*evap3 + Et*evap4

write(2,401) year,day,time,theta1
END DO
STOP
END PROGRAM SITEMOISTURE
```

Appendix 4

Derivation of terms from AWS data (following Allen 1998)

G, soil heat flux, (MJ $m^{-2}h^{-1}$) is assumed to be equal to 0.5 R_n at night and 0.1 R_n during daylight.

γ, the psychrometer constant, is approximated as 0.067 kPa C^{-1} between 100-200m above sea level.

e_s saturation vapour pressure at air temperature (kPa) is equal to

$$e_s = 0.6108 \exp(17.27\ T/(T+237.3))$$

where T is air temperature (°C)

e_a vapour pressure of air (kPa) is calculated by

$$e_a = e_s\ (T_{wet}) - \gamma\ (T - T_{wet})$$

where T_{wet} is wet-bulb temperature (°C).

Δ, the slope of saturation vapour pressure curve at air temperature (kPa C^{-1}) is equal to

$$\Delta = (4098(0.6108 \exp(17.27T / T+237.3)))/ (T+237.3)^2$$